An investigation into novel synaptic plasticity mechanisms which are disrupted in a mouse model of fragile-X syndrome

Erik A Larson

December 2020
Integrated Program in Neuroscience

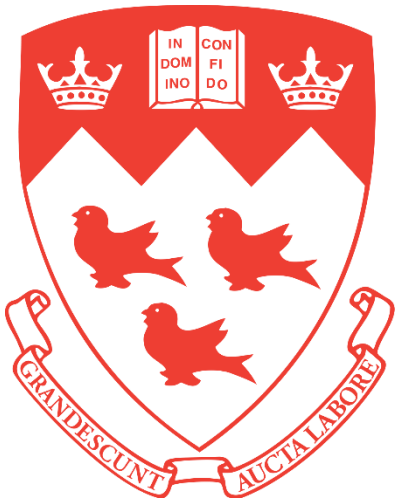

McGill University
(Montreal, Canada)

A thesis submitted to the Faculty of Graduate and Postdoctoral Studies in partial fulfillment of the requirement of the degree of
DOCTOR OF PHILOSOPHY

Copyright © 2020 Erik A Larson

To all my loved ones,

Especially my mom

“Of course it is happening inside your head…
but why on earth should that mean that it is not real?”

-Albus Percival Wulfric Brian Dumbledore
(J.K. Rowling)

ABSTRACT

Synaptic neurotransmission is a fundamental process which enables signaling between neurons. All voluntary animal behaviour relies on proper synaptic function, and many neurological diseases have their origins in synaptic disruptions. In particular, the neurodevelopmental disease fragile-X syndrome (FXS) has notable defects in synaptic transmission across the brain. FXS is the most common single gene cause of intellectual disability and autism, and is caused by interruptions in the expression or function of the protein FMRP. Like many neurodevelopmental diseases, FXS is characterized in part by an imbalance in excitation and inhibition in the brain. While there is a general consensus regarding the defects in FXS excitatory signaling, there is considerably less known about defects to inhibitory neurotransmission. In particular, there has been no comprehensive study on the synapses of the inhibitory cerebellar molecular layer interneurons (MLIs) in the pathophysiology of FXS. Accordingly, this thesis addresses this gap in our understanding FXS, while also uncovering novel plasticity mechanisms in MLI inhibitory neurotransmission.

Neurotransmission is very dynamic and synapses regularly change their efficacy in a process known as synaptic plasticity. Most research into synaptic plasticity has focused on excitatory synapses, but there is a new interest in studying the mechanisms that lead to long term changes of inhibitory synaptic signaling. One of these mechanisms includes a novel role for reactive oxygen species (ROS) to potentiate inhibitory GABAergic signaling of MLIs. Given this, the first objective of this thesis was to identify the physiological signaling pathways of ROS-dependent inhibitory plasticity using an approach involving both pharmacological and genetic

manipulations. I found that NMDA receptor activation generates physiological ROS through a nNOS-cGMP-NOX2 pathway. Furthermore, this pathway recruited α3-containing $GABA_A$ receptors to the synapse following PKC activation and GABARAP trafficking.

The second half of this thesis was a study on the role of MLIs in the neurodevelopmental disease, FXS. In these chapters, I start by describing a novel defect in MLI NMDA receptor signaling. Consequently, this impacts multiple plasticity mechanisms which regulate inhibition in the CNS. First, MLIs are unable to modulate their firing properties in response to NMDA receptor activation. Second, there is an inability to potentiate inhibitory signaling onto MLIs. Inhibitory plasticity can be restored by the inclusion of a small molecule which potentiates the intracellular signaling pathway. Third, there is a significant impact on the regulation of blood flow through the cerebellum. Together, the lack of these plasticity mechanisms likely impacts the cerebellar circuit which I predict would have downstream consequences on motor learning. Finally, I have also found a defect in dendritic filtering of cerebellar MLIs in FXS. MLIs from FXS mice fire more action potentials following afferent stimulation, which is linked to a larger evoked postsynaptic potential (ePSP) amplitude. Moreover, acute reintroduction of the N-terminal fragment of FMRP reduces the ePSP amplitude in FXS mice. Taken together, this thesis presents original findings on GABAergic plasticity and multiple defects in inhibitory signaling of FXS mice in the cerebellum. Based on our new understanding of inhibitory signaling, this thesis also demonstrates mechanisms to overcome these defects in FXS which could lead to therapeutics in a future clinical setting.

ABÉRGÉ

La neurotransmission synaptique est un processus fondamental qui permet la signalisation entre les neurones. Tout comportement animal volontaire repose sur une fonction synaptique appropriée, et de nombreuses maladies neurologiques ont pour origine des perturbations synaptiques. En particulier, le syndrome de l'X fragile (FXS), un maladie neurodéveloppementale, présente des défauts notables dans la transmission synaptique à travers le cerveau. Le FXS est la plus courante de déficience intellectuelle et d'autisme cause de une gêne unique, et est causée par des interruptions dans l'expression ou la fonction de la protéine FMRP. Comme de nombreuses maladies neurodéveloppementales, le FXS présente un déséquilibre dans l'excitation et l'inhibition dans le cerveau. Bien qu'il existe un consensus général concernant les défauts de la signalisation excitatrice FXS, on en sait considérablement moins sur les défauts de la neurotransmission inhibitrice. En particulier, il n'y a pas eu d'étude complète sur les synapses des interneurones des cellules inhibitrices interneurone moléculaire de cervelet (MLI) dans la physiopathologie du FXS. En conséquence, cette thèse aborde cette lacune dans la connaissance du FXS, tout en découvrant de nouveaux mécanismes de plasticité dans la neurotransmission inhibitrice de MLI.

Le processus de neurotransmission est très dynamique et les synapses changent régulièrement leur efficacité dans un processus appelé plasticité synaptique. La plupart des recherches sur la plasticité se sont concentrées sur les synapses excitatrices, mais il existe un nouvel intérêt pour l'étude des mécanismes qui conduisent à des changements à long terme de la signalisation synaptique inhibitrice. L'un de ceux-ci comprend un nouveau rôle pour les espèces

réactives de l'oxygène (ROS) dans la potentialisation de la signalisation inhibitrice GABAergique des MLI. Compte tenu de cela, le premier objectif de cette thèse était d'identifier les voies de signalisation physiologiques de la plasticité inhibitrice ROS-dépendante. J'ai trouvé que l'activation du récepteur NMDA génère des ROS physiologiques via une voie nNOS-cGMP-NOX2. En outre, cette voie a recruté des récepteurs $GABA_A$ contenant α3 dans la synapse après l'activation de PKC et le trafic de GABARAP.

La deuxième moitié de cette thèse était une étude sur le rôle des MLI dans la maladie neurodéveloppementale, FXS. J'ai trouvé un défaut précédemment non décrit dans la signalisation du récepteur MLI NMDA. Par conséquent, cela a un impact sur plusieurs mécanismes de plasticité qui régulent l'inhibition dans le SNC. Premièrement, les MLI sont incapables de moduler leurs propriétés de déclenchement en réponse à l'activation du récepteur NMDA. Deuxièmement, il existe une incapacité à potentialiser la signalisation inhibitrice sur les MLI. La plasticité inhibitrice peut être restaurée par l'inclusion d'une petite molécule qui potentialise la voie intracellulaire. Troisièmement, il y a un impact significatif sur la régulation du flux sanguin à travers le cervelet. L'absence de ces mécanismes de plasticité a probablement un impact sur le circuit cérébelleux, ce qui aurait des conséquences en aval sur l'apprentissage moteur. Enfin, j'ai également trouvé un défaut dans le filtrage dendritique des MLI cérébelleuses dans FXS. Les souris FXS tirent plus de potentiels d'action après une stimulation afférente, qui est liée à une plus grande amplitude du potentiel postsynaptique évoqué (ePSP). De plus, la réintroduction aiguë du fragment N-terminal de FMRP réduit l'amplitude de l'ePSP chez les souris FXS. Pris ensemble, cette thèse présente des découvertes originales sur la plasticité GABAergique et de multiples défauts dans la signalisation inhibitrice des souris FXS. Sur la base de notre

nouvelle compréhension de la signalisation inhibitrice, cette thèse démontre également des mécanismes pour surmonter ces défauts dans FXS qui pourraient conduire à des traitements pour une utilisation clinique future.

TABLE OF CONTENTS

LIST OF FIGURES

PART I: REVIEW OF THE LITERATURE

PART II: EXPERIMENTAL RESULTS

Chapter 1

Chapter 2

Chapter 3

PART III: GENERAL DISCUSSION

LIST OF ABBREVIATIONS

7-chlorokynurenate (7CK)
acetylcholine (ACh)
acetylcholine binding protein (AChBP)
afterhyperpolarization (AHP)
amino-terminal domain (ATD)
AMPA receptor (AMPAR)
autism spectrum disorders (ASD)
big conductance Ca2+-activated K+ (BK)
Brain-derived neurotrophic factor (BDNF)
Ca2+/calmodulin-dependent protein kinase II (CaMKII)
calcium ions (Ca2+)
carboxy-terminal domain (CTD)
chloride ions (Cl-)
climbing fiber (CF)
cornichon homologue proteins (CNIH)
cytokine tumour-necrosis factor-α (TNF-α)
endogenous cannabinoid (eCB)
evoked excitatory postsynaptic potential (eEPSP)
excitatory postsynaptic current (EPSC)
excitatory postsynaptic potential (EPSP)
extracellular domain (ECD)
fragile-X syndrome (FXS)
G protein-coupled receptors (GPCRs)
GABAA receptor-associated protein (GABARAP)
GABAA receptors (GABAAR)
GABAB receptors (GABABR)
glycine receptors (GlyR)
inhibitory long term potentiation (iLTP)
inhibitory post synaptic potential (IPSP)
inhibitory post synaptic potentials (IPSP)
inhibitory postsynaptic current (IPSC)
intrinsic plasticity (IP)
Ionotropic glutmate receptors (iGluRs)
K+- Cl- transporter member 5 (KCC2)
kainite receptors (KAR)
ligand binding domain (LBD)
long term depression (LTD)
long term potentiation (LTP)
magnesium ions (Mg2+)
metabotropic glutamate receptors (mGluRs)
molecular layer interneurons (MLIs)
mossy-fibre (MF)
Na+-activated, K+-selective ion channels (Slack)
Na+-K+-Cl- cotransporter (NKCC1)
neuromuscular junction (NMJ)
nicotinic acetylcholine (nAChR)
nitric oxide (NO)
NMDA receptor (NMDAR)
N-methyl- d-aspartic acid (NMDA)
N-terminal domain of FMRP (N-FMRP)
parallel fiber (PF)
post translational modifications (PTM)
postsynaptic density (PSD)
Potassium ion (K+)
Purkinje cell (PC)
readily releasable pool (RRP)
rebound potentiation (RP)
Schaffer collateral (SC)
small conductance Ca2+-activated K+ (SK)
transmembrane AMPAR regulatory protein (TARP)
transmembrane domain (TMD)
untranslated region (UTR)
ventral tegmental area (VTA)
vestibulo-ocular reflex (VOR)
voltage gated Ca2+ channels (VGCCs)
voltage gated Ca2+ channels (VGCCs)
α-amino-3-hydroxy-5-methyl-4-isoxazolepropionic acid (AMPA)
γ-aminobuteryic acid (GABA)

ACKNOWLEDGMENTS

If you are reading this, you should know that none of it would be possible without the support of the people that I will mention here. They have meant more to me than words can do justice, but I will try and express their importance to my life, and to this work, as a way of thanks.

First I would like to thank Derek, who has had the greatest influence on my development as a scientist. The lab that he has fostered over the years has made it the best learning environment. After a full week of experiments, Friday beers were always at the front of his mind and this attitude of work/life balance spread through the rest of the lab. Beer hour(s) discussions have covered topics from interesting lab results, current events, or obscure facts/statistics that someone had found on the internet. More often than not, some of our greatest insights were made during those beer hours and many of my fondest lab memories are from Friday at 4:55 to the end of the day.

This collegial attitude of the lab continued through the week but without the influence of beer discussions were typically more tailored to the new papers of the day, or some wacky experiments that we would be starting. This day to day was how we “cut our teeth” and is where I credit my real education at McGill. While discussions often lead to arguments, they were always made in good faith and in an attempt to come to a better understanding. Most importantly, the input from lab members during formal lab meetings improved the quality of my work and presentations. At first, I was awed by the older members of the lab. Mark, Patricia, Brent, and Bryan – all had an expertise that was incredibly intimidating. Their knowledge eventually trickled down and I eventually learned how to keep up with the rapid pace discussions could take. Specifically I would like to thank Mark for being a mentor to everyone in the lab. Not only are his molecular biology skills extensive, he was always willing to help anyone wherever he could both technically and by providing valuable feedback. When I joined, Bryan was the most senior member of the lab and he helped sharpen my critical thinking skills while teaching me to properly think through my experiments. Patricia was one of my best lab-friends and we had many good times both inside and outside the lab. She is also the best technical experimentalist and set impossibly high standards for electrophysiology in the lab. Brent, was the publishing star during

my early years and represented the best of the lab for chasing cool ideas and executing challenging experiments. On a more personal level he was also the smartest trivia player I have ever seen and has remained a great friend.

More recently, I have learned more from the newer lab members. Adamo has been the great lab maverick and he has approached research with a gusto that is inspiring. Edward was one of the most talented and intelligent young students that I have had the pleasure of working with and I also enjoyed discussing, and eating, great food with him. Other members of the Lab who I am grateful to are Hugo, Marika, Niklas, Martina, Sara, Alek, Karelle, Jihane, Frédérique, Kaitlin, Rafael, Tian, Kat, Arjun, Alexia, and Xin-Tong.

There are a few lab members who I have specifically left to the end. First, Mike was the most important Bowie Lab member for my early years. He trained me in the mysterious ways of patch-clamp electrophysiology, and laid the groundwork for everything that has gone into this thesis. I would also like to specifically thank Amanda. Her editing skills are beyond amazing, and she taught me the difference between “effect and affect”. More importantly, her kindness has been a constant source of support over the last 3 years. Finally, Ryan has been the lab-mate that I have shared the most with. We started around the same time and together formed the new wave of the “cerebellum side of the lab”. Throughout that time, we have been international traveling partners, and enjoyed the office, comic book movies, discussed the latest news or statistics of the day, and we have celebrated each other’s triumphs and commiserated when needed. Ryan has also been my guide through the modern world of the pop culture, and has expanded my appreciation for different types of music all while being the best lab-mate/friend anyone could ask for.

Within the Bellini building, I have also been fortunate to have close friendships with people from other labs. I spent most of my time sitting next to Sandra from the Munter lab. Not only was she one of the hardest working people I have ever seen but she has a great infectious love of life that is centered on sports. She made every Olympics or World Cup an event to remember. While we might not see eye to eye on our favourite athletes, our banter has always been in good fun and brings smiles to our faces (except perhaps for the years that Munich has

won the treble). I am also grateful to another German, Filip who was always happy to share some beer or play soccer. Corey was the person I met first in the building and helped to bring everyone from different labs together, generally over a beer (there is a theme developing here). Finally Mark J, Britt, Paoula, Pheobe, Shireen, Mel, and Andy have all made my time in the lab brighter and more enjoyable.

Outside the lab, but with the McGill community, this thesis also owes much to Dr. Charles Bourque and Dr. Ellis Cooper who have been nothing short of the best PhD committee members one could ask for. They have consistently challenged me and provided suggestions for experiments that have truly improved the science presented here in this thesis.

More friends whom I would like to thank are the ones I played trivia, soccer or shared good food and drinks with. In no particular order, thank you to Matt, Rob, Ali, Charbel, Josh, Sienna, Alan, Kate, Ana, Fe, Steve, Kai, Holly, AC, Marwan, Nikki, Kristy, Andrew, Julia, Lindsay, Lisa and so many others for making the time during my PhD unforgettable. I would also like to thank my friends in the GC who might not really know what I do but have always been there for me.

Finally, I would like to thank my family. First and foremost, thank you to my parents. I do not know how I could have done this without their love and support. From a young age, they have instilled a thirst for knowledge which has stayed with me. They have given me the unconditional love that has made me the person I am today. Everything in this thesis exists because of what they have done for me. Alongside my parents, my sister Tina has been my closest friend. We have shared all of the victories and tragedies of life and helped take each other through it all. She is a source of support that I have relied on through my entire life. Finally, I have an extensive family, both in and out of Montreal. Thank you to my Grandma, all my aunts and uncles, my cousins (first and second), and all their significant others.

I would like to extend a special thank you to Bram for help in editing this thesis. His infectious and youthful love of life has helped kept me steady through the writing process.

And last, but certainly not least, thank you to Kathleen. She is the brightest light in my life and helped get me over the finish line.

CONTRIBUTIONS OF AUTHORS

This thesis is written in a manuscript-based format, as outlined in the McGill guidelines. The body of the thesis is composed of three chapters, the first being a published manuscript and the second and third which will be submitted for publication in a similar form. All manuscripts are co-authored, and a detailed description of authors' contributions follows below, as required by McGill guidelines.

Chapter 1: "Physiological ROS signaling induces iLTP in cerebellar MLIs" was published in the Journal of Neuroscience in 2020 as:

> **Larson, E. A.,** Accardi, M. V., Wang, Y., D'Antoni, M., Karimi, B., Siddiqui, T. J., & Bowie, D. (2020). Nitric oxide signaling strengthens inhibitory synapses of cerebellar molecular layer interneurons through a GABARAP-dependent mechanism. Journal of Neuroscience, 40(17), 3348-3359.

For this work I designed the experiments with Dr. Bowie. I then collected, analyzed, and plotted all the data presented in Figures 1.1, 1.2, 1.3, 1.4, 1.5, and 1.6. I also prepared the summary Figure 1.8 as well as drafted the entirety of the manuscript with Dr. Bowie. Together Dr. Bowie and I revised the manuscript and provided all the responses to the reviewers. Martina D'Antoni contributed data to Figure 1.5. Dr. Michael Accardi contributed data to Figure 1.1, 1.3, 1.4, and 1.5. Figure 1.7 was created entirely by our collaborators in the Siddiqui lab at the University of Manitoba.

Chapter 2: in its current form will have the authors as listed:

Larson, E. A., Alexander, R.P.D., Trigiani, L.J., Hamel, E, & Bowie, D

For this work I designed the experiments with Dr. Bowie. I then collected, analyzed, and plotted all the data presented in Figures 2.1, 2.3, 2.4. I also prepared the summary Figure 2.6 as well as drafted the entirety of the manuscript. Figure 2.2 was created entirely by Dr. Alexander from the Bowie Lab. Figure 2.5 was created in collaboration with Dr. Alexander who help collect, analyze and plot all of the data for panels A, B, D, and E. All of the data for panel C was collected and analyzed by Dr. Lianne Trigiani from Dr. Hamel's lab.

Chapter 3: in its current form will have the authors as listed:

Larson, E. A. & Bowie, D

For this work I designed the experiments with Dr. Bowie. I then collected, analyzed, and plotted all the data presented in all the Figures with analysis help from Dr. Ryan Alexander for Figure 3.2. I have then drafted the entirety of the manuscript.

FOREWORD

The brain is a marvelous and intricate organ responsible for coordinating voluntary control over the rest of the body. All of the complex integrating and processing of information necessary for an animal to interact with its environment occurs throughout the specialized structures found in the brain. This processing of information is all accomplished through a network of neurons, which produce a wide range of behaviours such as memory, emotions, and movement. These neural circuits are connected by synapses which coordinate the activity of many neurons – a theory rooted in the work of Ramon y Cajal and championed by Sir Charles Scott Sherrington. One of the most important features about these synapses are that they are dynamically regulated. Small changes to the strength of a synapse adjusts the function of the neural circuit and ultimately underlies the physiological basis for Donald Hebb's theory of learning. As synapses have long been appreciated as one of the most important parts of the nervous system, attempts to understand the way the brain works has focused heavily on the anatomy and physiology of synapses.

Despite many decades of research, we are still learning how synapses function and change over time. Changes to synapses can broadly be referred to as synaptic plasticity and occurs during development and throughout life. During development, there are many important milestones that occur which change the way that synapses function to ensure that the brain matures properly. Of critical importance is that the strength of the many synaptic inputs for each neuron is appropriately weighted and fine-tuned. Synapses can be classified as either excitatory or inhibitory, and a delicate balance must be maintained between their relative strengths. This is a tightly regulated process controlled and many different molecules and proteins constantly act

to change the functional properties of synapses. In recent years there has been a realization that the origins for many neurodevelopmental disorders are found in synapses. More specifically, the proteins that shape synapses are often dysfunctional or improperly controlled in different neurodevelopmental disorders (Heavner and Smith, 2020).

With new advances in the field of human genetics, neurodevelopmental diseases have increasingly been classified based on mutations found within genes encoding proteins highly expressed in synapses. In order to better understand the neurobiology of these diseases, the mutations have been reproduced in transgenic rodent models which has allowed researchers to more closely examine their role in the brain and within synapses. During my PhD I wanted to understand how synapses function in both health and disease with a focus on inhibitory synaptic signaling. This thesis was guided by the questions: how do synapses function and how can their malfunction lead to disease? These two questions have been at the forefront of attempts to develop therapeutic interventions which eventually could be used for treating the symptoms of disease. By having a better understanding of the function of synapses, we can have a new appreciation of the pathophysiology of neurodevelopmental disorders. In turn, by studying the synaptic defects in animal models of neurodevelopmental diseases we can have new insights into synapse physiology. Accordingly, this thesis is organized into three **PARTS** to address these questions. **PART I** is a literature review which covers synapses; including the history of synaptic signaling, excitatory and inhibitory synapses, synaptic integration, and the role of synapses in neurodevelopmental disease. **PART II** contains my original work from my time in the Bowie lab. It is organized in a manuscript format and has three chapters which (1) describes a novel signaling pathway for the induction and expression of inhibitory long term potentiation, (2) investigates

how defects in excitatory signaling leads to plasticity defects in neurodevelopmental disease, and (3) explores how a novel role for the fragile-X mental retardation protein is important for dendritic filtering. **PART III** contains a general discussion of the results, with a focus on how the plasticity mechanisms in thesis could interact. Finally, I also discuss how my results could be translational and illustrate aims for future therapeutic development.

PART I: REVIEW OF THE LITERATURE

R.1 The Synapse

The synapse is one of the most important structures in the central nervous system (CNS) and allows for signals to pass throughout the brain. Since its discovery it has remained one of the most significant concepts for describing the function of the nervous system. Nevertheless, the theory of a synapse was hotly debated among early neuroscientists whom were trying to understand the cellular anatomy of the brain. Joseph von Gerlach and Camillo Golgi proposed that the nervous system consisted primarily of a large net of processes with a connected continuous cytoplasm across the entire CNS and referred to this as the reticular theory (Sotelo, 2020). This was contrasted by a theory called the "neuron doctrine", which argued that the nervous system was made up of many individual cells called neurons which formed invisible microscopic connections to each other. The neuron doctrine was championed by the work of August Forel and Wilhelm His, and illustrated by the precise staining of Santiago Ramon y Cajal (Sotelo, 2020). Ultimately, it was the neuron doctrine which would prove to be correct, but a key question remained – how do neurons signal to one another? This question was answered through physiology experiments done by Sir Charles Scott Sherrington. He noted a delay from the stimulation of an afferent and the expected time for reflex response to occur. The explanation that he provided was that this was due to signal transmission between nerves and coined the term "synapse", which denoted the place where information passes from a presynaptic neuron to a postsynaptic neuron (Sherrington, 1906).

With the concept of synapses in the CNS becoming established, it still remained to be seen if the synaptic transmission signal was an electrical or chemical messenger. A key observation supporting the chemical transmission hypothesis was made by Langley, who

conceptualized the idea of a "receptor" which responds to chemical signals – in his case, exogenous nicotine (Langley, 1905). Endogenous chemical transmission was demonstrated by Otto Loewi who showed that a substance he called "vagusstoff" could slow the heart rate of an isolated heart (Loewi, 1921). Vagusstoff was later confirmed to be acetylcholine by Dale and colleagues, which provided abundant support for the idea of chemical transmission (Dale and Gaddum, 1930; Dale et al., 1936). Nevertheless, others such as Sir John Carew Eccles doubted that chemical transmission was fast enough to function in the CNS and favoured the electrical neurotransmission theory for synapses in the brain and at the neuromuscular junction (Eccles, 1937). Incidentally, it was Eccles and colleagues who would eventually provide the conclusive demonstration that chemical synaptic transmission was the predominant form of neurotransmission in the CNS. They determined that it was the only explanation which could support their observations of inhibitory post synaptic potentials (IPSP) during recordings of spinal cord stimulations (Brock et al., 1952).

As the foundational work on the synapse brought it into the center of the molecular neuroscience world, its importance in understanding brain function has only grown. A revolutionary discovery found that high frequency neurotransmission can induce long term changes increasing the synaptic efficacy with an effect lasting for hours (Bliss and Lømo, 1973). This observation was called long term potentiation (LTP) and provided the first evidence in support of Donald Hebb's theory on learning and memory. Hebb had stated that neurons which are concurrently active will undergo a change to increase the likelihood that they will further coordinate their activity – a mechanism now called Hebbian Plasticity (Hebb, 1949).

"When an axon of cell A is near enough to excite a cell B and repeatedly or persistently takes part in firing it, some growth process or metabolic change takes place in one or both cells such that A's efficiency, as one of the cells firing B, is increased" (Hebb, 1949)

Amazingly this concept had been postulated as early as the time of Cajal, but Hebb defined the rules and then Bliss and Lømo provided the key experiments to link the synapse to learning and memory (Sotelo, 2003). Further experiments have shown that different stimulation patterns are able to reverse LTP (Staubli and Lynch, 1990; Fujii et al., 1991), or reduce the basal synaptic strength through a process called long term depression (LTD) (Dudek and Bear, 1992). Together, the study of synapses through the years has revealed that they are very dynamic and now changes to their function are considered the locus of Donald Hebb's rules for learning and memory (Nicoll, 2017).

Through these mechanistic insights into the function of synapses it has also become apparent that many CNS diseases involve synaptic defects. Notably neurodevelopmental diseases such as autism have long been thought to arise due to defects in one or more synaptic proteins. The list of synaptic proteins linked to autism is extensive and includes the Shank family of scaffolding proteins (Monteiro and Feng, 2017), FMRP which regulate synapses through local control of translation (Contractor et al., 2015), PTEN and the TSC family of proteins which control cellular signaling (Auerbach et al., 2011; Zhou and Parada, 2012), and synaptic kinase CDKL5 (Weaving et al., 2004). A common factor among all of these proteins is that they regulate synaptic transmission and that mutations/deletions within their genes are associated with neurodevelopmental diseases (Heavner and Smith, 2020). In other instances, defective synapses are linked to neuropsychiatric diseases like epilepsy (Ben-Ari, 2010; Lachance-Touchette et al.,

2011) or neurodegenerative diseases such as Alzheimer's (Nisticò et al., 2012; Sheng et al., 2012). While this list is far from comprehensive, it begins to highlight the importance of understanding the role that individual proteins play in forming synapses and understanding the basic fundamentals of synapses in the hopes of also understanding how diseases develop. Knowledge of the molecular mechanisms regulating synapses can lead to better insight of the nature of disease. Moreover, studying diseases at the synaptic level can lead to greater understanding of both the basic function of a synapse while learning about the pathophysiology of the disease.

R.1.1 Synapse anatomy and physiology

Even though the synapse was generally well accepted from Sherrington's work, it was not until imaging experiments using electron microscopy on nervous system tissue was the presence of the synapse confirmed. Two independent groups: Sanford Palay and George Palade (Palay and Palade 1955; Palay, 1956), and de Robertis and Bennett (De Robertis and Bennett, 1955), confirmed and described the presence of the synapse as the interface between two neurons. Follow-up experiments have highlighted synaptic structures, including the presynaptic terminal which has an area called the active zone containing the vesicles filled with neurotransmitter ready for release (Südhof, 2012)(see Fig. R.1). On the other side of the synapse is the postsynaptic density (PSD) which consists of a number of structural proteins as well as receptors to respond to neurotransmitter release (Sheng and Kim, 2011). Helping to provide organization to the synapse are a number of trans-synaptic cell-adhesion proteins such as neuroligins, neurexins, netrin, cadherins, ephrin, and LRRTMs (Südhof, 2018). These help to ensure that synapses are targeted, developed, organized, or eliminated appropriately.

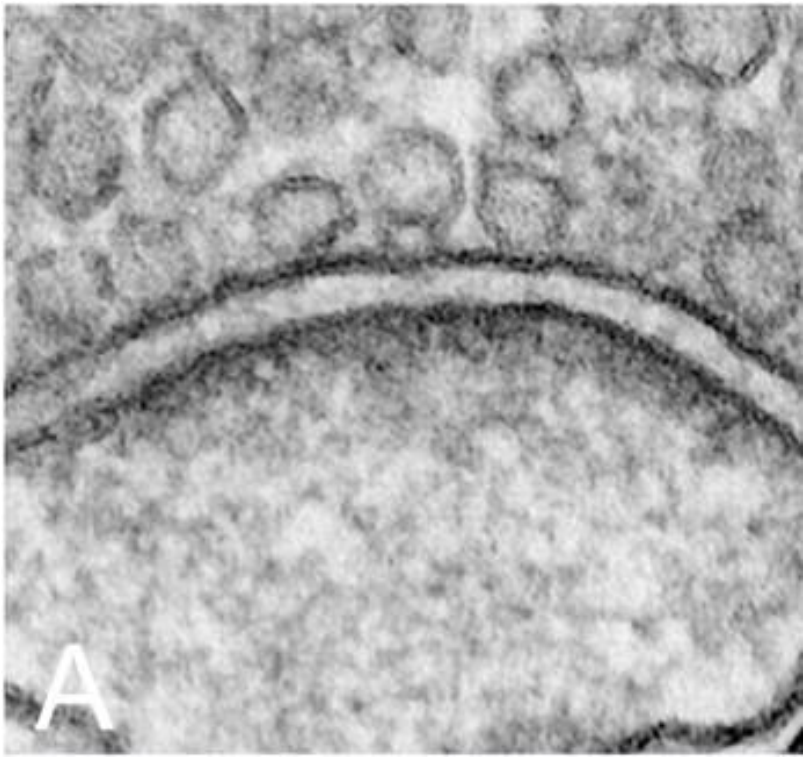

Figure R.1: Electron microscopy image of a chemical synapse
(A) An electron microscopy image from a hippocampal culture of a synapse. Note the synaptic vesicles on the presynaptic side (top), opposite of the dark post synaptic density which contains the receptor proteins (bottom). Reprinted with permission from (Chen et al., 2008)

While the basic description of a synapse, concerning the flow of information from the presynaptic to the postsynaptic cell, has remained relatively unchanged since Sherrington's time, the level of understanding about the mechanisms of neurotransmission have advanced significantly. Furthermore, changes to synaptic efficacy, also known as synaptic plasticity, have been extensively studied since the work of Bliss and Lømo. Researchers have uncovered the presence of pre and postsynaptic plasticity, revealing a rich set of mechanisms by which the brain is regulated. These neurophysiology concepts will be considered throughout this thesis and discussed at length in this literature review. Synaptic plasticity is a major theme in results Chapters 1 and 2, while Chapter 3 focuses primarily on synaptic integration.

R.1.2 Presynaptic physiology

The primary signaling unit of the nervous system is the action potential (AP) which propagates in the form of a rapid all or none electrical depolarization to the presynaptic terminal. The presynaptic terminal is a specialized structure which responds to the depolarization of the AP and releases neurotransmitter into the synaptic cleft – the space between the two neurons. This occurs through a series of sequential steps which was described by Bernard Katz and colleagues. They found that the release of neurotransmitter relied on the presence of Ca^{2+} (Fatt and Katz, 1952) and the amplitude of response corresponded to a minimum amplitude (quanta) which can sum into larger amplitudes if more units are released (del Castillo and Katz, 1954).

The presynaptic terminal is full of vesicles containing neurotransmitters – each one is thought to correspond to the quanta described by Katz. The sequence of presynaptic AP, to Ca^{2+} entry, to neurotransmitter release is incredibly fast – on the order of 10 µs (Sabatini and Regehr, 1996). Ca^{2+} concentration rapidly rises in the presynaptic terminal due to the high concentration of P/Q and N-type voltage gated Ca^{2+} channels in the presynaptic active zone (Südhof, 2012). Vesicle fusion and neurotransmitter release is facilitated by a complex set of proteins which respond to the entry of Ca^{2+} and support synaptic vesicle exocytosis. These proteins include the Ca^{2+} sensor synaptotagmin (Geppert et al., 1994), and a SNARE complex consisting of syntaxin-1A, SNAP-25, synaptobrevin-2/VAMP2 (Sutton et al., 1998). Together these form a structure which binds to both the plasma membrane and vesicle membrane. Ca^{2+} then binds to synaptotagmin which induces a conformational change leading to vesicle fusion with the plasma membrane, this occurs on a sub-millisecond timescale allowing for rapid neurotransmitter exocytosis (Zhou et al., 2017).

R.1.2.1 Presynaptic plasticity

Even though the presynaptic machinery described above is similar across neurons, different synapses respond in unique ways to AP patterns. The heterogeneous nature of synaptic release is due to different factors and synapses can also dynamically change their release probability. Depending on the synapse, the presynaptic vesicle release can be modulated by both short (Regehr, 2012) and long term changes (Castillo, 2012). Changes lasting for minutes or less are called short term presynaptic plasticity. They can be classified as either depression, if there is a reduction to the subsequent stimulations, facilitation, if there is a potentiation to the subsequent stimulations, or post-tetanic potentiation (PTP) if continued high frequency presynaptic activity leads to an increasingly larger current (Regehr, 2012). Long term presynaptic changes are also known as presynaptic long term potentiation (LTP) or long term depression (LTD) and occur due to changes in the probability of release or in the number of active release sites (Castillo, 2012).

R.1.2.2 Short term presynaptic plasticity

Short term changes to presynaptic release are dependent on presynaptic Ca^{2+} signaling (Burnashev and Rozov, 2005) and the availability of vesicle pools – also known as the readily releasable pool (RRP) (Kaeser and Regehr, 2017). Proposed models for short term depression have generally focused on the depletion of the RRP following trains of APs (Betz, 1970; Zucker and Regehr, 2002). A competing hypothesis suggests that contrary to the RRP hypothesis, short term depression is mostly caused by short term changes to Ca^{2+}entry into the presynaptic terminal (Catterall and Few, 2008). The primary evidence in support of this comes from the calyx of Held synapse where Ca^{2+}-induced inhibition of presynaptic Ca^{2+} channels are the cause of short

term depression. Moreover, in low Ca^{2+}conditions the synapse facilitates as Ca^{2+}-induced inhibition no longer occurs (Xu and Wu, 2005; Luo and Südhof, 2017).

Katz and Miledi hypothesized that short term synaptic facilitation was caused by residual Ca^{2+} in the presynaptic terminal which allows for a larger second Ca^{2+} signal if two incoming APs occurred within a short time of each other (Katz and Miledi, 1968). A key part of this hypothesis is that it requires a second Ca^{2+} sensor distinct from the sensor that triggers the initial fusion. Recent evidence has found a possible candidate for this second sensor. Different isoforms of synaptotagmin are critical for fulfilling both the role of triggering the initial fusion, and mediating synaptic facilitation (Chen and Jonas, 2017; Jackman and Regehr, 2017). Specifically synaptotagmin-1 and -2 are important for the initial vesicle fusion while synaptotagmin-7 is necessary for synaptic facilitation at cerebellar basket cell – Purkinje cell (PC) synapses (Chen et al., 2017), cerebellar granule cell synapses (Turecek and Regehr, 2018), PC – DCN synapses (Turecek et al., 2017), hippocampal Schaffer collateral (SC) – CA1, mossy-fibre (MF) – CA3, lateral-performant-path synapses in the dentate gyrus, and corticothalamic relay synapses (Jackman et al., 2016). Even at the short term depressing calyx of Held, synaptotagmin-7 is critical for a small basal current that underlies the peak current and contributes to high frequency synaptic transmission (Luo and Südhof, 2017). These studies also demonstrated the relationship between facilitation and depression as in the absence of facilitation (due to KO of synaptotagmin-7) the synapses all became depressing.

Synaptotagmin-7 works as a sensor for facilitation because it has very slow binding kinetics but binds Ca^{2+} with high affinity. Accordingly, it is hypothesized to bind to vesicles and boost the size of the RRP (Chen et al., 2017) while it has also been shown to contribute to a slower

asynchronous release (Bacaj et al., 2013; Turecek and Regehr, 2018). Importantly, the discovery of synaptotagmin-7 has revealed the mechanism by which residual Ca^{2+} contributes to facilitation and how both facilitation and depression can occur simultaneously and compete against each other.

R.1.2.3 Long term presynaptic plasticity

Long term changes to the presynaptic probability of release can last for hours or longer and occur at both excitatory and inhibitory synapses. The mechanisms underlying these can be entirely presynaptic in nature, involve retrograde signaling from the postsynaptic to presynaptic terminal or involve neighbouring cells (Monday and Castillo, 2017). Plasticity mechanisms which are entirely presynaptic typically involve a rise in intracellular Ca^{2+}, followed by a signaling cascade involving kinase/phosphatase activation. A model form of presynaptic plasticity is the MF-CA3 pyramidal neurons where cAMP/PKA activation leads to a long lasting increase in the probability of release and potentiation of the synapse (Nicoll and Schmitz, 2005). Similar mechanisms of potentiation involving cAMP/PKA have also been described in the subiculum (Behr et al., 2009), corticothalamic relay (Castro-Alamancos and Calcagnotto, 1999), and cerebellar parallel fiber (PF) synapses (Salin et al., 1996). Other signaling molecules which can induce presynaptic LTP include nitric oxide (NO) in the ventral tegmental area (VTA) (Nugent et al., 2007; Nugent et al., 2009) and brain-derived neurotrophic factor (BDNF) at the MF-CA3 synapse (Sivakumaran et al., 2009).

Many forms of presynaptic LTD involve activation of G protein-coupled receptors (GPCRs). Bidirectional LTD has also been shown at the MF-CA3 synapse (Kobayashi et al., 1996) which requires activation of $G_{i/o}$ through mGluR activation (Atwood et al., 2014). Another common form

of presynaptic LTD involves endogenous cannabinoid (eCB) signaling. Contrasting the induction of presynaptic LTP via NO (Nugent et al., 2007), midbrain dopaminergic neurons in the VTA experience presynaptic LTD following retrograde eCB signaling which inhibits presynaptic release (Pan et al., 2008; Haj-Dahmane and Shen, 2010). This also occurs in the striatum (Gerdeman et al., 2002) and neocortex (Sjöström et al., 2003) suggesting that this is a common mechanism in the CNS. Other mechanisms which have been described to induce presynaptic LTD include serotonin acting on 5-HT_{1b} receptors in the striatum (Mathur et al., 2011) and opioid signaling in the hypothalamus (Iremonger and Bains, 2009).

R.1.3 Postsynaptic physiology

As the presynaptic side of the synapse is specialized for releasing neurotransmitter, the postsynaptic side is primed to respond to the neurotransmitter. In general the postsynaptic membrane is made up of neurotransmitter receptors which are organized by a matrix of proteins to form the PSD (Sheng and Kim, 2011). Excitatory and inhibitory synapses have dramatically different PSDs which will be discussed in more depth in later sections. The majority of excitatory synapses are found on small specialized structures protruding from the dendrites called spines (Bourne and Harris, 2008). On the other hand inhibitory synapses are usually found on the dendritic shaft or soma (Sheng and Kim, 2011). Similarly to the presynaptic side, there are abundant plasticity mechanisms which occur in the postsynaptic side that effect the efficacy of synaptic transmission. For the next few sections I will go into more specific detail about the components of the postsynaptic membrane for excitatory and inhibitory synapses.

R.2 General introduction to excitatory synapses: glutamatergic signaling

In the simplest terms, excitatory neurotransmission can be described as a signal that increases the likelihood of a postsynaptic neuron to generate an AP. The synaptic response properties underlying excitatory neurotransmission were first studied at the neuromuscular junction (NMJ). With early recording techniques being relatively crude compared to modern electrophysiology, the large NMJ synapses and postsynaptic muscle were an attractive experimental preparation to study the nature of synapses. The first descriptions of excitatory neurotransmission were made at the frog sartorious, and cat soleus NMJs (Katz and Kuffler, 1941), and were referred to as the excitatory endplate potential (Eccles et al., 1941). Previous work had already identified that acetylcholine (ACh) release from the presynaptic neuron underlies the depolarization at the NMJ (Brown et al., 1936; Dale et al., 1936) which was then demonstrated to depolarize the membrane by a transient increase in ion permeability (Fatt and Katz, 1951). This was important evidence for an ion channel receptor.

As improvements in electrophysiology techniques allowed for recordings in central neurons it later demonstrated that excitatory depolarizations also occur in the CNS (Brock et al., 1952).Somewhat surprisingly, it was only much later that glutamate was generally accepted as the excitatory neurotransmitter in the brain. Glutamate is widely found throughout the brain (Berl and Waelsch, 1958) and elicits excitatory postsynaptic responses (Curtis et al., 1959). Nevertheless, glutamate was not considered a likely neurotransmitter because depolarized all neurons, suggesting it was nonspecific, and moreover, it was found in high concentrations throughout the brain (Curtis et al., 1960; Curtis and Watkins, 1960b). A few important discoveries cemented the role of glutamate as the main excitatory neurotransmitter in the CNS. Specifically,

the reuptake (Balcar and Johnston, 1972), and Ca^{2+} induced release of glutamate (Roberts, 1974), were the key observations which convinced neuroscientists that glutamate was a bonafide neurotransmitter.

The development of pharmacological tools helped identify specific functional subtypes of glutamate receptors which were eventually cloned and classified (Watkins and Jane, 2006; Lodge, 2009; Krnjević, 2010). Ionotropic glutamate receptors (iGluRs) can be classified into 3 families called α-amino-3-hydroxy-5-methyl-4-isoxazolepropionic acid (AMPA), kainate, and N-methyl- d-aspartic acid (NMDA) receptors based on the receptor responses to agonists (Traynelis et al., 2010). AMPA and NMDA receptors are the workhorse receptors and are the predominant mediators of excitatory synaptic transmission and synaptic plasticity in the CNS (Traynelis et al., 2010). On the other hand, kainate receptors (KAR) aren't as ubiquitously expressed and have different biophysical properties compared to AMPA receptors (Contractor et al., 2011). Their primary roles are to modulate postsynaptic excitability (Contractor et al., 2011) and modulate presynaptic neurotransmitter release (Pinheiro and Mulle, 2008).

There also exists a family of metabotropic glutamate receptors (mGluRs) which act on slower timescales by coupling up to G proteins (Niswender and Conn, 2010). Similar to KARs, the function of mGluRs are varied, and in large part depend on their subcellular localization. For instance, presynaptic mGluRs can increase or decrease the probability of release depending on the synapse (Pinheiro and Mulle, 2008). Activation of mGluRs in the spinal cord increase the probability of release (Cochilla and Alford, 1998), but at the inhibitory interneuron-CA1 synapses, mGluR activation inhibits vesicle release (Mannaioni et al., 2001). One of the most well studied forms of plasticity is the mGluR-dependent postsynaptic LTD. First described in cerebellar PCs,

this form of LTD occurs when climbing fibers (CF) are stimulated in conjunction with PFs and requires mGluR1 activation (Ito et al., 1982). A similar postsynaptic mGluR-dependent form of LTD occurs at CA1 pyramidal neurons but involves mGluR5 activation which is closely related to mGluR1 (Oliet et al., 1997; Huber et al., 2000). Interestingly, enhanced mGluR-dependent LTD has been heavily tied into the pathophysiology of the neurodevelopmental disease fragile X syndrome (Bear et al., 2004).

R.2.1 Excitatory postsynaptic density

As previously mentioned, excitatory AMPA receptor synapses are typically found on specialized dendritic compartments called spines (Bourne and Harris, 2008). Not surprisingly AMPA and NMDA receptors are especially concentrated at the PSD (Craig et al., 1993). The organization of these receptors relies heavily on the scaffolding proteins which make up the intracellular side of the PSD. Chief among these scaffolding proteins is PSD-95 (Cho et al., 1992) which directly binds to NMDAR through PDZ domains (Kornau et al., 1995). PDZ domains are modular protein interaction domains which recognize and bind to short motifs on other proteins (Kim and Sheng, 2004). AMPA receptors lack PDZ domains but are shuttled to the synapse through their interactions with trafficking proteins that contain PDZs (Sheng and Sala, 2001). These trafficking proteins include GRIP 1 and 2 (Dong et al., 1997; Dong et al., 1999), PICK1 (Xia et al., 1999), TARPs (Schnell et al., 2002), and SAP97 (Leonard et al., 1998).

R.2.2 AMPA receptors

The vast majority of excitatory neurotransmission in the mammalian brain is mediated by glutamatergic AMPA receptors. AMPA receptors, like all iGluRs, are tetrameric ion channels which are comprised of four different subunits which make up the family (GluA1 - GluA4)

(Traynelis et al., 2010). Each subunit maintains a similar structure which includes a large amino-terminal domain (ATD), a ligand binding domain (LBD), a transmembrane domain (TMD) and an intracellular carboxy-terminal domain (CTD) (Sobolevsky et al., 2009). The first full length AMPA receptor crystal structure revealed some interesting structural features in the quaternary structure. Most notable was that the protein assembles as a dimer of dimers, with subunits A and B forming one dimer unit, and C and D forming the other dimer unit. It was also found that the A and C subunit and B and D subunits occupy equivalent positions within the tetramer, but A/C and B/D interact differently with each other (Sobolevsky et al., 2009). Furthermore, it is interesting to note that while the structure has two-fold symmetry in the extracellular regions (ATD and LBD), there is a rearrangement of the structure for a four-fold symmetry in the TMD which forms the ion channel pore (Sobolevsky et al., 2009) (see Fig. R.2).

The four domains illustrated above give AMPA receptors important properties which can be modified. An alternative splice locus in the LBD called the flip/flop cassette (Sommer et al., 1990) changes many of the biophysical properties of the AMPA receptor including deactivation, desensitization, and sensitivity to allosteric modulators (Partin et al., 1996). Moreover the flip/flop cassette effects the resting state mobility of AMPA receptors (Dawe et al., 2019). Immediately adjacent to the flip/flow cassette is the “R/G” site which is an alternative splice variant effecting channel desensitization in GluA2-4 (Lomeli et al., 1994). A specific GluA2 subunit modification is the glutamine to arginine substitution which is at the narrowest segment of the pore and is known as the “Q/R” site (Sommer et al., 1991). It is estimated that almost all native GluA2 receptors are edited to arginine (Sommer et al., 1991). This editing makes GluA2 containing receptors somewhat special as they have different biophysical properties. Edited

GluA2 containing receptors have reduced rectification (Verdoorn et al., 1991) and lower Ca^{2+} permeability (Hume et al., 1991; Burnashev et al., 1992) when compared to unedited receptors. The mechanism underling AMPA receptor rectification was later found to be due to channel block by intracellular polyamines. Crucially, Ca^{2+} permeability is inversely related with polyamine induced rectification which is directly linked to the edited status of the "Q/R" site (Bowie and Mayer, 1995; Donevan and Rogawski, 1995; Kamboj et al., 1995). These basic differences in the AMPA receptor structure confer a wide range of possible functional response properties which have been observed in native tissue and are important for when considering how synapses function.

R.2.3 AMPA receptor auxiliary proteins

R.2.3.1 Stargazin and TARPs

While the AMPA receptor structure is complex in itself, native receptors are also adorned by a number of auxiliary subunits (Jackson and Nicoll, 2011). It is becoming abundantly clear that auxiliary proteins fill a critical role in AMPA receptor synaptic signaling as they are have been shown to be important for trafficking and modulating AMPA receptor channel properties. The first AMPA receptor auxiliary protein discovered was the transmembrane AMPAR regulatory protein (TARP) γ-2, also known as the stargazin protein. Stargazin was first observed as the result of a spontaneous mutation in the inbred stargazer mouse line. The stargazer mice were named after their head tossing and staring up at the stars but were also noted to have severe motor ataxia and seizures (Noebels et al., 1990). The underlying cause of this phenotype was mutations in the gene for what became known as the stargazin protein (Letts et al., 1998).

It was soon found that the stargazer mouse has almost a complete absence of AMPA receptor mediated excitatory postsynaptic currents (EPSC) in cerebellar granule cells. Meanwhile, NMDA receptor EPSCs are maintained demonstrating that presynaptic release of glutamate is functional and the deficit occurs due to poor postsynaptic AMPA receptor expression (Chen et al., 1999; Hashimoto et al., 1999). The reintroduction of stargazin was found to rescue functional AMPA receptor currents in granule cells and it forms a key interaction with AMPA receptors and PSD-95 (Chen et al., 2000b). An important structural element to the stargazin protein is its PDZ domains which targets it, and AMPA receptors bound to it, to PSD-95 in excitatory synapses (Schnell et al., 2002).

In addition to its role of receptor trafficking stargazin/TARP γ-2 has many roles modulating the biophysical properties of AMPA receptors. The first observations showed that γ-2 slows desensitization and deactivation, increases single channel open time, and increases kainate efficacy (Priel et al., 2005; Tomita et al., 2005). AMPA receptors interacting with γ-2 are also more likely to transition into a single channel high open probability mode (Zhang et al., 2014a), and have altered responses to common antagonists (Menuz et al., 2007) due to increased agonist affinity (MacLean and Bowie, 2011). Another key function of γ-2 is to relieve block by intracellular polyamines (Soto et al., 2007) by allowing polyamine permeation through AMPA receptors (Brown et al., 2017). These effects are imparted by at least two important interactions between γ-2 and AMPA receptors. First the gating properties such as desensitization were shown to rely on the 'KGK' motif on the LBD (Dawe et al., 2016) which was found to have a structural interaction with γ-2 (Twomey et al., 2016). The second site involves the intracellular C-tail of γ-2 which is crucial for the relief of polyamine block (Soto et al., 2014).

TARP γ-2 is part of the TARP family of proteins and each of the proteins in the family have interaction effects with AMPA receptors. These can be divided into two subgroups called Type-I TARPs which include γ2, γ3, γ4 and γ8 and Type-II TARPs which include γ5 and γ7 (Jackson and Nicoll, 2011). All Type-I TARPs generally have similar homology and introduction of them into cerebellar granule cells can rescue the stargazer AMPA receptor trafficking deficit (Tomita et al., 2003). They also impart qualitatively similar biophysical properties on AMPA receptors (Milstein et al., 2007). Type-II TARPs have a smaller intracellular region and consequently have less of an impact on AMPA receptors (Kato et al., 2007; Kato et al., 2008; Soto et al., 2009).

R.2.3.2 Other AMPA receptor auxiliary proteins

In addition to the TARP family of proteins, AMPA receptors also interact with other auxiliary subunits which confer different functional properties. Cornichon homologue proteins (CNIH-2 and CNIH-3) have similar effects as TARPs in that they dramatically slow channel deactivation and desensitization kinetics, and promote surface trafficking (Schwenk et al., 2009). Furthermore CNIH relieves polyamine block (Coombs et al., 2012) by increasing the permeability of polyamines through AMPA receptors (Brown et al., 2017). GSG1L is another AMPA receptor auxiliary protein with a similar homology to TARPs but slows desensitization and recovery from desensitization (Shanks et al., 2012) while increasing block by polyamines (McGee et al., 2015). An additional family of AMPA receptor auxiliary proteins is the CKAMP, or Shisa protein, family which include CKAMPs 39, 44, 52, and 59 (Farrow et al., 2015). CKAMP-44 speeds entry into and slows recovery from desensitization (von Engelhardt et al., 2010) which is crucial for of short term plasticity in the hippocampus (von Engelhardt et al., 2010; Khodosevich et al., 2014) and LGN relay neurons (Chen et al., 2018).

Excitatory signaling becomes increasingly complex when consideration is given to the number of combinations of AMPA receptors that can exist in nature. All of the possible alternative splice variants and associations with auxiliary subunits diversify AMPA receptors which ultimately endows the CNS to with specialized synaptic responses at different synapses. While the exact composition of native synapses is unknown for the vast majority of neurons in the brain, attempts to categorize them have been made by comparing synaptic responses to the responses of recombinant AMPA receptors with fixed configurations. These experiments were first carried out to differentiate the AMPA receptor subunits most likely expressed in native neurons. This was accomplished by comparing the kinetic properties of native pulled patches with those from recombinant data, while also considering mRNA expression patterns (Geiger et al., 1995; Koh et al., 1995). More recently this has been expanded to include auxiliary subunits in an attempt to map their expression patterns. Some studies of note have attempted to demonstrate the influence of auxiliary subunits on synaptic properties in the cerebellum (Dawe et al., 2019), hippocampus (Kato et al., 2010), and thalamic relay neurons (Chen et al., 2018).

R.2.4 NMDA receptor physiology

While the NMDA receptor is structurally closely related to the AMPA receptor, it is functionally quite different. Like the AMPA receptor, the NMDA receptor is a tetrameric ion channel which is formed from 7 different subunits: GluN1, GluN2A–GluN2D, GluN3A, and GluN3B (Traynelis et al., 2010) (see Fig R.2). Unlike other glutamate receptors, NMDA receptors are obligatory heterotetramers which are assembled from two GluN1 and two GluN2 or GluN3 subunits (Glasgow et al., 2015). They are commonly thought to be diheteromeric receptors which contain two GluN1 and two GluN2 subunits, but have also exist as triheteromeric receptors containing

two GluN1 subunits and two subunits of different identities (i.e. any of the GluN2 or GluN3 subunits) (Glasgow et al., 2015).

While considered an excitatory neurotransmitter receptor, NMDA receptors do not bind glutamate alone. Full activation of the receptor requires the presence of glutamate and either the co-agonist glycine (Johnson and Ascher, 1987) or D-serine (Mothet et al., 2000). Analysis of the activation kinetics in response to different concentrations of glutamate and glycine ligands revealed that NMDA receptors have two glycine and two glutamate binding locations (Clements and Westbrook, 1991). Subsequent work has revealed that glycine/D-serine binds to the GluN1 subunit while glutamate binds to all the GluN2 subunits (Hansen et al., 2018).

Several properties of NMDA receptors distinguish them from other glutamate receptors. NMDA receptors have a strong voltage dependent block by Mg^{2+} at negative membrane potentials (Mayer et al., 1984; Nowak et al., 1984). They also have slow deactivation kinetics (Forsythe and Westbrook, 1988; Lester et al., 1990) and high permeability to Ca^{2+} (MacDermott et al., 1986; Burnashev et al., 1992; Schneggenburger, 1996). The slow gating properties of NMDA receptors contribute to the slow synaptic response when observing an ensemble EPSC composed of both the fast AMPA and slow NMDA receptor responses (Hestrin et al., 1990; Sah et al., 1990; Geiger et al., 1997). Meanwhile, Mg^{2+} block and high permeability to Ca^{2+}, are important NMDA receptor properties which explain the induction requirements of LTP and LTD. In recent years, a novel metabotropic form of NMDA receptor activation has been discovered which does not require ion flux and adds even further diversity to this important signaling receptor protein (Nabavi et al., 2013; Dore et al., 2015).

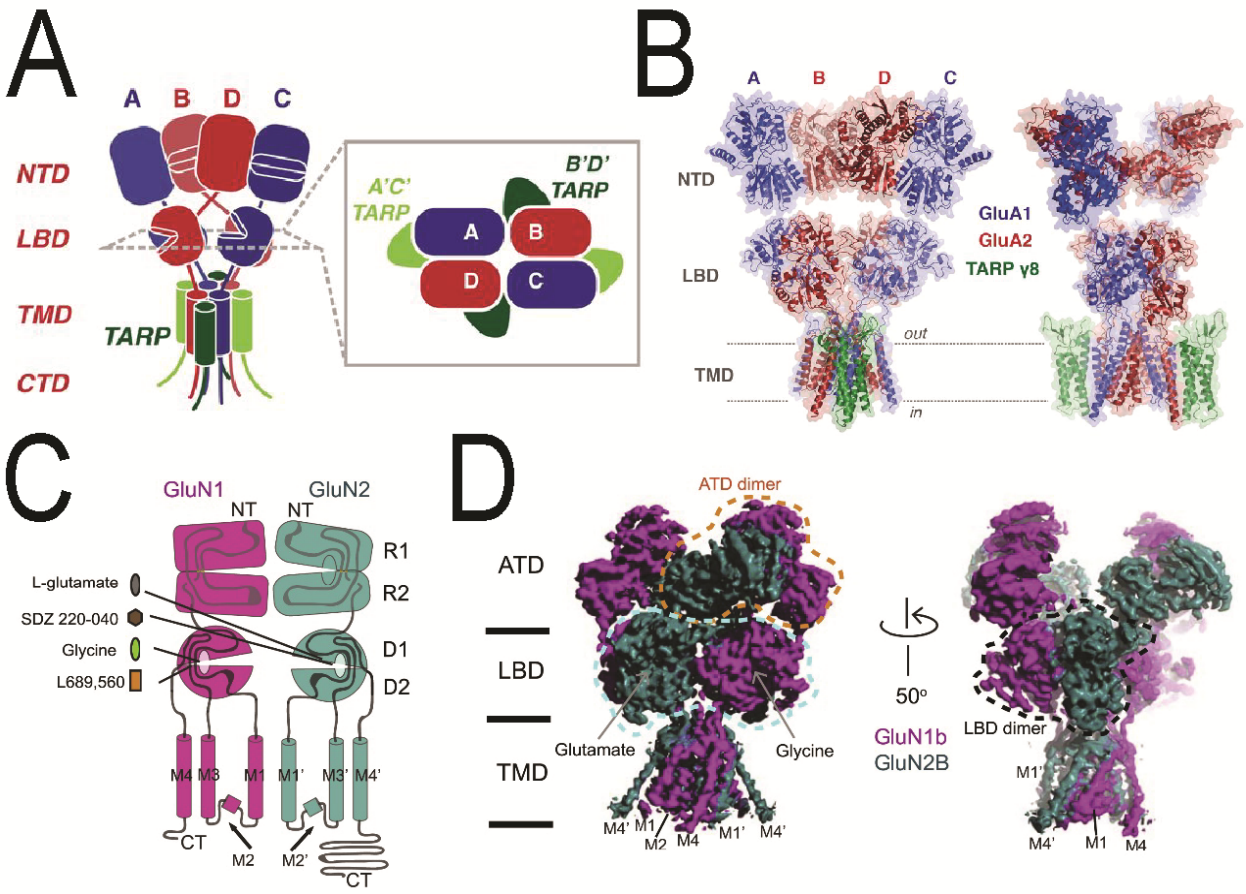

Figure R.2: Structure and organization of glutamate receptors
(A) Schematic of the AMPA receptor tetramer in complex with TARP auxiliary proteins. Identified are the four domain layers (NTD, N-terminal domain; LBD, ligand-binding domain; TMD, transmembrane domain; and CTD, C-terminal domain) as well as the position of the TARPs (green) located on either the A'C' or B'D' positions. (B) Structure of the atomic model for a heteromeric GluA1/2 receptor with TARP γ8 auxiliary subunits. Reprinted with permission from (Herguedas et al., 2019). (C) Organization of the domains of the NMDA receptor showing the NT (N-terminal domain) D1 and D2 lobes of the LBD, TMD, and CTD. Also illustrated are the glycine binding site with the specific blocker L689 and glutamate binding site with the specific blocker SDZ. (D) Cryo-EM density of heteromeric GluN1b/2B receptor. Reprinted with permission from (Chou et al., 2020).

R.2.5 Excitatory synapse plasticity: long term potentiation

As previously mentioned, synapses can be a very dynamic locale involving changes to synaptic efficacy. Synaptic plasticity is thought to be the basis for learning and memory and there is a great interest in uncovering the molecular mechanisms mediating these behaviours. For excitatory synapses, postsynaptic changes involve the insertion or removal of AMPA receptors from the

synapse which increases or decreases the overall strength of the EPSC response (Huganir and Nicoll, 2013). This involves post-translational modifications like phosphorylation which happen on the CTD of AMPA receptors. The CTD contains serine, threonine, and tyrosine residues which can be phosphorylated by PKA, PKC, PKG, CaMKII, FYN, and Src kinases (Lu and Roche, 2012; Diering and Huganir, 2018). The physiological activation of these kinases, and downstream functional consequences for synaptic signaling has been one of the most heavily researched fields in neuroscience.

R.2.5.1 Hippocampal CA1 NMDA receptor dependent long term potentiation

Research following Bliss and Lømo's initial descriptions of LTP (Bliss and Lømo, 1973) focused on identifying the induction pathway leading to LTP. A major finding showed that Ca^{2+} entry into the postsynaptic neuron is a key trigger for the induction of LTP (Lynch et al., 1983; Malenka et al., 1988). Additional experiments revealed that LTP induction requires simultaneous NMDA receptor activation and depolarization of the post synaptic neuron (Malinow and Miller, 1986; Gustafsson et al., 1987). The importance of NMDA receptors relies on two important biophysical properties. First, NMDA receptors are very permeable to Ca^{2+} (MacDermott et al., 1986; Ascher and Nowak, 1988) which is necessary for the induction of LTP (Lynch et al., 1983). Second, NMDA receptors are blocked by Mg^{2+} at negative membrane potentials and Ca^{2+} entry thus requires a depolarizing stimuli to occur simultaneously with the receptor activation (Mayer et al., 1984; Nowak et al., 1984). These properties of NMDA receptors thus explain the need for either a stimulus paired with a postsynaptic depolarization or tetanus stimulation to induce LTP (see Fig R.3).

Following NMDA receptor activation and Ca^{2+} entry, the induction of LTP then involves Ca^{2+}/calmodulin-dependent protein kinase II (CaMKII) activation (Malenka et al., 1989). CaMKII can be activated directly from rises to intracellular Ca^{2+} (Miller and Kennedy, 1986) and has been proposed to be a molecular switch for memory (Lisman and Goldring, 1988). Strengthening this line of thinking were observations which showed that CaMKII directly associates with NMDA receptors at the PSD (Leonard et al., 1999). While the induction mechanism up until this point has been generally agreed upon the expression mechanisms are still being worked out. In part, this is due to the complexity of the number of AMPA receptor phosphorylation sites and interacting proteins regulating receptor trafficking.

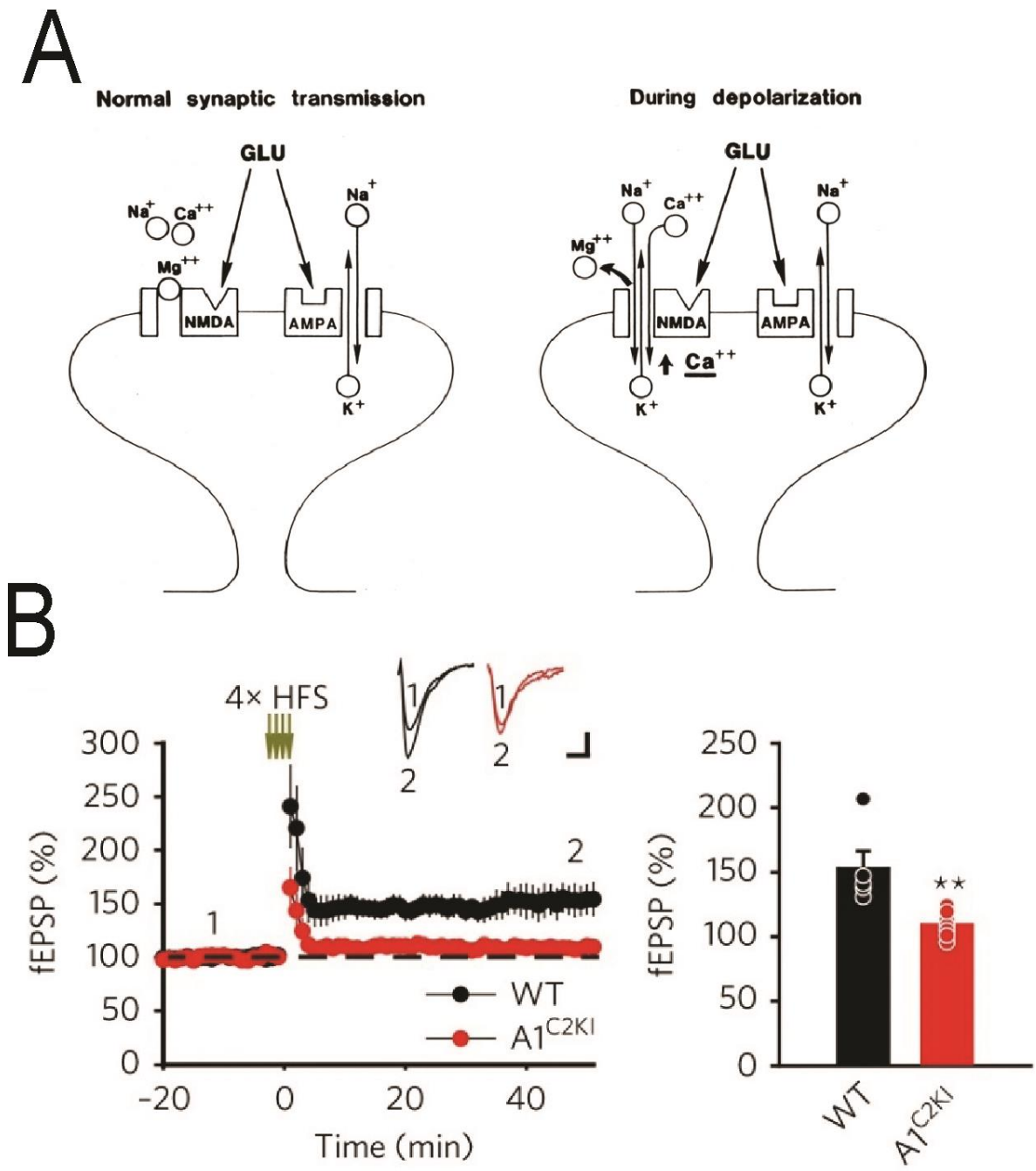

Figure R.3: Induction and expression of excitatory LTP requiring the GluA1 subunit
(A) Schematic of the induction protocol required for LTP. Note that LTP induction involves depolarization and removal of Mg^{2+} block of NMDA receptors. This causes an increase in intracellular Ca^{2+} acting as the trigger for LTP. Reprinted with permission from (Nicoll, 2017). (B) A high frequency stimulation (HFS) induction of LTP at CA1 pyramidal neuron synapses. Black traces represent WT experiments with a robust LTP response while red traces show a lack of LTP in neurons where the GluA1 C-tail has been substituted with the GluA2 C-tail. Adapted and reproduced with permission from (Zhou et al., 2018).

There has been an increasing number of proteins which have been deemed to be important to LTP, but most of them have focused on the GluA1 subunit in the expression of LTP. For instance mice were found to not express LTP if the GluA1 subunit is knocked out (Zamanillo et al., 1999) whereas they have enhanced LTP if GluA2 and GluA3 are knocked out (Meng et al., 2003). Furthermore, the expression of LTP involves the phosphorylation of residues on the CTD of GluA1 and mutations to those residues impair LTP expression (Lee et al., 2003). Together these observations led to the hypothesis that GluA1 containing receptors are inserted in the synapse during LTP (Kessels and Malinow, 2009). However, this hypothesis has been called into question as it has been shown that given a sufficient induction stimuli, and a large reserve pool of receptors, any AMPA or KAR combination is sufficient for the expression of LTP (Granger et al., 2013). A more recent study used a more subtle approach to replace the CTD of GluA1 with the CTD of GluA2. They found that while basal synaptic transmission is unchanged, LTP is completely lost (Zhou et al., 2018). Furthermore performing the reverse experiment and replacing the C-terminus of GluA2 with the C-terminus of GluA1 enhanced LTP expression. This work from Zhou and colleagues, and earlier work from (Zamanillo et al., 1999) and (Lee et al., 2003), demonstrate that the GluA1 CTD is a privileged domain for the expression of LTP in CA1 neurons. Accordingly it appears that under normal physiological conditions GluA1 plays an important role in the expression of LTP. When considering the body of work it is likely that there is some AMPA receptor redundancy and that any receptor can fulfill the role of LTP but different subunits are favoured to be recruited during LTP.

R.2.5.2 Other forms of LTP

So far I have highlighted LTP at the CA3-CA1 synapse as it has been the most well studied, but there are many other forms of LTP found elsewhere in the brain. For instance, the cerebellum has a different form of LTP where the induction and expression mechanisms are quite different from the hippocampus. Cerebellar LTP is non-associative and requires a sustained 1Hz stimulation of PF afferents (Lev-Ram et al., 2002). Furthermore this form of LTP is Ca^{2+} independent but requires the production of NO. Interestingly, PC LTP is expressed through an increase in the single channel conductance of GluA3 containing AMPA receptors (Gutierrez-Castellanos et al., 2017). It has also been argued that similar mechanisms occur in hippocampal CA1 pyramidal neurons adding further complexity to the story of LTP (Renner et al., 2017).

Another form of LTP that has been well studied is between the VTA and nucleus accumbens (NAc). This is part of the mesolimbic system and has been studied for its role in maladaptive behaviours such as addiction. The VTA-NAc synapse undergoes an NMDA receptor dependent LTP (Thomas and Malenka, 2003). Drugs of abuse associated with addiction such as cocaine (Ungless et al., 2001), amphetamine, opioids, and alcohol (Saal et al., 2003) can also trigger LTP at this synapse. Induction of LTP at the VTA-NAc synapse requires concurrent dopamine release and NMDA receptor activation (Cahill et al., 2014). Interestingly, VTA-NAc LTP preferentially occurs at the VTA-D1-medium spiny neuron of the NAc and involves insertion of GluA2 lacking receptors (Terrier et al., 2016).

This review is far from comprehensive for all the brain regions and forms by which LTP occurs, but instead illustrates some of the more common forms of LTP to provide a sample of how diverse the mechanisms of the brain are. Many of the mechanisms underlying LTP at

different synapses are shared, such as the need for NMDA receptor activation, but each synapse has slightly different rules which makes them unique. Accordingly, a careful dissection of the mechanisms underlying plasticity can yield interesting insights into neurophysiology and also the pathophysiology of disease. Insights like these are important for the results which I present in Chapters 1 and 2.

R.2.6 Long term depression

Long term depression (LTD) of synaptic signaling is the opposite of LTP which together forms a bidirectional switch regulating synaptic strength. While LTD is relatively less well studied compared to LTP, it has an important functional role in reducing synaptic strength in the CNS. LTD was first described in the cerebellum at PF–PC synapses, and is a key component of cerebellar motor learning (Ito et al., 1982). Induction of PC LTD occurs when CF stimulation is paired with PF stimulation and requires mGluR1 activation. There is also a well-studied form of NMDA receptor dependent LTD at the hippocampal CA3-CA1 synapse (Dudek and Bear, 1992) as well as a mGluR5 dependent LTD (Huber et al., 2000; Huber et al., 2001). Both mGluR- and NMDA receptor dependent LTD have been characterized in nearly all brain regions including the amygdala, neocortex (all layers), hypothalamus, striatum, midbrain, brain stem and spinal cord (Collingridge et al., 2010). The following sections will briefly describe the molecular mechanisms for some of the more well studied forms of LTD.

R.2.6.1 Cerebellar Purkinje cell long term depression

Cerebellar LTD is a form of spike-timing-dependent plasticity (STDP) and relies on precise timing of the concurrent inputs of two different synapses. The paired PF and CF induction stimulation of cerebellar LTD relies on mGluR1 receptor activation, Ca^{2+} entry through voltage-gated Ca^{2+}

channels, and PKC activation. Experiments implicating the role of mGluR1 in the induction pathway revealed that mice with mutant mGluR1 (Alba et al., 1994), mGluR1 KO mice (Conquet et al., 1994), or antibodies blocking mGluR1 activation (Shigemoto et al., 1994) had impairments in cerebellar LTD and notable deficits in motor learning. Ca^{2+} entry was also implicated from experiments chelating intracellular Ca^{2+} which disrupted LTD (Sakurai, 1990), and observations that LTD requires both extracellular Ca^{2+} and a depolarizing stimulus to activate voltage-gated Ca^{2+} channels (Linden et al., 1991; Konnerth et al., 1992). LTD in PCs also requires proteins such as stromal interaction molecule 1 (STIM1), to properly regulate Ca^{2+} levels (Hartmann et al., 2014). Furthermore, several groups have also demonstrated the importance of PKC in this pathway by using PKC specific pharmacology to block or stimulate LTD (Linden and Connor, 1991), or using transgenic inhibition of PKC to block LTD (De Zeeuw et al., 1998). Finally there is an important role for protein translation in the induction of mGluR dependent LTD involving an intracellular ERK signaling pathway (Ito-Ishida et al., 2006). The protein translation dependent nature of mGluR-dependent LTD is found in other brain regions and is known to be one of the key defects in the neurodevelopmental disease fragile-X syndrome (Bear et al., 2004).

Recently, the rules for the induction of mGluR-LTD have been found to be more complex than the initial descriptions. There is a difference in sensitivity to the associated timing rules for concurrent PF and CF activation in the induction of LTD across the cerebellum (Suvrathan et al., 2016). Different areas of the cerebellum, such as the floccus or vermis, have different STDP tuning requirements which closely match their expected physiological input frequencies (Suvrathan et al., 2016). Moreover, increasing inhibition by activation of molecular layer interneurons (MLI) changes the expression of LTD into LTP by regulating Ca^{2+} entry into PC dendrites (Rowan et al.,

2018). Accordingly, it should be noted that the induction of LTD is likely quite different when considering the whole cerebellar circuit rather than just the concurrent activation of the PF and CF synapses.

The expression of cerebellar LTD involves phosphorylation of the GluA2 subunit which is subsequently internalized through endocytosis. This occurs due to a PKC phosphorylation on the GluA2 CTD which limits its interaction with GRIP1, and maintains binding to PICK1 which promotes internalization (Matsuda et al., 1999; Chung et al., 2000; Chung et al., 2003). Later studies have confirmed the role of these proteins as targeted PC deletions of either PICK1 (Steinberg et al., 2006) or GRIP1/2 (Takamiya et al., 2008) to prevent PC LTD.

R.2.6.2 Hippocampal LTD

There are two other notable forms of LTD which have been described at the CA3-CA1 synapse in the hippocampus. They can be broken down by their induction mechanisms, with one mechanism involving Group I mGluRs (mGluR1 and mGluR5) activation, and the other NMDA receptor activation. Interestingly, both of these mechanisms rely on the same neurotransmitter, glutamate, but released at different frequencies. While these two mechanisms have been explored beyond the hippocampus in the rest of the brain, they have been most extensively studied at the CA3-CA1 synapse and this section will accordingly focus primarily on the mechanisms underlying the hippocampal LTD mechanisms (Collingridge et al., 2010).

R.2.6.2.1 NMDA receptor dependent LTD

NMDA receptor dependent LTD was first observed in response to a continual low frequency (900 pulses at 1-3Hz) stimulation of SC–CA1 pyramidal neuron synapses (Dudek and Bear, 1992). The first mechanistic insights into NMDA receptor dependent LTD found that chelating Ca^{2+} with high

concentrations of BAPTA eliminated LTD expression. A follow up study implicated the activation of the phosphatase calcineurin downstream of Ca^{2+} entry as a critical step in LTD (Mulkey et al., 1994). LTD expression then requires receptor internalization following post translational modifications (PTM) on AMPA receptors. Similar to LTP, the CTD of AMPA receptors are targets for these PTMs, which are necessary for the receptor internalization occurring during LTD (Diering and Huganir, 2018). Specifically, dephosphorylation of serine 845 occurs during LTD (Lee et al., 1998) and mutations at this residue are associated with defects in the expression of LTD (Lee et al., 2010).

An interesting question emerges when considering that both LTP and LTD rely on intracellular Ca^{2+} signaling through NMDA receptors. How do neurons differentiate an LTP from an LTD signal if they involve the same intracellular messenger pathway (NMDA receptor/Ca^{2+})? To address this question, it has been proposed that the low Ca^{2+} affinity CaMKII can only be properly activated to stimulate LTP when there is a relatively large Ca^{2+} influx. Conversely, calcineurin is a high affinity Ca^{2+} binding protein which can respond best to a smaller increase in intracellular Ca^{2+} (Lisman, 1989; Malenka and Bear, 2004). Therefore, the proposed difference arises due to the intensity of the Ca^{2+} signal in the postsynaptic neuron whereby a sufficiently strong input will reach the Ca^{2+} threshold needed to activate CaMKII.

In the last few years there have been experiments that have directly challenged the mechanism outlined above. Experiments have revealed that MK-801 (pore channel blocker of NMDA receptors), and 7-chlorokynurenate (7CK, a glycine site specific blocker of NMDA receptors) do not prevent NMDA receptor dependent LTD (Nabavi et al., 2013). These results demonstrate NMDA receptors act in a metabotropic manner without ion flux. Follow-up studies

have revealed that this mechanism relies on movement occurring in the intracellular CTD of the NMDA receptor GluN2 subunits (Dore et al., 2015). Metabotropic NMDA receptor activation has also been shown to induce LTD in other brain regions (Carter and Jahr, 2016) and found to induce dendritic spine shrinkage (a correlate of LTD) (Stein et al., 2015). While these results seem to be difficult to reconcile with the literature demonstrating a need for ion flux (Babiec et al., 2014; Volianskis et al., 2015; Sanderson et al., 2016), there is a new model proposed suggesting that PSD-95 expression levels determine if ion flux dependent or independent NMDA receptor dependent LTD occurs (Dore and Malinow, 2020). Ion-flux independent NMDA receptor LTD does not occur at mature synapses or those with high levels of PSD-95, which could explain the differences in NMDA receptor dependent LTD findings (Dore and Malinow, 2020).

R.2.6.2.2 mGluR dependent LTD

While both mGluR and NMDA receptor dependent LTD occur at the hippocampal SC-CA1 synapse, the induction patterns are quite different. There were two early stimulation protocols which induced mGluR-dependent LTD. One protocol delivered a 5 Hz stimulation for 3 minutes (Oliet et al., 1997) and another was a paired pulse protocol (50ms inter-pulse interval) performed at 1hz for 15 mins (Huber et al., 2000). The second protocol has also been demonstrated to be comparable to direct mGluR5 activation by chemical agonists (Huber et al., 2001). Both stimulation protocols activate mGluR5 receptors and cause a long lasting internalization of AMPA receptors in the presence of NMDA receptor antagonists. Downstream signaling from mGluR activation is quite different in the hippocampus compared to the cerebellum. In response to mGluR5 activation, AMPA receptor internalization occurs due to activation of a tyrosine phosphatase and dephosphorylation of GluA2 (Moult et al., 2006; Gladding et al., 2009).

Unlike NMDA receptor dependent LTD, mGluR dependent LTD requires post synaptic protein synthesis (Huber et al., 2000). Translation is initiated downstream of mGluR activation through ERK-MAPK (Gallagher et al., 2004) and PI3K-mTOR pathways (Hou and Klann, 2004). These two pathways converge during mGluR LTD to stimulate new protein synthesis (Banko et al., 2006). AMPA receptor internalization is then maintained through rapid synthesis of Arc which maintains a persistent AMPA receptor endocytosis rate (Waung et al., 2008). Furthermore proper temporal dynamics of Arc expression are critical for mGluR-dependent LTD as well as hippocampal learning (Wall et al., 2018).

R.2.7 Homeostatic synaptic scaling

Thus far this review has focused on describing LTP and LTD which form the Hebbian plasticity mechanisms, however there is another form of plasticity called synaptic scaling. Synaptic scaling addresses a fundamental problem that arises from the associative nature of Hebbian plasticity. As Hebbian plasticity increases the strength of synapses, it risks starting a positive feedback process of increasing circuit excitability and leading to further unconstrained LTP (Turrigiano, 2008). On the other hand, homeostatic plasticity, or synaptic scaling, prevents destabilizing runaway LTP by globally reducing overall synaptic strength to reduce excitability (Turrigiano, 2008). The effect of synaptic scaling is to increase the global EPSC amplitude in response to chronic low activity (experimentally by blocking activity with either TTX or AMPA receptor antagonists) or decrease the global EPSC amplitude in response to chronic high activity (experimentally by blocking inhibition) (Turrigiano et al., 1998). Induction of homeostatic plasticity has been described in response altering cellular or network firing rates both *in vitro*

(Turrigiano et al., 1998; Burrone et al., 2002) and *in vivo* (Hengen et al., 2013; Keck et al., 2013; Barnes et al., 2015b).

There are a wide range of induction mechanisms that have been attributed to synaptic scaling. BDNF was an early molecule which was linked to homeostatic plasticity. Interestingly, BDNF was found to have opposite effects on inhibitory interneurons and excitatory pyramidal neurons demonstrating a circuit level effect for balancing excitation-inhibition (Rutherford et al., 1998). Another secreted molecule which stimulates synaptic scaling is the cytokine tumour-necrosis factor-α (TNF-α). TNF-α release from glia increase the surface trafficking of AMPA receptors and decrease the surface levels of inhibitory $GABA_A$ receptors (Beattie et al., 2002). Furthermore TNF-α is released during TTX induction of synaptic scaling and blocking TNF-α signaling prevents homeostatic plasticity but does not affect Hebbian plasticity in hippocampal cultures (Stellwagen and Malenka, 2006). New protein synthesis of activity-induced genes also play an important role in homeostatic plasticity. In response to hyperactivity Arc protein expression is induced (Shepherd et al., 2006) and increased AMPA receptor internalization occurs (Chowdhury et al., 2006) during a process called down scaling. Similar to Hebbian plasticity, synaptic scaling occurs throughout the brain and often has conserved mechanisms (Keck et al., 2017). Together, Hebbian and homeostatic plasticity provide the major mechanistic insights into how learning and memory in the CNS can occur and maintain stability.

R.3 General Introduction to inhibitory synapses: GABA and Glycine

As the name suggests, the role of inhibition is to limit activity in the central nervous system. More specifically, at the neuronal level activation of an inhibitory synapse reduces the likelihood that the postsynaptic neuron will generate an AP. Until the end of the first half of the 20th century, there was uncertainty about the existence of inhibition. A prominent early advocate for the existence of inhibition was Sherrington who suggested that different parts of the brain are likely to inhibit another part (Sherrington, 1906). Conversely, Cajal had largely ignored any role for inhibition in his work (Ramon y Cajal, 1911) and this idea was shared by others who thought did not generally accept inhibition in the CNS during the first half of the 20th century (Fulton, 1951). Proper descriptions of synaptic inhibition came from Eccles and colleagues, who published a series of papers in the 1950s describing inhibition and the ionic currents underlying the IPSP at the motor-neuron junction (Brock et al., 1952; Coombs et al., 1955). Subsequently, others showed that this type of signaling occurs in the CNS which firmly established a role for inhibitory synaptic signaling (Phillips, 1959; Stefanis and Jasper, 1964).

In contrast to excitation, inhibition in the CNS is typically mediated by many different types of local interneurons modulating the activity of principal neurons (Pelkey et al., 2017). Accordingly, there is a great diversity in the physiological effects of inhibition on the postsynaptic neuron. Some of the physiological purposes of inhibition is to filter synaptic inputs, and to modulate gain, tuning and firing properties of the post synaptic neuron (Isaacson and Scanziani, 2011; Roux and Buzsáki, 2015). There is a diverse cast of interneurons in the CNS which each play a role in producing these effects. These interneurons are generally grouped in three classes: paravalbumin (PV), somatostatin (SOM), or 5-HT3a expressing interneurons (Rudy et al., 2011).

Their function is largely dictated by their anatomical and physiological properties as well as their post-synaptic targeting (Pelkey et al., 2017). For example, PV basket cells primarily targeting somatic or perisomatic synapses and strongly inhibit postsynaptic firing whereas SOM interneurons target dendrites and inhibit a local dendritic branch (Chiu et al., 2019)

Further variety in inhibitory signaling comes from the expression patterns of the postsynaptic receptors. In the nervous system, most inhibitory signaling occurs through either GABAergic (in the brain) or glycinergic (in the spinal cord and periphery) neurotransmission (Olsen and DeLorey, 1999). Both of these signaling molecules act through their respective receptors to generate an IPSP. $GABA_A$ receptors ($GABA_ARs$) and glycine receptors (GlyRs) are ionotropic receptors permeable to anions and their currents are primarily due to Cl^- or HCO_3^- flux (Curtis and Watkins, 1960a; Krnjević and Schwartz, 1967; Werman et al., 1967). Additionally there are another class of GABA receptors called $GABA_B$ receptors ($GABA_BRs$) which exert their inhibitory effects via a K^+ conductance (Bowery et al., 1980) through a G-protein mechanism (Nicoll, 1988).

R.3.1 The history of GABAergic signaling

The observation of inhibitory signaling in the CNS (Phillips, 1959; Stefanis and Jasper, 1964) had left a big question on the identity of the chemical neurotransmitter. Early neurochemistry experiments demonstrated that the chemical γ-aminobuteryic acid (GABA) is inhibitory (Hayashi and Nagai, 1956; Kuffler and Edwards, 1958), and is widespread in the CNS (Awapara et al., 1950; Roberts and Frankel, 1950; Udenfriend, 1950) hinting that it could be the inhibitory chemical neurotransmitter. Seminal work in 1967 firmly established GABA as the predominant inhibitory neurotransmitter in the CNS by demonstrating that direct GABA application stimulates the same

currents as a synaptic evoked IPSP in cortical neurons (Krnjević and Schwartz, 1967). In the following years, there has been a great deal of research which has uncovered the nature of GABAergic signaling from its release to the properties of its receptors.

Some of the early research on the molecular aspects of inhibitory signaling focused on identifying the proteins involved in GABAergic signaling. These investigations found a critical role for the protein GAD in the metabolic pathway in the synthesis of GABA (Wu et al., 1973). Electron microscopy evidence found GAD located at presynaptic terminals which supported a role for GABA in inhibitory neurotransmission (McLaughlin et al., 1974). Later experiments identified the presence and amino acid sequence of two forms of GAD. First, GAD67 was identified (Kaufman et al., 1986; Kobayashi et al., 1987) and then GAD65 (Erlander et al., 1991) which were eventually tied into two separate genes (GAD1 and 2 respectively) (Bu et al., 1992). While both forms of GAD are known to produce GABA, they have distinct roles. Not surprisingly, both GAD65 and GAD67 have fairly similar amino acids in their catalytic domain but they have quite unique sequences in the domains responsible for subcellular targeting, membrane interaction, and protein regulation (Soghomonian and Martin, 1998). GAD65 is localized to presynaptic terminals and produces GABA for neurotransmission while GAD67 is found throughout the cell and is involved in general metabolism in neurons (Soghomonian and Martin, 1998). These roles do not appear to be redundant as GAD65 KO mice have poor inhibitory synaptic transmission (Hensch et al., 1998; Tian et al., 1999).

Much like AMPA receptors, the classification of GABA receptors has benefited greatly from advances in pharmacology. Two major classes of GABA receptors have been identified since the discovery of drugs which specifically block the GABAergic IPSP. First are the $GABA_A$ receptors

which are blocked by bicuculline, picrotoxin, and gabazine (Takeuchi and Takeuchi, 1969; Curtis et al., 1971; Ueno et al., 1997) and generate an IPSP due anion permeation. Second are the $GABA_B$ receptors which are quite different in both structure and function to the $GABA_A$ receptors. $GABA_B$ receptors generate an IPSP by a K^+ conductance and are blocked by baclofen but not any of the traditional $GABA_A$ receptor blockers (Bowery et al., 1980; Hill and Bowery, 1981).

Concurrent with the initial descriptions of the receptors were discoveries that showed how important clinical drugs modulate the effects of $GABA_A$ receptors. The barbiturate class of drugs had long been prescribed as a anticonvulsant, sedative, and anesthetic, and in the 1970s their mechanism of action was found as an allosteric modulator of $GABA_A$ receptors (Macdonald and Barker, 1978). Around the same time, the benzodiazepine class of drugs were shown to similarly modulate $GABA_A$ receptor function (Choi et al., 1977), but in a subunit selective manner and affecting only a subset of synaptic $GABA_A$ receptors (Lüddens and Wisden, 1991; Smith and Olsen, 1995). This provided a useful early tool to study diversity in $GABA_A$ receptor expression and has ultimately been an important consideration for the classification of $GABA_A$ receptors (Olsen and Sieghart, 2008). As modern techniques have developed, the study of $GABA_A$ receptors has revealed a rich diversity of ion channel function and plasticity mechanisms which regulate inhibitory signaling in the CNS.

R.3.2 $GABA_A$ Receptors: Structure and Function

GABAergic signaling is incredibly diverse in part because of the number of different subunits which can makeup functional post synaptic receptors. The ionotropic $GABA_A$ receptor is a member of the Cys-looped family of ion channels which include the nicotinic acetylcholine receptor (nAChR), GlyR, and 5-HT3 receptor, all of which share a similar pentameric structure

(Miller and Smart, 2010). The first cloning studies and comparative sequence analysis of the Cys-loop ion channels revealed similar architectural features. From the primary amino acid sequence it was found that they all possess the same cystine residues which form cys-loops and give the family its name. Moreover they were all predicted to have similar 4 transmembrane helices (Barnard et al., 1987). Further cloning and genomic analysis of the $GABA_A$ receptors revealed that humans have genes encoding 19 different subunits; α1-6, β1-3, γ1-3, δ, ε, θ, π, and ρ1-3 (Simon et al., 2004). Alternative splicing provides additional variety in $GABA_A$ receptors and the most notable splice variant being the γ2 short/long (γ2S/ γ2L) form (Olsen and Sieghart, 2008).

Despite the abundance of subunits, which theoretically could combine to make thousands of different $GABA_A$ receptors, it appears that $GABA_A$ receptors only exist in limited varieties. Only 36 distinct subtypes have been found or predicted to be found in nature (Olsen and Sieghart, 2008; Fritschy and Panzanelli, 2014). *In vivo* $GABA_A$ receptors typically assemble as heteropentameric channels with a two α, two β and γ subunit stoichiometry (Sigel and Steinmann, 2012). A notable exception to this rule is the $GABA_A$ ρ subunit (formerly referred to as the $GABA_C$ class), which makes functional homopentameric channels (Zhang et al., 2001). Based on mRNA expression, the α1, β2 and γ2 are the most ubiquitous subunits in the adult brain (Laurie et al., 1992b; Laurie et al., 1992a; Poulter et al., 1992; Sur et al., 2001) and are thought to form the most common $GABA_A$ receptor which is arranged in an α/β/α/β/γ stoichiometry (Olsen and Sieghart, 2008; Sigel and Steinmann, 2012) (see Fig. R.4). In the next few sections I will delve deep into the GABAA receptor structure-function world. This is inspired by some recently published papers with new structural insight which expands our knowledge of the function of GABA receptors.

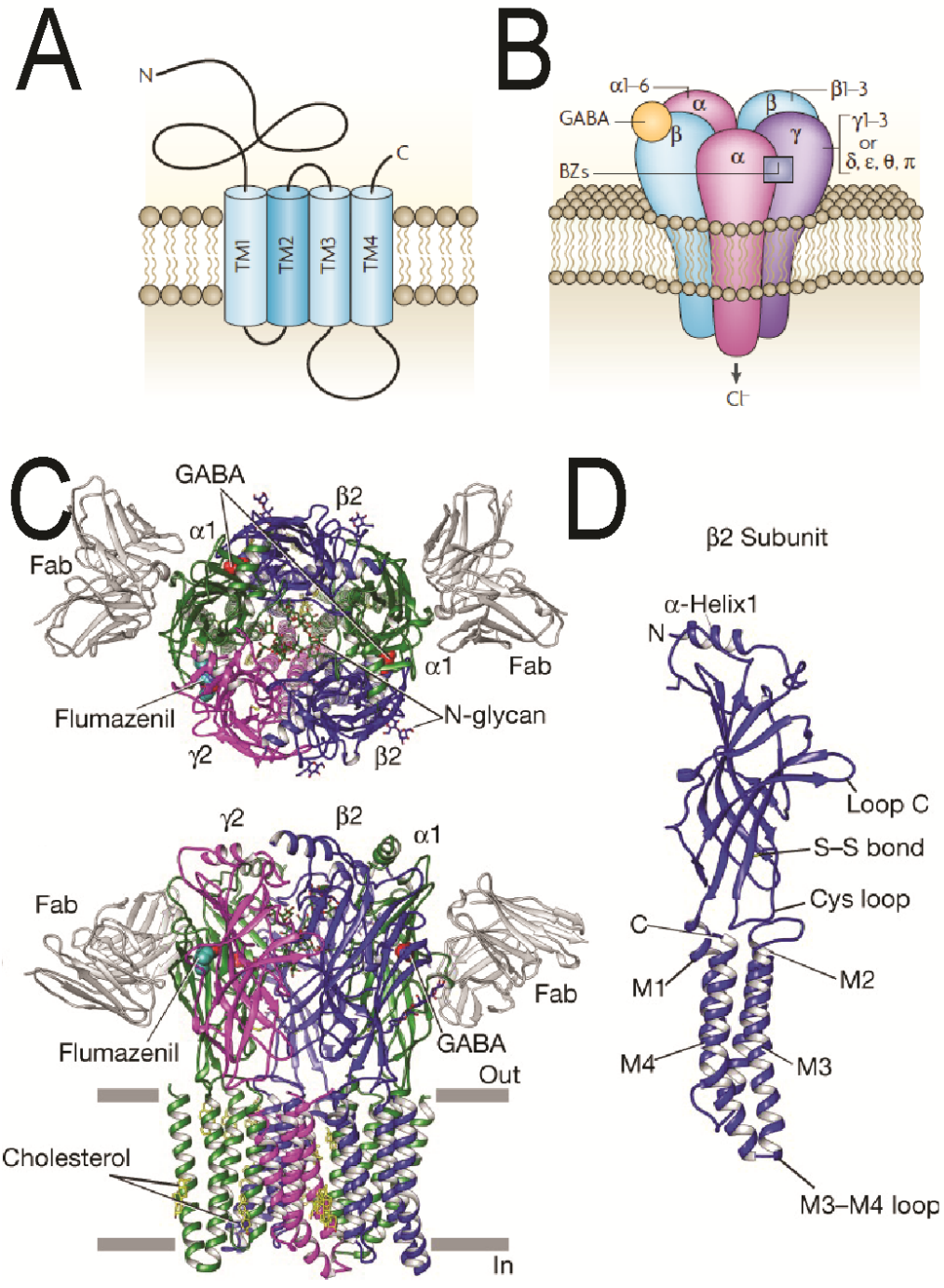

Figure R.4: Structure of a GABAA receptor

(A) Cartoon structure of one of the subunits for the Cys-loop family of ion channels. The 4 transmembrane domains (TM1-4) are identified as well as the large extracellular loops. (B) Cartoon of the assembly of the pentameric $GABA_A$ receptor structure found in the common α/β/α/β/γ arrangement with all of the possible subunits also identified. The GABA and benzodiazepine (BZ) binding sites are labeled. Reprinted with permission from (Jacob et al., 2008). (C) Structure of the atomic model for a human $GABA_A$ receptor

(α1/β2/γ2) in complex with Fab tags. GABA is shown in its binding pocket as a red sphere while flumazenil is found in the BZ binding pocket as a cyan sphere. (D) Atomic model of the structure for a single β2 subunit. Reprinted with permission from (Zhu et al., 2018b)

R.3.2.1 $GABA_A$ Receptor Structure

Structurally, $GABA_A$ receptors are quite different from AMPA receptors. Like all Cys-loop receptors, $GABA_A$ receptors are pentameric ion channels. Each subunit of the Cys-loop family is similar and are made up of a large extracellular domain (ECD) of 200-250 amino acids, 4 α-helical TMDs (M1-4), a longer intracellular loop between M3 and M4, and an extracellular c-terminus (Karlin and Akabas, 1995). The ECD includes the cys-loop, and is then primarily made up of amino acids arranged in 10 β-strands (Miller and Aricescu, 2014). These β-strands in the ECD form the GABA binding pocket which is found at the two β and α interface of subunits (Zhu et al., 2018b). The ion channel pore and gate is formed by the 5 M2 α-helices of each subunit. Most of the $GABA_A$ receptor PTMs occur in the long intracellular domain between M3 and M4 (Moss and Smart, 1996; Nakamura et al., 2015). At the narrowest part of the ion channel near the cytoplasm is the selectivity gate which is determined by the amino acids facing into the pore (Miller and Smart, 2010).

One of the major advantages afforded to the study of $GABA_A$ receptors, and Cys-loop ion channels, is the significant structural homology shared within the family (Olsen and Sieghart, 2008). The first structural insights came from high resolution images of the extracellular regions of the mollusc acetylcholine binding protein (AChBP) receptor (Brejc et al., 2001). While this structure was not full length, it provided good resolution of the N-terminal extracellular hydrophilic region containing the ligand-binding domain and the important complimentary subunit interactions. Specifically the paper identified the 6 key loops formed by β-strands naming

them loop A-F, with loops A, B, and C coming from the principal subunit and D, E, and F from the complimentary subunit (Brejc et al., 2001). A follow up crystal structure of the same protein illustrated a ligand bound receptor identifying the key aromatic amino acids on loop B which provided the principal cation-π binding site (Celie et al., 2004).

Mutagenesis and electrophysiology experiments suggested that there are similar cation-π binding site on the $GABA_A$ ρ subunit (Lummis et al., 2005) which is unique among $GABA_A$ receptors in that it makes functional homodimers (Zhang et al., 2001). The principal aromatic residue responsible for the cation-π interaction of GABA with the $GABA_A$ receptor was hypothesized to be Tyr97, found on loop A of the β subunit (Padgett et al., 2007). However, three recent full length $GABA_A$ receptor cryo-EM structures have demonstrated that the principal cation-π interacting site for GABA is more likely Tyr205 found on loop C of the β subunit (Liu et al., 2018a; Phulera et al., 2018; Zhu et al., 2018b). Importantly the Tyr205 residue is conserved across subunit types and these three papers used different $GABA_A$ receptor subunit compositions. This was also in agreement with previous electrophysiology experiments illustrating the importance of the Tyr205 amino acid for GABA efficacy (Amin and Weiss, 1993). Nevertheless each paper also confirmed that other aromatic residues, important for GABA efficacy, increase the stability of GABA in the binding pocket. Specifically these included Tyr 97 and Tyr 157 of the β subunit which form putative hydrogen bonds with GABA (Liu et al., 2018a; Phulera et al., 2018; Zhu et al., 2018b). Finally, as with all Cys-loop receptors, GABA binding involves interactions with the complimentary subunit on loops D-F of the ligand binding pocket (Miller and Smart, 2010). While this involves large aromatic residues forming a hydrophobic binding area, it also requires a key arginine residue which is important for GABA recognition and

efficacy (Boileau et al., 1999) and acts to stabilize GABA in the binding pocket of all three structures (Liu et al., 2018a; Phulera et al., 2018; Zhu et al., 2018b).

Upon neurotransmitter binding, the receptor must transduce the signal from the ECD to the TMD for the channel gate to open. As first noted in nAChRs (Lee and Sine, 2005), there are a number of important sites maintaining the interface between the ECD to the TMD (Miller and Aricescu, 2014). In particular there are a number of contact points between the β6-7 linker and the extracellular M2-M3 loop. The β1-2 linker also contacts the same M2-3 loop alongside with the β10-strand (Miller and Aricescu, 2014). These contact points are relatively conserved among the Cys-loop family as they have also been observed in structures of AChBP, and the full length bacterial Cys-loop ELIC and GLIC ion channels (Hilf and Dutzler, 2008; Bocquet et al., 2009). Tight coupling of ECD and TMD is maintained through these interactions which facilitate a high amount of surface area contact between the two domains (Miller and Aricescu, 2014).

Ion permeation through $GABA_A$ receptors begins in the ECD where a vestibule coordinates ion flow into the pore and is critical for ion channel conductance (Hansen et al., 2008; Miller and Aricescu, 2014). Within this structure, the amino acid residues are conserved among the anion permeable members of the Cys-loop family, and are charge reversed for cation permeable ion channels (Hansen et al., 2008). Recent high resolution structures have suggested that fenestrations in the subunit interface could be an alternative pathway by which ions enter into the ion channel pore (Phulera et al., 2018; Zhu et al., 2018b). The pore of the ion channel is made up of the M2 α-helices from each subunit, which are quite homologous within the $GABA_A$ receptor family (Miller and Smart, 2010). The two most critical sites within the pore are the activation and desensitization gates which are found at the 9' (Bali and Akabas 2007) and 2'

(Gielen et al., 2015) positions in the pore structure respectively. Binding of GABA induces an anticlockwise asymmetric rotation of all the subunits in the ECD (Masiulis et al., 2019). This new confirmation influences the M2 9' residues to move away from the pore towards the inter-subunit interface allowing ion permeation (Masiulis et al., 2019).

For most Cys-loop receptors, ion selectivity is determined by the same set of amino acids lining the pore. Interestingly, the cation ion permeable nACh (Galzi et al., 1992; Corringer et al., 1999) and 5-HT3 receptors (Gunthorpe and Lummis, 2001) can be changed into anion permeable receptors by introducing mutations on three key residues which mimic GlyRs. GlyRs can also be similarly changed from anion to cation permeable ion channels by the reverse mutations at the same sites (Keramidas et al., 2000; Keramidas et al., 2002). Ion selectivity of $GABA_A$ receptors is more complex as there are different rules for different subunit combinations. Homomeric $GABA_A$ ρ receptor ion selectivity is governed by a single amino acid at the 2' location along the pore. Mutating Pro to Glu at the 2' site is sufficient to convert the ion channel from anion to cation permeable (Wotring et al., 2003; Carland et al., 2004). Meanwhile, the β subunit dominates the ion selectivity of the typical heteromeric α/β/γ $GABA_A$ receptors (Jensen et al., 2002).

R.3.2.2 $GABA_A$ receptor electrophysiology properties

Since the discovery of inhibitory signaling, there has been a concerted effort to identify and categorize the receptor proteins and electrophysiology was the first technique to study this in detail. The first evidence that GABAergic signaling was the predominant inhibitory CNS signaling molecule was made by comparing the anion permeation of the electrically evoked IPSP and the GABA evoked IPSP (Krnjević and Schwartz, 1967). Following the initial description of a Cl^- mediated GABAergic IPSP, it was found that $GABA_A$ receptors are also permeable to HCO_3^-, Br^-, I^-

and F^-. The relative permeability for each anion suggested that $GABA_A$ receptors have an open channel pore diameter of 5.6Å (Bormann et al., 1987). In the presence of a predominantly Cl^- containing solution, the $GABA_A$ receptor has multiple conductance states of 44, 30, 19 and 12 pS but 30 pS is the most common (Bormann et al., 1987).

As previously mentioned, the binding site for GABA is between the β/α-subunit and full activation of the receptor requires full occupancy of these two sites. This was hypothesized following dose response observations on GABA concentration to $GABA_A$ receptor activation, which predicted the two binding sites (Constanti, 1979) (Sakmann et al., 1983). Recently, these early hypothesis have been confirmed by the identification of the two ligand binding sites in a ligand bound $GABA_A$ receptors structure (Zhu et al., 2018b). Nevertheless, it has also been hypothesized that a mono-ligand bound receptor can reach an active state (Macdonald et al., 1989), which was observed during fast deactivating $GABA_A$ receptor currents in response to low concentrations (10μM) of GABA (Jones and Westbrook, 1995). Similar fast deactivating kinetics were observed when one of the ligand binding sites was removed through site directed mutagenesis, confirming that $GABA_A$ receptors activate in a monoligand bound state (Petrini et al., 2011). Upon binding of the GABA ligand, the receptor can either enter into the conducting active state or into a non-conducting desensitized state. Typically the channel favours entering the active state before desensitizing (Jones and Westbrook, 1995). For low concentrations of GABA, the rate of limiting step of receptor activation is the GABA binding step but as the concentration of GABA reaches the saturating levels typically seen during phasic synaptic transmission the limiting step becomes the rate at which the channel opens (Maconochie et al., 1994).

The channel properties such as activation, deactivation and desensitization of $GABA_A$ receptors are heavily dependent on the α-subunits in the receptor (Farrant and Nusser, 2005). The subtype of α-subunit expressed can change the receptor sensitivity to GABA by up to 20x. This is due to 4 key amino acids in the α-subunits which results in an order of α6<α1<α2<α4<α5<α3 for sensitivity to GABA (Böhme et al., 2004). Additionally there are other notable differences in $GABA_A$ receptor gating properties based on the α-subunit composition. Specifically α3-containing $GABA_A$ receptors have slower rise time for activation and significantly slower rates of desensitization and deactivation when compared to α1-containing receptors (Gingrich et al., 1995; Barberis et al., 2007). Likewise, α2-containing $GABA_A$ receptors also deactivate more slowly than α1-containing receptors (Lavoie et al., 1997). These slower rates of deactivation has been attributed to an increased affinity of GABA for both α2- (Dixon et al., 2014) and α3- containing $GABA_A$ receptors (Keramidas and Harrison, 2009).

Moreover, the presence or absence of γ or δ subunits alter the biophysical properties of $GABA_A$ receptors and provide additional flavours to GABAergic signaling. Importantly, the single channel conductance of $GABA_A$ receptors is roughly doubled (from ~15 to ~30pS), with the presence of either a γ or δ subunit (Puia et al., 1990; Verdoorn et al., 1990; Angelotti and Macdonald, 1993; Fisher and Macdonald, 1997). Of note, the presence of γ2 was shown to speed up activation of $GABA_A$ receptors while δ subunits slow desensitization (Haas and Macdonald, 1999). Within the γ class of subunits there is further variety that is introduced in GABAergic signaling. For instance, γ1-containing receptors are significantly slower in both activation and deactivation compared to γ2 containing receptors which could be reflected by differences in synaptic clustering (Dixon et al., 2014). Furthermore, the expression of either the γ2L or γ2S splice

variant changes the overall kinetic profile of $GABA_A$ receptor responses (Benkwitz et al., 2004). Together, the expression of different subunit isoforms can dramatically alter the response properties of GABAergic signaling which ultimately determines the response properties of inhibitory synapses.

R.3.3 Phasic and tonic GABAergic inhibition

GABAergic synaptic signaling can be grouped into two major functional groups based on their response characteristics: tonic or phasic inhibition (Semyanov et al., 2004; Farrant and Nusser, 2005)(see Fig R.5). Both types of signaling involve activation of $GABA_A$ receptors but their response properties are quite distinct and rely on different receptor compositions and subcellular localization. Phasic inhibition, or fast synaptic inhibitory transmission, is characterized by a rapid, brief response with a distinct inhibitory postsynaptic current (IPSC). Conversely tonic GABA signaling involves sustained receptor activation which consistently provides an inhibitory tone (Farrant and Nusser, 2005) (see Fig. R.5).

In some neurons, like cerebellar granule cells, both types of inhibition play an important role in neuronal signaling. Unsurprisingly, cerebellar granule cells use two compositions of $GABA_A$ receptors to facilitate tonic and phasic inhibition. Specifically granule cells express α1- and α6-containing receptors with the latter being primarily found at extrasynaptic sites (Nusser et al., 1996). Further experimental evidence has identified that the δ subunit is critical for the extrasynaptic localization of $GABA_A$ receptors and together with α6 subunits make up the tonic inhibitory $GABA_A$ receptors in cerebellar granule cells (Nusser et al., 1998). In the absence of the α6 receptor, cerebellar granule cell lack tonic inhibition but also do not express any surface δ subunits demonstrating that the granule cell δ subunits preferentially assemble with α6-

containing receptors (Jones et al., 1997; Nusser et al., 1999). Moreover, mice cerebellar granule cells from mice lacking the α6 receptor do not have any tonic inhibition while having minimal disruption to phasic inhibition (Brickley et al., 2001). Meanwhile, tonic inhibitory transmission is maintained by the α1/β2,3/γ2 receptors which are found directly in the synapse (Nusser et al., 1999).

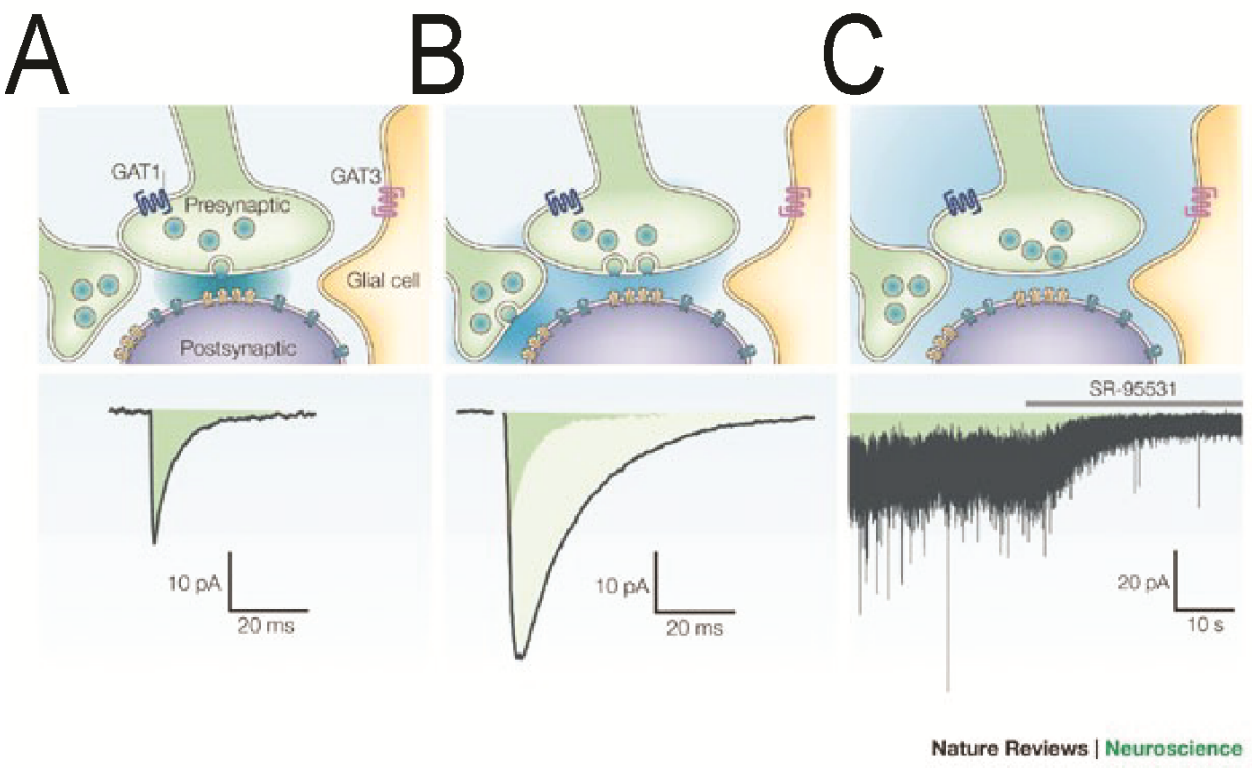

Figure R.5: Response properties of GABAergic synapses
(A) The release of a single GABA containing vesicle from the presynaptic terminal activates postsynaptic $GABA_A$ receptors directly across from the release site. Example inhibitory GABAergic current is under the schematic. (B) A large release of multiple GABA containing multiple vesicles from either a single synapse or release from several terminals promotes GABA 'spillover', which activates both synaptic receptors and perisynaptic or extrasynaptic receptors (blue). The trace shows the averaged waveform of the larger evoked IPSC with the area of the trace from A superimposed for comparison. (C) An example of how low concentrations of ambient GABA tonically activate high affinity $GABA_A$ receptors. Tonic inhibition causes a noisy inhibitory membrane current which can be blocked by $GABA_A$ receptor blockers such as SR-95531. Reproduced with permission from (Farrant and Nusser, 2005)

R.3.4 GABAergic plasticity

R.3.4.1 GABA and chloride

As previously mentioned, $GABA_A$ receptors are anion permeable channels and the main permeant ion during synaptic transmission is Cl^-. As such, the reversal potential of $GABA_A$ receptors is essentially equivalent to the reversal potential of Cl^- which is determined by the relative concentration of Cl^- both inside and outside the neuron. Cl^- is actively transported into and out of the neuron by Na^+-K^+-Cl^- cotransporter (NKCC1) and the K^+- Cl^- transporter member 5

(KCC2) respectively (Ben-Ari, 2002; Ben-Ari et al., 2007). In the developing nervous system there is a notable shift in the reversal potential of GABA currents from -40 to -70 mV during the first two weeks of postnatal rodent development (Ben-Ari et al., 2007). This shift in reversal potential occurs due to shifts in the expression patterns of NKCC1 and KCC2. KCC2 expression gradually increases from almost no expression at birth to adult levels within the first 2 weeks of development (Rivera et al., 1999). Simultaneously, there is high levels of NKCC1 at birth which decrease during those same first 2 weeks (Clayton et al., 1998). The expression patterns of these two proteins are developmentally anti-correlated and this ultimately determines if GABA is hyperpolarizing or depolarizing (Yamada et al., 2004; Ben-Ari et al., 2007).

R.3.4.2 $GABA_A$ receptor trafficking and modulation

While the plasticity mechanisms of excitatory AMPA receptor signaling has been extensively studied since the work of Bliss and Lømo, considerably less focus has been directed to postsynaptic plasticity of GABAergic signaling. Nevertheless, there is still considerable literature regarding the nature of inhibitory synaptic plasticity. Similar to AMPA receptor plasticity, postsynaptic $GABA_A$ receptor plasticity typically involves the insertion or removal of receptors into the synapse (Chiu et al., 2019). $GABA_A$ receptor insertion/removal involves two mechanisms which regulate synaptic receptor density; endocytosis and exocytosis of $GABA_A$ receptors (Luscher et al., 2011), and lateral diffusion of receptors into and out of the synapse (Triller and Choquet, 2008; Bannai et al., 2009).

The synaptic stability of $GABA_A$ receptors depends on their mobility and cell surface dynamics. In part, this is regulated by interactions between $GABA_A$ receptors and the protein gephyrin, which forms the core scaffolding protein of inhibitory synapses (Fritschy et al., 2012).

Experiments with gephyrin KO mice have demonstrated that gephyrin expression is not necessarily required for functional GABAergic synapses to form, but the absence of gephyrin does correspond to weaker GABAergic synapses (Lévi et al., 2004) and a reduced amount of $GABA_A$ receptor clustering (Jacob et al., 2005). Another important $GABA_A$ receptor targeting proteins is $GABA_A$ receptor-associated protein (GABARAP), which promotes $GABA_A$ receptor synaptic clustering (Chen et al., 2000a) and $GABA_A$ receptor exocytosis during inhibitory synapse strengthening (Marsden et al., 2007). Other proteins involved in activity dependent $GABA_A$ receptor trafficking include NSF, PRIP1/2, and GRIP (Luscher et al., 2011).

R.3.4.3 $GABA_A$ receptor plasticity mechanisms

The earliest evidence of inhibitory LTP (iLTP) was called rebound potentiation (RP) and discovered in cerebellar PCs in following bursts of APs (Kano et al., 1992). RP is postsynaptic and requires an increase in intracellular Ca^{2+} (Kano et al., 1992), and activation of CaMKII (Kano et al., 1996), and PKA (Kawaguchi and Hirano, 2000)**.** Interestingly, this form of iLTP only occurs at the somatic - basket cell-PC synapses, but not at the dendritic stellate cell-PC synapses (He et al., 2015). Furthermore this plasticity acts on the $GABA_A$ receptor β2-subunit, which is found at the basket cell-PC synapses (He et al., 2015). The two observations demonstrating that postsynaptic GABA plasticity is $GABA_A$ receptor composition dependent, and presynaptic neuron specific, is a common observation which has been found across other forms of GABAergic plasticity.

Outside the cerebellum, other forms of iLTP have been found which are similar to RP but rely on NMDA receptor activation and downstream CaMKII activation. This mechanism was first described in hippocampal cultures, where stimulation of NMDA receptors promotes the recruitment of $GABA_A$ receptors to synapses through a CaMKII and GABARAP trafficking

dependent mechanism (Marsden et al., 2007; Marsden et al., 2010). As in RP, this mechanism also relies on a specific subunit composition. NMDA receptor driven iLTP in the hippocampus involves CaMKII phosphorylation of the $GABA_A$ receptor β3 subunit, at the Ser-383 position (Petrini et al., 2014). Furthermore this plasticity also involves the clustering of gephyrin (Petrini et al., 2014), a protein which helps promote $GABA_A$ receptor clustering at inhibitory synapses (Tretter et al., 2012; Tyagarajan and Fritschy, 2014). A similar NMDA receptor, CaMKII dependent iLTP was found in cortical layer 2/3 pyramidal cells. Notably this plasticity was specific to the distal SOM-pyramidal cell synapses and did not occur at PV or VIP synapses (Chiu et al., 2018). Moreover this plasticity mechanism requires β2 containing $GABA_A$ receptors which are enriched at SOM synapses (Chiu et al., 2018) (see Fig. R.6).

In addition to the mechanisms described above, these plasticity mechanisms also depend on PTMs of gephyrin. Hippocampal NMDA receptor dependent iLTP involves CaMKII phosphorylation of gephyrin at Ser-305 which increases the size of gephyrin puncta (Flores et al., 2015). Gephyrin phosphorylation of Ser-268 by extracellular signal-regulated kinase (ERK) (Tyagarajan et al., 2013) and Ser-270 by glycogen synthase kinase 3β (GSK3β) (Tyagarajan et al., 2011) promotes gephyrin cleavage by calpain-1 and reduces gephyrin clustering. Other PTMs of gephyrin include palmitoylation of Cys-212 and Cys-284 which stabilize gephyrin in the synapse (Dejanovic et al., 2014) and gephyrin nitrosylation (Dejanovic and Schwarz, 2014), and SUMOylation (Ghosh et al., 2016) which result in decreased clustering. Together, these PTMs all contribute to shaping the strength of GABAergic synapses by dictating the clustering of gephyrin and $GABA_A$ receptors.

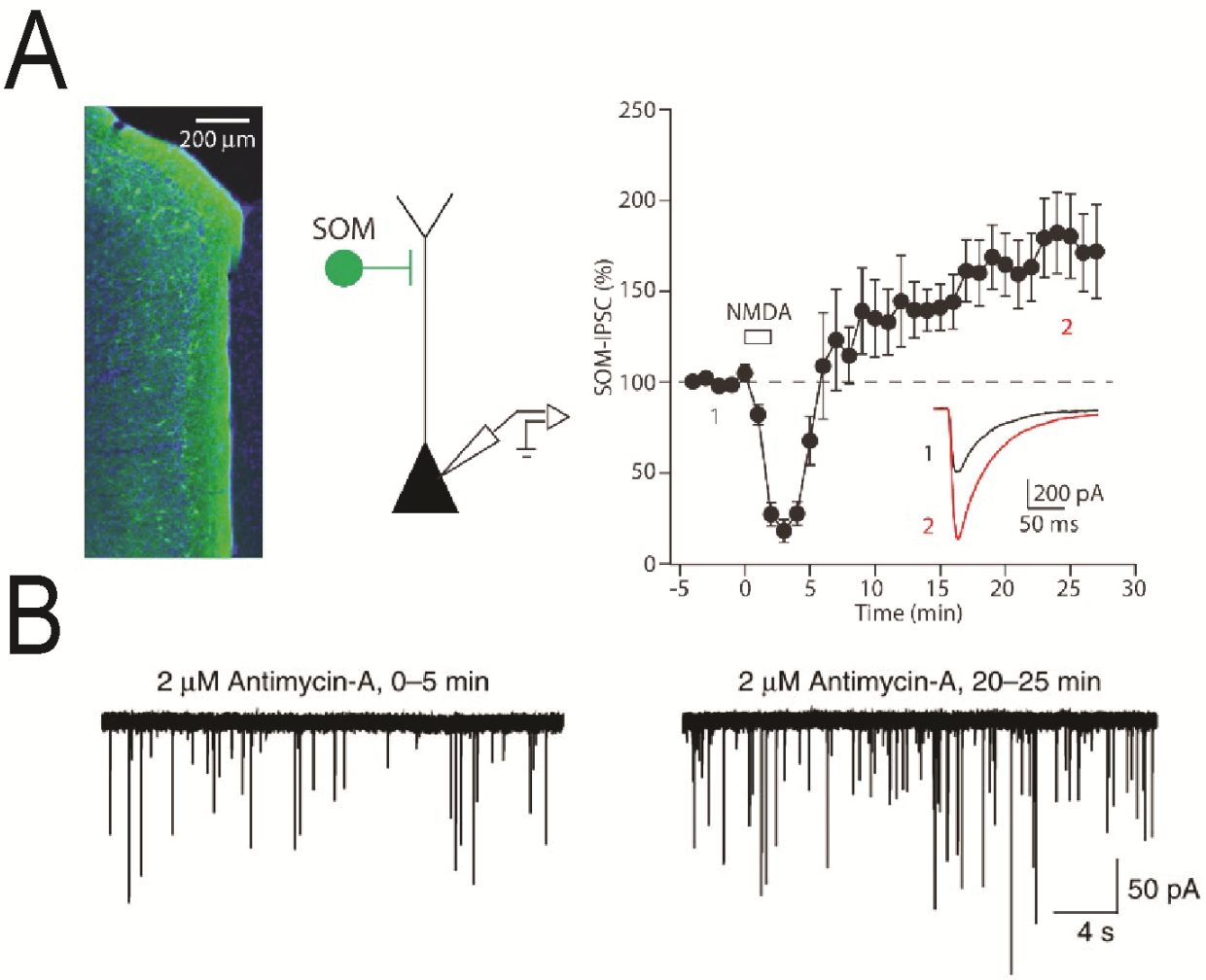

Figure R.6: Long term potentiation of inhibitory GABAergic synapses

(A) Inhibitory GABAergic currents in cortical pyramidal neurons evoked by excitatory channel-rhodopsin activation of somatostatin interneurons before and after the application of NMDA. NMDA acts to selectively stimulate potentiation of GABAergic synapses with specific presynaptic partners (in this case SOM neurons). Reproduced with permission from (Chiu et al., 2018). (B) Miniature GABAergic currents from cerebellar molecular layer interneurons before (left) and after (right) the presence of the mitochondrial poison antimycin-A. Antimycin-A increases the frequency of $GABA_A$ receptor currents through a postsynaptic recruitment of α3-containing $GABA_A$ receptors. Reproduced with permission from (Accardi et al., 2014).

R.3.4.4 Reactive Oxygen Species and inhibitory plasticity

A relatively novel inhibitory plasticity mechanism involves the generation of reactive oxygen species (ROS) as a signaling molecule. While classically thought of as a molecule of cytotoxic consequence of oxidative stress, different forms of ROS are known to act as physiological signaling molecules (Dickinson and Chang, 2011). In terms of inhibitory transmission, $GABA_A$ receptors are directly modulated by ROS at key redox sensitive cysteine residues in the ECD (Beltrán González et al., 2020). In recent years, ROS has been shown to modulate GABAergic signaling through both extracellular and intracellular means. For instance, application of extracellular H_2O_2 to CA1 pyramidal neurons potentiates tonic GABA currents through an extracellular redox mechanism which increases the potency of GABA at low concentrations (Penna et al., 2014). As with the CaMKII specific GABA plasticity, H_2O_2 potentiation of GABA currents also seems to be subunit specific as it selectively potentiates tonic GABA currents while leaving synaptic GABA currents unaffected (Penna et al., 2014).

More important to this thesis, the generation of intracellular ROS modulates GABAergic signaling in the cerebellum. Both cerebellar granule cells (Accardi et al., 2015), and stellate cells (Accardi et al., 2014), experience $GABA_A$ receptor potentiation in response to mitochondrial generation of ROS (see Fig R.6). Insulin application can also cause potentiation of GABAergic signaling in cerebellar granule cells through a ROS dependent manner (Accardi et al., 2015). Moreover, these plasticity mechanisms also target specific populations of $GABA_A$ receptor subunits much like other physiological induction protocols. Cerebellar granule cells undergo ROS-dependent iLTP through recruitment of α6-containing $GABA_A$ receptors (Accardi et al., 2015) while stellate cells recruit α3-containing $GABA_A$ receptors (Accardi et al., 2014). The plasticity of

GABAergic signaling in stellate cells is a particular focus of this thesis and experiments presented in Chapter 1 were designed to explore the physiological induction and molecular pathway underlying this mechanism. The results presented in Chapter 2 relied on the careful dissection of this novel plasticity mechanism. Due to new understanding of inhibitory LTP from Chapter 1, I was able to provide further insight into the pathophysiology of the neurodevelopmental disease, fragile-X syndrome.

R.4 Dendritic Integration

The integration of all excitatory and inhibitory synaptic inputs occurs throughout the branches of the dendritic tree. The dendrites thus fulfill a primary roles of neurons in information processing by regulating synaptic integration. As the AP is the primary signaling unit of a neuron and is typically generated at the axon initial segment (AIS) (Kole et al., 2008), excitatory postsynaptic potentials (EPSP) generated at synapses must pass through the dendritic arbours, the soma, and to the AIS to generate an AP. EPSPs from synapses in different parts of the dendrites can summate causing a larger EPSP as the signal approaches the soma and AIS. Repetitive stimulation of a single synapse can also summate if subsequent EPSPs occur quickly. These two actions are called spatial and temporal summation, respectively. Signal propagation, EPSP summation, and ultimately AP generation depend on how the post synaptic potentials travel through the dendrite branches which are influenced by passive and active dendritic properties (Stuart et al., 2016).

R.4.1 Passive dendritic properties

Passive dendrite properties rely on three main electrical properties denoted from cable theory, membrane resistance (*R*m), membrane capacitance (*C*m), and intracellular resistance (*R*i) (Spruston et al., 1994). These all influence the summation of synaptic inputs but one of the critical factors affecting summation is the membrane time constant (τ_m) which is a function of *C*m and *R*m. Following any post synaptic potential change, the slow component of voltage decay is determined by τ_m (Stuart et al., 2016). In effect, τ_m sets the window by which temporal summation can occur. While τ_m could be considered a passive property it would be more appropriate to call it a resting property. This is because at resting membrane potential, τ_m is

unchanging, but there are voltage sensitive currents such as I_h or rectifying K^+ channels which change τ_m (Spruston and Johnston, 1992; Stuart and Spruston, 1998; Golding et al., 1999). Therefore properties like τ_m can vary along a dendrite and depend on the location, expression, and function of voltage gated ion channels. For example, there is a greater density of I_h in the distal apical dendrites of pyramidal effecting dendritic properties and signal propagation (Magee, 1998; Stuart and Spruston, 1998; Williams and Stuart, 2000). Finally, the location of the synapse and the structure of the dendrites strongly influence the EPSP propagation to the axon initial segment. The effect of the EPSP rise time, and fast component of the decay is heavily influenced by the location of the synapse on the dendrites independent of any voltage dependent properties (Stuart et al., 2016).

R.4.2 Active dendritic properties

While the passive dendritic properties discussed above are important in shaping the propagation of the synaptic response, there are also many other active properties. In fact, some dendrites in the hippocampus (Sun et al., 2014) and olfactory bulb (Chen et al., 1997; Urban and Castro, 2005) are so active that they are capable of generating APs. The voltage gated ion channels present in dendrites can also modulate the EPSP waveform shaping the response found at the soma. Activation of Na_V channels at subthreshold membrane potentials amplifies the EPSP without necessarily generating an AP (Deisz et al., 1991; Stuart and Sakmann, 1995). Furthermore voltage gated Ca^{2+} channels (VGCCs) can also contribute to EPSP amplification (Urban et al., 1998). Both VGCCs and Na_V channels can function together with concurrent activation of NMDA receptors. This mechanism relies on depolarization to relieve NMDA receptor Mg^{2+} block and concurrent glutamate release for NMDA receptors with activation of VGCCs and Na_V (Losonczy and Magee,

2006; Branco and Häusser, 2011). However, block of only NMDA receptors is sufficient to eliminate this EPSP amplification demonstrating they provide a regulation over the voltage gated ion channels (Losonczy and Magee, 2006; Branco and Häusser, 2011).

As VGCCs and Na_V act to potentiate the EPSP amplitude, dendritic voltage gated K^+ channels (K_V) attenuate the EPSP waveform. A-type potassium channels are found in high densities of dendrites and block by 4-AP will increase the EPSP amplitude (Hoffman et al., 1997; Cash and Yuste, 1999). Additionally, Ca^{2+}-activated K^+ channels also play an important role in attenuating the EPSP amplitude. Small conductance Ca^{2+}-activated K^+ (SK) channels are often found coupled close to VGCCs and dampen the EPSP amplitude (Ngo-Anh et al., 2005; Gu et al., 2008; Jones et al., 2017). There are also the big conductance Ca^{2+}-activated K^+ (BK) channels which limit dendritic excitability in the context of regulating Ca^{2+} spikes (Berkefeld et al., 2006; Benhassine and Berger, 2008; Bock and Stuart, 2016).

R.4.3 The role of inhibition on dendritic signaling

Perhaps most important in the context of this thesis is the role of inhibition in regulating the EPSP waveform. The main role of inhibition is to oppose the depolarization caused by excitatory synapses. Much like excitatory synapses, inhibition is also subject to the cable properties of the neuron and activation of inhibitory synapses can have dramatic changes to neuron activity. Neurons can receive vastly different types of inhibition depending on the type of presynaptic inhibitory neurons driving the response (Klausberger and Somogyi, 2008; Pelkey et al., 2017). As Cl^- is the primary permeant ion through the inhibitory $GABA_A$ receptors, the ability for them to mediate inhibition relies on the local Cl^- gradient across the cell membrane which is set by local Cl^- transporters (Farrant and Kaila, 2007; Kaila et al., 2014). The Cl^- gradient can vary dramatically

in different cells which greatly impacts inhibition in a cell-type specific manner (Martina et al., 2001; Gulledge and Stuart, 2003). In cells with a relatively depolarized Cl^- reversal potential GABA can still cause inhibition in the absence of a proper IPSP due to shunting which dampens excitatory transmission. Moreover, shunting can spread so that in some instances inhibition could theoretically be stronger outside of the synapse (Gidon and Segev, 2012). Physiologically, $GABA_A$ receptor activation can also compartmentalize activity in dendrites, which can be seen by restrictions in Ca^{2+} rises to specific dendritic branches in both cortical (Chiu et al., 2013) and cerebellar neurons (Rowan et al., 2018; Gaffield et al., 2019).

R.5 Neurodevelopmental Disorders

Neurodevelopmental disorders are an umbrella term for disorders which disrupt the maturation of the brain and cause delays or failure to meeting developmental milestones. Within this group are autism spectrum disorders (ASD), which are a collection of common phenotypes which must include social deficits and repetitive behaviors. While ASDs are all neurodevelopmental in nature, there is not one singular cause, instead ASDs are a collection of many rare diseases (Bagni and Zukin, 2019; Heavner and Smith, 2020). To date there are up to 1000 genes that have been implicated in causing ASDs (Ramaswami and Geschwind, 2018), but genetic causes only accounts for less than half of the total ASD cases and any one gene typically account for less than 1% of known cases (Heavner and Smith, 2020). Many of the known genetic causes of autism converge on defects of proteins which are important for synapse formation or function (see Fig. R.7). These include mutations encoding genes for trans-synaptic cell adhesion molecule neuroligins 1-3 (Jamain et al., 2003), neurexin-1 and -3 (Kim et al., 2008; Vaags et al., 2012) the post-synaptic family of scaffolding proteins SHANK1-3 (Durand et al., 2007; Monteiro and Feng, 2017), and CNTNAP2 (Strauss et al., 2006). Furthermore, there are mutations in individual synaptic genes which do not necessarily cause autism but increase the risk of developing a neurodevelopmental disease. These are considered “highly vulnerable genes” and cumulative mutations affecting multiple at risk genes increases the likelihood of ASD onset (Parenti et al., 2020).

In addition to the above mentioned genetic causes, there are over 100 neurodevelopmental syndromes which have comorbidity with ASD (Betancur, 2011). Most of these syndromes have known defects in synapse function, development, and/or plasticity (Grant, 2012; Zoghbi and Bear, 2012). Rett syndrome is a severe disease which is caused by mutations in

the gene encoding the MeCP2 protein (Amir et al., 1999; Ip et al., 2018). Loss of function in MeCP2 results in decreased soma size, spine size, and shifts in excitability (Ip et al., 2018). Another syndrome affecting synaptic development and function is tuberous sclerosis complex (TSC). TSC is an autosomal dominant disorder caused by mutations to *TSC1* and *TSC2* which often presents with autism in patients (Jeste et al., 2016). The gene products of *TSC1* (hamartin), and *TSC2* (tuberin), are tumor supressing proteins which regulate the activity of the mTOR pathway (Lipton and Sahin, 2014). The mTOR pathway plays a key part in regulating activity dependent local protein translation which is important in synaptic plasticity (Jung et al., 2014). Finally, fragile-X syndrome (FXS) is the most common single gene cause of intellectual disability and is the result of mutations affecting the *FMR1* gene (Bagni and Zukin, 2019). FXS is associated with a number of defects in plasticity and neuron hyperexcitability. A focus of this thesis is to provide better understanding of the synaptic defects in FXS. Results Chapters 2 and 3 have used a mouse model of FXS, the *Fmr1*-KO mouse, and the next sections will review the current literature of this disease in more detail.

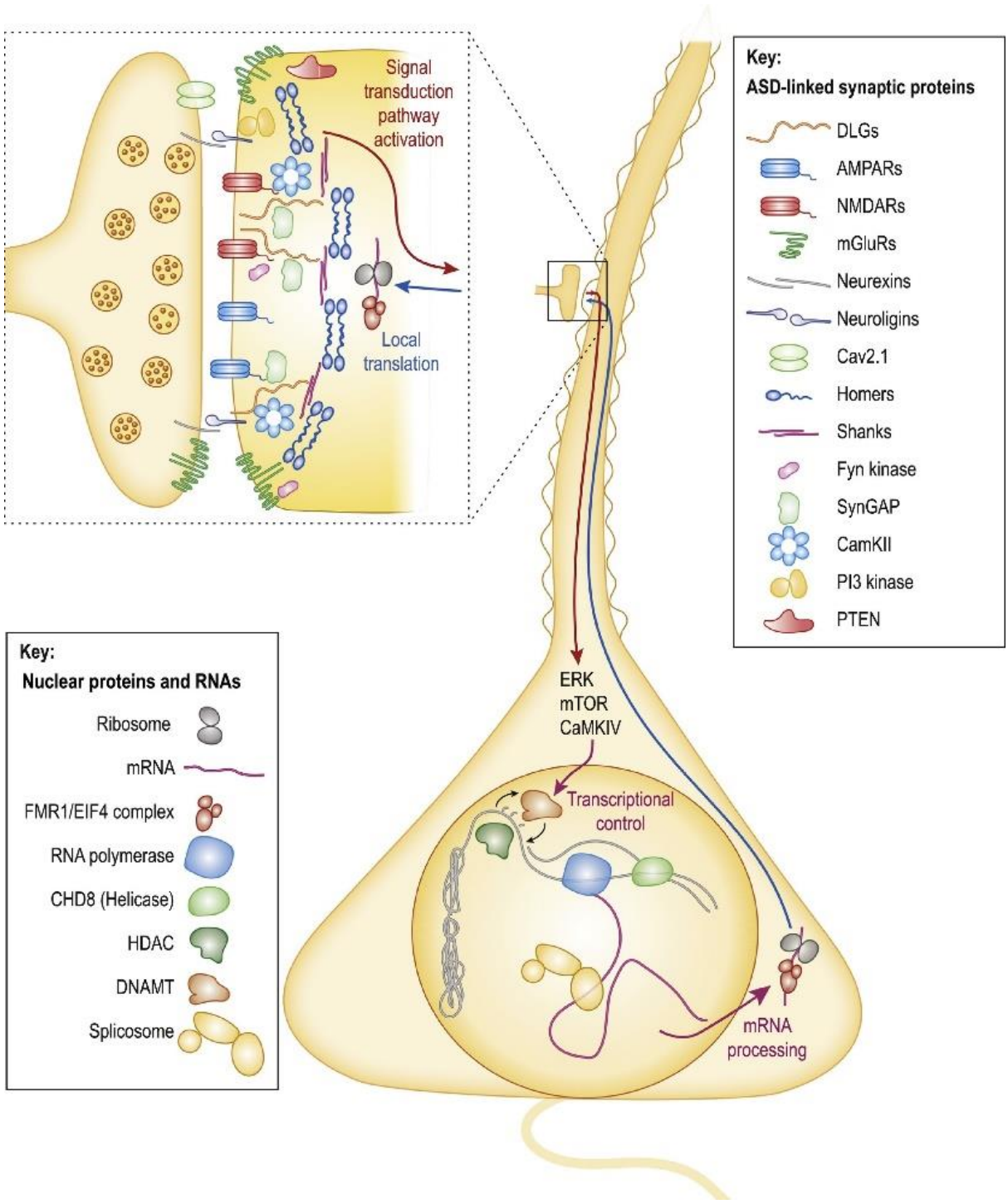

Figure R.7: Synaptic proteins functionally dysregulated in Autism Spectrum Disorders
A cartoon view of the synapse identifying synaptic proteins linked to ASDs including cell adhesion molecules (neuroligin), scaffolding proteins, intracellular signaling pathways, voltage gated ion channels, and ion channel receptors. Reproduced with permission from (Heavner and Smith, 2020)

R.5.1 Fragile-X Syndrome

Fragile-X syndrome (FXS) is a neurodevelopmental disorder which results in mild to severe intellectual disability and autism, which is a comorbidity in half of people diagnosed with the syndrome (Bagni et al., 2012; Santoro et al., 2012). People with FXS also have a common set of physical traits such as macroorchidism (enlarged testes), a long face with protruding ears, flat feet, and lax joints (Santoro et al., 2012). FXS was first described by in a 1943 paper by Martin and Bell where they described a sex-linked trait causing intellectual disability in the males from the pedigree of one family (Martin and Bell, 1943). They found that while the males of the family had the most severe phenotypes, some of the females also presented with similar but milder symptoms (Martin and Bell, 1943). Further studies have identified that severity of symptoms, correlates with the presence of a fragile site on the X chromosome (Silverman et al., 1983) which was found to be the chromosome location Xq27.3 (Krawczun et al., 1985). Eventually this site was found to harbour the gene *FMR1,* which encodes the fragile X mental retardation protein (FMRP) (Verkerk et al., 1991). The vulnerable nature of the site was then linked to hypermethylation of in the 5'-untranslated region (UTR) of the FMR1 gene which silences the gene and prevents expression of FMRP (Pieretti et al., 1991). Hypermethylation occurs as a result of an expansion CGG repeats in the 5'-UTR. Healthy individuals typically have 6 to 54 CGG repeats while individuals with greater than 200 CGG repeats have a "full mutation" which completely silences FMR1 and causes the development of FXS (Santoro et al., 2012). Individuals with 55-200 CGG repeats have the FXS permutation and develop an array of symptoms which include tremors, cerebellar ataxia, and eventual cognitive decline (Hagerman et al., 2003).

Under normal conditions FMRP is expressed in virtually all cells but is found to be most expressed highly in neurons (Devys et al., 1993; Hinds et al., 1993). Functionally, FMRP fulfills many roles but it is best known as an mRNA binding protein. Early biochemistry experiments revealed that FMRP has multiple binding domains with high affinity for RNA including two KH domains and a RGG box (Ashley et al., 1993; Siomi et al., 1993). As an mRNA binding protein, FMRP mainly acts to inhibit protein translation and FXS mouse models, which lack FMRP, have excess protein synthesis (Richter et al., 2015; Banerjee et al., 2018). Many of the mRNA targets of FMRP are expressed in the postsynaptic density, and thus, FMRP has a key role in shaping the synaptic response (Darnell et al., 2011). In addition to its canonical role as a regulator of protein translation, FMRP also makes direct protein-protein interactions to regulate ion channels. Structural biology experiments on the N-terminal domain of FMRP (N-FMRP) identified this region as a candidate to make these protein-protein interactions (Ramos et al., 2006) and later, N-FMRP was found to regulate many different ion channels (to be discussed in depth below). Taken together, FMRP fulfills many roles in cellular physiology, but a common theme among them is that FMRP regulates synapse function.

In addition to the complete gene silencing caused by the CGG repeats, there are some point mutations which affect the function of FMRP and lead to FXS. There are two known missense FMRP mutations in the RNA binding domains which are known to cause FXS symptoms in humans, G266E in the KH1 domain (Myrick et al., 2014), and I304N (De Boulle et al., 1993). The G266E mutation results in full FXS symptoms due to a loss of FMRP binding to RNA. Another mutation, R138Q, is found in the N-terminal domain and is associated with the nuclear localization signal (Collins et al., 2010). R138 is important as a binding site for direct protein-

protein interactions with the BK channel which is abolished by the R138Q mutation (Myrick et al., 2015; Kshatri et al., 2020).

For humans, the lack of FMRP causes changes to overall brain white matter structure (Villalon-Reina et al., 2013; Hall et al., 2016; Swanson et al., 2018) and functional connectivity (van der Molen et al., 2014; Wang et al., 2017). In part, this is linked to brain hyperexcitability (Wang et al., 2017) which is a common symptom found in general ASDs and FXS (Rubenstein and Merzenich, 2003; Contractor et al., 2015; Nelson and Valakh, 2015). Hyperexcitability in FXS arises from changes to brain function across the CNS. For instance, there is an increased risk for seizures in FXS patients (Berry-Kravis, 2002) and a reduced threshold for audiogenic seizures in *Fmr1*-KO mice (Musumeci et al., 2000; Chen and Toth, 2001), the most common animal model to study FXS. This is found at the level of sensory processing where auditory cortex of *Fmr1*-KO mice have greater responsiveness to sound (Rotschafer and Razak, 2013). Hyperexcitability is also found in somatosensory processing with defects in BK and I_h channel function causing increases in neuron excitability (Zhang et al., 2014b).

R.5.1.1 The RNA binding role of FMRP

Since FMRP was found to bind mRNA and regulate protein translation, there has been an effort to identify its interacting targets. A seminal paper came out in 2011 which used crosslinking-immunoprecipitation and high throughput screening to derive an extensive list of FMRP mRNA targets (Darnell et al., 2011). Insight from this work showed that FMRP is frequently bound to mRNA targets of proteins typically expressed in synapses and it was estimated that FMRP interacts with mRNA encoding for up to 30% of the proteins found in the PSD (Darnell et al., 2011). Some of the more notable mRNA binding partners of FMRP include the NMDA receptor

subunits NR1, 2A, 2B and 3A, PSD-95, Shank1–3, neuroligins 1–3 the mGluR5 receptor, and other proteins interacting with NMDA and mGluR5 receptor signaling (Darnell et al., 2011). The Darnell study also revealed that FMRP regulates protein translation by binding to the mRNA coding regions and represses translation through ribosomal stalling (Darnell et al., 2011). The ribosomal stalling mechanism was further supported by evidence showing that the ribosome transit rate, a measurement of translation, is faster in mice lacking FMRP (Udagawa et al., 2013).

FMRP also regulates mRNA translation through interactions with components of the RNA-Induced Silencing Complex (RISC). FMRP interacts with the microRNA (miR) miR-125a to regulate translation of PSD-95 (Muddashetty et al., 2011). When FMRP is phosphorylated it forms a protein complex with AGO2-miR-125a to inhibit translation (Muddashetty et al., 2011). In response to mGluR signaling, FMRP is dephosphorylated and the complex breaks down to release mRNA and allows translation to occur (Muddashetty et al., 2011). A similar mechanism occurs regulating the mRNA of NMDA receptor subunit GluN2A. In hippocampal neurons FMRP forms a complex with miR-125b and Argonaute 1 to limit GluN2A subunit expression (Edbauer et al., 2010).

R.5.1.2 FXS, mTOR, and mGluR-LTD

A well-studied mechanism by which FMRP regulates translation is through its effects on the mTOR signaling pathway. mTOR signaling involves an evolutionarily conserved pathway which is responsible for controlling protein synthesis and regulates cell growth, proliferation, and metabolism (Hay and Sonenberg, 2004) (see Figure R.8). There are two distinct mTOR complexes with distinct pathways called mTOR complex 1 and 2 (mTORC1 and 2) (Hay and Sonenberg, 2004). Dysfunction in mTOR signaling has been reported in FXS studies and is linked to mGluR-LTD

(Sharma et al., 2010). These observation were built off earlier studies which revealed that mGluR-LTD is enhanced in *Fmr1*-KO mice (Huber et al., 2002; Koekkoek et al., 2005).

The downstream targets of mTORC1 signaling are the eukaryotic translation initiation factor 4E (eIF4E)-binding proteins (4E-BPs), and p70S6 kinase 1 (p70S6K1) (Hay and Sonenberg, 2004). 4E-BPs act to limit protein synthesis by binding to eIF4E and preventing its interaction with translation machinery. Activation of mTOR leads to phosphorylation of 4E-BP causing it to dissociate from eIF4E. The three subunit complex called eIF4F is then assembled which includes eIF4G, eIF4A, eIF4E and is critical for the initiation of translation (Hay and Sonenberg, 2004). This pathway is also regulated by FMRP which binds to cytoplasmic FMR1-interacting protein 1 (CYFIP1) to inhibit eIF4E through a similar mechanism as 4E-BP (Napoli et al., 2008). Under normal conditions, the FMRP-CYFIP1 complex restricts local dendritic translation of proteins and is under the control of mGluR and BDNF signaling (Napoli et al., 2008). The FMRP-CYFIP1 complex regulates actin remodeling and protein synthesis which is required for synaptic plasticity (De Rubeis et al., 2013).

As previously mentioned, hippocampal mGluR-LTD is a translation dependent process (Huber et al., 2000) and requires activation of the mTOR through a phosphoinositide 3-kinase (PI3K)-mTOR signaling pathway (Hou and Klann, 2004). Originally thought to involve mTORC1 (Hou and Klann, 2004), recent evidence has implicated mTORC2 as the molecule responsible for mGluR-LTD (Zhu et al., 2018a). An important early observation in the understanding of the pathophysiology of FXS was that *Fmr1*-KO mice had enhanced hippocampal mGluR-LTD (Huber et al., 2002). This lead to the mGluR theory of FXS which hypothesized that downregulating mGluR signaling could rescue behavioural phenotypes and lead to a putative treatment (Bear et

al., 2004). While this has been a successful approach at reducing the severity of FXS phenotypes in mice (Dölen et al., 2007), it has yet to translate to success in treating humans.

Unlike in WT neurons, mGluR-LTD is independent of protein synthesis in *Fmr1*-KO mice (Nosyreva and Huber, 2006). This is thought to be because the proteins required for LTD have already been synthesized (Richter et al., 2015). Accordingly, part of the nature of the disease involves general translational control and correcting the disease requires a rebalance of protein expression. As FMRP is critical to inhibiting mTOR translation and regulating overall protein synthesis, drugs targeting mTOR signaling have recently been proposed as novel treatments. Experiments inhibiting eIF4E phosphorylation, and thus reducing mTOR induced translation have been able to rescue many FXS phenotypes in mice (Gkogkas et al., 2014). More recently metformin, an FDA approved inhibitor of the mTOR pathway, has been shown to rescue mGluR-LTD, dendritic abnormalities, and behavioural phenotypes (Gantois et al., 2017). These advances have brought a new dimension to the development of FXS therapeutics which may lead to new treatments for people with the disease in the future (Gantois et al., 2019).

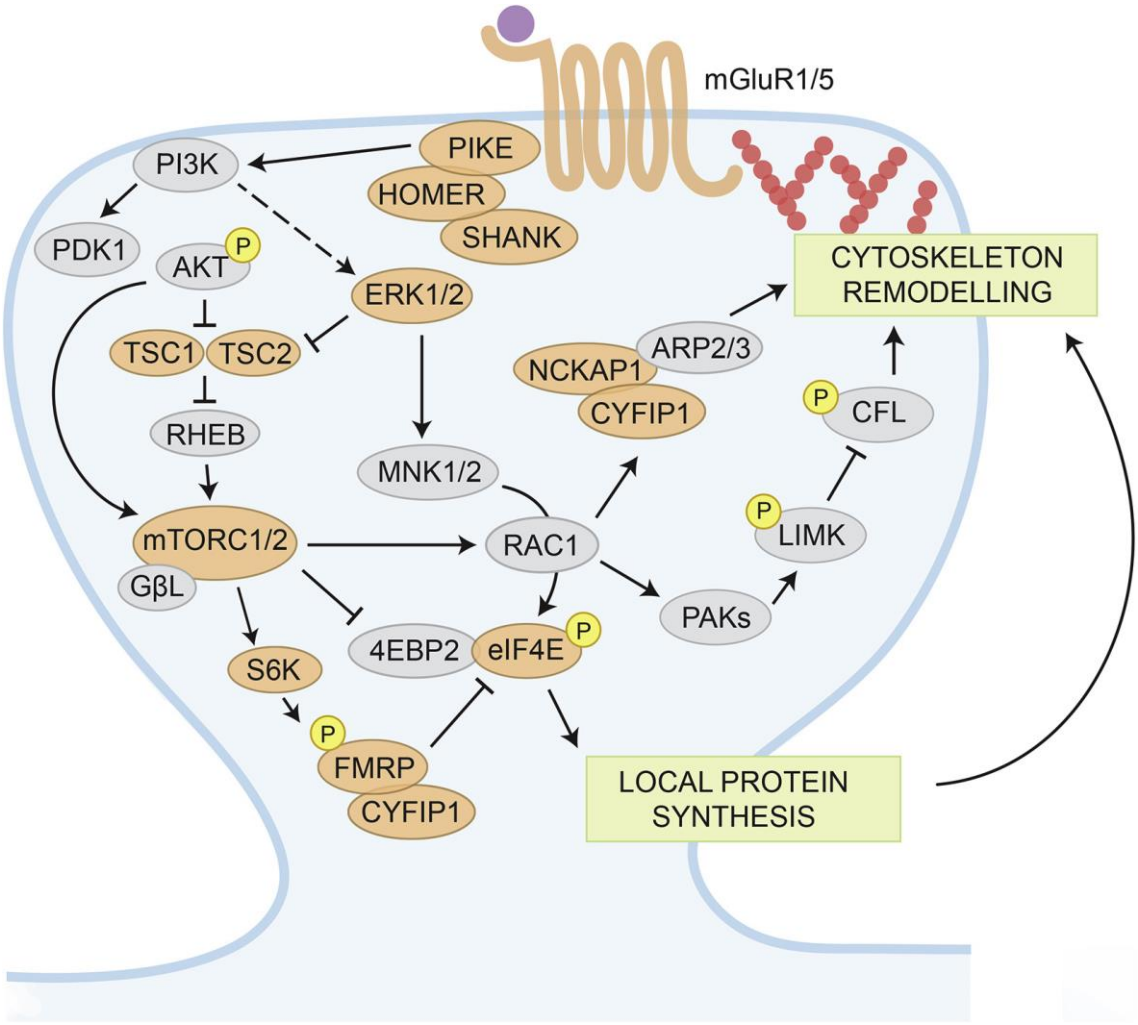

Figure R.8: A model of the mTOR and mGluR signaling pathway in synapses
A cartoon view of the synapse summarizing the activation pathway of mTOR signaling following mGluR activation and the regulation of local protein synthesis. Reproduced with permission from (Bagni and Zukin, 2019)

R.5.1.3 The novel structural role of FMRP

Over the last 10 years, a new translation independent role for FMRP in the direct modulation of ion channel function. While originally unexpected, these interactions have come to be recognized as an important function of FMRP in regulation of the biophysical properties of ion channels. Moreover, this functional regulation has been tied into the overall hyperexcitability that has been described in the FXS brain (Contractor et al., 2015). Prior to direct evidence demonstrating the

effects of FMRP on ion channel function, structural analysis of the N-terminal fragment revealed motifs which could facilitate protein-protein interactions (Ramos et al., 2006). Later experiments then revealed that this fragment was crucial for mediating binding and modulation of ion channel functions. FMRP was first shown to modulate the Na^+-activated, K^+-selective ion channels (Slack or K_{Na}) by direct protein-protein interactions (Brown et al., 2010). Two important pieces of evidence were used to demonstrate the protein-protein interactions between FMRP and Slack. First, FMRP was shown to co-immunoprecipitate with Slack from WT neurons but not from *Fmr1*-KO mice. Second, introducing the N-terminal fragment of FMRP (amino acids 1–298), promoted a shift in channel gating to a higher conductance mode which was eliminated upon the removal of FMRP. This effect was also lost when using heat inactivated FMRP, or when paired with a truncated Slack channel without a C-tail. Altogether, the N-terminus of FMRP (N-FMRP) was shown to modulate Slack channel gating through a binding site found on the C-tail (Brown et al., 2010). A follow study has shown that the regulation of Slack channel function by FMRP normalizes neuron firing properties (Zhang et al., 2012).

Additional studies have revealed that similar interactions happen with other ion channels and a well-studied interaction happens with FMRP and the BK channel-β4 auxiliary subunit complex. Deng and colleagues first showed that FMRP is critical for regulating presynaptic release by regulating BK channel function (Deng et al., 2013). BK channels are important for AP repolarization as well as the fast phase of the afterhyperpolarization (AHP) (Bean, 2007). In CA3 hippocampal neurons, *Fmr1*-KO mice have a more broad AP shape due to dysregulation of BK channels (Deng et al., 2013) which affects short term plasticity (Deng et al., 2011). The regulation of AP shape relies on an interaction of N-FMRP and BK channels with the β4 auxiliary subunit

(Deng et al., 2013; Kshatri et al., 2020). Furthermore, the FMRP R138Q mutation abolishes most of the functional interactions between FMRP and the BK channel complex (Myrick et al., 2015; Kshatri et al., 2020). Deng and colleagues have also implicated a role for FMRP to regulate SK channels (Deng et al., 2019). SK channels normally regulate a slower component of the AHP (the medium AHP or mAHP) (Bean, 2007), which is also dysregulated In *Fmr1*-KO mice (Deng et al., 2019). Allosteric modulators promoting SK channel opening or introduction of N-FMRP rescues AP firing in *Fmr1*-KO mice suggesting that SK channels are also regulated in a similar manner as BK channels (Zhang et al., 2012).

There has been an ever expanding list of ion channels which are directly regulated through protein-protein interactions with N-FMRP. There is a notable deficit in cerebellar GABAergic signaling onto PCs due to a presynaptic decrease in delayed-rectifier K^+ currents found in basket cells (Yang et al., 2018). PCs in *Fmr1*-KO mice receive excessive GABA release due to diminished $K_V1.2$ currents. The reintroduction of N-FMRP through patch pipette perfusion can rescue cerebellar basket cell GABA release. Furthermore, a FMRP antibody can remove the FMRP interaction in WT mice to mimic the *Fmr1*-KO phenotype demonstrating that endogenous FMRP regulates presynaptic release (Yang et al., 2018). FMRP can also potentiate $K_V1.2$ currents in recombinant experiments, directly illustrating this interaction (Yang et al., 2018). Hyperpolarization-activated cyclic nucleotide–gated (HCN) channels, which mediate the I_h current, are bi-directionally controlled by FMRP. The reintroduction of FMRP rescues dendritic function by potentiating I_h in prefrontal cortex while reducing I_h in CA1 pyramidal neurons through yet unknown mechanisms (Brandalise et al., 2020). Finally N-FMRP shifts the biophysical properties of $Ca_V3.1$ and K_V4, and reintroduction restores mossy fiber-granule cell synapse

function (Zhan et al., 2020). Over the last 10 years, the interactions between N-FMRP and the ion channels listed above have revealed that the pathophysiology of FXS extends past the role of translation, and illustrates an important need to reconsider how the disease manifests.

R.6 Thesis rational and objectives

The overall goal of my thesis was to gain better understanding about the nature of inhibitory signaling in the cerebellum, and to advance our knowledge about the pathophysiology of fragile X syndrome. These investigations were guided by an idea that understanding normal synaptic function can yield insights into the manifestation of disease, and the study of disease can inform our understanding of how synapses function. The first objective was to study a novel form of inhibitory plasticity which had recently been described in the cerebellum. Prior to beginning my PhD, the Bowie lab had recently published a study identifying an inhibitory plasticity mechanism which involved the generation of ROS to recruit α3-containing $GABA_A$ receptors in cerebellar MLI synapses (Accardi et al., 2014). While this work revealed a new way to regulate inhibitory synapses, the iLTP induction required delivering intracellular mitochondrial poisons to generate ROS. A follow-up study demonstrated that cerebellar granule cells similarly recruit α6-containing $GABA_A$ receptors through a ROS dependent mechanism (Accardi et al., 2015). Importantly, this study also revealed that insulin could induce iLTP through activation of physiological receptors and signaling (Accardi et al., 2015). Nevertheless, at the time it was unknown if any physiological pathways could induce iLTP in MLIs. In particular, we were interested to explore if there was a role for synaptic activity to induce iLTP.

Previous work had established that excitatory synaptic activation can generate ROS through NMDA receptor activation (Dugan et al., 1995; Reynolds and Hastings, 1995). Therefore, the initial goal was to examine if iLTP could be induced by excitatory synaptic activity in MLIs. I achieved this objective by using the “bread and butter” of the Bowie lab, whole-cell patch clamp electrophysiology with a stimulating electrode to activate synaptic afferents. Through a series of

pharmacological and genetic experiments presented in **PART II: Chapter 1 "Physiological ROS induces iLTP in cerebellar MLIs"**, we were able to elucidate a biochemical pathway starting with NMDA receptor activation and leading to $GABA_A$ receptor recruitment. Thanks to biochemistry data provided in collaboration with the Siddiqui lab at the University of Manitoba, we implicated an important role of GABARAP in the recruitment of $GABA_A$ receptors. The insights gained through our understanding of the biochemical signaling pathway downstream of NMDA receptor activation were critical for subsequent experiments detailed in Chapter 2.

After dissecting the basic synaptic plasticity mechanisms presented in Chapter 1, my goal was to focus on the role of MLIs in the pathology of disease. Chapters 2 and 3 describe the results from studies looking at the function of MLIs in the neurodevelopmental disease fragile-X syndrome (FXS). Classically, the cerebellum has been studied for its role in motor learning (Ito, 2006). Recent advances have led to an emerging hypothesis where the cerebellum plays an important role in the development of the CNS and, moreover, that dysfunction to the cerebellum is an important factor in the development and pathophysiology of neurodevelopmental diseases (Wang et al., 2014; Sathyanesan et al., 2019; Schmahmann et al., 2019; Streng and Krook-Magnuson, 2020). While the cerebellum has been extensively studied, most of the research at the cellular level has been focused understanding the properties of PCs, the sole output of the cerebellar cortex (Apps and Garwicz, 2005). Conversely, less is known about molecular layer interneurons (MLIs) which constitute the dominant inhibitory input onto PCs, and provide a critical regulation of their activity (Jörntell et al., 2010). More recently, studies genetically targeting and regulating MLI activity have confirmed the important role of MLIs *in vivo* during

learning and behaviour (Astorga et al., 2017; Gaffield and Christie, 2017; Rowan et al., 2018; Brown et al., 2019).

While there is now a general acceptance of the important role that MLIs have in shaping cerebellar output, there also exist a number of mechanisms by which they are functionally regulated. For instance, they have a well characterized excitatory plasticity mechanism in response to PF stimulation which changes composition of synaptic AMPA receptors (Liu and Cull-Candy, 2000; Liu and Cull-Candy, 2002). Moreover the PF-MLI synapse also undergoes LTD in response to low frequency stimulation (2Hz) which can be shifted to LTP if paired with a depolarizing protocol (Rancillac and Crépel, 2004). Finally we have shown that NMDA receptor activation regulates MLI inhibitory synapses which is presented as Results Chapter 1 (Larson et al., 2020). Prior to the work presented in this thesis, there has yet to be a comprehensive study examining any of these synaptic properties in a FXS mouse model.

To address this, I performed experiments in the cerebellum using *Fmr1*-KO mice, a common model to study the neurodevelopmental disease FXS. In **Results Chapter 2**, **"Excitatory synaptic defects have knock-on effects for plasticity in FXS mice"**, I found that excitatory synaptic transmission is defective in *Fmr1*-KO mice. *Fmr1*-KO mice have a decreased NMDA receptor current which impacts the induction of two MLI plasticity mechanisms. Notably, in *Fmr1*-KO mice there is an inability to induce iLTP even though the downstream biochemical signaling pathway is functional. We were able to restore iLTP in *Fmr1*-KO mice by using a small molecule to directly activate the signaling pathway identified in Results Chapter 1. These results from Chapter 2 demonstrate the advantage of carefully dissecting the biochemical signaling pathway in Chapter 1.

Results Chapter 3, "FMRP acts as a regulator of MLI dendritic signaling", is a follow-up study to an observation initially made during Chapter 2. During our initial experiments with *Fmr1*-KO mice stimulating PFs, we found that they had consistently larger EPSPs. Nevertheless we also noted that the evoked AMPA receptor currents are similar between WT and *Fmr1*-KO mice suggesting that this defect is not a synaptic defect in nature. Therefore, the objective of Chapter 3 was to further explore the nature of the larger EPSP, both in terms of the functional consequences on MLI activity and the underlying cause of the large EPSP amplitude. I addressed these questions by again performing whole-cell patch clamp electrophysiology and stimulating presynaptic afferents. We show that in response to parallel fiber stimulation, MLIs from *Fmr1*-KO mice fire more APs. Furthermore, this is due to the absence of FMRP which plays an important role in regulating dendritic filtering. Acute reintroduction of the N-terminal fragment of FMRP is sufficient to rescue the increase in EPSP amplitude that we have observed.

PART II: EXPERIMENTAL RESULTS

CHAPTER 1

A physiological ROS signaling pathway induces iLTP in cerebellar MLIs

1.1 Foreword to Chapter 1

This chapter originates as the follow up to the project of a previous PhD student in the Bowie Lab, Mike Accardi. In the winter before I joined the lab, Mike had published a beautiful study linking the generation of ROS to iLTP in cerebellar MLIs (Accardi et al., 2014). During my first few months he was working on a follow up study into a similar mechanism in cerebellar granule cells and exploring a role for insulin in stimulating the same pathway (Accardi et al., 2015). These two studies were incredibly novel, but they lacked insight into how ROS dependent iLTP could occur in normal brain function. My first experiments in the lab were to follow up this work by studying if excitatory afferent stimulation could produce a similar effect on GABAergic signaling. We knew that excitatory synapses had been shown to produce ROS in other preparations – particular following NMDA receptor activation (Dugan et al., 1995; Reynolds and Hastings, 1995). Accordingly, we adopted a stimulation protocol that had been reliably used to stimulate NMDA receptors in MLIs (Carter and Regehr, 2000; Clark and Cull-Candy, 2002) and found that it was successful in inducing iLTP. The rest of the study presented in this Chapter was carried out to identify the biochemical signaling pathway responsible for iLTP.

While this pathway was ultimately found to involve ROS, it did not necessarily have to even though the pathway was stimulating NMDA receptor activation. In other neurons, NMDA receptor activation induces iLTP through a (presumably) ROS independent pathway (Marsden et al., 2007; Petrini et al., 2014; Chiu et al., 2018). In these experiments we found that a ROS pathway is immediately activated following Ca^{2+} entry through NMDA receptors. This pathway includes nitric oxide synthase (nNOS), which couples directly to PSD-95, cGMP production, and superoxide production from NOX2 activation (see Fig 1.4*G*). The involvement of the nNOS-cGMP

pathway was particularly important for experiments that were carried out in Chapter 2. I was also able to link the activation of PKC to the production of ROS by using different combinations of pharmacological activators. These experiments were done specifically to test if Mike's previously published work was acting on the same pathway that I was studying. Finally, a collaboration with the Siddiqui group at the University of Manitoba helped us demonstrated that the pathway expresses iLTP by the recruitment of α3-containing $GABA_A$ receptors with the trafficking protein GABARAP.

During the publication process, I ended up repeating many of the experiments in voltage clamp due to reviewer comments. Initially we had performed all of the experiments in current clamp in an attempt to perform experiments with a more physiological condition. In the end, repeating much of the work in voltage clamp strengthened the results and provided us with a better visualization of iLTP. Furthermore, we tested a diverse arrangement of pharmacology in both conditions and demonstrated that the results could be achieved by two different approaches. Furthermore, the voltage clamp experiments were done with high internal Cl^-, while the current-clamp experiments were performed with a solution containing primarily gluconate. Thus we could rule out any role in changes to Cl^- concentration having an effect on the iLTP mechanism. In the end, the results supported our initial hypothesis that NMDA receptors could generate ROS to induce iLTP, but also provided greater insight into the signaling pathway than we initially expected. This has become even more valuable since I was able to make use of it when designing experiments in Chapter 2.

Article Title:

Nitric oxide signaling strengthens inhibitory synapses of cerebellar molecular layer interneurons through a GABARAP-dependent mechanism

Erik A. Larson[1,3], Michael V. Accardi[2,3], Ying Wang[4,5,6], Martina D'Antoni[1,3], Benyamin Karimi[4,5,6], Tabrez J. Siddiqui[4,5,6], & Derek Bowie[3*]

[1]Integrated Program in Neuroscience; McGill University; Montréal, Québec, Canada
[2]Graduate Program in Pharmacology; McGill University; Montréal, Québec, Canada
[3]Department of Pharmacology and Therapeutics; McGill University; Montréal, Québec, Canada
[4] Department of Physiology and Pathophysiology, Max Rady College of Medicine, Rady Faculty of Health Sciences, University of Manitoba, Winnipeg, Canada
[5] Neuroscience Research Program, Kleysen Institute for Advanced Medicine, Health Sciences Centre, Winnipeg, Canada
[6] The Children's Hospital Research Institute of Manitoba, Winnipeg, Manitoba, Canada

Reproduced with permission from: **Larson, E. A.,** Accardi, M. V., Wang, Y., D'Antoni, M., Karimi, B., Siddiqui, T. J., & Bowie, D. (2020). Nitric oxide signaling strengthens inhibitory synapses of cerebellar molecular layer interneurons through a GABARAP-dependent mechanism. Journal of Neuroscience, 40(17), 3348-3359.

1.2 Abstract

Nitric oxide (NO) is an important signaling molecule that fulfills diverse functional roles as a neurotransmitter or diffusible second messenger in the developing and adult CNS. Although the impact of NO on different behaviours such as movement, sleep, learning, and memory has been well documented, the identity of its molecular and cellular targets is still an area of ongoing investigation. Here, we identify a novel role for NO in strengthening inhibitory $GABA_A$ receptor-mediated transmission in molecular layer interneurons (MLIs) of the mouse cerebellum. NO levels are elevated by the activity of neuronal nitric oxide synthase (nNOS) following Ca^{2+} entry through extrasynaptic NMDA-type ionotropic glutamate receptors (NMDARs). NO activates protein kinase G (PKG) with the subsequent production of cyclic GMP (cGMP) which prompts the stimulation of NADPH oxidase and protein kinase C (PKC). The activation of PKC promotes the selective strengthening of α3-containing $GABA_A$ receptor synapses through a □-aminobutyric acid receptor-associated protein (GABARAP)-dependent mechanism. Given the widespread but cell type specific expression of the NMDAR/nNOS complex in the mammalian brain, our data suggest that NMDARs may uniquely strengthen inhibitory GABAergic transmission in these cells through a novel NO-mediated pathway.

1.3 Introduction

The NMDA receptor (NMDAR) is an abundant neurotransmitter-gated ion-channel that orchestrates the formation, maintenance and plasticity of almost all glutamatergic synapses in the developing and adult brain (Hardingham and Bading, 2003; Paoletti et al., 2013a). It is implicated in numerous neurological diseases from neurodevelopmental disorders (Bello et al., 2013; Hu et al., 2016) to neurodegenerative disease including Huntington's (Milnerwood and Raymond, 2010) and Alzheimer's disease (Liu et al., 2019). Two synergistic features of the NMDAR critical for its role in synaptic signaling are its slow channel gating (Glasgow et al., 2015) and high Ca^{2+} permeability (Gnegy, 2000). These properties of the NMDAR act together to ensure that the presynaptic release of L-glutamate elevates postsynaptic Ca^{2+} and triggers a cascade of Ca^{2+}-dependent biochemical events inside the cell. Much of the activity initiated by NMDARs is relayed through the actions of Ca^{2+}/calmodulin-dependent protein kinase II (CaMKII) (Sanhueza and Lisman, 2013) which is anchored to the NMDAR (Bayer et al., 2006) and thus ideally suited to act as a signaling hub. For example, it has been shown that this pathway originating at glutamatergic synapses strengthens GABAergic synapses (Marsden et al., 2007; Petrini et al., 2014; Chiu et al., 2018).

NMDA receptor signaling is also tightly coupled to neuronal nitric oxide synthase (nNOS) activity through the postsynaptic scaffold of PSD-95 and -93 (Brenman et al., 1996b; Brenman et al., 1996a). By elevating cytosolic Ca^{2+}, synaptic NMDARs activate nNOS generating nitric oxide (NO) which has a variety of roles in neuronal communication and blood vessel modulation (Bredt, 1999; Kiss and Vizi, 2001). Accordingly, NO participates in numerous CNS functions including learning and memory, sleep and feeding behavior, movement, pain, anxiety and reproductive

activity (Garthwaite, 2019). An area of ongoing investigation is to identify the molecular and cellular targets of NO. What is known is that physiological levels of NO elevated by NMDAR stimulation act as a retrograde signal (Garthwaite, 2016), stimulate gene expression (Lu et al., 1999) and/or promote AMPA receptor (AMPAR) trafficking (Serulle et al., 2007). Conversely, excessive levels of NO promote neurotoxicity (Brown, 2010).

Here, we identify a new role for NO in strengthening GABAergic synapses of cerebellar molecular layer inhibitory neurons. We show that an elevation in cytosolic Ca^{2+} mediated by NMDARs triggers a cascade of signaling events that begin with nNOS activation and release of NO which through the generation of cyclic GMP (cGMP) activates protein kinase G (PKG). This pathway stimulates NADPH oxidase and protein kinase C to strengthen α3-containing $GABA_A$ receptor synapses through a γ-aminobutyric acid receptor-associated protein (GABARAP)-dependent mechanism. Given the widespread but cell-type specific expression of the NMDAR/nNOS complex in the mammalian CNS, our data suggest that NMDARs may uniquely strengthen inhibitory GABAergic transmission through a novel NO-mediated pathway in cerebellar MLIs and other nNOS positive ($nNOS^+$) neurons.

1.4 Materials and Methods

Animals

Wild-type mice with a C57BL/6 background were obtained from Charles River Laboratories (Wilmington, MA, USA) and maintained as a breeding colony at McGill University. Mice (male and female) used for the experiments ranged from eighteen to thirty days old. All experiments have been approved and were performed in accordance with the guidelines of the Canadian Council on Animal Care and were approved by the Animal Care Committee of McGill University. Breeder pairs of Gabra3 KO (1-Gabra3tm2Uru/Uru), C57BL/6 background, were kindly provided by Dr. Rudolph (Harvard Medical School, McLean Hospital, MA 02478, USA)(Yee et al., 2005).

Cerebellum slice preparation

Mice were anaesthetized with isoflurane and immediately decapitated. The cerebellum was rapidly removed from the whole brain while submerged in oxygenated (95% O_2, 5% CO_2) ice-cold cutting solution which contained (in mM): 235 sucrose, 2.5 KCl, 1.25 NaH_2PO_4, 28 $NaHCO_3$, 0.5 $CaCl_2$, 7 $MgSO_4$, 28 D-glucose (pH 7.4; 305 - 315 mOsmol/L). The tissue was maintained in ice-cold solution while sagittal slices of cerebellar vermis (300 µm) were cut using a vibrating tissue slicer (Leica VT1200, Leica Instruments, Nussloch, Germany). The slices were transferred to oxygenated artificial cerebrospinal fluid (aCSF) and held at room temperature (20–23°C) for at least 1 hr before recordings were performed. aCSF contained (in mM): 125 NaCl, 2.5 KCl, 1.25 NaH_2PO_4, 26 $NaHCO_3$, 2 $CaCl_2$, 1 $MgCl_2$, 25 D-glucose (pH of 7.4; 305 - 315 mOsmol/L).

Electrophysiology

Slice experiments were performed on an Olympus BX51 upright microscope (Olympus, Shinjuku, Tokyo, Japan) equipped with differential interference contrast/infrared (DIC/IR) optics. Whole-

cell patch-clamp recordings were made from visually-identified molecular layer interneurons (MLIs), primarily in lobules IV and V, which were distinguished from misplaced or migrating granule cells by their soma diameter (8-9 μm) and location in the molecular layer. For current-clamp experiments, patch pipettes were prepared from thick-walled borosilicate glass (GC150F-10, OD 1.5 mm, ID 0.86 mm; Harvard Apparatus Ltd, Holliston, Massachusetts) and had open tip resistances of 4-10 MΩ when filled with an intracellular solution that contained (in mM): 126 K-Gluconate, 0.05 $CaCl_2$, 0.15 K_4BAPTA, 4 NaCl, 1 $MgSO_4$, 5 HEPES, 3 Mg-ATP, 0.1 NaGTP, 15 D-Glucose, 2 QX314 to block voltage-activated Na^+ channels and 0.5 mg/ml Lucifer Yellow as a post-hoc dye indicator (pH 7.4 with KOH, 300-310 mOsmol/L). High BAPTA intracellular current-clamp solution contained (in mM): 110 K-Gluconate, 0.05 $CaCl_2$, 10 K_4BAPTA, 4 NaCl, 5 HEPES, 4 Mg-ATP, 0.1 NaGTP, 15 D-Glucose and 2 QX314 (pH 7.4 with KOH, 300-310 mOsmol/L). Voltage-clamp recordings were made with patch pipettes prepared as described above but filled with an intracellular solution that contained (in mM): 140 CsCl, 4 NaCl, 0.5 $CaCl_2$, 10 HEPES, 5 EGTA, 2 Mg-ATP, 2 QX314 (pH 7.4 with CsOH, 300–310 mOsmol/L). High BAPTA voltage-clamp solution contained 110 CsCl, 4 NaCl, 10 HEPES, 10 Cs_4BAPTA, 2 Mg-ATP, and 2 QX314 (pH 7.4 with CsOH, 300–310 mOsmol/L). Specific n numbers reported refer to technical replications (i.e. patch clamp recordings) while each experiment was replicated using at least 3 different mice.

In each case, recordings were made with a Multiclamp 700A amplifier (Molecular Devices, Sunnyvale, CA, USA) in voltage- or current-clamp mode. Series resistance and whole-cell capacitance were corrected and estimated by cancelling the fast current transients evoked at the onset and offset of brief (10-20 ms) 5 mV voltage-command steps. Series resistance during postsynaptic whole-cell recording (10-25 MΩ) was checked for stability throughout the

experiments (<20% drift tolerance). The capacitance of the MLIs was in the range of 5-14 pF. The bath was continuously perfused at room temperature (22-23 ^{o}C) with aCSF at a rate of 1–2 ml/min. We chose to perform recordings at room temperature rather than physiological temperature because it tended to increase the viability of the slice tissue and slowed the time course of synaptic events making them easier to resolve. Membrane currents were filtered at 5 kHz with an eight-pole low-pass Bessel filter (Frequency Devices, Haverhill, MA, USA) and digitized at 25 kHz with a Digidata 1322A data acquisition board and Clampex9 (Molecular Devices) software. Curve fitting and figure preparation of all electrophysiology data was performed using Origin 7.0 (OriginLab, Northampton, MA, USA), Microsoft Excel, and Clampfit 10 (Molecular Devices) software.

For extracellular stimulation, thin walled borosilicate glass electrodes (OD 1.65mm, ID 1.15mm; King Precision Glass Inc, Claremont, CA, USA) were used with a tip resistance of < 3 MΩ when filled with aCSF. The ground electrode for the stimulation circuit was made with a platinum wire wrapped around the stimulation electrode. The stimulating electrode was positioned in the molecular layer at or just beneath the slice surface. Voltage pulses (10—25 V in amplitude, 200-400 □s in duration) were applied at low frequency stimulation (0.1 Hz) through the stimulating electrode. To minimize variability between responses, the stimulating electrode was positioned 50-100 µm away from the recorded cell. The stimulus voltage used during each experiment was at the lowest intensity to elicit the maximal eEPSP/IPSC response within the range described above. Stimulation strength and duration were kept constant throughout the experiment. For high frequency stimulation (HFS), trains of six stimuli were delivered at 100 Hz (inter-train interval of 20 s) as described previously (Li et al., 2011). This HFS protocol has been previously shown to

generate ROS (Li et al., 2011) and mimics somatosensory stimulation patterns (Jorntell and Ekerot, 2006; Saviane and Silver, 2006; Rancz et al., 2007; Arenz et al., 2008; Coddington et al., 2013). The HFS was performed every five minutes to ensure a continual accumulation of ROS. During the voltage-clamp experiments of evoked GABA currents (cf Fig. 1.2), we performed the HFS protocol at a holding potential of +40 mV to relieve Mg^{2+} block of NMDARs. We performed the single stimulation recordings at -60 mV to isolate the response from NMDA currents and used GYKI 53655 to pharmacologically block AMPA currents. For all experiments which included perfusion of either pharmacological or peptide blocker compounds in the internal solution we waited 15 minutes prior to beginning the HFS induction protocol. In experiments where the antioxidant N-acetyl-cysteine (NAC) was included in the patch electrode solution, we unexpectedly observed that NAC alone increased the amplitude of baseline responses to 191.5 % ± 36 (n=4) of the starting response which stabilized 20 mins after whole-cell breakthrough. Since this was not observed in the absence of NAC ($Peak_{15}$, 100.2 ± 5.5 %, n = 21), we concluded that the resting redox state of the cell affects the synaptic properties of MLIs. Antioxidants have been shown to potentiate both AMPARs (Lee et al., 2012) and NMDARs (Köhr et al., 1994). As our plasticity mechanism relies on NMDAR activation we would expect that any potentiating effect of NAC on the NMDAR current would be more likely to strengthen iLTP. Given this, HFS was commenced only after the effect of NAC on basal synaptic properties stabilized.

Pharmacological compounds

NMDAR antagonist, D-(-)-2-Amino-5-phosphonopentanoic acid (D-APV; 10 µM), AMPA antagonist 1-(4-Aminophenyl)-3-methylcarbamyl-4-methyl-3,4-dihydro-7,8-methylenedioxy-5H-2,3-benzodiazepine hydrochloride (GYKI 53655; 10 µM), and the $GABA_A$ receptor antagonist

bicuculline (10 µM) were purchased from Tocris Bioscience (Ellisville, MO, USA). Stock solutions of these antagonists were prepared in water and were stored at −20°C and working solutions were diluted with aCSF shortly before application to the bath. N-acetylcysteine (NAC, 1 mM) (Sigma-Aldrich Canada, Oakville, ON, Canada), PKA inhibitor fragment (6-22) amide (PKA 6-22, 5µM, Tocris), Ruthenium Red (1 µM, Tocris), and cGMP analogue pCPT-cGMP (10 µM, Tocris) were prepared as a stock solution in water and dissolved in patch electrode solution on the day of the experiment. Apocynin (100 µM, Tocris), 3-bromo-7-nitroindazole (3-Br-7-NI; 10 µM, Tocris), KN-93 (5 µM, Tocris), Gö 6983 (5 µM, Tocris), phorbol 12-myristate 13-acetate (PMA, 100nM, Tocris), 1H-[1,2,4]Oxadiazolo[4,3-a]quinoxalin-1-one (ODQ; 10 µM, Tocris), KT 5823 (5 µM, Tocris), and Antimycin-A (2 µM, Sigma) were dissolved in DMSO and stored at −20°C. The K1 GABARAP, K1 GABARAP scrambled, and α3-derived peptides (all 100µM, Genscript, Piscataway, NJ, USA) were dissolved in DMSO and stored at -20°C. The final maximum DMSO concentration for all experiments (0.1% v/v) had no effect on GABAergic responses which was consistent with other studies (Nakahiro et al., 1992).

cDNA constructs

HA-$GABA_AR$-α3 contains the signal sequence of rat neuroligin1, the HA tag and mature sequence of rat $GABA_AR$-α3 (NM_017069) included in the Clontech EGFP-C1 vector. Human $GABA_AR$-β2 (NM_000813) and human $GABA_AR$-γ2 (NM_000816) were cloned into the pcDNA3 vector. Mouse GABARAP (BC030350) was C-terminally tagged with CFP in the Clontech ECFP-N1 vector. Rat Gephyrin (NM_022865), N-terminally tagged with YFP, was cloned in the Clontech EYFP-C1 vector. All expression constructs were driven by the CMV promoter.

Co-immunoprecipitation protocol

Semi-confluent HEK 293 cells were plated on 60mm dishes and transfected with YFP-Gephryin, GABARAP-CFP or negative control YFP. Co-transfections were done with equivalent amounts of HA-$GABA_AR$-α3, $GABA_AR$-β2 and $GABA_AR$-γ2 (short). Cells were then allowed to grow for 24h post-transfection. 50 µl Protein-G sepharose beads slurry was incubated with 5 µg of rat anti-HA antibody (3F10, Sigma) for 4h at 4°C. Cells were subsequently washed twice and collected in cold phosphate-buffered saline (PBS). Harvested cells were lysed using 250 µl of complexiolyte-48 (Logopharm) and further disrupted by passaging 10-15 times through a 25G needle. Lysed cells were incubated at 4°C for 1h on an end-over rotator. Subsequently, lysates were centrifuged at 14,000 x g at 4°C for 10 min. The resulting supernatants were incubated overnight at 4°C with Protein-G beads conjugated with anti-HA antibody. The beads were washed 3 to 4 times with complexiolyte-48 dilution buffer and eluted in 2x SDS-PAGE sample buffer. The resulting eluates along with 10 µl of the supernatants used as expression control (input) were subjected to SDS-PAGE electrophoresis, immunoblotted on PVDF membranes and probed with rabbit anti-GFP antibody (A11122, Life Technologies, 1:1000) followed by anti-rabbit HRP antibody (4030-05, Southern Biotech, 1:7000). The blots were developed using chemiluminescence in the ChemiDoc imaging system (Bio-Rad). For peptide interference experiments, the same protocol was followed with a third of the antibody, beads and lysates used. The scrambled GABARAP and GABARAP peptides were added to the lysates just before they were added to the beads with a final concentration 2.5 mM.

Statistical analysis

Data were analyzed using SPSS (IBM) and custom statistical software kindly provided by Dr. Joe Rochford (McGill University). All data were tested for normality and appropriate parametric or

nonparametric tests were conducted accordingly. For all repeated measures ANOVA presented, Tukeys post hoc tests were conducted as indicated in the figure legends. For all Friedman tests, a Wilcoxon signed-rank test with a Bonferroni-Holmes correction was conducted on the combinations. All statistical analysis of amplitudes (repeated measures ANOVA or Friedman tests) were conducted comparing the baseline 5 min average of the data sets and each subsequent 5 minute intervals following treatment up to 25mins post treatment.

1.5 Results

High frequency stimulation of glutamatergic synapses strengthens inhibitory transmission

To study activity-dependent plasticity of GABAergic synapses, we performed whole-cell current- and voltage-clamp electrophysiological recordings on cerebellar MLIs which receive synaptic input from both excitatory and inhibitory neurons (Fig. 1.1*A*). Current-clamp recordings were performed to examine the effect of GABAergic signaling on neuronal excitability whereas we used voltage-clamp recordings to study the $GABA_A$ receptor response in isolation. Previous work from our lab has shown that GABAergic synapses of MLIs can be strengthened by elevating cytosolic reactive oxygen species (ROS) with the mitochondrial uncoupler, antimycin-A (Accardi et al., 2014). It remains to be established, however, if cytosolic ROS levels can be elevated by physiologically relevant stimuli, for example, through synaptic transmission. Since MLIs express extrasynaptic NMDARs (Clark and Cull-Candy, 2002), we reasoned that activation of these receptors by neurotransmitter spillover from glutamatergic fibers might elevate cytosolic ROS through a non-canonical signaling pathway that has been previously described in cultured neurons (Dugan et al., 1995; Reynolds and Hastings, 1995).

To test this, we performed stimulation experiments of MLI glutamatergic synapses using a field-stimulating electrode placed in the molecular layer of the cerebellum to activate the parallel fiber axons from granule cells (Fig. 1.1*A*). Using this approach, two types of responses were observed in current-clamp recordings (Fig. 1.1*B,C*). In most of the recordings (n=10), a single stimulation elicited a compound response composed of an initial excitatory postsynaptic potential (EPSP) that overlapped with an inhibitory postsynaptic potential (IPSP) (Fig. 1.1*B*)

suggesting that both excitatory parallel fiber-MLI (PF-MLI) synapses and inhibitory synapses had been stimulated. MLIs receive input from many inhibitory cells in the cerebellar cortex; therefore, the observed inhibitory signal could arise from the axons of adjacent MLIs and/or Lugaro and globular cells (Fritschy and Panzanelli, 2006). In other recordings (n=8), field stimulation evoked a monophasic EPSP without any detectable hyperpolarization, suggesting that only PF-MLI excitatory synapses were activated (Fig. 1.1*C*).

To study GABAergic synapse plasticity, we adapted a high frequency stimulation (HFS) protocol used in other studies to elevate ROS (Li et al., 2011). This HFS protocol is also in line with *in vivo* firing rates of cerebellar granule cells and the frequency of synaptic transmission for cerebellar MLIs (Chadderton et al., 2004). Using this protocol, a decline in the eEPSP amplitude was observed in recordings with a biphasic response over the 25 minutes following HFS ($Peak_{25}$ 48.6 ± 5% of initial response, n=10, $F(5,45)=34.55$, $p<0.00001$, repeated measures ANOVA) (Fig. 1.*1B,E,F*). In contrast, the EPSP amplitude was unchanged in cells exhibiting a monophasic response ($Peak_{25}$, 98.3 ± 2 %, n=8, $F(5,40)=1.70$, $p=0.15$, repeated measures ANOVA) suggesting that HFS did not directly affect the efficacy of glutamatergic transmission (Fig. 1.1*C,E,F*). We therefore reasoned that the decline elicited by HFS in cells with a biphasic response was due to a strengthening of inhibitory transmission. In agreement with this, application of 10 µM bicuculline, to block $GABA_A$ receptors and the observed hyperpolarization, prevented the decline in the eEPSP amplitude ($Peak_{25}$, 115.6 ± 17 %, n=4, $x^2(5)=2.74$, $p=0.74$, Friedman test) (Fig. 1.1*D,E,F*).

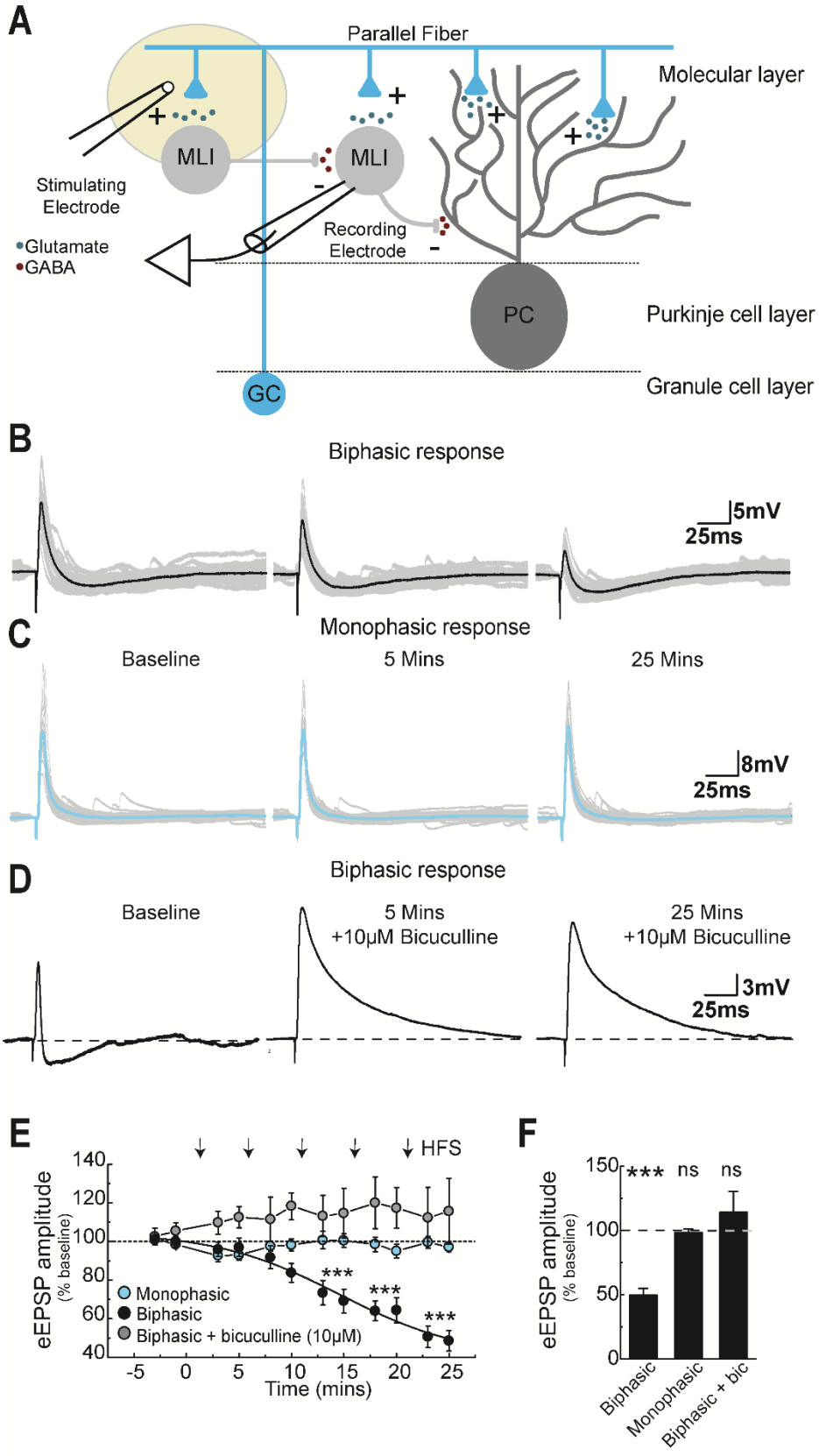
A
Parallel Fiber
Molecular layer
MLI
MLI
Stimulating Electrode
Recording Electrode
Glutamate
GABA
PC
Purkinje cell layer
GC
Granule cell layer
B
Biphasic response
5mV
25ms
C
Monophasic response
Baseline
5 Mins
25 Mins
8mV
25ms
D
Biphasic response
Baseline
5 Mins
+10μM Bicuculline
25 Mins
+10μM Bicuculline
3mV
25ms
E
HFS
eEPSP amplitude
(% baseline)
Monophasic
Biphasic
Biphasic + bicuculline (10μM)
***
***
***
Time (mins)
F
eEPSP amplitude
(% baseline)
***
ns
ns
Biphasic
Monophasic
Biphasic + bic

Figure 1.1: Repetitive stimulation of MLI excitatory synapses strengthens inhibitory neurotransmission
*(A) Schematic illustrating the arrangement of stimulating and recording electrodes. Stimulating electrode was positioned to focally depolarize (yellow circle) excitatory and inhibitory axons of cells innervating MLIs (MLI = molecular layer interneuron, PC = Purkinje cell, GC = granule cell). (B,C) Representative current-clamp recordings from two MLIs with either a biphasic or monophasic response at three time points; before (baseline) and after (5 mins or 25 mins) HFS. (D) Representative current-clamp recordings from a MLI with a biphasic response at three time points; before (baseline) and 5 mins after application of the $GABA_AR$ antagonist bicuculline and 25 mins after HFS + bicuculline treatment. (E) Time course plot of the eEPSP amplitude before and after HFS from monophasic (n = 7) or biphasic (n = 10) cells or biphasic cells in the presence of the bicuculline (n = 4). (F) Summary plot of the eEPSP amplitude at 25 mins following HFS shown as a percentage of the initial baseline (Tukey's post-hoc contrasts: ***=p<0.001).*

To better quantify the increase in GABAergic transmission, we performed the same HFS protocol in voltage-clamp mode and measured the evoked inhibitory postsynaptic currents (eIPSCs) (Fig. 1.2). We observed a two-fold increase in the eIPSC amplitude following the HFS protocol (HFS $Peak_{25}$, 200.3 ± 35 %, n = 7, $F(5,30)=5.97$, $p=0.0006$, repeated measures ANOVA) which was accompanied by a slowing in decay kinetics (Fig. 1.2*A*-*D*). This latter observation is consistent with our previous finding showing that elevation in ROS levels promotes the recruitment of α3-containing $GABA_A$ receptors into inhibitory MLI synapses (Accardi et al., 2014). Potentiation was absent in experiments where the recorded cell did not receive HFS reaffirming that GABAergic transmission is stable under basal conditions (Control $Peak_{25}$, 105.5 ± 8 %, n=8, $x^2(5)=2.67$, $p=0.75$, Friedman test). Furthermore, the potentiation of eIPSC amplitude was present only when the HFS protocol was paired with a depolarization to +40mV and not when HFS was performed at -60mV ($Peak_{25}$ 95.6 ± 9 %, n=6, $x^2(5)=0.57$, $p=0.98$, Friedman test) (Fig. 1.2*A*-*C*). This latter finding suggests that the induction of long-term potentiation in GABAergic transmission (i.e. iLTP) may be postsynaptic and also involve an elevation in cytosolic Ca^{2+}. In agreement with this, inclusion of 10 mM BAPTA, to chelate cytosolic Ca^{2+}, eliminated the increase

in eIPSC amplitude ($Peak_{25}$, 89 ± 5 %, n=5, $x^2(5)=9.45$, p=0.06, Friedman test) and prevented the slowing in decay kinetics (control τ, 15.3 ± 1.1ms, +40mV HFS τ, 20.1 ± 1.9ms, +BAPTA τ, 14.1 ± 1.7ms) observed when HFS was paired with a depolarization step to +40 mV (Fig. 1.2*A-D*).

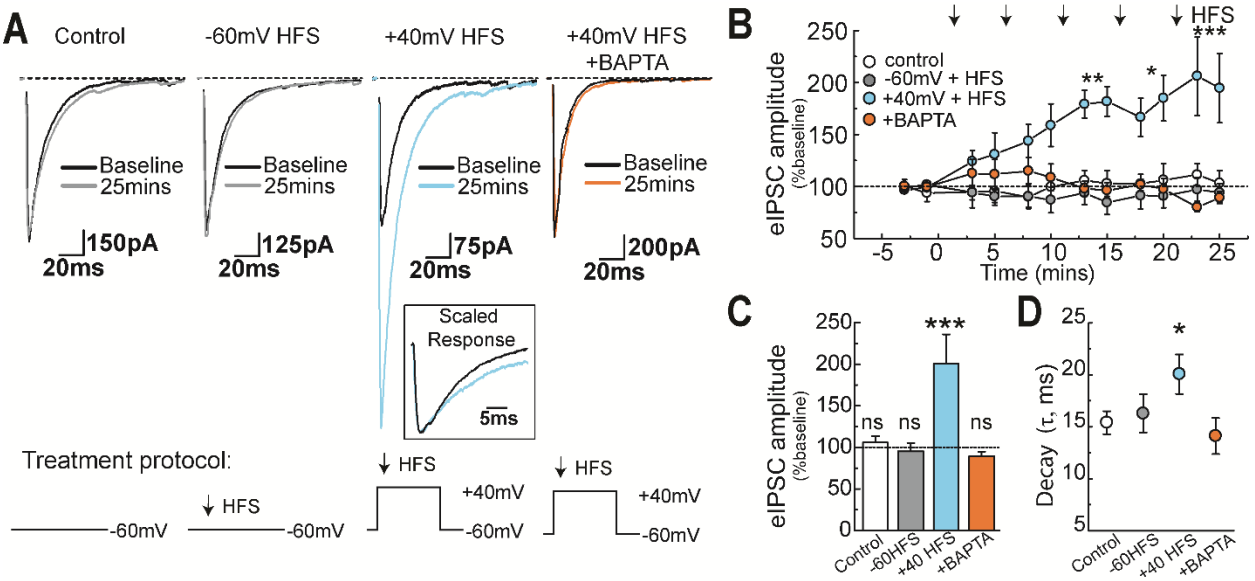

Figure 1.2: High frequency stimulation evokes an increase in eIPSC amplitude and a slowing of decay kinetics.

*(A) $GABA_AR$ currents from different MLIs just before the start (i.e. baseline) of the HFS protocol at t=0 mins and after 25 mins. (Inset) Scaled response from the same trace as the +40HFS demonstrating the slowing of decay kinetics following the HFS treatment. (B) Summary plot of the time course of eIPSC amplitude during and following HFS expressed as a percentage of the baseline. (C) Summary bar graph of the eIPSC amplitude observed in different experimental conditions at 25 mins after HFS and expressed as a percentage of the baseline. (D) Summary plot comparing the decay kinetics of eIPSCs at 25 mins in different experimental conditions after HFS. Error bars, s.e.m (Tukey's post hoc contrasts: *=p<0.05, **=p<0.01, ***=p<0.001).*

Activation of NMDARs strengthens postsynaptic inhibitory synapses

Previous work has shown that fast glutamatergic signaling in MLIs is primarily mediated by synaptic AMPA receptors (AMPARs), with a smaller contribution from extrasynaptic NMDARs (Clark and Cull-Candy, 2002). To determine the impact of each receptor subtype following a single

stimulus or HFS, we compared the effect of AMPAR and NMDAR selective antagonists on the glutamatergic response (Fig. 1.3*A*-*D*). Given the strong voltage-dependent block of NMDARs by external Mg^{2+} at negative membrane potentials, we recorded membrane currents at both -60 and +40 mV. As previously reported (Clark and Cull-Candy, 2002), most of the glutamatergic response from a single stimulation at a holding potential of -60 mV was blocked by the selective AMPAR antagonist, GYKI 53655 (10 µM) demonstrating the predominant contribution of postsynaptic AMPARs (Fig. 1.3*A,D*). In contrast, the glutamatergic response after HFS stimulation at +40 mV, exhibited a greater APV-sensitive component due to a greater contribution of NMDARs (Fig. 3*B*-*D*). In keeping with this, the charge transfer (Q) observed in control conditions at +40 mV (Q = 49.1 ± 8.6 pC, n = 10) was similar to the charge transfer measured following bath application of 10 M GYKI 53655 to isolate the NMDAR response (Q=41.7 ± 12.3 pC, n=10, W(9)=12, p=0.25, Wilcoxon signed-rank test) (Fig. 1.3*B*-*D*). To directly test the hypothesis that NMDAR activation is required for strengthening GABAergic signaling, we repeated the HFS protocol in slices pre-incubated with 10 µM D-APV to block NMDARs (Fig. 1.3*E,F,*G). Under these conditions, the reduction in peak eEPSP of the biphasic response failed to occur ($Peak_{25}$, 111.2 ± 8 %, n=4, F(5,15)=0.33, p=0.88, repeated measures ANOVA) (Fig. 1.3*E,F,G*) establishing that extrasynaptic NMDARs couple signaling between glutamatergic and GABAergic synapses in cerebellar MLIs. In agreement with our previous result in voltage-clamp (Fig. 1.2), inclusion of high concentrations of BAPTA in the patch electrode also eliminated the reduction in the eEPSP amplitude (Fig. 1.3*G*) demonstrating that NMDARs strengthen GABAergic transmission through an elevation in cytosolic Ca^{2+}.

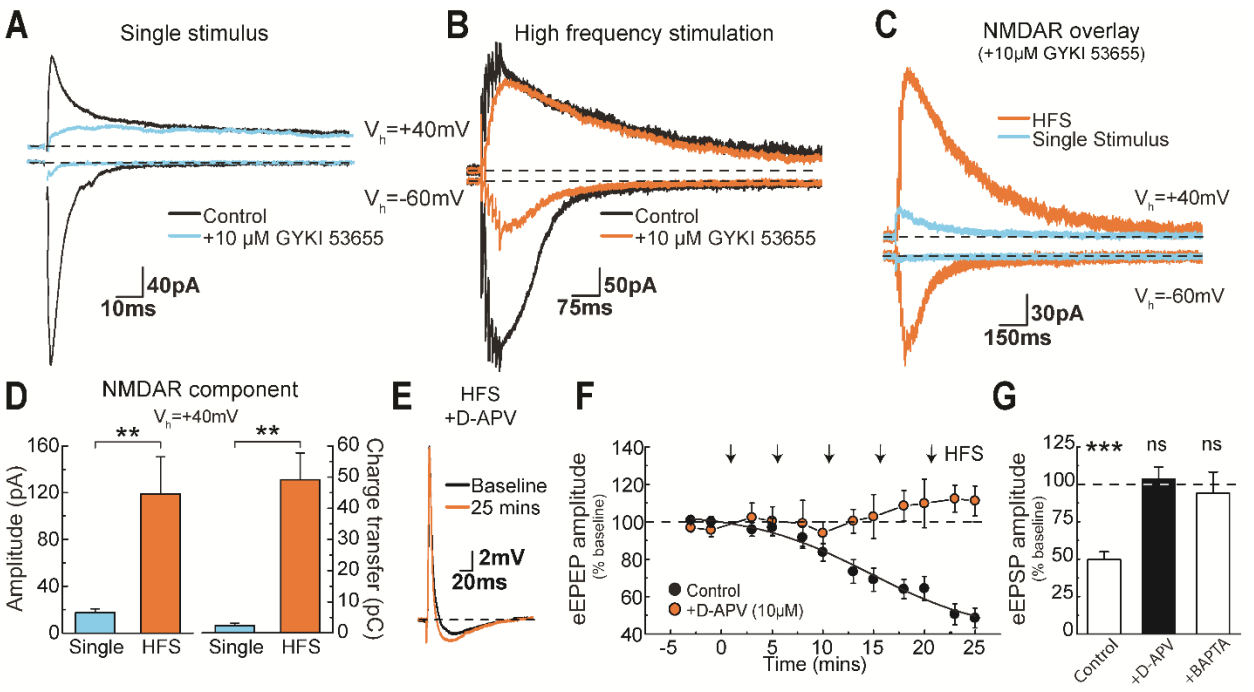

Figure 1.3: GABAergic synapses are strengthened by the activation of extrasynaptic NMDARs.
*(A) Representative traces of evoked currents from a single stimulus at +40 mV (top) or -60 mV (bottom) membrane potential. Traces in blue or black denote responses observed in the presence or absence of the AMPAR antagonist, GYKI 53655 (10 μM), respectively. (B) Representative traces of evoked currents (from the same cell as (A)) during a 100 Hz 6 train stimulus (or HFS) at a membrane potential of +40 mV (top) and -60 mV (bottom) in the presence (orange trace) and absence (black trace) of GYKI 53655. (C) Overlay of pharmacologically-isolated NMDAR currents (same traces as in A and B) following a single stimulus (blue trace) or during a 100 Hz 6 stimulus train (orange trace, HFS) at +40 mV and -60 mV membrane potential. Stimulation artifacts have been removed for clarity. (D) Bar graph of the peak amplitude (left, t(9)=3.43, p=0.007, paired t-test) or charge transfer (right, t(9)=3.32, p=0.009, paired t-test) of NMDAR responses following a single stimulus or during a HFS train. (E) Representative current-clamp recordings from a MLI with a biphasic response in the presence of the NMDAR antagonist D-APV before and after HFS treatment. (F) Time course plot of the eEPSP amplitude before and after HFS in the presence (n = 4; open circle) and absence (n = 10; filled circles) of D-APV. Arrows indicate when the HFS protocol was performed. (G) Summary plot of the eEPSP amplitude at 25 mins following HFS expressed as a percentage of the baseline. Error bars, s.e.m. Control data represents the biphasic response from figure 1 and is shown for comparison purposes. (**=p<0.01, ***=p<0.001).*

NMDA receptors strengthen GABAergic synapses via a NO-dependent pathway

Since NMDARs can elevate ROS levels in other neurons (Dugan et al., 1995; Reynolds and Hastings, 1995) and strengthen GABAergic signaling in cerebellar MLIs (Accardi et al., 2014), we tested whether a ROS-dependent mechanism could be responsible for the induction of iLTP in

this study. To do this, we first included the antioxidant, N-acetylcysteine (NAC, 1 mM), in the patch electrode solution (Fig. 1.4*A*) which, as anticipated, eliminated the decline in the net depolarization following HFS ($Peak_{25}$, 117 ± 21 %, n = 4, F(5,15)=0.35, p=0.87, repeated measures ANOVA) (Fig. 1.4*B*). Since intracellular NAC does not antagonize $GABA_A$ receptor responses (Accardi et al., 2014; Accardi et al., 2015), we concluded that the failure of the HFS protocol to reduce the net depolarization was due to the antioxidant properties of NAC. To determine the origin of ROS production, the pharmacological agents 3-Br-7-Nitroindazole (10 μM 3-Br-7-Ni), apocynin (100 μM Apo), and ruthenium red (1 μM RR) were included in the patch electrode solution to selectively inhibit the activity of neuronal nitric oxide synthase (nNOS or NOS-1), NADPH oxidase (NOX2) and the mitochondrial Ca^{2+} uniporter, respectively. Although 3-Br-7-Ni also inhibits the other NOS isoforms, iNOS (or NOS-2) and eNOS (NOS-3), RNAseq and data from nNOS specific KO animals reveal that only nNOS is expressed in cerebellar MLIs (Huang et al., 1993; Zeisel et al., 2018). The decline in the net depolarization was greatly attenuated by pharmacological block of nNOS and NOX2 with peak responses at 25 mins of 87.1 ± 5 % (3-Br-7-Ni, n=5 F(5,20)=2.40, p=0.073, repeated measures ANOVA) and 100.6 ±7 % (Apocynin, n=5, $x^2(5)=6.371$, p=0.272, Friedman test) respectively (Fig. 1.4*A,B*). In contrast, inhibition of the mitochondrial Ca^{2+} uniporter with 1 μM RR did not affect the ability of the HFS protocol to attenuate the eEPSP amplitude ($Peak_{25}$, 45.5 ± 10 %, n = 4, $x^2(5)=17.857$, p=0.003, Friedman test) (Fig. 1.4*A,B*). These results demonstrate that nNOS and NOX2 are responsible for the iLTP observed following NMDAR activation.

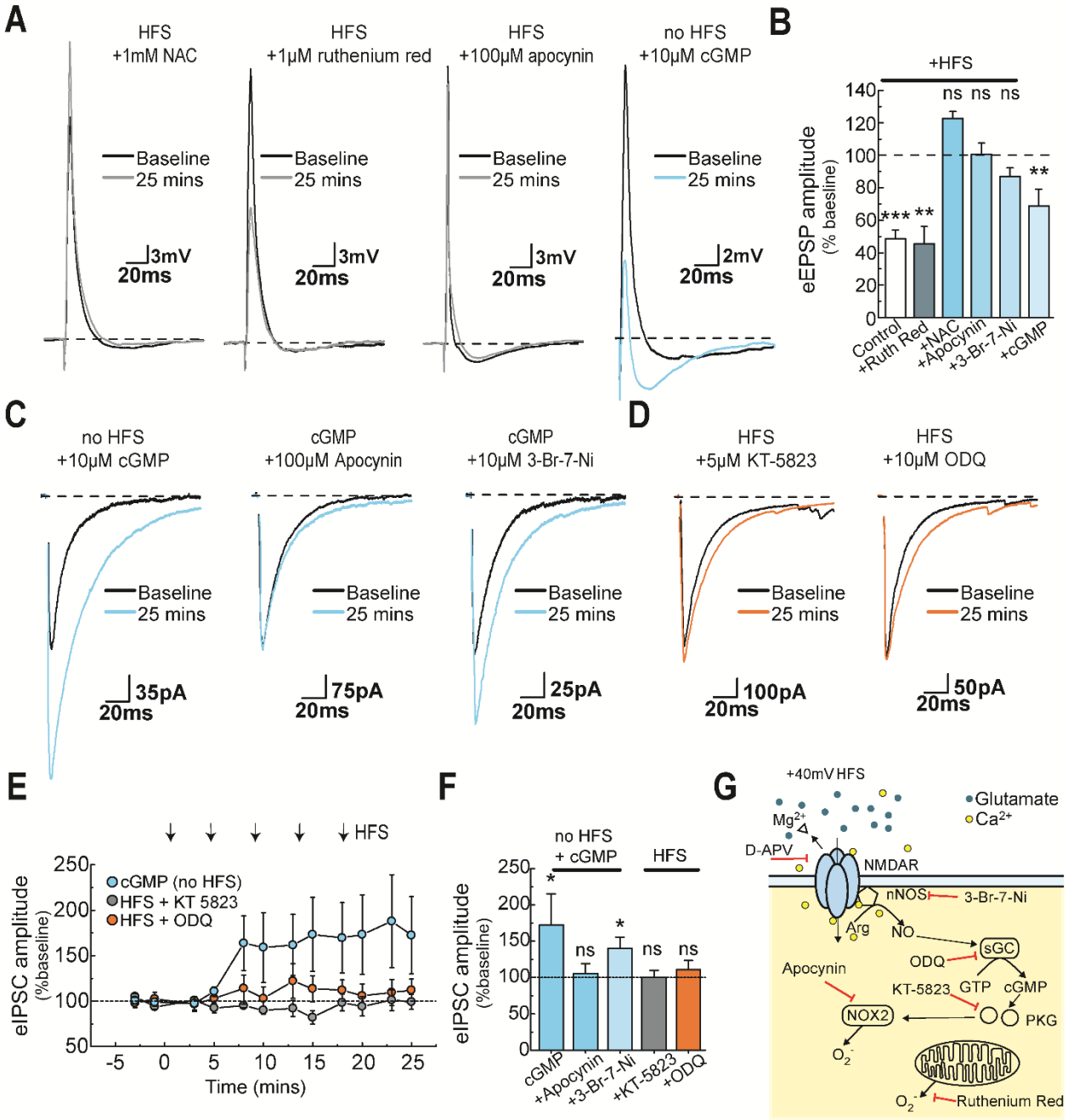

Figure 1.4: Inhibition of nitric oxide synthase and NADPH oxidase blocks iLTP

(A) Representative recordings from four different MLIs in current-clamp showing the response to patch electrode perfusion with different pharmacological agents. The first three traces show the overlay of responses before (black) and after (gray) HFS. In each case, the recording electrode solution contained either N-acetylcysteine, ruthenium red or apocynin. The rightmost trace shows the overlay of two averaged EPSPs at the beginning (black) of patch perfusion with cGMP and after 25 mins (blue). (B) Summary bar graph of the eEPSP amplitude at 25 mins under different conditions expressed as a percentage of the baseline. Error bars, s.e.m. (C) Representative $GABA_AR$ membrane currents from three different voltage-clamped MLIs at the start (black) and after 25 mins (blue) of internal patch perfusion with cGMP. (D)

Representative $GABA_AR$ currents from two different voltage-clamped MLIs at baseline (black) and 25 mins after HFS (orange) with internal patch perfusion of KT-5823 (PKG inhibitor) or ODQ (guanylate cyclase inhibitor). (E) Summary plot of the time course of eIPSC amplitude during internal perfusion of cGMP or HFS treatment. (F) Summary bar graph of the change in eIPSC amplitude after 25 mins perfusion with internal perfusion of cGMP or HFS treatment with pharmacological blockers. Data is expressed as a percentage of the baseline. (G) Schematic diagram outlining the key signaling steps triggered by Ca^{2+} influx through NMDARs. An elevation in cytosolic Ca^{2+}, activates nNOS which generates NO from arginine (Arg). NO's action on guanylate cyclase (sGC) generates cGMP from GTP which, in turn, signals to PKG and NOX2 to generate the ROS, superoxide (O_2^-). Line markers in red denote the pharmacological target of 3-Br-7-Ni (nNOS), apocynin (NOX2), ruthenium red (mitochondria), D-APV (NMDAR), KT-5823 (PKG) and ODQ (sGC). Error bars, s.e.m. (=p<0.05, **=p<0.01, ***=p<0.001)*

The fact that iLTP can be eliminated by pharmacological block of nNOS or NOX2 suggests both enzymes share a common signaling pathway. Since prior work has shown that nNOS activity is upstream of NOX2 in neurons (Girouard et al., 2009), we reasoned that a similar sequence of events may occur in MLIs. For example, a rise in nitric oxide levels through nNOS activity is known to first elevate cGMP levels via guanylate cyclase which in turn activates protein kinase G (PKG) with downstream activation of NOX2 (Girouard et al., 2009). To determine if a similar sequence of events occurs in MLIs, we directly stimulated PKG by perfusing a non-hydrolysable cGMP analog through our patch pipette (Fig. 1.4*A C,E,F*). In separate current- and voltage-clamp experiments, direct activation of PKG resulted in a decrease in eEPSP amplitude ($Peak_{25}$, 68.7 ± 10 %, n=7 F(6,30)=4.56, p=0.003, repeated measures ANOVA) and a potentiation of the eIPSC amplitude ($Peak_{25}$, 180.3 ± 10 %, n=6 F(5,25)=3.09, p=0.02, repeated measures ANOVA) respectively (Fig. 1.4*A,C*) demonstrating that iLTP is regulated by cGMP. Consistent with our HFS treatment, intracellular perfusion of cGMP also resulted in a slowing of decay kinetics (cGMP τ, 21.8 ± 3.7ms). Furthermore, pharmacological block of nNOS with 3-Br-7-Ni failed to eliminate the eIPSC potentiation ($Peak_{25}$, 139.9 ± 15 %, n=6 F(5,25)=2.87, p=0.03, repeated measures ANOVA)

whereas block of NOX2 activity with apocynin eliminated the effect of the cGMP analog ($Peak_{25}$, 105 ± 14 %, n=6, $x^2(5)=5.33$, p=0.37, Friedman test) (Fig. 1.4*C,F*). Conversely, including the PKG antagonist, KT-5823 (5 μM), in our internal patch solution eliminated any potentiation of the eIPSC amplitude following HFS (Peak25, 99.3 ± 8 %, n=7 F(6,30)=0.92, p=0.48, repeated measures ANOVA) (Fig. 1.4*D,E,F*). Finally, pharmacological block of guanylate cyclase by internal perfusion of ODQ (10 μM) also prevented any potentiation of the eIPSC following HFS (Peak25, 112 ± 12%, n=7, F(6,30)=0.78, p=0.57, repeated measures ANOVA) (Fig. 1.4*D,E,F*). Together, these data demonstrate that nNOS activation is upstream of NOX2 in a PKG-dependent pathway as summarized in Fig. 1.4*G*.

Protein kinase C strengthens GABAergic synapses following NMDA receptor activation

Several kinases have been shown to regulate the strength of GABAergic synapses by triggering the recruitment of synaptic $GABA_A$ receptors (Luscher et al., 2011). Many of these kinases also possess ROS-sensitive amino-acid residues in their regulatory or catalytic domains which can affect kinase activity. Specifically protein kinase A (PKA), protein kinase C (PKC) and CaMKII can be activated by ROS in addition to their canonical activation pathways (Knock and Ward, 2011). Given this, we reasoned that the iLTP observed in the present study could be due to ROS action on kinase activity.

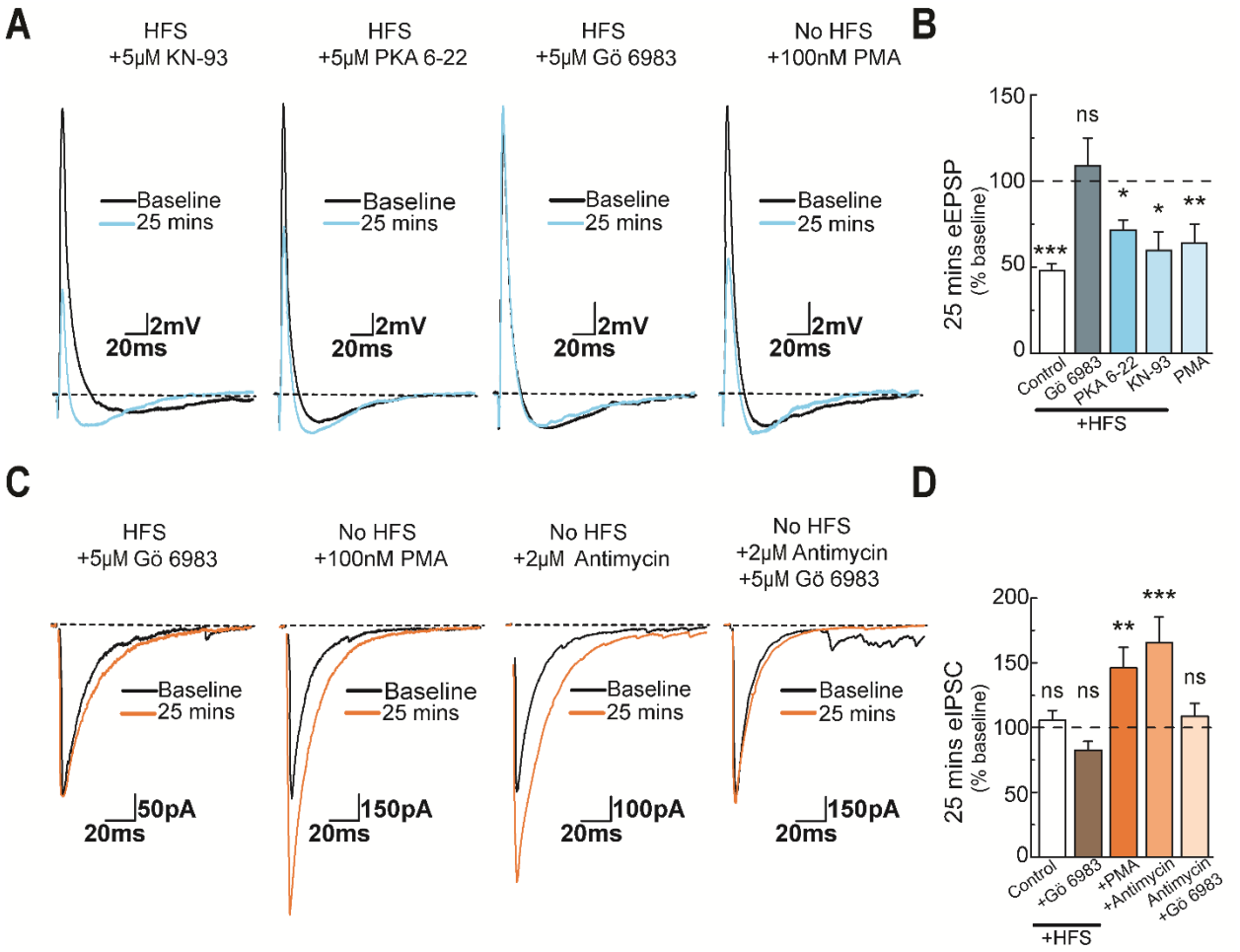

Figure 1.5: Activation of protein kinase C strengthens GABAergic synapses

(A) Representative recordings from four different MLIs in current-clamp showing the response to patch electrode perfusion with different kinase inhibitors or activators. The first three traces (left to right) show the overlay of responses before (black) and after (blue) HFS. In each case, the recording electrode solution contained either KN-93, PKA 6-22 or Gö 6983. The rightmost trace shows the overlay of two averaged EPSPs at the beginning (black) of patch perfusion with the phorbol ester, PMA, and after 25 mins (blue). (B) Summary bar graph of the eEPSP amplitude at 25 mins under different conditions expressed as a percentage of the baseline. Error bars, s.e.m. (C) Representative $GABA_AR$ membrane currents from four different MLIs in the voltage-clamp configuration. Synaptically-evoked membrane currents observed prior to the onset of HFS (black) and after 25 mins (orange) in the presence of the PKC inhibitor, Gö 6983 (left). The remaining traces correspond to eIPSCs observed at the start (black) and after 25 mins (orange) of patch perfusion with PMA, antimycin-A and antimycin-A + Gö 6983. (D) Summary bar graph of the data shown in panel C expressed as a percentage of the baseline. Error bars, s.e.m. (=p<0.05, **=p<0.01, ***=p<0.001)*

To test this, we performed the HFS experiment while perfusing individual MLIs with either KN-93 (5 μM), protein kinase inhibitor-(6-22)-amide peptide (5 μM) or Gö 6983 (5 μM) to selectively inhibit CaMKII, PKA and PKC respectively (Fig. 1.5). Pharmacological inhibition of PKA and CaMKII still resulted in a decline in the eEPSP amplitude following HFS with peak responses after 25 mins of 71.5 ± 5 % (n=6 $x^2(5)=23.23$, p=0.0003, Friedman test) and 57.2 ± 9 % respectively (n = 4 $x^2(5)=11.43$, p=0.04, Friedman test) (Fig. 1.5 *A,B*). In contrast, inhibition of PKC by 5 M Gö 6983 eliminated the induction of iLTP by the HFS protocol (Fig. 1.*5A*) with peak responses at 25 mins of 108.7 ± 16 % (n = 5 $x^2(5)=5.43$, p=0.36, Friedman test) (Fig. 1.*5B*). Similarly, inclusion of 5 M Gö 6983 in voltage-clamp experiments also prevented iLTP (Fig. 1.*5C,D*). In support of this, direct activation of PKC with phorbol myristate acetate (PMA, 100nM), elicited a similar time-dependent onset of iLTP in both current- and voltage-clamp experiments (Fig. 1.*5A-D*). We observed a decrease in the eEPSP to 63.9 ± 12 % of the baseline eEPSP (n=4, $x^2(4)=13.8$, p=0.008, Friedman test) in current-clamp recordings and an increase to 146 ± 16 % of the baseline eIPSC (n=6, repeated measures ANOVA $F(4,20)=4.77$, p=0.007) in voltage-clamp (Fig. 1.*5A-D*). Interestingly, we also observed iLTP following the inclusion of the metabolic uncoupler, antimycin A, to generate mitochondria ROS in MLIs which was eliminated by the PKC inhibitor (Fig. 1.5*C,D*). This latter finding demonstrates that our previous study linking mitochondrial ROS (mROS) to the strengthening of GABAergic signaling in cerebellar MLIs is mediated through PKC (Accardi et al., 2014). A similar PKC-dependent pathway may also explain the effect of mROS on α6-containing $GABA_A$Rs of cerebellar granule cells (Accardi et al., 2015). Taken together, these data show that ROS-induced iLTP in MLIs relies on a PKC-dependent signaling pathway.

Synapse strengthening requires GABARAP and recruitment of α3-containing $GABA_A$ receptors

Although MLIs express both α1- and α3-containing $GABA_A$ receptors (Laurie et al., 1992c), previous work from our lab has shown that ROS-mediated synapse strengthening relies exclusively on the recruitment of postsynaptic α3-containing receptors (Accardi et al., 2014). Though more numerous, α1-containing $GABA_AR$ synapses are unaffected by ROS in both stellate and granule cells of the cerebellum (Accardi et al., 2014; Accardi et al., 2015). To determine whether NMDAR-dependent strengthening of GABAergic transmission also relies upon α3-containing receptors, we repeated the HFS protocol in cerebellar slices from α3 KO mice (Fig. 1.6). As anticipated, GABAergic strengthening elicited by HFS was absent in MLIs lacking the α3-subunit ($Peak_{25}$, 115.3 ± 15 %, n = 7, $x^2(5)=6.59$, p=0.25, Friedman test) (Fig. 1.6 *A*-*C*) confirming that the strengthening of MLI inhibitory synapses is subunit-dependent.

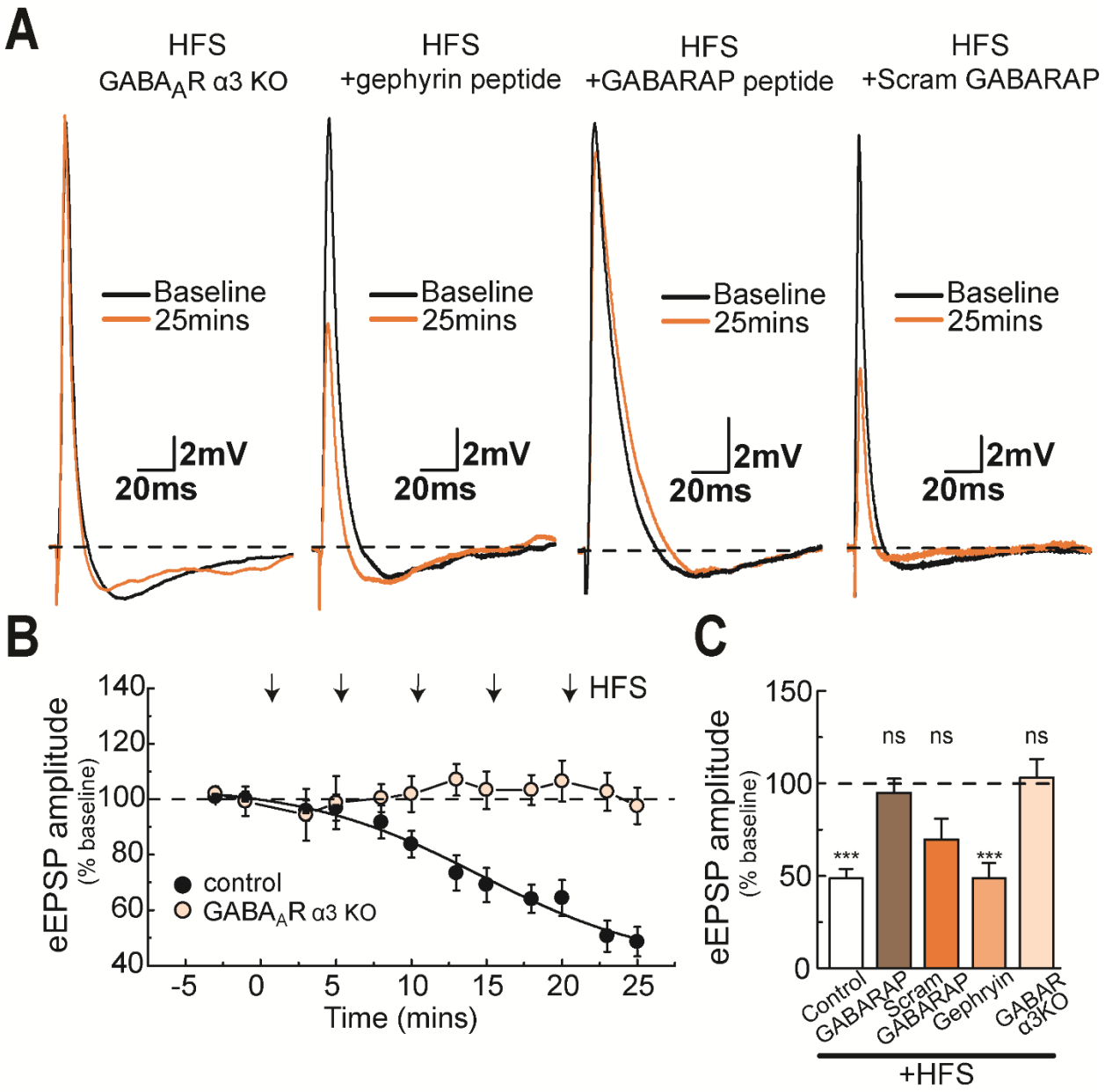

Figure 1.6: iLTP is dependent on α3-containing GABAA receptors and GABARAP

(A) Overlay of eEPSP recordings from four different MLIs in current-clamp configuration before the start of HFS (black) and after 25 mins (orange). (left to right) Representative examples of recordings from MLIs from a GABA$_A$R α3 KO mouse (cell #151110r1) and wildtype cells perfused with the gephyrin interfering peptide (cell #150612r1), GABARAP interfering peptide (cell #150518r1) and scrambled GABARAP peptide (cell # 150908r1). (B) Time course of the averaged eEPSP amplitude before and after HFS for the biphasic response from figure 1 and in recordings from GABA$_A$R α3 KO mice. (C) Summary bar graph of eEPSP amplitude at 25 mins following HFS expressed as a percentage of the baseline. Error bars, s.e.m. (=p<0.05, **=p<0.01, ***=p<0.001).*

$GABA_A$Rs interact with a number of scaffolding proteins which regulate receptor trafficking and clustering at inhibitory synapses. To investigate which protein interactions are responsible for synaptic targeting of α3-containing $GABA_A$ receptors, we focused on two prominent $GABA_A$R scaffolding proteins linked to inhibitory synapse plasticity (Petrini and Barberis, 2014): gephyrin (Tyagarajan and Fritschy, 2014) and GABA(A)-receptor-associated protein (GABARAP) (Wang et al., 1999). Previous work has identified that gephyrin binds directly to the GABA α3-subunit (Tretter et al., 2011) while GABARAP is known to bind to the γ2-subunit (Wang et al., 1999). In keeping with this, co-expression of recombinant α3β2γ2 $GABA_A$ receptors in HEK293 cells with either gephyrin or GABARAP revealed that both scaffolding proteins co-immunoprecipitate with the ion-channel complex (Fig. 1.7). Consequently, we used two short-chain peptides, namely α3-derived peptide (Tretter et al., 2011; Maric et al., 2014) and K1 GABARAP peptide (Weiergräber et al., 2008), to interfere with the binding of gephyrin or GABARAP, respectively to recombinantly expressed α3-containing $GABA_A$ receptors (see Methods) (Fig. 1.7*B*). These peptides were then used in separate electrophysiology experiments to test for the role of gephyrin and/or GABARAP in MLI inhibitory synapse strengthening.

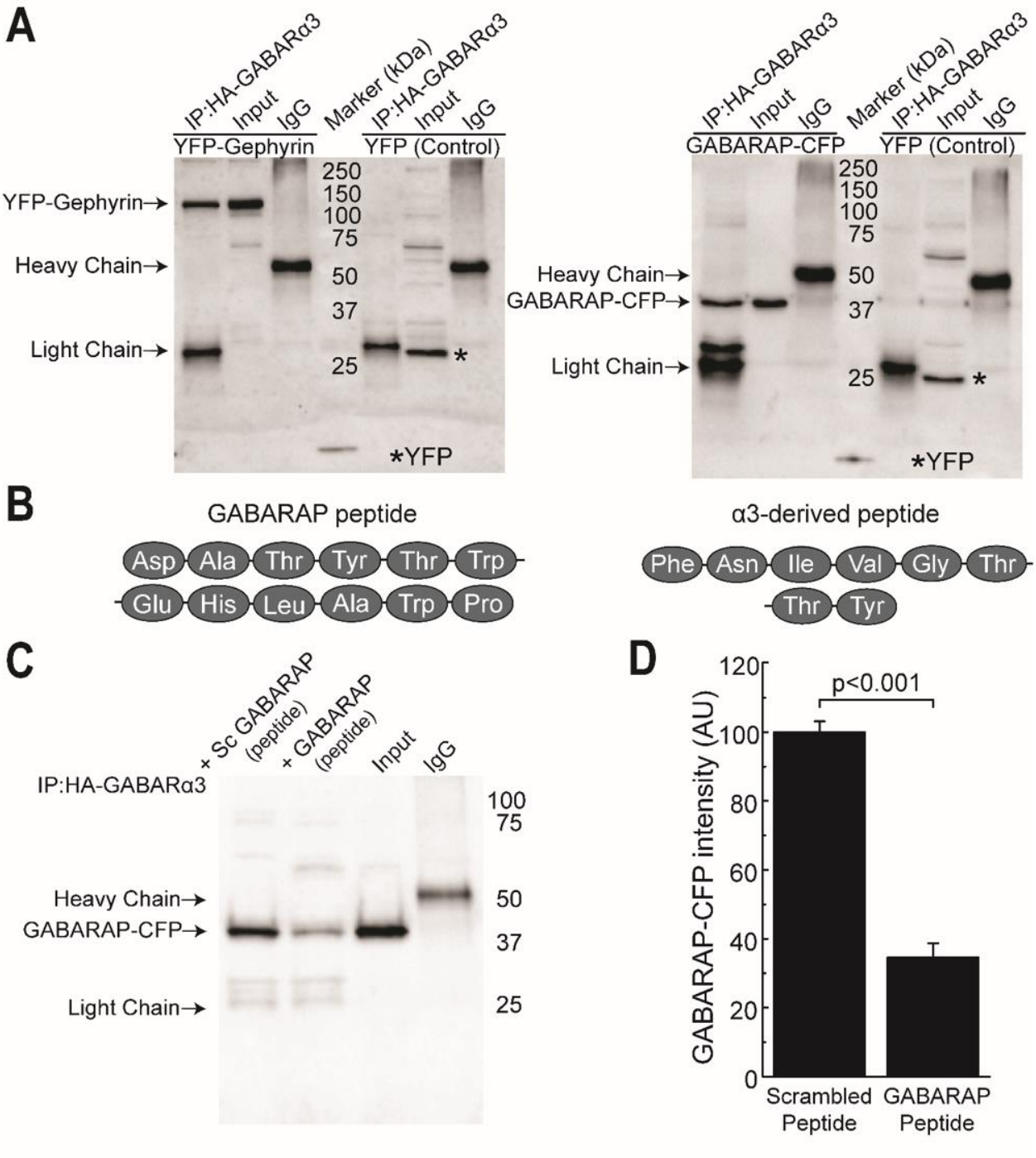

Figure 1.7: Co-assembly of α3-containing GABAA receptors with GABARAP can be disrupted by short-chain interfering peptides

(A) Western blots of lysates from HEK 293 cells transfected with HA-GABA$_A$R-α3, GABA$_A$R-β2 and GABA$_A$R-γ2 (short) to form $\alpha 3\beta 2\gamma 2$ GABA$_A$R channels that have been co-expressed with either Gephyrin-YFP (left) or GABARAP-CFP (right). (A-left) Blot with eluates and inputs (n = 3) of cell lysates immunoprecipitated with an anti-HA antibody and analyzed by immunoblotting with an anti-GFP antibody. YFP is presented as

a negative control (Note that the anti-GFP antibody recognizes both YFP and CFP). (A-right) Blot with eluates and inputs (n = 3) of cell lysates immunoprecipitated with an anti-HA antibody and analyzed by immunoblotting with an anti-GFP antibody. (B) Primary amino-acid sequence of the K1-GABARAP blocking peptide and the α3-derived-gephyrin blocking peptide. (C) Scrambled GABARAP peptide or GABARAP peptide were added to lysates from the same transfections and pulled down with anti-HA antibody. Immunoblotting was performed with an anti-GFP antibody, as in panel A. (D) Bar graph comparing GABARAP immunoblot levels after pre-incubation with GABARAP or scrambled peptide (p< 0.001, n=4, Student's t test; error bars, s.e.m.).

Each peptide was included in the patch electrode solution during HFS protocols to interfere with the binding of the target protein (Fig. 1.6*A,C*). In all cases, we waited 15 mins from breakthrough before beginning the HFS protocol to allow the peptide to dialyze throughout the neuron and prevent protein-protein interactions. We observed that the rate and degree of onset of synapse strengthening induced by HFS was unaffected by the 3-derived, gephyrin-inhibiting peptide ($Peak_{25}$, 48.7 ± 8 %, n = 5, F(4,20)=6.86, p=0.0007, repeated measures ANOVA, Fig. 1.6*A,C*) suggesting that α3-containing $GABA_A$ receptors are not recruited to inhibitory synapses via a gephyrin-dependent mechanism. In contrast, inclusion of the K1 GABARAP peptide in the patch electrode solution eliminated the induction of synapse strengthening (Fig. 1.6*A,C*; F(5,40)=1.22, p=0.35, repeated measures ANOVA) indicating that GABARAP is required for the synaptic recruitment of α3-containing $GABA_A$ receptors. In agreement with this, pre-incubation of the K1 GABARAP peptide with lysates of cells co-expressing α3-containing $GABA_A$ receptors disrupted GABARAP binding establishing the specificity of the interaction (Fig. 1.7*C,D*). Moreover, a scrambled version of the K1 GABARAP peptide failed to disrupt the binding of GABARAP to the $GABA_AR$ complex (Fig. 1.7*C,D*). Additionally, the scrambled peptide failed to prevent the induction of iLTP by the HFS protocol (n = 4, 69.6 ± 11 %) (Fig. 1.6*A,C*) further confirming the specificity of the K1 GABARAP peptide interaction with α3-containing $GABA_A$ receptors.

1.6 Discussion

The present study advances our understanding of how NO signaling regulates the excitatory/inhibitory balance in the mammalian brain in several new and important ways. First, we show that NO generated by NMDAR activation strengthens inhibitory GABAergic synapses through a series of sequential steps involving nNOS, NADPH oxidase, and PKC as outlined in figure 8. These observations are distinct from previous work which has shown that NMDARs strengthen GABAA receptor synapses through a different pathway involving CaMKII. Second, we show that the strengthening of α3-containing GABAAR synapses in MLIs is reliant on the scaffolding protein, GABARAP, rather than gephyrin. Our data does not exclude a role for gephyrin at α3-receptor synapses but nevertheless highlights that GABARAP has a prominent role in the recruitment process. Finally, given the widespread but cell-selective expression of the NMDAR/nNOS complex, our findings suggest that NO control of GABAergic synapses through NMDARs may be more widespread in the vertebrate brain than has been appreciated.

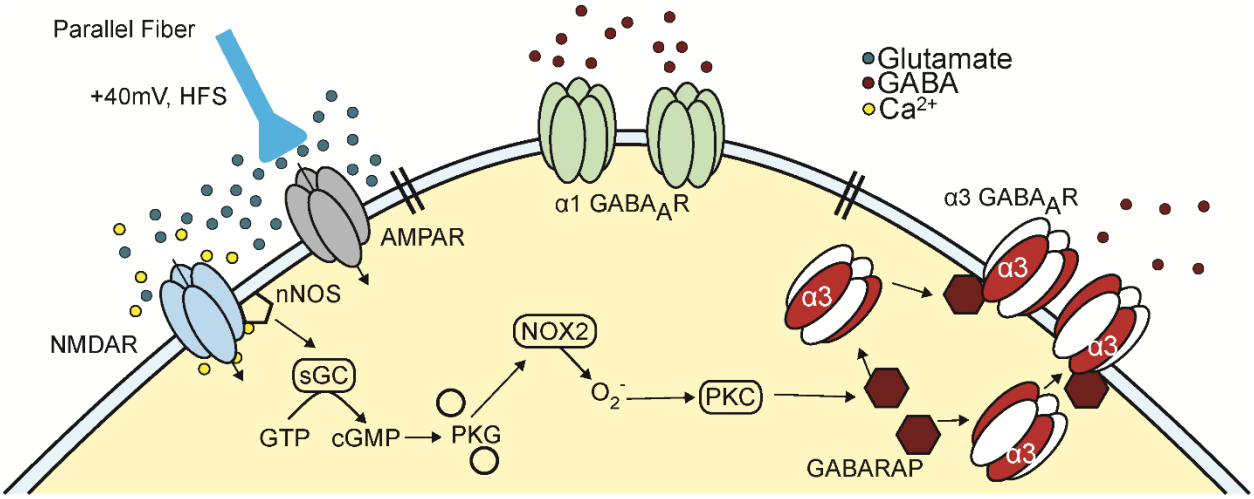

Figure 1.8. Summary of iLTP signaling pathway

Schematic diagram summarizing the main signaling events and molecules that lead to the selective recruitment of α3-containing $GABA_AR$s into inhibitory synapses of cerebellar MLIs. HFS of parallel fibers from granule cells stimulates extrasynaptic NMDARs of MLIs and activates nNOS through the influx of external Ca^{2+}. nNOS generates NO which acts on guanylate cyclase (sGC) elevating cGMP which, in turn, stimulates PKG and NOX2. We speculate the production of superoxide by NOX2 leads to the activation of PKC and the recruitment of $GABA_AR$s via a GABARAP-dependent pathway. This signaling pathway selectively acts on α3-containing $GABA_AR$s and does not affect synapses containing α1-$GABA_AR$s.

Nitric oxide strengthens inhibitory GABAergic synapses following NMDAR activation

Multiple pre- and postsynaptic mechanisms elicit long-term changes in the efficacy of GABAergic synapses (Kullmann et al., 2012) with one of the most prominent pathways involving an increase in the number of GABAA receptors per synapse (Luscher et al., 2011). NMDAR-mediated strengthening of GABAergic synapses has been linked to an increase in cytoplasmic Ca2+ and subsequent activation of CaMKII (Marsden et al., 2007; Luscher et al., 2011; Chiu et al., 2019). Although Ca2+ entry through NMDARs is still a requirement in inhibitory synapse strengthening of MLIs, we excluded a role for CaMKII since its specific kinase inhibitor, KN-93, did not affect synaptic plasticity (cf. Fig. 1.5).

A recent study has shown that postsynaptic NMDARs of granule cells can enhance inhibitory transmission by the retrograde action of NO on presynaptic GABA terminals of Golgi cells in the rat cerebellum (Mapelli et al., 2016). Although we cannot completely exclude a presynaptic role of NO in the present study on the mouse cerebellum, our data suggest that almost all the molecular events triggered by NMDARs in MLIs are predominantly postsynaptic. For example, it is unlikely that a presynaptic mechanism could explain the effect of internal patch perfusion of the GABARAP blocking peptide on inhibitory synapse strengthening (Figs. 6 and 7) given that the peptide is membrane impermeant and thus confined to the cytoplasm of the recorded cell. Likewise, the effect of internal patch perfusion with cGMP and its inhibition by apocynin (Fig. 1.4) suggests that the signaling pathway involving both cGMP and NOX2 is postsynaptic. Furthermore, if NO was acting through a purely presynaptic mechanism, enhanced release of presynaptic GABA by NO would be expected to be observed at all inhibitory synapses. However, our data demonstrate that the enhancement of GABAergic transmission by NMDARs and NO occurs only at α3-containing inhibitory synapses and not α1-receptor synapses (Fig. 1.6). It is possible that NO has both pre- and postsynaptic targets at inhibitory synapses of MLIs. In this case, NO would selectively enhance presynaptic GABA release from α3- and not α1-receptor synapses whilst triggering the postsynaptic cell to generate NO, cGMP, activate NOX2 and PKC and finally promote the recruitment of postsynaptic α3-receptors.

Interestingly, a similar dual effect of NO might be at play at the inhibitory Golgi cell-granule cell synapse. In agreement with this, we have previously shown that reactive oxygen species enhance recruitment of postsynaptic α6- but not α1-containing $GABA_A$Rs in mouse granule cells (Accardi et al., 2015) whilst others have shown a presynaptic action of NO on GABA

release from rat Golgi cells (Mapelli et al., 2016). Differential regulation of input-specific GABAergic synapses onto the same neuron has recently been described in the cerebral cortex (Chiu et al., 2018) and striatum (Paraskevopoulou et al., 2019), consequently, it is possible that a similar arrangement is found in both inhibitory synapses of MLIs and granule cells of the cerebellum. An important caveat to both pre- and postsynaptic roles of NO in granule cells, however, is that nNOS expression in the presynaptic terminals of Golgi cells is high in the rat but almost completely absent from the mouse, particularly mice with the C57BL/6 background used in this study (Kaplan et al., 2013). Accordingly, NO may act primarily on presynaptic Golgi cell terminals in the rat and through a postsynaptic pathway in granule cells of the mouse. Whether nNOS expression at MLI inhibitory synapses is similarly species-dependent has yet to be examined.

GABAergic synapse strengthening is dependent on the scaffolding protein, GABARAP

Our experiments establish a key role for GABARAP in the strengthening of GABAergic synapses. Although different mechanisms may anchor $GABA_A$Rs at central synapses, the prevalent view is that gephyrin plays a prominent role in binding the α1-3 (Tretter et al., 2008; Mukherjee et al., 2011; Tretter et al., 2011) and/or 2-3 (Kowalczyk et al., 2013) $GABA_A$R subunits to the cytoskeleton (Tyagarajan and Fritschy, 2014). Although gephyrin-independent clustering of postsynaptic $GABA_A$ receptors has been reported (Kneussel et al., 2001; Lévi et al., 2004; Panzanelli et al., 2011) the role of other accessory proteins, such as GABARAP (Wang et al., 1999) and/or the dystrophin–glycoprotein complex (DGC) (Pribiag et al., 2014), has received less attention. Our data argue in favor of GABARAP playing an important role in the recruitment of α3-containing $GABA_A$ receptors during synapse strengthening (cf. Fig. 1.6). Although, we cannot

exclude a role for gephyrin at α3-receptor synapses, co-staining for the α3 subunit and gephyrin show very little overlap (Accardi et al., 2014) suggesting that α3 $GABA_AR$ subunits may associate with another trafficking/scaffolding protein in MLIs. Our findings are consistent with studies on cultured hippocampal neurons showing that there are low GABARAP levels at inhibitory synapses under basal conditions (Kittler et al., 2001) and that the levels increase following chemically-induced strengthening of inhibitory synapses (Marsden et al., 2007).

Widespread and cell-selective expression of $nNOS^+$ neurons in the mammalian brain

$nNOS^+$ neurons are expressed throughout the CNS (Vincent and Kimura, 1992; Southam and Garthwaite, 1993; Rodrigo et al., 1994) and are involved in many different CNS functions that include learning and memory, sleep, feeding behaviors, movement, pain, anxiety, and reproductive activity (Garthwaite, 2008; Steinert et al., 2010; Chachlaki et al., 2017; Garthwaite, 2019). It has long been recognized that nNOS activation and the downstream production of cGMP is linked to glutamatergic signaling, primarily through NMDARs in the cerebellum (Southam et al., 1991). Of note, nNOS activity is highest in the cerebellum compared to other brain regions (Forstermann et al., 1990) due to several $nNOS^+$ neuronal types, including granule cells and MLIs, but is curiously absent from PCs, the sole output neuron of the cerebellar cortex (Vincent and Kimura, 1992; Rodrigo et al., 1994). Our data establish a new function for nNOS in MLIs which is part of a sequential signaling pathway that strengthens inhibitory GABAergic synapses following NMDAR activation. NMDARs of MLIs are also involved in the tight coupling between neuronal communication and local blood flow during functional hyperemia where activation of NMDARs generates NO which promotes vasodilation of local capillaries (Rancillac et al., 2006).

Taken together, these observations suggest that NMDARs expressed by MLIs fulfill multiple functions that control the excitability of MLIs whilst impacting the physiological state of the surrounding cells and tissue. In keeping with this, unpublished data from our lab reveals that NMDARs also directly modulate MLI excitability (Alexander & Bowie, unpublished observation) through a signaling pathway that leads to a hyperpolarizing shift in sodium channel (Nav) activation and inactivation recently described (Alexander et al., 2019). Interestingly, this pathway does not involve PKC but instead signals through the actions of CaMKII (Alexander & Bowie, unpublished observation) suggesting that Ca^{2+}-influx through NMDARs in MLIs triggers a bifurcating pathway involving both CaMKII and nNOS. Given the multiple actions of NMDARs and nNOS in MLIs, it is tempting to speculate that similar roles are found in other $nNOS^{+}$ cells of the CNS. On that note, NMDAR activation and the generation of ROS or NO also lead to the strengthening of GABAergic transmission in cerebellar granule cells (Accardi et al., 2015; Mapelli et al., 2016) and vasodilation of local blood vessels (Mapelli et al., 2017) in a manner reminiscent of MLIs. Given this, it would be interesting in future studies to examine whether NMDAR activation of other $nNOS^{+}$ neurons outside the cerebellum similarly regulate $GABA_AR$ plasticity and local blood flow.

Author contributions:

E.A.L., M.V.A., T.J.S. and D.B. designed research; E.A.L., M.V.A., Y.W., M.D., and B.Y. performed experiments; E.A.L. M.V.A., Y.W., M.D., B.Y., and D.B. analyzed data; E.A.L. and D.B. wrote the manuscript.

Acknowledgements

This work was supported by Canadian Institutes of Health Research Operating Grants CIHR MOP-342247 to D.B. and by CIHR MOP-142209 to TJS. We thank members of the Bowie laboratory, for discussions and comments on the manuscript.

The authors declare no competing financial interests.

CHAPTER 2

Excitatory synaptic defects have multiple physiological consequences for cerebellum function in FXS mice

2.1 Foreword to Chapter 2

Chapter 2 of this thesis was originally prepared as a single manuscript with some of the experiments from Chapter 1. When I began my PhD, I was recording synaptic currents from both WT and *Fmr1*-KO mice as a way to make comparisons. Early on in my recordings I had found that *Fmr1*-KO mice lacked inhibitory plasticity. In uncovering the signaling cascade responsible for the induction of iLTP in WT mice, we were able to start dissecting apart the differences between the mice and locate defects in *Fmr1*-KO mice. As more and more of the pathway was revealed in WT mice, we decided that it was more appropriate to publish a study on the induction and expression of iLTP in WT mice alone. Fortunately, the data we had collected in WT mice allowed us to identify that while NMDA receptors are functionally absent in MLIs lacking FMRP, the rest of the signaling cascade appeared to be intact. We then developed a strategy using a small molecule (Drug-X[1]) to boost the limited residual NMDA receptor signal.

At the same time as I was working on the experiments that were published in Chapter 1 and contained in this chapter, my lab mate Ryan had been preparing two manuscripts about an intrinsic plasticity (IP) mechanism which regulates MLI excitability. One manuscript, which has since been published, identified that IP involves the phosphorylation of voltage-gated Na^+ channels to lower the action potential threshold (Alexander et al., 2019). In his recently published paper, he performed elegant experiments identifying that the same high frequency stimulation

[1] I have been asked to not disclose the name or nature of Drug-X by McGill's patent office

(HFS) that I have used to activate NMDA receptors, can induce IP in MLIs. It was then a natural question to ask if *Fmr1*-KO mice have defects in the induction of IP. Not surprisingly, we found that MLIs lacking FMRP do not have any changes to their firing properties following HFS of excitatory PF afferents. These two observations on defective IP and iLTP have provided a nice compliment to each other and demonstrate the functional downstream consequences of the lack of NMDA receptors. It still remains to be seen how the induction of these IP and iLTP interact and affect the overall excitability of MLIs, but it is likely that they play an important physiological role. I will speculate about this further in the general discussion.

Article Title:

NMDA receptor/NOS-related signaling deficits drive inhibitory circuit dysfunction in fragile X syndrome

Erik A. Larson[1,2], Ryan P.D. Alexander[2], Lianne J. Trigiani[3], Edith Hamel[3], & Derek Bowie[2]

[1]Integrated Program in Neuroscience, McGill University, Montréal, QC, Canada, H3A 2B4
[2]Department of Pharmacology and Therapeutics, McGill University, Montréal, QC, Canada, H3G 1Y6
[3]Laboratory of Cerebrovascular Research, Montréal Neurological Institute, McGill University, Montréal, QC, Canada H3A 2B4

To be submitted to the *Journal of Neuroscience*

2.2 Abstract

Fragile X syndrome (FXS) is a neurodevelopmental disorder associated with deficits in several neurotransmitter systems. Although defects in GABAergic transmission are implicated in FXS, the nature of the aberrancies is still being resolved. Here, we show two novel GABAergic plasticity mechanisms which are absent in cerebellar molecular layer interneurons (MLIs) from *Fmr1*-KO mice. In WT mice, MLIs typically strengthen their GABAergic synapses while also increasing their firing rate in response to NMDA receptor (NMDAR) activation. In *Fmr1*-KO mice, NMDAR signaling is markedly diminished and consequently, these two plasticity mechanisms modulating inhibitory signaling are absent. Inhibitory synapse strengthening requires the downstream activation of PKC. Bypassing NMDAR signaling and directly activating PKC restores inhibitory synapse strengthening in *Fmr1*-KO mice demonstrating that this intracellular signaling pathway remains functional. Taken together, our data identify an important disruption in the crosstalk between glutamatergic and GABAergic signaling in FXS. Since MLI connectivity shapes cerebellar output, the absence of plasticity in GABAergic signaling further ties defects in the cerebellum to the pathophysiology of FXS. Furthermore we provide evidence that Drug-X can correct NMDAR driven GABAergic plasticity in *Fmr1*-KO mice which may represent a novel therapeutic strategy for FXS. Finally, we demonstrate that there is a disruption in cerebellar neurovascular coupling and overall blood vessel function in dysfunctional *Fmr1*-KO mice. This study reveals multiple novel defects in a mouse model of FXS which add to the pathophysiology of the disease.

2.3 Introduction

Fragile X syndrome (FXS) is a neurodevelopmental disorder representing the most common form of inherited autism and intellectual disability (O'Donnell and Warren, 2002). It is caused by the transcriptional silencing of the *FMR1* gene which eliminates expression of the corresponding Fragile X mental retardation protein (FMRP) (Verkerk et al., 1991). FMRP is an mRNA binding protein which is localized to synapses and regulates local translation of many proteins critical to synaptic function (Greenough et al., 2001; Darnell et al., 2011). Early investigation into these synapse specific dysfunctions uncovered defects in spine morphology in tissue from both FXS patients (Rudelli et al., 1985) and *Fmr1*-KO mice (Comery et al., 1997). Since then, FXS has been commonly viewed as a disease affecting neuronal circuit development as well as synaptic function and plasticity (O'Donnell and Warren, 2002; Contractor et al., 2015). Accordingly, one of the main goals for developing novel FXS therapeutics has been to understand the molecular defects underlying synaptic dysfunction in the FXS brain.

Like many other autistic disorders, FXS has been characterized by an imbalance of excitation and inhibition in the brain (Nelson and Valakh, 2015). A significant emphasis has been placed on studying defects associated with glutamatergic transmission and in particular focusing on mGluR-LTD. Enhanced mGluR-LTD is one of the most well studied FXS phenotypes and was first reported in the hippocampus of *Fmr1*-KO mice (Huber et al., 2002). Similar results were subsequently found in the cerebellum (Koekkoek et al., 2005), amygdala (Suvrathan et al., 2010), and neocortex (Hays et al., 2011). These discoveries spurred the development of therapeutic tools targeting mGluR signaling for the treatment of FXS. While these therapies targeting mGluR signaling have had success in ameliorating defects in *Fmr1* KO mice (Dölen et al., 2007) they have

been unsuccessful in human clinical trials (Scharf et al., 2015). Complicating the challenges for the development of therapeutics is that additional research has revealed numerous other defects in cell signaling pathways. In part, this is due to the role of FMRP as an RNA binding agent and regulator of local protein synthesis. For instance, there are many proteins in the excitatory postsynaptic density which have altered expression in *Fmr1*-KO mice (Darnell et al., 2011). Specifically, expression of PSD-95 (Todd et al., 2003; Zalfa et al., 2007), Homer (Giuffrida et al., 2005), and neuroligins (Dahlhaus and El-Husseini, 2010) are all disrupted in *Fmr1*-KO mice. Consequently, there are also notable dysfunctions in ionotropic glutamatergic neurotransmission and notably disruptions in NMDA receptor (NMDAR) signaling (Gocel and Larson, 2012; Toft et al., 2016). There are also other knock-on implications impacting downstream secondary signaling pathways including those signaling through CaMKII, whose activation relies on proper coupling to proteins in the post synaptic density (Guo et al., 2015). All together these molecular defects contribute in part to the overall CNS hyperactivity in FXS (Contractor et al., 2015).

There has also been an effort to understand the role of the inhibitory GABAergic system in the pathophysiology of the disease (Rudolph and Mohler, 2014). A number of GABAergic defects have been found in *Fmr1*-KO mice including downregulated expression levels of α1, α2 and δ $GABA_A$ receptor ($GABA_AR$) subunits (Paluszkiewicz et al., 2011) as well as a dysregulation of enzymes involved in GABA synthesis and degradation (Paluszkiewicz et al., 2011). Furthermore, *Fmr1*-KO mice show a developmental delay in switching $GABA_AR$ polarity from excitatory to inhibitory transmission (He et al., 2014). Together, these observations can begin to explain the overall hyperexcitability observed in FXS brain which correlates with a high rate of seizures in people with FXS (Contractor et al., 2015). To that end there has been a focus on the

clinical use of drugs that enhance GABAergic signaling with which there has been some success at relieving FXS symptoms (Lozano et al., 2014b). Nevertheless, it remains to be established if plasticity mechanisms affecting the long-term efficacy of GABAergic signaling are also affected in FXS. For example we have recently identified two plasticity mechanisms modulating inhibition in the cerebellum which have yet to be evaluated in a FXS model (Alexander et al., 2019; Larson et al., 2020).

In this study, we set out to study the properties of MLIs in the *Fmr1*-KO mouse model of FXS. For the first time we reveal that activity dependent plasticity mechanisms are lost in *Fmr1*-KO mice due to dysfunctional excitatory neurotransmission. We have found that cerebellar MLIs from *Fmr1*-KO mice have dramatically smaller NMDAR currents. Consequently, MLIs from *Fmr1*-KO mice are unable to potentiate their firing properties – a mode of long-term intrinsic plasticity (IP) dependent on NMDAR signaling (Alexander and Bowie, 2020). Furthermore, there is an inability to recruit postsynaptic $GABA_A$ receptors ($GABA_AR$) during NMDAR dependent inhibitory long term potentiation (iLTP) (Larson et al., 2020).Together, these defects correspond to an inability to regulate cerebellar MLI output which we predict would ultimately cause a dysregulation of Purkinje cell (PC) activity. Given the important role that the excitation/inhibition balance plays in the development of FXS, our data provides novel insights into how these mechanisms interact with each other and advances our understanding of the neurobiology of the disease.

2.4 Materials and Methods

Ethical approval

All experiments were performed in accordance with the guidelines of the Canadian Council on Animal Care and were approved by the Animal Care Committee of McGill University.

Animals

Wild-type mice with a C57BL/6J background were obtained from Charles River Laboratories (Wilmington, MA, USA) and maintained as a breeding colony at McGill University. Breeder pairs of *Fmr1*-KO mice and *Gabra3* KO (1-Gabra3tm2Uru/Uru), C57BL/6 background, were kindly provided by Dr. Greenough (University of Illinois, Urbana-Champaign, IL 61801, USA)(Comery et al., 1997) and Dr. Rudolph (Harvard Medical School, McLean Hospital, MA 02478, USA)(Yee et al., 2005). Both male and female wild-type mice used for experiments ranged from postnatal days 18 to 30.

Slice preparation

Mice (P21-35) were anesthetized with isoflurane and immediately decapitated. A block of cerebellar vermis was rapidly dissected from the mouse head and submerged in ice-cold cutting solution perfused with carbogen gas (95% O_2, 5% CO_2). Cutting solution contains (in mM): 235 sucrose, 2.5 KCl, 1.25 NaH_2PO_4, 28 $NaHCO_3$, 0.5 $CaCl_2$, 7 $MgCl_2$, 28 D-glucose, 1 ascorbic acid, 3 sodium pyruvate (pH 7.4; 305–315 mOsmol/L). The block of vermis was then fastened to a platform, transferred to the slicing chamber and again submerged in ice-cold cutting solution, bubbled with carbogen throughout the remainder of the procedure. Thin slices of cerebellar vermis (300 µm) were obtained with a vibrating tissue sectioner (Leica VT1200; Leica

Instruments, Nussloch, Germany). The slices were transferred to oxygenated artificial cerebrospinal fluid (ACSF) and held at room temperature (21°C-23°C) for at least 1 h before recordings were performed. ACSF contained the following (in mM): 125 NaCl, 2.5 KCl, 1.25 NaH_2PO_4, 26 $NaHCO_3$, 2 $CaCl_2$, 1 $MgCl_2$, and 25 D-glucose (pH of 7.4; 305–315 mOsmol/L).

Electrophysiology

Slice experiments were performed on an Olympus BX51 upright microscope (Olympus, Southall, UK) equipped with differential interference contrast/infrared optics. Whole-cell patch-clamp recordings were made from either visually-identified MLIs in acute sagittal slices of cerebellar vermis. MLIs were distinguished from misplaced or migrating granule, glial by their small soma diameter (8–9 µm), location in the outer two-thirds of the molecular layer and whole-cell capacitance measurement (4-12 pF). Patch pipettes were prepared from thick-walled borosilicate glass (GC150F-10, OD 1.5 mm, ID 0.86 mm; Harvard Apparatus Ltd, Kent, UK) and had open tip resistances of 4–7 MΩ when filled with an intracellular recording solution. Recordings were made with a Multiclamp 700A amplifier (Molecular Devices, Sunnyvale, CA, USA) at a holding potential of -60 mV. Series resistance and whole-cell capacitance were estimated by cancelling the fast transients evoked at the onset and offset of a 10 ms, 5 mV voltage-command steps. Access resistance during whole-cell recording (10–25 MΩ) was compensated between 60 and 80% and checked for stability throughout the experiments (~15% tolerance). The bath was continuously perfused at room temperature (21–23 °C) with ACSF at a rate of 1–2 mL/min. Currents were filtered at 5 kHz with an eight-pole low-pass Bessel filter (Frequency Devices, Haverhill, MA, USA) and digitized at 25 kHz with a Digidata 1322A data acquisition board and Clampex 10.1 (Molecular Devices) software.

For extracellular stimulations, thin walled borosilicate glass electrodes (OD 1.65mm, ID 1.15mm; King Precision Glass Inc, Claremont, CA, USA) were used with a tip resistance of < 3 MΩ when filled with aCSF. The ground electrode for the stimulation circuit was made with a platinum wire wrapped around the stimulation electrode. The stimulating electrode was positioned in the molecular layer at or just beneath the slice surface. Voltage pulses (10—25 V in amplitude, 200-400 μs in duration) were applied at low frequency stimulation (0.1 Hz) through the stimulating electrode. To minimize variability between responses, the stimulating electrode was positioned 50-100 μm away from the recorded cell. The stimulus voltage used during each experiment was at the lowest intensity to elicit the maximal eEPSP/IPSC response within the range described above. Stimulation strength and duration were kept constant throughout the experiment. For high frequency stimulation (HFS), trains of six stimuli were delivered at 100 Hz (inter-train interval of 20 s) as described previously This HFS protocol has been used previously to potentiate inhibitory signaling through a ROS mediated pathway (Larson et al., 2020) and mimics somatosensory stimulation patterns (Jorntell and Ekerot, 2006; Saviane and Silver, 2006; Rancz et al., 2007; Arenz et al., 2008; Coddington et al., 2013). We performed the HFS protocol every five minutes. During the voltage-clamp experiments of evoked GABA currents (see Fig. 2.3, 2.4), we performed the HFS protocol at a holding potential of +40 mV to relieve Mg^{2+} block of NMDARs. We performed the single stimulation recordings at -60 mV to isolate the response from NMDA currents and used GYKI 53655 to pharmacologically block AMPA currents. For all experiments which included perfusion of either pharmacological or peptide blocker compounds in the internal solution we waited 10 minutes prior to beginning the HFS induction protocol.

Recording solutions

All chemicals were obtained from Sigma Aldrich (St. Louis, MO, USA) unless otherwise indicated. Internal pipette solution for current-clamp experiments contained (in mM): 126 K-gluconate, 5 HEPES, 4 NaCl, 15 D-glucose, 0.05 $CaCl_2$, 1 $MgSO_4$, 0.15 K_4-BAPTA, 3 Mg-ATP, 0.1 Na-GTP, 2 QX314 (adjusted to pH 7.4 with KOH, 300-310 mOsmol/L). Voltage-clamp recordings were made with an intracellular solution that contained (in mM): 140 CsCl, 4 NaCl, 0.5 CaCl2, 10 HEPES, 5 EGTA, 2 Mg-ATP, 2 QX314 (pH 7.4 with CsOH, 300-310 mOsmol/L). For cell-attached experiments, internal solution contained (in mM): 125 NaCl, 10 HEPES, 40 D-Glucose, 2.5 $MgCl_2$ (adjusted to pH 7.4 with NaOH, 300-310 mOsmol/L).

Pharmacological compounds

NMDAR antagonist, D-APV (10 µM) and MK-801 (10 µM), AMPA antagonist 1-(4-Aminophenyl)-3-methylcarbamyl-4-methyl-3,4-dihydro-7,8-methylenedioxy-5H-2,3-benzodiazepine hydrochloride (GYKI 53655; 10 µM), and the $GABA_A$ receptor antagonist bicuculline (10 µM) were purchased from Tocris Bioscience (Ellisville, MO, USA). Stock solutions of these antagonists were prepared in water and were stored at −20°C and working solutions were diluted with aCSF shortly before application to the bath. Phorbol 12-myristate 13-acetate (PMA, 100nM, Tocris) was dissolved in DMSO and stored at −20°C. The final maximum DMSO concentration for all experiments (0.1% v/v).

Vascular reactivity

Middle or posterior cerebral arteries were isolated from both WT (n=9) and Fmr1-KO (n=4) mice and vessel diameter was measured using video microscopy (Living Systems Instrumental,

Burlington, VT) as previously described (Trigiani et al., 2019). Blood vessels were cannulated in a closed sac preparation in 1xKREBS buffer, and gradually pressurized to 60mmHg. Vasoconstriction was measured in response to extraluminal application of thromboxane A2 receptor agonist, U46619 at increasing concentrations (10−9 to 10−3 mol/L, Tocris Bioscience Ellisville, MO, USA). Data is presented as a percentage change from the basal diameter.

Blood vessel imaging

Cerebellar vermis slices were prepared in the sagittal orientation as described above for electrophysiology experiments. Imaging experiments were performed on an Olympus BX51 upright microscope (Olympus, Southall, UK) equipped with infrared optics. Blood vessels were visually identified in the molecular layer and images were taken at 4 Hz with an Olympus XM10 camera. Baseline recordings were then conducted for 5 mins to ensure stability which was followed by perfusion of the thromboxane A2 receptor agonist, U46619 (75/150 nM) to saturation within 10 mins. Upon saturation of U46619 (10 mins), NMDA (50 μM) was washed into the slice chamber for 5 mins while U46619 concentrations were maintained. Imaging then continued for 15 mins after the application of NMDA with only U46619 in the slice chamber. Blood vessel diameters were analyzed using a custom Matlab script kindly provided by Drs. Bruno Cauli (Sorbonne Université, France) and Elizabeth Hillman (Columbia University, USA).

2.5 Results

Glutamatergic transmission is defective in MLIs from *Fmr1*-KO mice

To study synaptic properties of cerebellar MLIs from *Fmr1*-KO mice, we first performed whole-cell patch clamp electrophysiology recordings and placed a field stimulating electrode to evoke excitatory post synaptic currents (eEPSCs). We specifically placed our stimulating electrode in the molecular layer to activate parallel fiber (PF) -MLI synapses and pharmacologically isolated either AMPA receptor (AMPAR) or NMDAR currents with D-APV or NBQX respectively (Fig. 2.1*A*). Interestingly, when performing a single stimulation at a -60 mV holding potential we found no differences in the functional properties of the evoked AMPAR currents. Both WT and *Fmr1*-KO mice had similar measurements of peak AMPAR response amplitude (WT amplitude; -166.9 ± 21.5 pA, *Fmr1*-KO amplitude; -203.5 ± 22.2 pA; unpaired t-test t(16) 1.251, p= 0.23), decay kinetics as fit by an exponential (WT τ; 1.88 ± 0.3 ms , *Fmr1*-KO τ; 2.27 ± 0.3 ms; unpaired t-test t(13)=0.898, p= 0.38; Fig 2.1 *B,C,D*). Furthermore, they also had a similar voltage-dependent block by 60 μM of intracellular spermine indicating that they express a similar AMPAR composition (Fig. 2.1*E,F*).

Unlike most glutamatergic synapses, MLI-PF synapses contain AMPARs only while nearby NMDARs are extrasynaptic (Clark and Cull-Candy, 2002). Consequently to activate NMDARs a high frequency PF stimulation is required for a large glutamate release which spills onto the extrasynaptic receptors (Carter and Regehr, 2000; Clark and Cull-Candy, 2002). To record evoked NMDAR currents from WT and *Fmr1*-KO mice we again performed whole cell patch clamp at +40 mV to relieve Mg^{2+} block and used a high frequency stimulation protocol (HFS, 100Hz) to activate PF afferents (see Methods). This frequency has previously been shown to sufficiently activate

NMDARs (Clark and Cull-Candy, 2002; Larson et al., 2020) and is comparable to firing rates seen *in vivo* (Chadderton et al., 2004). In contrast to our observations on evoked AMPAR currents, there was a greatly diminished NMDAR response in the *Fmr1*-KO mice compared to WT (Fig 2.1*G,H*). First the NMDAR peak amplitude was significantly reduced in *Fmr1*-KO mice compared to WT (WT; 119.1 ± 31.6 pA, n=10, *Fmr1*-KO; 42.1 ± 11.6 pA, n=8, unpaired t-test t(16)=2.162, p=0.046). We also observed that the overall NMDAR charge transfer was significantly lower in the *Fmr1*-KO mice compared to WT mice (WT; 41.7 ± 12.4 pC, n=10, *Fmr1*-KO; 7.8 ± 3.5 pC, n=8 unpaired t-test t(16)=2.373, p=0.03) further demonstrating the lack of NMDAR signaling in the *Fmr1*-KO mice (Fig. 2.1*G,H*).

To determine if this NMDAR deficit is a general defect in *Fmr1*-KO MLIs or a specific defect to PF-MLI synapses we performed a second set of experiments and stimulated climbing fiber (CF) afferents. While CFs do not directly synapse onto MLIs, they release a large volume of glutamate which activates NMDARs through spillover (Szapiro and Barbour, 2007; Coddington et al., 2013). Unlike PFs, which have a short term facilitation to a paired-pulse stimuli, CFs have a very strong short term depression (Szapiro and Barbour, 2007; Coddington et al., 2013). Thus to distinguish CF from PF responses we used a paired pulse protocol and placed our stimulating electrode at the base of the PC layer (see methods, Fig 2.1*A,I*). Consistent with our results from PF stimulation, NMDAR evoked CF responses were significantly smaller in amplitude (WT; 14.9 ± 1.2pA, n=5, *Fmr1*-KO; 4.5 ± 0.5pA, n=4, unpaired t-test t(7)=4.896, p=0.0017) and changer transfer (WT; 2.19 ± 0.02pC, n=5, *Fmr1*-KO; 0.143 ± 0.004pC, n=4 unpaired t-test t(7)=2.529, p=0.039) in MLIs from *Fmr1*-KO mice compared to WT mice(Fig 2.1*I,K*).

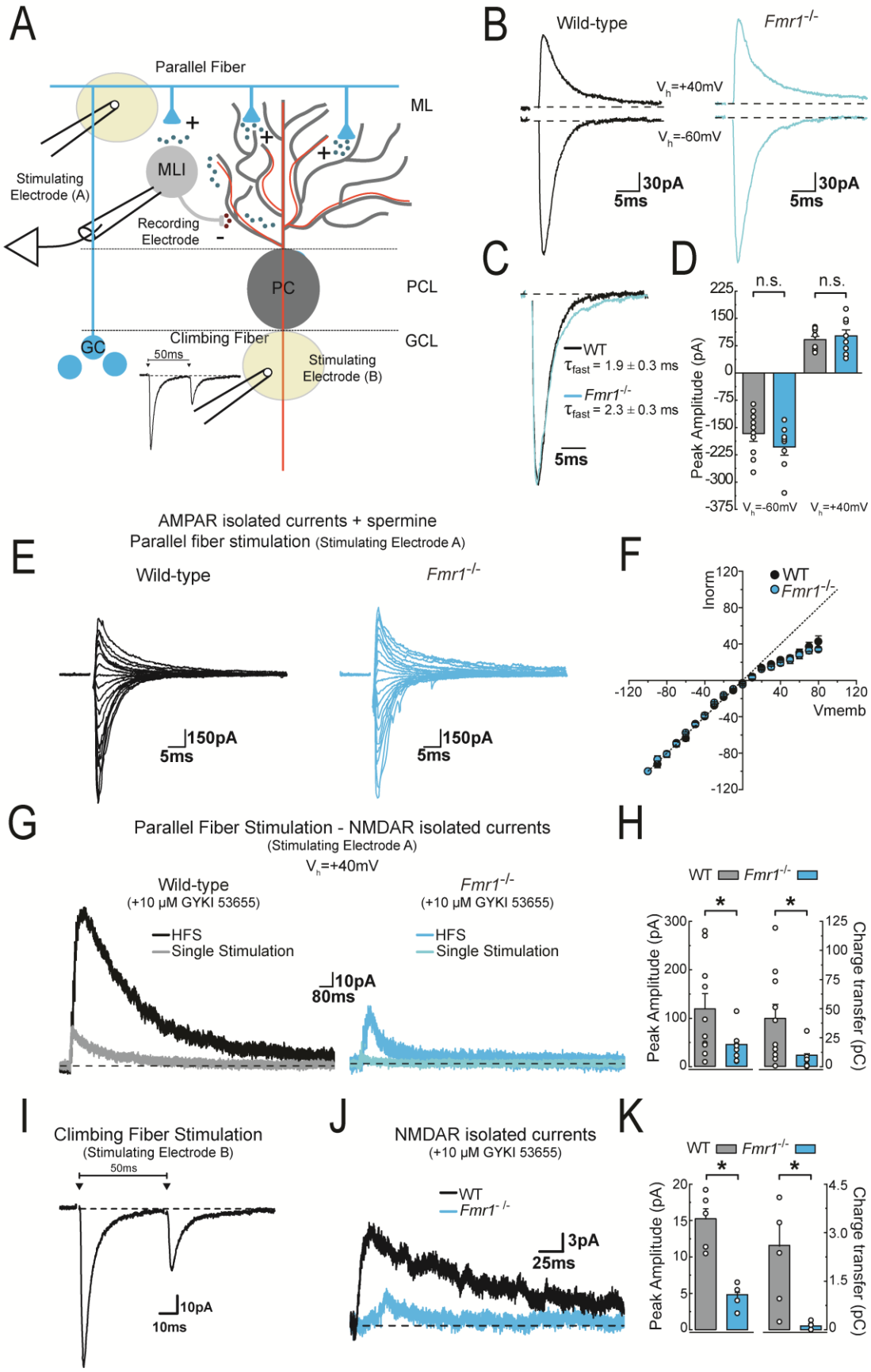
A
Parallel Fiber
ML
MLI
Stimulating Electrode (A)
Recording Electrode
PC
PCL
GC
Climbing Fiber
50ms
Stimulating Electrode (B)
GCL
B
Wild-type
Fmr1-/-
Vh=+40mV
Vh=-60mV
30pA
5ms
C
WT
τfast = 1.9 ± 0.3 ms
Fmr1-/-
τfast = 2.3 ± 0.3 ms
5ms
D
n.s.
Peak Amplitude (pA)
Vh=-60mV
Vh=+40mV
E
AMPAR isolated currents + spermine
Parallel fiber stimulation (Stimulating Electrode A)
Wild-type
Fmr1-/-
150pA
5ms
F
Inorm
WT
Fmr1-/-
Vmemb
G
Parallel Fiber Stimulation - NMDAR isolated currents
(Stimulating Electrode A)
Vh=+40mV
Wild-type
(+10 μM GYKI 53655)
Fmr1-/-
(+10 μM GYKI 53655)
HFS
Single Stimulation
10pA
80ms
H
WT
Fmr1-/-
Peak Amplitude (pA)
Charge transfer (pC)
I
Climbing Fiber Stimulation
(Stimulating Electrode B)
50ms
10pA
10ms
J
NMDAR isolated currents
(+10 μM GYKI 53655)
WT
Fmr1-/-
3pA
25ms
K
WT
Fmr1-/-
Peak Amplitude (pA)
Charge transfer (pC)

Figure 2.1: NMDA receptors are downregulated in cerebellar MLIs of Fmr1-KO mice
(A) Schematic illustrating the arrangement of stimulating and recording electrodes. Stimulating electrode was positioned to focally depolarize (yellow circle) excitatory parallel fiber (stimulating electrode A) or climbing fiber axons (stimulating electrode B); MLIs (MLI = molecular layer interneuron, PC = Purkinje cell, GC = granule cell). (B) Representative voltage-clamp recordings of evoked MLI AMPAR currents at holding potentials of -60mV and +40mV from a WT (left) and Fmr1-KO (right) mouse. (C) Voltage-clamp traces from the -60mV holding potential in panel (B) scaled and overlaid to compare AMPAR kinetics. (D) Summary plot of the AMPAR eEPSC amplitude for WT and Fmr1-KO mice (Error bars, s.e.m.). (E) AMPAR eEPSC recordings at holding potentials from -100mV to +40mV in the presence of internal spermine. (F) I/V plot of the AMPAR eEPSC from both WT and Fmr1-KO mice. (G) Representative voltage-clamp recordings of evoked MLI NMDAR currents at +40mV from a WT (left) and Fmr1-KO (right) mouse in response to a single or high frequency stimulation (overlaid). (H) Summary plot of the NMDAR eEPSC amplitude for WT and Fmr1-KO mice following parallel fiber stimulation (Error bars, s.e.m.). (I) Representative voltage-clamp recordings of the paired-pulse protocol (from stimulating electrode location B) used to identify climbing fiber responses in MLIs. (J) Representative voltage-clamp recordings at +40mV of the NMDAR currents following climbing fiber stimulation from a WT and Fmr1-KO mouse (overlaid). Summary plot of the NMDAR eEPSC amplitude for WT and Fmr1-KO mice following climbing fiber stimulation (Error bars, s.e.m.).

Taken together, these observations demonstrate that MLIs lacking FMRP have a substantial deficit in NMDAR signaling. Importantly a smaller charge transfer would result in a decreased Ca^{2+} entry and potentially limit NMDAR/Ca^{2+}-dependent plasticity mechanisms. NMDAR signaling has recently been shown to be important for a number of signaling pathways in MLIs including the regulation of IP (Alexander and Bowie, 2020) and inhibitory long term potentiation (iLTP) (Larson et al., 2020). We therefore reasoned that the lack of NMDAR signaling in the *Fmr1*-KO mice would have impacts on both of these important physiological mechanisms. Accordingly, we performed experiments to examine the consequences of the NDMAR defect on both IP and inhibitory LTP.

NMDAR-dependent intrinsic plasticity is lost in MLIs lacking FMRP

A recent publication from the Bowie lab has identified an NMDAR-dependent plasticity of intrinsic excitability, or IP, that relies on CaMKII signaling to potentiate Na^+ channel function in

cerebellar MLIs (Alexander and Bowie, 2020). Given the loss of NMDAR-mediated EPSCs in MLIs of *Fmr1*-KO mice, we reasoned that this firing rate plasticity mechanism would also be affected. To that end we recorded spontaneous firing rates in MLIs from WT and *Fmr1*-KO mice in loose-seal cell-attached configuration to avoid changes in excitability associated with whole-cell recording (Alexander et al., 2019; Alexander and Bowie, 2020). We then used the same HFS protocol from Figure 2.1 to drive PF synapses and activate NMDARs. Unsurprisingly, in WT MLIs we found that 30 mins after the onset of the HFS protocol the firing rate was significantly higher compared to the baseline frequency (218 ± 38% frequency at 25 min compared to baseline; p = 0.021; n = 7) (Fig. 2.2*A,B*). Furthermore this potentiation of firing rate was prevented by blocking NMDARs. In cells that were treated with the NMDAR pore channel blocker MK-801, we found there was no significant change from baseline firing rate at 30 mins after performing the HFS protocol (130 ± 20% frequency at 25 min compared to baseline; p = 0.17; n = 8) (Fig. 2.2*A,B*). MLIs from *Fmr1*-KO mice also did not have any changes to their firing rate following HFS treatment which is unsurprising given that they lack robust NMDAR signaling (110 ± 10% 25 min frequency compared to baseline; t = 1.29, p = 0.24; n = 8). Importantly, firing rates did not change in the baseline 15 minutes in either WT (2.9 ± 0.3 Hz at 1 min vs. 3.0 ± 0.3 ± at 15 min; t = 1.02, p = 0.35; n = 7) or *Fmr1*-KO cells (4.7 ± 1.0 Hz at 1 min vs. 4.7 ± 1.0 ± at 15 min; t = 0.71, p = 0.50; n = 8). Finally we also found that baseline firing frequencies were not significantly different between genotypes demonstrating that the inability to potentiate the firing rate of *Fmr1*-KO MLIs is not due to a difference in basal frequency (2.9 ± 0.3 Hz for WT vs. 4.7 ± 1.0 Hz for *Fmr1*-KO; t = 1.76, p = 0.10).

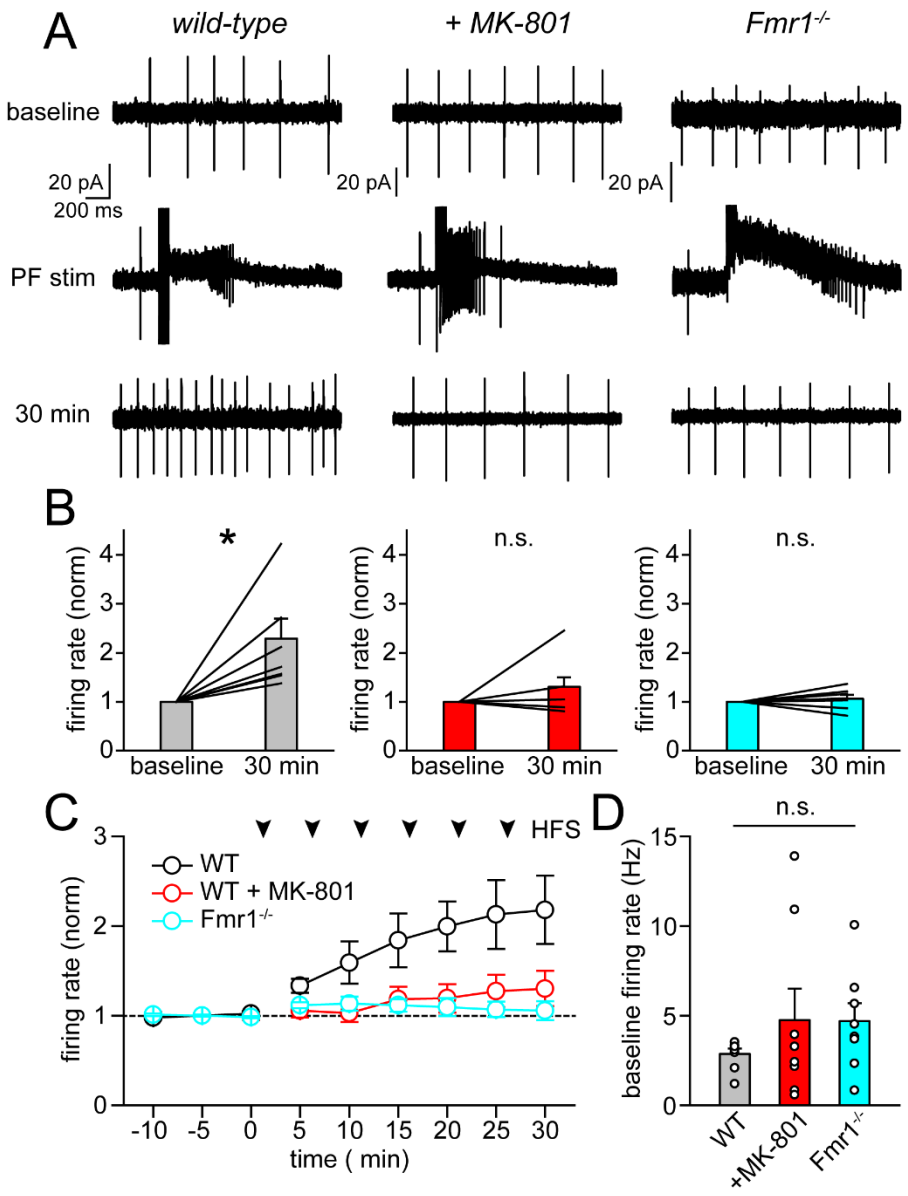

Figure 2.2: Intrinsic plasticity following NMDA receptor activation is absent in Fmr1-KO MLIs
(A) Representative loose-seal cell attached recordings from WT MLIs (left), WT MLIs in the presence of MK-801 (centre), and Fmr1-KO MLIs (right), before, during and after an extracellular parallel fiber HFS protocol. Note that experiments included the GABA antagonist bicuculine in the bath to eliminate any contribution of inhibition on the induction of IP. (B) Summary plot of the action potential frequency before and 30 mins following HFS normalized to baseline (Error bars, s.e.m.). (C) Time course plot of the normalized action potential frequency of the above traces throughout the duration of the recordings from the 10 min baseline period through 30 mins of HFS protocols. (D) Firing rate frequency of WT MLIs, WT MLIs in the presence of MK-801, and Fmr1-KO MLIs, during the first 5 mins prior to HFS treatment.

NMDAR- dependent inhibitory LTP is lost in MLIs of FXS mice

A recent study from our lab has described a novel form of iLTP in MLIs which also relies on NMDAR activation (Chapter 1) (Larson et al., 2020). To probe if this plasticity mechanism is similarly disrupted in the *Fmr1*-KO mice we repeated the same experiments as previously described (Chapter 1)(Larson et al., 2020). In current clamp we stimulated PF afferents and recorded biphasic responses consisting of an evoked EPSP (eEPSP) followed by an IPSP (Fig. 2.3*A*). We then used the same HFS protocol (100Hz) previously used to activate NMDARs which has been shown to strengthen GABAergic signaling in MLIs (Chapter 1)(Larson et al., 2020). Although the evoked biphasic responses recorded from *Fmr1*-KO MLIs consistently had larger eEPSP depolarizations (see Chapter 3), repetitive HFS failed to elicit a reduction in the response after 25 mins of the protocol. In WT MLI recordings we observed a significant decrease in the eEPSP amplitude to 48.6 ± 5.0 % of the baseline amplitude (reproduced data from Chapter 1) (Fig. 2.3*A,C,D*). Conversely, recordings from *Fmr1*-KO mice did not have a significant change to the eEPSP amplitude following the HFS protocol ($Peak_{25}$ 97.5 ± 5.8 %, n=7, $F(5,45)=1.59$, $p=0.18$, repeated measures ANOVA, Fig. 2.3A,C,D).

To confirm that our observation in current clamp reflects an inability to potentiate GABAergic signaling we performed additional experiments in voltage clamp to isolate the IPSC component. We isolated and recorded isolated GABAergic currents with a high Cl^- solution at -60 mV (see Methods). In order to activate NMDARs in voltage clamp, we paired our HFS with a depolarization to +40 mV to relieve Mg^{2+} block of NMDARs. Similar to our results in current clamp, we did not see any changes to the evoked IPSC amplitude in *Fmr1*-KO mice ($Peak_{25}$ 115 ± 7.1 %, n=6, $F(5,25)=2.33$, $p=0.07$, repeated measures ANOVA, Fig. 2.3*B,E*). With our observations

in both current- and voltage-clamp we concluded that GABAergic plasticity is defective in MLIs from *Fmr1*-KO mice.

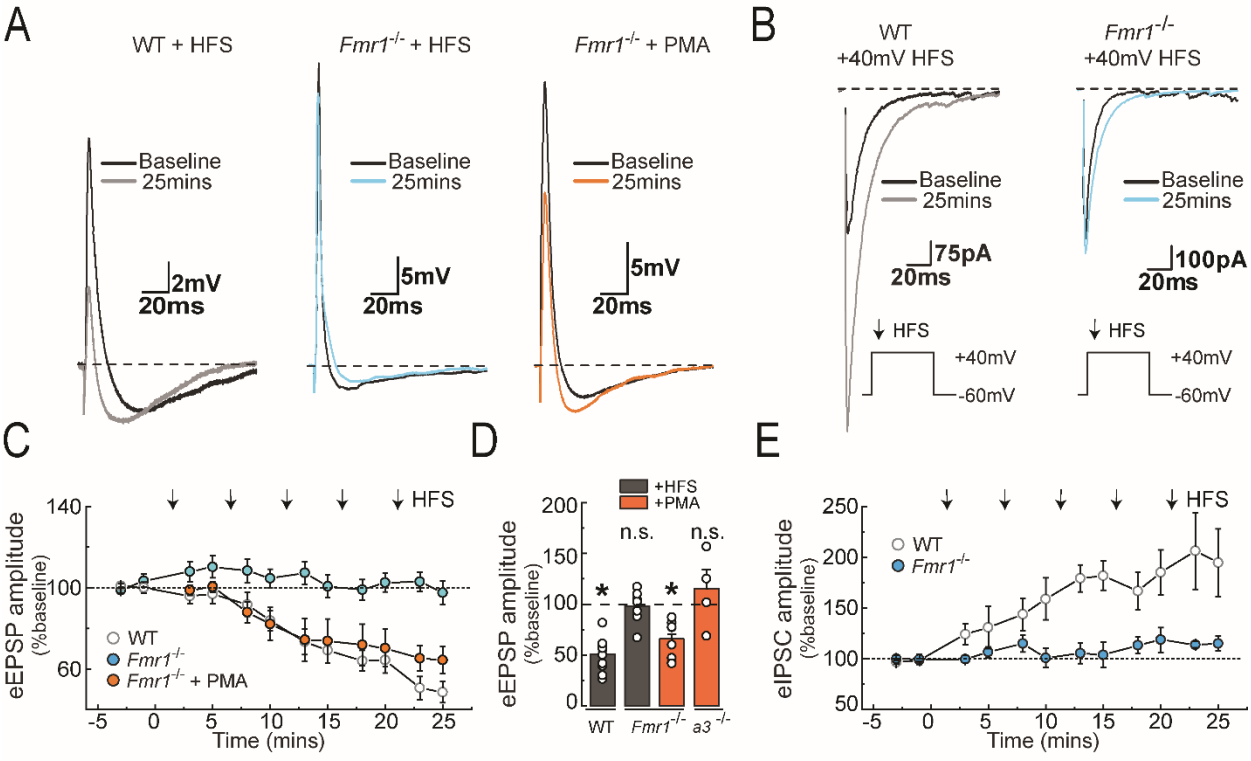

Figure 2.3: NMDA receptor dependent iLTP is lost in MLIs from Fmr1-KO mice
(A) Representative recordings from three different MLIs in current-clamp before and 25 mins after treatment with either HFS (left and center) or PMA (right). (B) Representative recordings from two different MLIs in voltage-clamp before and 25 mins after HFS (WT data reproduced from Chapter 1 for comparative purposes). (C) Summary plot of the time course of the eEPSP amplitude during HFS treatment or internal perfusion with PMA (Error bars, s.e.m). (D) Summary plot of the eEPSP amplitude as a percentage of the baseline amplitude at 25 mins following the onset of treatment (Error bars, s.e.m). (E) Summary plot of the time course of the eIPSC amplitude during HFS treatment (Error bars, s.e.m).

To better understand the absence of iLTP in *Fmr1*-KO mice we wanted to test if the intracellular signaling mechanisms mediating iLTP were similarly defective. As we have previously described, this mechanism involves activation of PKC in the recruitment of $GABA_AR$s into the synapse. We therefore included PMA, a PKC activator, in our internal patch pipette to bypass NMDAR signaling and directly stimulate iLTP. In *Fmr1*-KO mice we found that direct activation of

PKC with 100nM internal PMA elicited a reduction to in the eEPSP amplitude consistent with our observations form WT cells ($Peak_{25}$, 64.3 ± 6 %, n=8, F(4,28)=4.68, p=0.005, repeated measures ANOVA, Fig. 2.3*A,C,D*). This demonstrated that downstream signaling from NMDAR activation remains intact in *Fmr1*-KO mice. Since iLTP relies on the recruitment of α3-containing $GABA_A$Rs, we tested the specificity of PMA by performing the same experiments in *Gabra3* KO mice (Accardi et al., 2014; Larson et al., 2020). As expected, PMA failed to affect the eEPSP amplitude in *Gabra3* KO mice, indicating that the effect of PMA is primarily to stimulate recruitment of α3-containing $GABA_A$Rs ($Peak_{25}$, 115 ± 18%, n=4, F(4,12)=0.42, p=0.79, repeated measures ANOVA, Fig. 2.3*D*). Taken together, reduced functional expression of NMDARs in *Fmr1*-KO is the key impairment in the signaling pathway that limits recruitment of α3-containing $GABA_A$Rs into inhibitory synapses during HFS.

Drug-X rescues iLTP in stellate cells of FXS mice

Since downstream the secondary signaling pathway downstream of NMDAR signaling is intact we hypothesized that it might be possible to potentiate the residual NDMAR currents observed in *Fmr1*-KO mice. Full NMDAR activation requires the presence of a co-agonist, either D-serine (Mothet et al., 2000) or glycine (Johnson and Ascher, 1987) and the decrease in NMDAR signaling we have observed in *Fmr1*-KO mice could be due to a lack of co-agonist availability. This is the case in the dentate gyrus of *Fmr1*-KO mice, as application of NMDAR of co-agonists has been shown to rescue deficits in NMDAR-dependent LTP (Bostrom et al., 2013). To test if this would potentiate NMDAR signaling in MLIs we performed PF HFS (see Figure 2.1, Methods) before and after wash-in of D-serine (100μM). As D-serine did not significantly change the basal NMDAR charge transfer in WT or *Fmr1*-KO mice (Fig. 2.4*A*), the nature of the *Fmr1*-KO NMDAR deficit is

likely due to a limitation of the amount of functional NMDARs that are expressed in MLIs. Therefore, we took another approach to boost the intracellular signaling pathway for an attempt to rescue iLTP.

Our previous study characterizing the biochemical signaling pathway underlying MLI iLPT revealed a number of signaling molecules that we could target to rescue inhibitory plasticity. Specifically we identified that the pathway involves the stimulation of nNOS, production of cGMP, and the subsequent activation of PKG (see Chapter 1)(Larson et al., 2020). The nNOS-cGMP-PKG pathway is tightly controlled by proteins which produce and rapidly degrade the second messengers (Francis et al., 2010). We reasoned that we could target this pathway with Drug-X to potentiate the intracellular signaling pathway downstream of NMDAR activation. Accordingly we performed experiments introducing Drug-X (100μM) into MLIs through our patch pipette solution.

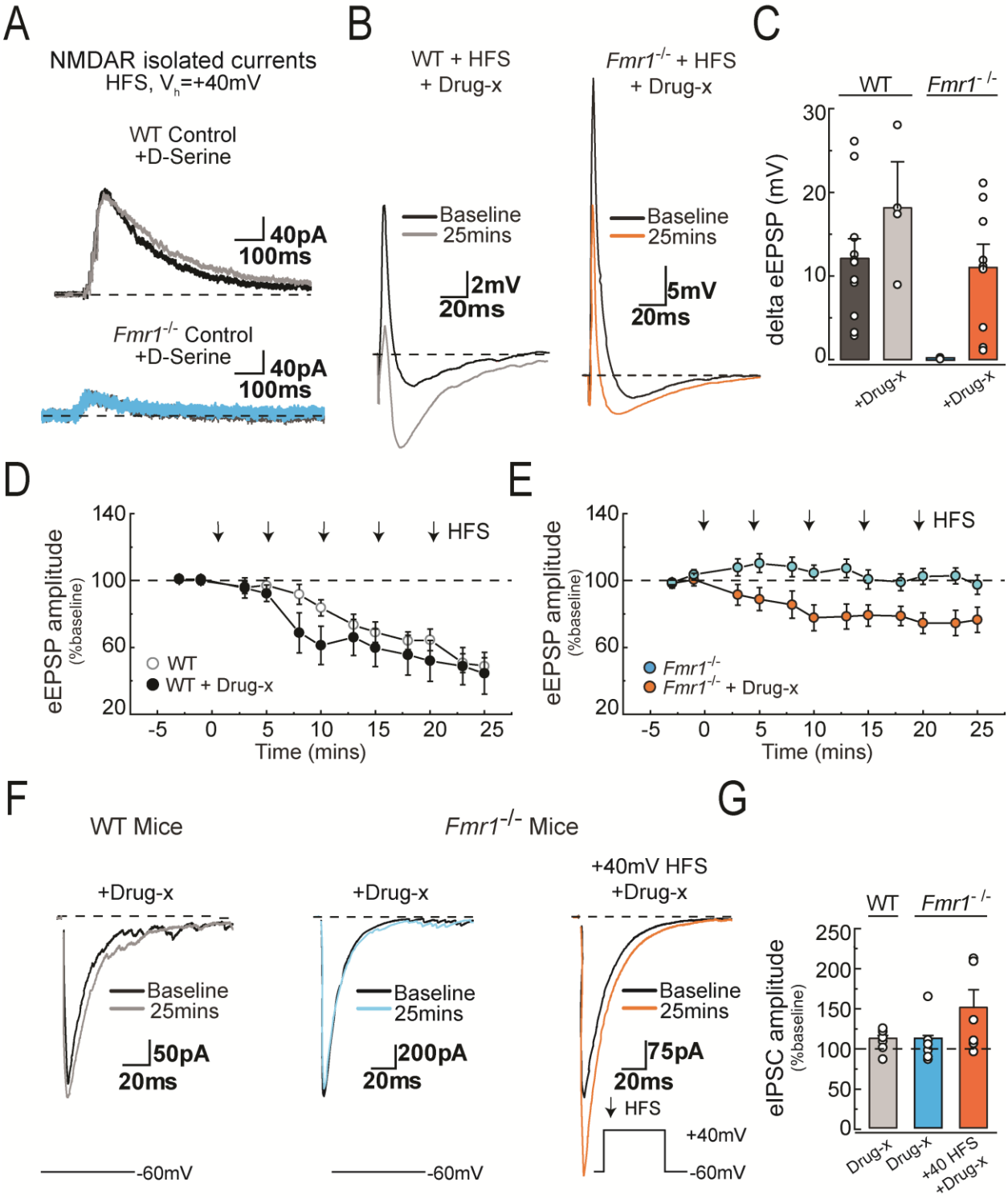

Figure 2.4: Drug-X rescues iLTP in Fmr1-KO mice

(A) Representative voltage-clamp recordings of evoked MLI NMDAR currents at +40mV from a WT (top) and Fmr1-KO (bottom) mouse in response to a HFS before and after D-Serine application (overlaid). (B) Representative recordings from two different MLIs in current-clamp before and 25 mins after HFS

treatment with internal perfusion of Drug-X. (C) Summary plot of the change in eEPSP amplitude in mV at 25 mins following HFS treatment (values represent the absolute change in overall amplitude from baseline to 30 mins). (D) Summary plot of the time course of the WT eEPSP amplitude during HFS treatment with or without internal perfusion of Drug-X. (E) Summary plot of the time course of the Fmr1-KO eEPSP amplitude during HFS treatment with or without internal perfusion of Drug-X. (Error bars, s.e.m). (F) Representative eIPSC recordings from three different MLIs in voltage-clamp at baseline and 25 mins after treatment (left; WT + Drug-X, center; Fmr1-KO + Drug-X, right; Fmr1-KO + Drug-X and HFS). (G) Summary plot of the eIPSC amplitude as a percentage of the baseline amplitude at 25 mins following the onset of treatment (Error bars, s.e.m)

First we examined if the introduction of Drug-X in the absence of HFS alters synaptic signaling. Under single pulse synaptic stimulations (no HFS), Drug-X had a very mild effect on the evoked IPSCs recorded in WT MLIs ($Peak_{25}$, 112.8 ± 5%, n=7, t(6)=2.484, p=0.047, paired t-test) but no effect on *Fmr1*-KO IPSCs ($Peak_{25}$, 109.5 ± 14%, n=6, t(5)=0.53, p=0.61, paired t-test) during 30 minutes of recording (Fig. 2.4*F,G*). This suggested that there is some downstream signaling in WT mice in the absence of NMDAR activation but likely almost negligible signaling in MLIs from *Fmr1*-KO mice. Next we performed our HFS protocol while including Drug-X in our patch pipette. Before starting the HFS protocol we allowed 10 minutes for the drug to wash into the neuron. Unsurprisingly, Drug-X did not prevent iLTP in WT mice and we were able to observe a large decrease in the peak eEPSP amplitude over 30 mins ($Peak_{25}$, 44.5 ± 12 %, n=4, F(5,15)=10.79, p=0.00015, repeated measures ANOVA). Most importantly, we were able to rescue iLTP in *Fmr1*-KO mice by performing HFS treatment in the presence of Drug-X ($Peak_{25}$, 72.6 ± 8 %, n=8, F(5,35)=7.48, p=0.00007, repeated measures ANOVA). When measuring the absolute difference before and after HFS treatment we observed a similar overall decrease in the eEPSP amplitude of *Fmr1*-KO MLIs treated with Drug-X compared to WT mice and WT mice treated with Drug-X (WT ΔeEPSP; -11.9 ±2.5 mV, n=10, WT +Drug-X ΔeEPSP; -15.5 ±4.6 mV, n=4; FXS ΔeEPSP; -1.8 ± 2.7 mV, n=8, FXS +Drug-X ΔeEPSP; -10.8 ± 3 mV, n=8). Finally, we performed a voltage clamp

experiment to directly measure GABAergic currents in the presence of Drug-X while performing HFS. We found that a significant potentiation of the eISPC amplitude in MLIs from *Fmr1*-KO mice in the presence of Drug-X ($Peak_{25}$, 157.8 ± 20%, n=5, t(4)=2.815, p=0.048, paired t-test). Taken together, we have demonstrated that Drug-X does not affect MLI GABAergic signaling under basal conditions, but Drug-X can boost intracellular signaling downstream of NMDAR activation. Furthermore, Drug-X is effective during instances where there are greatly diminished NMDAR currents as found in *Fmr1*-KO mice.

FXS mice have disruptions in the regulation of blood flow

In addition to the regulation of synaptic plasticity and intrinsic excitability that we have evaluated in this study, the stimulation of NMDARs in MLIs is responsible for the regulation of blood flow through the cerebellum. Nitric oxide production is a key molecule promoting blood vessel dilation and is the predominant molecule regulating blood flow in the cerebellum (Yang et al., 1999). Activation of NMDARs in MLIs increases local blood flow in the cerebellum because of their tight coupling to nitric oxide synthase (NOS) which produces nitric oxide following Ca^{2+} entry (Rancillac et al., 2006). Accordingly we reasoned that there could be a major impact on the local regulation of blood flow in the cerebellum of *Fmr1*-KO mice as this could be a further major unexamined defect in the disorder.

To test if there are defects in cerebellar blood vessel reactivity in the *Fmr1*-KO mice model, we performed experiments to measure blood vessel constriction and dilation (Rancillac et al., 2006). As previously noted, *in vitro* slice preparation blood vessels lack blood pressure and it is necessary to pharmacologically preconstrict blood vessels before the role of vasodilators, such as NO, can be properly assessed (Sagher et al., 1993; Cauli et al., 2004; Rancillac et al., 2006).

Importantly, it has also been established that the dilatory response is most noticeable on segments of blood vessels which are most strongly constricted (Rancillac et al., 2006). Accordingly, we first washed in the thromboxane agonist U46619 to establish an initial vasoconstriction. In WT slices, the standard concentration of U46619 (75 nM) was able to induce a significant vasoconstriction in the majority of blood vessels (Fig. 2.5*B*) (Rancillac et al., 2006). Surprisingly, we found that blood vessels from *Fmr1*-KO mice were mostly non-responsive to 75 nM indicating that the blood vessels from *Fmr1*-KO mice are less sensitive to activation of thromboxane A2 receptors (Fig. 2.5*B*). To further explore this observation, we extracted the middle and posterior cerebral arteries (MCA/PCA) and measured their reactivity in isolation. In agreement with our experiments conducted in slice, we found that blood vessels from *Fmr1*-KO mice respond less to U46619 confirming that *Fmr1*-KO mice have defects to their vasculature (Fig. 2.5*C*). As isolated blood vessels from *Fmr1*-KO mice still react to U46619, we reasoned that a higher concentration of the drug could induce significant vasoconstriction in slice. Accordingly, we used a higher concentration of U46619 (150 nM) and found that a higher proportion of blood vessels in both WT and *Fmr1*-KO mice responded with a significant constriction (Fig. 2.5*B*).

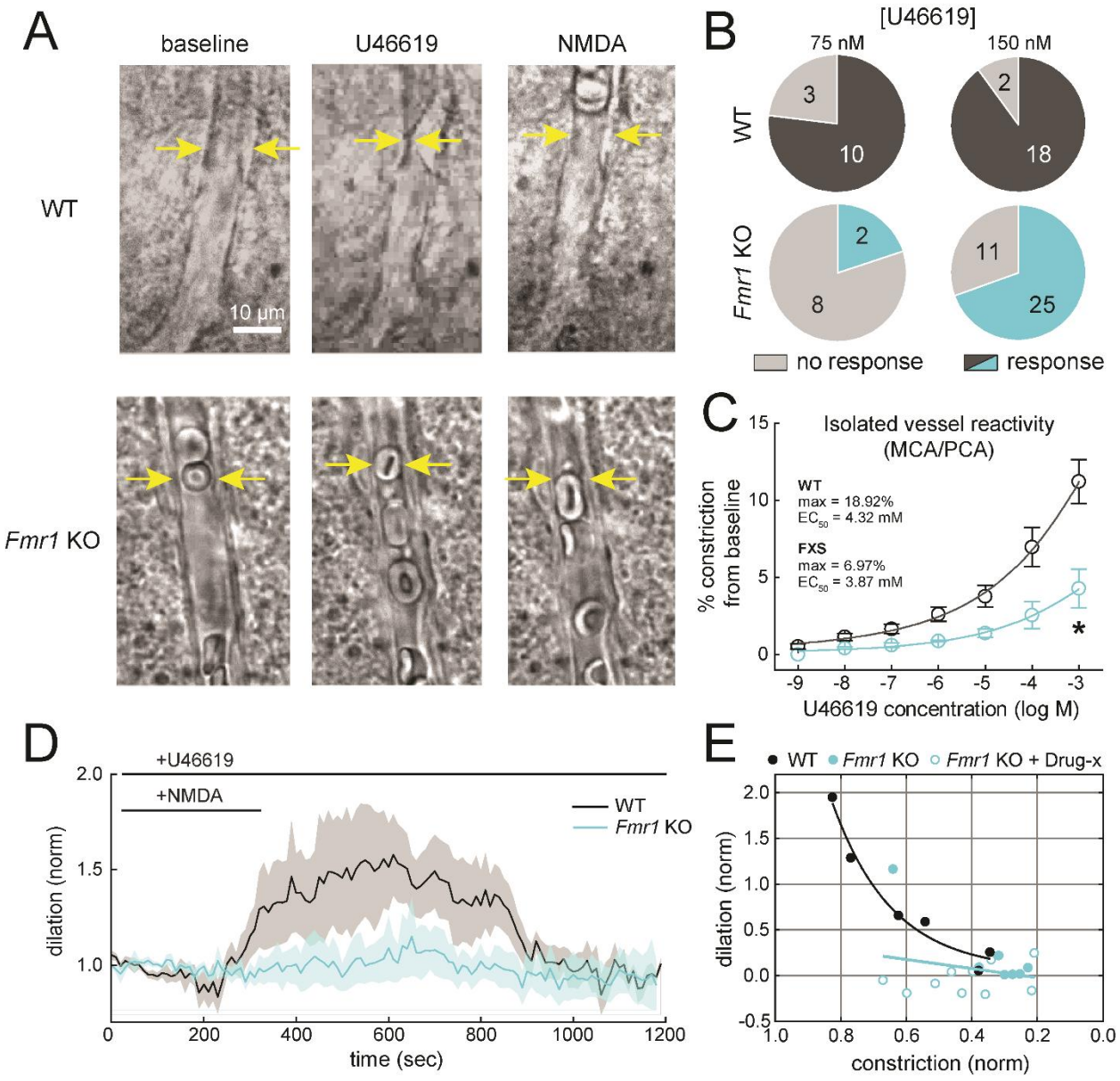

Figure 2.5 Neurovascular coupling is disrupted in the cerebellum of Fmr1-KO mice

(A) Representative images from two different cerebellar blood vessels from WT (top) and Frm1 KO (bottom) mice. Images are taken at baseline, application of the vasoconstrictor U46619, and application of NMDA. Yellow arrows indicate the analyzed pinch point for each blood vessel. (B) Pie charts categorizing the proportion of blood vessels which respond, or did not respond, to the application of 75 (left) and 150 nM (right) U46619 from both WT (top) and Fmr1 KO mice (bottom). (C) Dose-response plot of isolated blood vessels from WT and Fmr1 KO mice to U46619 fit with a logistic regression. (D) Time course plot of the normalized cerebellar blood vessel diameter in both WT and Fmr1 KO mice during the application of NMDA. Blood vessel diameter is initially normalized to the pre-constricted level (Error bars, s.e.m). (E) Plot of the blood vessel constriction compared with the blood vessel dilation in both WT and Fmr1 KO mice.

Only upon establishing a significant blood vessel constriction did we then proceed to test if the application of NMDA can induce vasodilation. First we applied 150 nM U46619 for 10 mins while constriction occurred. After visually identifying that cerebellar blood vessel were preconstricted, we bath applied NMDA (50 μM) for 5 mins to test if activation of NMDA receptors can induce dilation. In WT slices, we found that NMDA caused constricted blood vessels to dilate to 157.8 ± 21% (n=6, Fig. 2.5*A,D*) of the preconstricted diameter. Furthermore, we observed that the degree of blood vessel dilation was correlated with the amount of constriction we observed during application of U46619 (Fig 2.5*E*) which is consistent with previously published work (Rancillac et al., 2006). Conversely, while we were able to induce significant blood vessel constriction with application of 150 nM U46619 in cerebellum slices from *Fmr1*-KO mice, we did not observe similar dilation in response to NMDA (Fig 2.5 *D,E*). In *Fmr1*-KO mice we saw a peak dilation of 114.9 ± 20% (n=10, compared to 157.8 ± 21%, n=6 for WT) and the relationship between the degree of vessel constriction and dilation was lost (Fig 2.5 *D,E*). Finally, we tested to efficacy of Drug-X for restoring proper blood vessel function in Fmr1-KO mice. While we were still able to induce blood vessel constriction in the presence of Drug-X (Fig 2.5*E*), we did not observe a significant blood vessel dilation in response to NMDA (peak dilation 103.3 ± 1%) from the preconstricted blood vessel diameter.

2.6 Discussion

This study advances our understanding of inhibitory signaling and the role it plays in the pathophysiology of FXS in four important ways. First, we identify a novel defect in NMDAR mediated excitatory neurotransmission of cerebellar MLIs. NMDARs are a critical neurotransmitter receptor which have an important role in the development and maturation of the CNS (Paoletti et al., 2013b). In cerebellar MLIs, NMDARs are a central signaling hub responsible for stimulating multiple physiological plasticity mechanisms downstream of their activation (Alexander and Bowie, 2020; Larson et al., 2020) (Fig. 2.5). The decrease in NMDAR signaling in *Fmr1*-KO mice disrupts these downstream plasticity pathways impacting MLI function. Second, MLIs lacking FMRP do not exhibit activity-dependent upregulation of spontaneous firing due to the reduction of functional NMDARs. Third, NMDAR-dependent iLTP is also lost in *Fmr1*-KO mice due to the absence of NMDAR signaling. While these defects are downstream of NMDARs, we have shown through direct activation of PKC that the intracellular pathways stimulating iLTP remains functional. Furthermore, iLTP can be rescued by boosting the signaling molecules downstream of NMDAR activation and nitric oxide signaling with the use of molecules such as Drug-X. Finally, we have also shown that there are major disruptions to the regulation of blood vessels in *Fmr1*-KO mice which is a novel defect in the pathophysiology of the disease. Taken together, we have found a major synaptic deficit in NMDAR signaling in *Fmr1*-KO mice, described the physiological consequences, and provide a potential avenue for a novel therapeutic target for FXS syndrome.

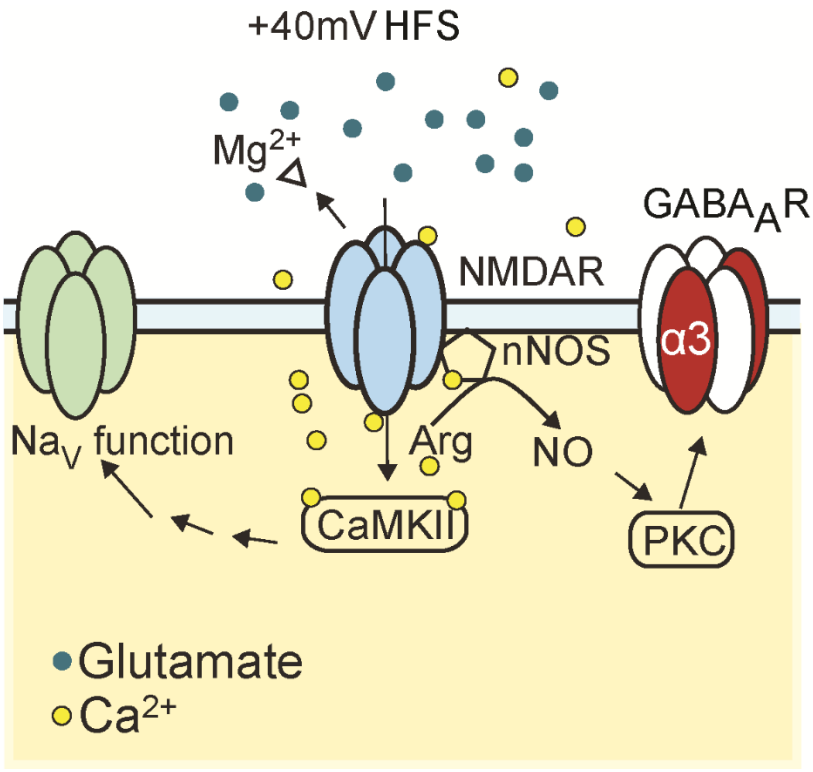

Figure 2.6: Summary of the IP and iLTP signaling pathways disrupted in Fmr1-KO mice
Schematic diagram summarizing the main signaling events and molecules that potentiate action potential frequency and GABAergic signaling. CaMKII activation is a necessary component for intrinsic plasticity (Alexander and Bowie, 2020) while PKC activation occurs downstream of NOS signaling for iLTP (Larson et al., 2020).

NMDAR defects have multiple downstream consequences impacting cerebellar function

Glutamatergic synapses in cerebellar MLIs are different from most conventional synapses as they mostly contain AMPARs, while NMDARs are thought to be only extrasynaptic (Clark and Cull-Candy, 2002). Interestingly, this uniqueness may render them particularly prone to disruption in autism-related disorders for several reasons. First, the extrasynaptic recruitment of NMDARs in MLIs requires the postsynaptic cell-adhesion molecule neuroligin-1 (Zhang and Sudhof, 2016). Neuroligins have already been linked to autism-related disorders (Bourgeron, 2015) and notably *Fmr1*-KO mice have decreased neuroligin-1 expression in the cerebellum (Dahlhaus and El-

Husseini, 2010). Second, FMRP and associated microRNAs, most notably miR-125b, regulate expression levels of the GluN2A NMDAR subunit (Edbauer et al., 2010) as well as regulating MEF-2 mediated PSD-95 degradation and synapse elimination (Tsai et al., 2012). Whether any of these molecules and/or mechanisms accounts for the defect in MLI NMDAR signaling awaits future investigation.

The defects in NMDAR signaling have also been shown to result in major impacts on the regulation of blood flow through the cerebellar cortex. As previously noted, the NMDAR-nNOS complex present on MLIs has an important role in neurovascular coupling in the cerebellum (Rancillac et al., 2006). We have found that cerebellar blood vessels from *Fmr1*-KO mice are unresponsive to the application of NMDA which is consistent with our observations demonstrating a lack of NMDAR signaling in MLIs. This is also similar with other experiments *in vivo* which have revealed that mice lacking MLIs have deficits in cerebellar blood flow regulation during sensory stimulation (Yang et al., 2000). Accordingly, we expect that there would similarly be a major impact on the local regulation of blood flow in the cerebellum of *Fmr1*-KO mice. It will be necessary to test the nature of cerebellar blood vessels defect during *in vivo* experiments in the *Fmr1*-KO mice model, as this is a major unexamined defect of the disorder. Further experiments in other brain regions should also be considered to see if NMDAR-NOS signaling is similarly disrupted throughout the CNS as this signaling complex is found across all brain regions (Bredt et al., 1990). While NMDAR-mediated activation of NOS also regulates blood flow in other brain regions (Faraci and Breese, 1993; Ayata et al., 1996; Lindauer et al., 1999), there are additional mechanisms by which blood flow is regulated including acetylcholine (Biesold et al., 1989) and noradrenaline (Toussay et al., 2013). Further experiments should begin to examine if

other mechanisms of neurovascular coupling are similarly disrupted. Finally, and perhaps most intriguingly, *Fmr1*-KO mice are also less responsive to vasoconstriction by thromboxane A2 activation by U46619. It is possible that this is a compensatory mechanism to allow blood flow in the absence of the endogenous NO dilatory signaling pathway but the nature of this defect remains to be resolved. Ultimately, these observations reveal that *Fmr1*-KO mice have an inability to regulate blood flow in response to neuronal activity.

Defective cerebellar circuits and the pathophysiology of fragile X syndrome

In this study, we have focused exclusively on the cerebellar cortex but there is evidence that the defects that we have described here could have implications across the CNS. Through a process termed *developmental diaschisis*, the cerebellum is thought to play a key role in guiding the maturation of circuits responsible for cognitive development (Wang et al., 2014). In recent years there is an increasing body of research which points to a link between the cerebellum and non-motor brain functions (Schmahmann and Sherman, 1998; Stoodley and Schmahmann, 2009; Badura et al., 2018; Deverett et al., 2018; Carta et al., 2019; Sathyanesan et al., 2019; Schmahmann et al., 2019; Streng and Krook-Magnuson, 2020). Dysregulated communication between the cerebellum and non-motor regions are also linked to the development of neurodevelopmental disorders such as autism spectrum disorders and FXS. Specifically, abnormalities in PCs have been found in patients with autism (Whitney et al., 2008; Jeong et al., 2014; Skefos et al., 2014) while cerebellar damage at a young age is also associated with autism (Limperopoulos et al., 2007; Bolduc and Limperopoulos, 2009; Catsman-Berrevoets and Aarsen, 2010; Wang et al., 2014). Furthermore, there is a strong relationship between disruptions in PC function and autistic like phenotypes in animals. Notably, autistic phenotypes have been

described in PC specific expression of mutations associated with autism including Shank2 (Peter et al., 2016), PTEN (Cupolillo et al., 2016), Tsc1 (Tsai et al., 2012), Tsc2 (Reith et al., 2013) and *Fmr1*-KO mice (Koekkoek et al., 2005).

The main role of MLIs are to modulate the firing properties of PCs (Mittmann et al., 2005; Jörntell et al., 2010) which are the sole output of the cerebellar cortex. In awake behaving animals the activity in MLIs has been directly linked with the cerebellar dependent motor learning that occurs during the vestibulo-occular (VOR) gain reflex. This mechanism relies on PC LTD and LTP which in turn is regulated by MLI activity (Rowan et al., 2018). Thus far there have not been any studies examining the nature of MLI regulation of non-motor activity but it is likely that MLIs would have a similar impact on non-canonical cerebellar function as they have on the motor learning underlying VOR. As defects in the output from the cerebellum are thought to contribute to the onset of autism spectrum disorders and FXS (Wang et al., 2014; Hampson and Blatt, 2015; Sathyanesan et al., 2019; Schmahmann et al., 2019), the defects from the loss of NMDAR signaling described in this study could have far reaching implications for overall brain function. In order to provide more insight into these questions, a more thorough investigation on the role of the MLI inhibitory and IP mechanisms on cerebellar function will need to be undertaken. Specifically the functional impact on PC firing properties following MLI iLTP and IP should be investigated.

Potential avenues for therapeutic development

From a therapeutic perspective, the most intriguing aspect of this study is the fact that the downstream secondary signaling cascade remains functional in the expression of iLTP. We were able to show with direct activation of PKC that the downstream signaling pathway

strengthening inhibitory GABAergic signaling is intact in *Fmr1*-KO mice. This observation is critical to demonstrating that the major defect in MLIs is found at the level of the NMDAR. Second, there are a wide range of potential signaling molecules which we have identified in Chapter 1 that could be targets for therapeutic interventions to prolong and strengthen the residual NMDAR signal. There is a large body of literature describing the biochemical signaling pathways involved in the NMDAR-nNOS pathway which we have previously used to inform our work on MLI iLTP (Larson et al., 2020). The signaling cascade downstream of NO production was first described in smooth muscle for the promotion of vasodilation (Palmer et al., 1987) through cGMP production (Ignarro et al., 1986). Similar biochemical signaling cascades have also been found in the CNS following NMDAR activation which regulate cerebral blood flow in the neocortex (Girouard et al., 2009) and cerebellum (Rancillac et al., 2006) while also being tied into synaptic plasticity (Bon and Garthwaite, 2003; Qiu and Knöpfel, 2007). A key part of the signaling pathway is the production/degradation of cGMP which can be regulated by small molecules (Goy, 1991). Since these pathways are well known they have been targeted in the past in the clinical setting, it will be interesting to see if targeting this pathway can restore normal cerebellar function in *Fmr1*-KO mice. In this study we have found a potential candidate drug to base future therapeutic research around. Critical to Drug-X's potential future use is that the presence of Drug-X has a modest effect under basal conditions which we have noted during our recordings (Fig. 2.4). This becomes more pronounced following activation of NMDAR and stimulation of nNOS. It will be interesting to see if Drug-X, or other drugs like it, can restore normal cerebellar behaviors in *Fmr1*-KO mice. As this NOS signaling pathway is ubiquitous, and regulates blood flow in smooth muscle outside the CNS (Bredt and Snyder, 1994), it will also be important to look for compounds to selectively target

neurons and avoid unintended off target effects. Future experiments should also test the cerebellar circuit functions in the context of the *Fmr1*-KO MLI phenotype.

Author Contributions:

E.A.L., R.P.D.A. L.J.T. and D.B. designed research; E.A.L., R.P.D.A., and L.J.T., performed research and analyzed data; E.A.L., R.P.D.A. L.J.T., and D.B. wrote the paper.

Acknowledgements

This work was supported by Canadian Institutes of Health Research Operating Grants CIHR MOP-342247 to D.B. We thank members of the Bowie laboratory, for discussions and comments on the manuscript.

The authors declare no competing financial interests.

CHAPTER 3

FMRP acts as a regulator of MLI dendritic signaling

3.1 Foreword to Chapter 3

This Chapter was a spinoff from a result we observed in Chapter 2. In addition to an inability for *Fmr1*-KO to induce iLTP in MLIs, we also found that they had a consistently larger EPSP amplitude from evoked stimulations. What had started out as a curious observation, has now ended up a comprehensive study to explain two things. First, we asked what is the consequence of the increased eEPSP amplitude on MLI excitability? Second, in what can only be described as true Bowie lab style, we asked what is the molecular mechanism that explains the larger EPSP amplitude? The first question was asked originally by Dr. Charles Bourque, from the Centre for Research in Neuroscience at the Montreal General Hospital. During a PhD committee meeting, he proposed that a larger EPSP would likely impact the firing properties of the neuron. I then performed the experiments presented in Figure 3.1 and found that his intuition was correct.

As for the second question, we knew from the results shown in Figure 2.1 of Chapter 2 that this defect was not due to increased AMPA receptor signaling. Furthermore, I had found that the action potential threshold could also not explain these results. Interestingly, we found that MLIs lacking FMRP have decreased A-type voltage gated K^+ currents. Nevertheless, this observation could not explain the larger EPSP amplitude for reasons that are outlined in the Discussion. What we ended up finding was an interesting role for the N-terminal fragment of FMRP. A number of studies over the last decade have revealed a role for N-FMRP to modulate voltage-gated ion channels and Derek suggested that we include the protein in my patch pipette solution. Admittedly, I was more skeptical at first but it ended up being successful at reducing the EPSP amplitude. By the end of this study, I had identified a second defect in MLI excitatory signaling, but one that was not synaptic and involved direct protein-protein modulation by FMRP.

Article Title:

Disrupted dendritic filtering contributes to hyperexcitability in the fragile-X syndrome cerebellum receptor

Erik A. Larson[1,2], & Derek Bowie[2]

[1]Integrated Program in Neuroscience, McGill University, Montréal, QC H3A 2B4, Canada
[2]Department of Pharmacology and Therapeutics, McGill University, Montréal, QC H3G 1Y6, Canada

To be submitted to the *Journal of Physiology*

3.2 Abstract

Fragile X syndrome (FXS) is the most common single gene cause of inherited intellectual disability and autism. The disease typically occurs because of the loss of expression of the Fragile X Mental Retardation Protein (FMRP) which causes hyperexcitability at the cellular and circuit level of the CNS. Here we show that the loss of FMRP causes defects in signaling from cerebellar molecular layer interneurons (MLIs). We observed increased action potential (AP) firing in MLIs from *Fmr1*-KO mice following excitatory PF stimulation. The nature of this increased firing is due to increased signaling from synapses, as intrinsic AP firing is similar between WT and *Fmr1*-KO mice. In voltage-clamp, evoked AMPA receptor EPSCs are similar between WT and *Fmr1*-KO mice while *Fmr1*-KO mice have significantly evoked EPSP amplitudes following synaptic stimulation. We attribute the larger depolarizations to decreased dendritic filtering in *Fmr1*-KO mice. T-type Ca^{2+} channels do not contribute to this difference in depolarization but *Fmr1*-KO mice have significantly smaller A-type K^{+} currents. Finally, reintroduction of an N-terminal fragment of FMRP (N-FMRP) reduces the EPSP depolarization in *Fmr1*-KO mice while having no effect in WT mice. This study reveals a novel defect in hyperexcitability and develops additional insight into the function of the N-FMRP in regulating neuronal excitability.

3.3 Introduction

Fragile X syndrome is the most common inheritable single gene cause of intellectual disability and autism. The disease is the result of the loss of expression or function of the Fragile X Mental Retardation Protein (FMRP). Typically, this disruption arises due to an expansion of CGG repeats in the 5'-untranslated region of the FMR1 gene (Pieretti et al., 1991; Verkerk et al., 1991). The full mutation occur when there are >200 CGG repeats and this results in hypermethylation and transcriptional silencing of FMRP – its gene product (Pieretti et al., 1991). FXS can also occur due to other disruptions to FMRP expression (Penagarikano et al., 2007) or from point mutations in FMR1. Notably, mutations in the FMRP amino terminal domain, R138Q (Collins et al., 2010; Myrick et al., 2015; Sitzmann et al., 2018), or the RNA binding region, G266E (Myrick et al., 2014), and I304N (De Boulle et al., 1993) are all known to cause FXS symptoms. The lack of FMRP, or disruptions to its function, cause phenotypes which include hyperactivity, anxiety, and neuronal circuit abnormalities (Contractor et al., 2015) which mirror observations from human patients (Lozano et al., 2014a).

Understanding the functional role of FMRP has been one of the main goals for understanding the pathophysiology of FXS. FMRP is a polyribosome mRNA binding protein which is highly enriched in synapses and controls local protein translation (Greenough et al., 2001). It has many mRNA targets, often for proteins enriched in synapses, and is responsible for translation-dependent long term changes to neuronal function (Brown et al., 2001; Darnell et al., 2011). A large body of FXS literature has focused on the role of FMRP in regulating cellular/circuit excitability (Contractor et al., 2015). At the molecular level, FMRP is responsible for transcriptionally regulating the expression, localization and function of voltage gated ion

channels critical to excitability (Brager and Johnston, 2014). Notably, FMRP interacts with the mRNA for $Na_V1.2$ and 1.6, and the K^+ channels $K_V4.2$ (A-type) (Gross et al., 2011), and $K_V1.2$, 2.1, and 3.1 (delayed rectifiers) (Strumbos et al., 2010; Darnell et al., 2011). FMRP also interacts with mRNA for the structural protein ankyrin-G (Darnell et al., 2011), which is critical for ion channel localization at the axon initial segment (Rasband, 2010). Furthermore, the biophysical properties of many of these ion channels are notably different in *Fmr1*-KO mice. For example, the activation A-type currents are significantly shifted in *Fmr1*-KO mice demonstrating there are multiple levels by which FMRP – or the lack thereof – can impact excitability (Routh et al., 2013; Kalmbach et al., 2015).

Contrasting early studies on the mRNA binding role of FMRP, recent advances in the last decade have revealed novel translation-independent roles for FMRP in the regulation of critical voltage-gated ion channels. Structural analysis of FMRP suggested that the N-terminal domain was a good candidate for forming protein-protein interactions (Ramos et al., 2006). Subsequently, FMRP was shown to interact with the sodium activated potassium channel (Slack) imparting functional changes (Brown et al., 2010). Additional studies have implicated dysfunctions in other ion channels in FXS and found that FMRP has a translation independent role in regulating their activity. Specifically, the delayed rectifier potassium ($K_V1.2$) (Yang et al., 2018), A-type potassium ($K_V4.3$) (Zhan et al., 2020), hyperpolarization-activated cyclic nucleotide–gated (HCN) (Brandalise et al., 2020), N-type calcium (Ca_V 2.2) (Ferron et al., 2014), T-type calcium ($Ca_V3.1$) (Zhan et al., 2020), small conductance calcium-activated potassium (SK2) (Deng et al., 2019), and big conductance calcium-activated potassium channels (BK) (Deng et al., 2013) have all been found to be regulated in some manner through a protein-protein interaction

with FMRP. Some of these interactions are modified by the presence of auxiliary proteins such as the BK channels β subunit (Kshatri et al., 2020). In other cases they depend on post-translational modifications such as phosphorylation of the $K_V1.2$ C-tail facilitate the interaction with FMRP (Yang et al., 2018).

While many of these observations link FMRP to excitability defects in the regulation of action potential (AP) firing, considerably less is known about how these defects are linked to excitability and dendritic signaling. Recent work has found defects in dendritic integration in cerebellar granule cells from *Fmr1*-KO mice (Zhan et al., 2020). Similar ion channels are found enriched in the dendrites of cerebellar molecular layer interneurons (Molineux et al., 2005) but the function of them has not been studied in the context of FXS. Here, we have tested the hypothesis that in the absence of FMRP, dysregulations of ion channel function causes disruptions in dendritic signaling. We found that cerebellar molecular layer interneurons from *Fmr1*-KO mice fire more APs in response to afferent stimulation compared to WT mice. Hyperexcitability in MLIs is caused by altered dendritic filtering which results in a larger response in *Fmr1*-KO mice compared to WT. In addition to our observed changes to dendritic signaling we have also found a decreased A-type K^+ current density. Finally, the defect in dendritic signaling can be rescued by acute reintroduction of the FMRP N-terminus fragment. Taken together we reveal a novel FXS defect in dendritic signaling which is due to the translation-independent role of FMRP.

3.4 Methods

Ethical approval

All experiments were performed in accordance with the guidelines of the Canadian Council on Animal Care and were approved by the Animal Care Committee of McGill University.

Animals

Wild-type mice with a C57BL/6J background were obtained from Charles River Laboratories (Wilmington, MA, USA) and maintained as a breeding colony at McGill University. Breeder pairs of *Fmr1*-KO mice, C57BL/6 background, were kindly provided by Dr. Greenough (University of Illinois, Urbana-Champaign, IL 61801, USA)(Comery et al., 1997). Both male and female mice used for experiments ranged from postnatal days 18 to 30.

Slice preparation

Mice were anesthetized with isoflurane and immediately decapitated. The cerebellar vermis was rapidly dissected from the mouse and submerged in ice-cold cutting solution perfused with carbogen gas (95% O_2, 5% CO_2). Cutting solution contains (in mM): 235 sucrose, 2.5 KCl, 1.25 NaH_2PO_4, 28 $NaHCO_3$, 0.5 $CaCl_2$, 7 $MgCl_2$, 28 D-glucose, 1 ascorbic acid, 3 sodium pyruvate (pH 7.4; 305–315 mOsmol/L). The vermis was then fastened to a platform, transferred to the slicing chamber and again submerged in ice-cold cutting solution, bubbled with carbogen throughout the remainder of the procedure. Slices of cerebellar vermis (300 µm) were made with a vibrating tissue sectioner (Leica VT1200; Leica Instruments, Nussloch, Germany). The slices were transferred to oxygenated artificial cerebrospinal fluid (ACSF) and held at room temperature (21°C-23°C) for at least 1 h before recordings were performed. ACSF contained the following (in

mM): 125 NaCl, 2.5 KCl, 1.25 NaH_2PO_4, 26 $NaHCO_3$, 2 $CaCl_2$, 1 $MgCl_2$, 25 D-glucose (pH of 7.4; 305–315 mOsmol/L).

Electrophysiology

Slice experiments were performed on an Olympus BX51 upright microscope (Olympus, Southall, UK) equipped with differential interference contrast/infrared optics. Whole-cell patch-clamp recordings were made from either visually-identified MLIs in acute sagittal slices of cerebellar vermis. MLIs were distinguished from misplaced or migrating granule, glial by their small soma diameter (8–9 µm), location in the outer two-thirds of the molecular layer and whole-cell capacitance measurement (4-12 pF). Patch pipettes were prepared from thick-walled borosilicate glass (GC150F-10, OD 1.5 mm, ID 0.86 mm; Harvard Apparatus Ltd, Kent, UK) and had open tip resistances of 4–7 MΩ when filled with an intracellular recording solution. Recordings were made with a Multiclamp 700A amplifier (Molecular Devices, Sunnyvale, CA, USA) at a holding potential of -60 mV. Series resistance and whole-cell capacitance were estimated by cancelling the fast transients evoked at the onset and offset of brief (10 ms) 5 mV voltage-command steps. Access resistance during whole-cell recording (7–25 MΩ) was compensated between 60 and 80% and checked for stability throughout the experiments (~15% tolerance). The bath was continuously perfused at room temperature (21–23 °C) with ACSF at a rate of 1–2 mL/min. Currents were filtered at 5 kHz with an eight-pole low-pass Bessel filter (Frequency Devices, Haverhill, MA, USA) and digitized at 25 kHz with a Digidata 1322A data acquisition board and Clampex 10.1 (Molecular Devices) software.

For extracellular stimulations, thin walled borosilicate glass electrodes (OD 1.65mm, ID 1.15mm; King Precision Glass Inc, Claremont, CA, USA) were used with a tip resistance of < 3 MΩ when filled with aCSF. The ground electrode for the stimulation circuit was made with a platinum wire wrapped around the stimulation electrode. The stimulating electrode was positioned in the molecular layer at or just beneath the slice surface. Voltage pulses (10—25 V in amplitude, 200 μs in duration) were applied at low frequency stimulation (0.1 Hz) through the stimulating electrode. To minimize variability between responses, the stimulating electrode was positioned 50-100 μm away from the recorded cell. The stimulus voltage used during each experiment was at the lowest intensity to elicit the maximal eEPSP/EPSC response within the range described above.

Recording solutions

All chemicals were obtained from Sigma Aldrich (St. Louis, MO, USA) unless otherwise indicated. Internal pipette solution for most current-clamp experiments contained (in mM): 126 K-gluconate, 5 HEPES, 4 NaCl, 15 D-glucose, 0.05 $CaCl_2$, 1 $MgSO_4$, 0.15 K_4-BAPTA, 3 Mg-ATP, 0.1 Na-GTP (adjusted to pH 7.4 with KOH, 300-310 mOsmol/L). Current-clamp recordings of evoked PSPs used the same solution with the addition of 2 mM QX314. Voltage-clamp recordings were made with an intracellular solution that contained (in mM): 140 CsCl, 4 NaCl, 0.5 CaCl2, 10 HEPES, 5 EGTA, 2 Mg-ATP, 2 QX314 (pH 7.4 with CsOH, 300-310 mOsmol/L). To isolate for AMPAR currents the external ACSF was supplemented with 10 μM bicuculine to block $GABA_A$ receptors. Internal solutions for voltage-clamp experiments examining A-type K^+ current (I_A) contained (in mM): 140 KCl, 10 HEPES, 2.5 $MgCl_2$, 0.15 K_4-BAPTA (adjusted to pH 7.4 with KOH, 300-310 mOsmol/L). The

external ACSF was supplemented with 5 mM TEA-Cl and 2 mM CsCl to block non-I_A K^+ channels, and 100 nM TTX to block AP firing.

Pharmacological compounds

NMDAR antagonist, D-APV (10 µM) and MK-801 (10 µM), AMPA antagonist 1-(4-Aminophenyl)-3-methylcarbamyl-4-methyl-3,4-dihydro-7,8-methylenedioxy-5H-2,3-benzodiazepine hydrochloride (GYKI 53655; 10 µM), and the $GABA_A$ receptor antagonist bicuculline (10 µM) were purchased from Tocris Bioscience (Ellisville, MO, USA). Stock solutions of these antagonists were prepared in water and were stored at −20°C and working solutions were diluted with aCSF shortly before application to the bath. Phorbol 12-myristate 13-acetate (PMA, 100nM, Tocris), and Drug-X (100µM) were dissolved in DMSO and stored at −20°C. The final maximum DMSO concentration for all experiments (0.1% v/v).

3.5 Results

MLIs from *Fmr1*-KO mice have increased excitability in response to PF stimulation

Neuron hyperexcitability is a common observation in FXS patients and animal models that explains many of the phenotypes and symptoms of the disease (Contractor et al., 2015), but less is known about how the absence of FMRP impacts dendritic signaling. Moreover there is a lack of knowledge regarding the general excitability of cerebellar MLIs in FXS, a key neuron type regulating the output of the cerebellar cortex circuit (Apps and Garwicz, 2005). To measure dendritic responses and neuronal excitability in MLIs, we performed whole-cell current-clamp electrophysiological recordings and compared the response properties from WT and *Fmr1*-KO mice. Upon breakthrough into whole-cell patch clamp configuration, we injected a hyperpolarizing current to maintain the holding potential at a -70 mV. We then recorded MLI APs in response to afferent stimulations by placing a stimulating electrode in the molecular layer and performing a single pulse protocol to activate PF afferents which form the primary excitatory synapse onto MLI dendrites (Apps and Garwicz, 2005).

By increasing the pulse intensity by 2V for each subsequent sweep, we probed responses across a range of intensities. At lower intensities (<10 mV), our stimulations failed to elicit any APs from either WT or *Fmr1*-KO MLIs. Upon reaching higher intensity stimulations, we began to reliably observe APs and eventually induced trains of APs at intensities closer to our peak stimulation of 24V (Fig. 3.1 *A,B*). Notably, MLIs from *Fmr1*-KO mice generated a significantly higher number of APs at higher stimulation intensities, demonstrating a hypersensitivity to afferent stimulation (average number of spikes at 24V: WT 2.3 ± 0.98 spikes per stim, n=6; *Fmr1*-KO 16.7 ± 7.6 spikes per stim, n=7).

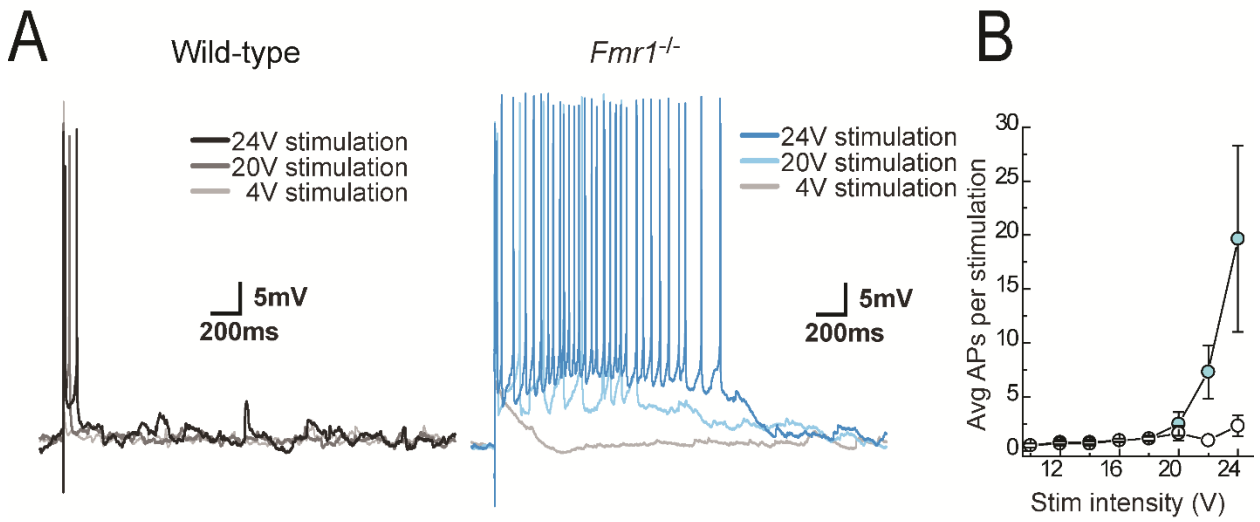

Figure 3.1: Parallel fiber stimulations onto MLIs generate more APs from Fmr1-KO mice
(A) Representative current clamp traces of action potentials evoked from parallel fiber stimulations of different intensities (4V, 20V, 24V) from a WT (left) and a Fmr1-KO mouse (right). (B) Summary plot of the average number of action potentials generated by parallel stimulations of increasing intensities. (Error bars, s.e.m).

Fmr1-KO and WT mice have different eEPSP properties

Next, we wanted to better understand the mechanism behind the increase in AP excitability following synaptic stimulation. The increase in AP excitability could be due to either increased synaptic signaling or to a change in MLI AP properties (Debanne et al., 2019). Altered synaptic signaling would generate a larger EPSP with a greater depolarization and overall a higher likelihood for more spikes. Alternatively, changes to AP properties such as a lowered spike threshold would also generate more APs from the same synaptic input. Accordingly we performed experiments to distinguish between these two hypotheses.

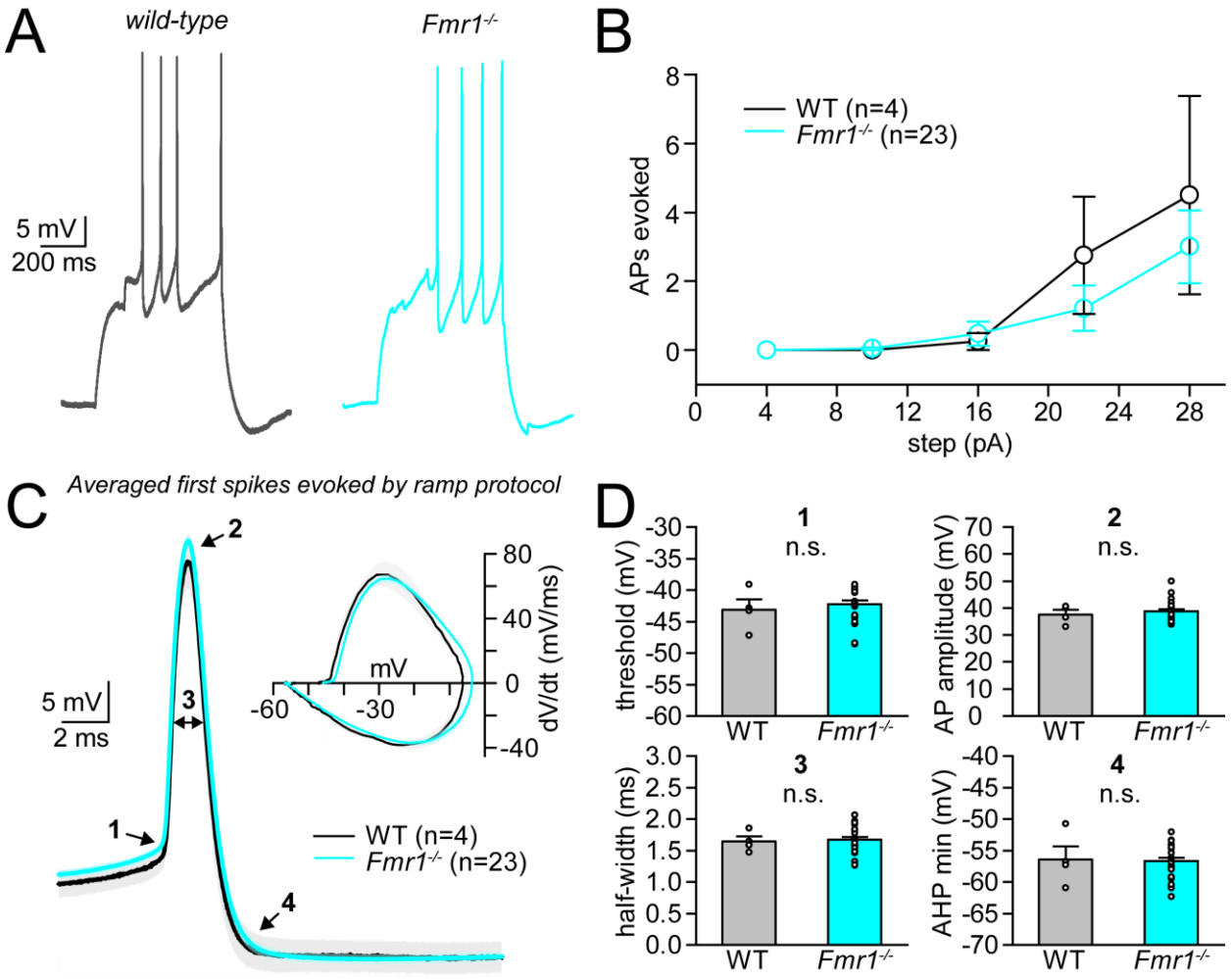

Figure 3.2: WT and Fmr1-KO mice have similar action potential properties
(A) Representative current-clamp recordings from a WT (left), and Fmr1-KO (right) MLI showing evoked action potentials from a 28pA depolarizing step. (B) Summary action potential frequency over a range of step amplitudes. (C) Action potentials overlaid next to the action potential cycle (calculated from voltage-time data) from a WT and Fmr1-KO MLI. (D) Summary plots comparing the action potential properties of threshold, action potential amplitude, half-width, and AHP minimum. (Error bars s.e.m.)

To assess AP properties, we performed experiments in current-clamp mode and injected incremental depolarizing currents (4-28pA) while recording the number of APs per step. At each step amplitude we observed a similar number of APs from both the WT and *Fmr1*-KO mice (28 pA step size; WT: 4.5 ± 2.8Hz, *Fmr1*-KO: 3.0 ± 1.1Hz) (Fig. 3.2 *A,B*). We then wanted to monitor the AP at the initiation of the upstroke so we performed a 1s ramp protocol to isolate the first

spike. To more carefully analyze the AP shape we transformed the AP by taking the derivative of the measured voltage plotted against membrane potential (Fig. 3.2 *C*). Then we overlaid the AP cycles from WT and MLIs and compared spike threshold (defined at the point where dV/dt=10mV/ms), amplitude, half-width, and after hyperpolarization minimum. Based on these measurements, we did not find any significant differences in the AP waveform which could explain the increased excitability observed in Figure 3.1. These results suggest that intrinsic membrane properties governing AP firing are largely comparable in MLIs from *Fmr1*-KO mice and that the hyperexcitability observed in Figure 3.1 must have another basis.

Next, we isolated the underlying evoked EPSP (eEPSP) waveform to observe the depolarization from a synaptic stimulus in the absence of APs. To do this we held MLIs at -60mV and performed the parallel fiber-MLI stimulation protocol as in Figure 3.1 with the inclusion of QX-314 in the patch pipette to block voltage gated Na^+ channels. Using a stimulating electrode we evoked a biphasic postsynaptic potential consisting of both excitatory glutamatergic and inhibitory GABAergic responses in WT and *Fmr1*-KO MLIs (Fig. 3.3 *A*). Compared to WT cells, the excitatory eEPSPs in *Fmr1*-KO MLIs had larger depolarizations (WT 22.5 ± 3.9 mV, n = 13; *Fmr1*-KO, 42.0 ± 3.1 mV, n=11; unpaired t-test t(22) 3.812, p= 0.00095) (Fig. 3.3*A,B*) and shorter half-widths (WT 11.0 ± 2.0 ms, n = 13; *Fmr1*-KO, 3.8 ± 0.7 ms, n = 11; unpaired t-test t(22)=3.048, p=0.006) (Fig. 3.3 *A,B*). The degree and duration of the hyperpolarization also tended to be larger in FMRP-lacking MLIs, but this was not statistically significant (WT -1.4 ± 0.4mV, n=13; *Fmr1*-KO, -2.4 ± 0.69mV mV, n=11; unpaired t-test t(22)=-0.639, p=0.52, Fig. 3.3 *A,B*). Additionally, we plotted an input/output relationship over the same range of intensities as in Figure 3.1 and found that *Fmr1*-KO mice consistently had larger eEPSP amplitudes compared to WT throughout the

range analyzed (Fig. 3.3 *C,D*). Accordingly, we reasoned that the larger eEPSP amplitudes in *Fmr1*-KO mice underlie the increased AP frequency observed in Figure 3.1 as the increased depolarization would sufficiently drive increased AP firing.

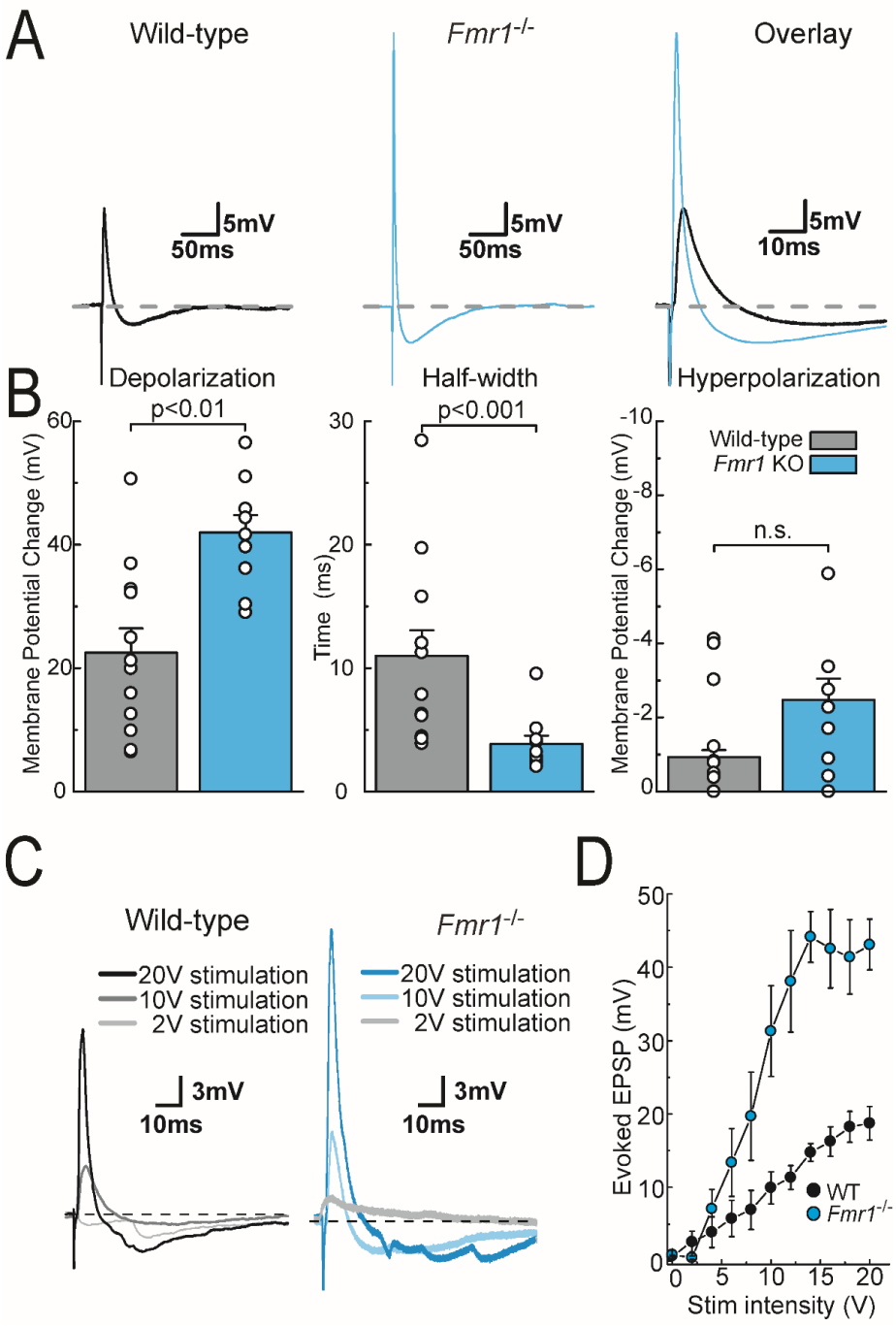

Figure 3.3: The ePSP waveform is larger and briefer in Fmr1-KO mice

(A) Representative ePSP recordings from a WT (left), and Fmr1-KO (center) MLI in current-clamp mode. The traces are then overlaid (right) to compare the differences in their properties. QX-314 was included in the patch pipette to block Na_V and action potential firing. (B) Summary plots comparing the overall depolarization amplitude, half-width, and hyperpolarization amplitude of the ePSP waveforms from panel A. (C) Representative current clamp traces of eEPSPs from parallel fiber stimulations at different intensities (2V, 10V, 20V) from a WT (left) and a Fmr1-KO mouse (right). (D) Summary plot of the average eEPSP amplitude generated by parallel stimulations of increasing intensities. (Error bars, s.e.m).

Fmr1-KO mice have disrupted dendritic filtering

After linking MLI hyperexcitability to increased eEPSP amplitude, we sought to better understand the molecular basis for this disruption. We were able to rule out any possibility that this could be linked to increased AMPA receptor synaptic currents because of our previous findings. While there is a notable deficit to high frequency stimulation of parallel fiber afferents, single stimulations of excitatory synapses are very similar between WT and *Fmr1*-KO mice and AMPAR currents are the same in both mice (see Chapter 2). We thus reasoned that the observed difference in eEPSP amplitude is likely due to disruption of an active conductance(s) affecting signal propagation along dendritic arbours. Outward currents such as voltage gated K^+ channels limit signal propagation along dendrites and an absence or reduction in this hyperpolarizing influence locally absence would allow for the greater eEPSP that we have observed in *Fmr1*-KO mice. Alternatively, the larger eEPSP could be the result of a larger inward depolarizing current such as those mediated by voltage gated Ca^{2+} channels which would potentiate the synaptic signal. Cerebellar MLIs express somatodendritic voltage gated channels which are known to modulate neuron excitability and changes to these ion channels could be responsible for this increased eEPSP. Specifically, they express Kv4.3 which mediates the A-type potassium current (I_A) and Cav3.2 which mediates the T-type Ca^{2+} current (I_T) (Molineux et al., 2005; Anderson et al., 2010; Anderson et al., 2013). Importantly, they have also been found to be disrupted in other cell types in *Fmr1*-KO Mice (Zhan et al., 2020). While dendritic Na_V channels also increase the eEPSP amplitude we ruled out any possibility of this due to our inclusion of the Na_V channel blocker QX314 during experiments in Figure 3.3 and the fact that MLIs do not express appreciable dendritic Na_V (Myoga et al., 2009).

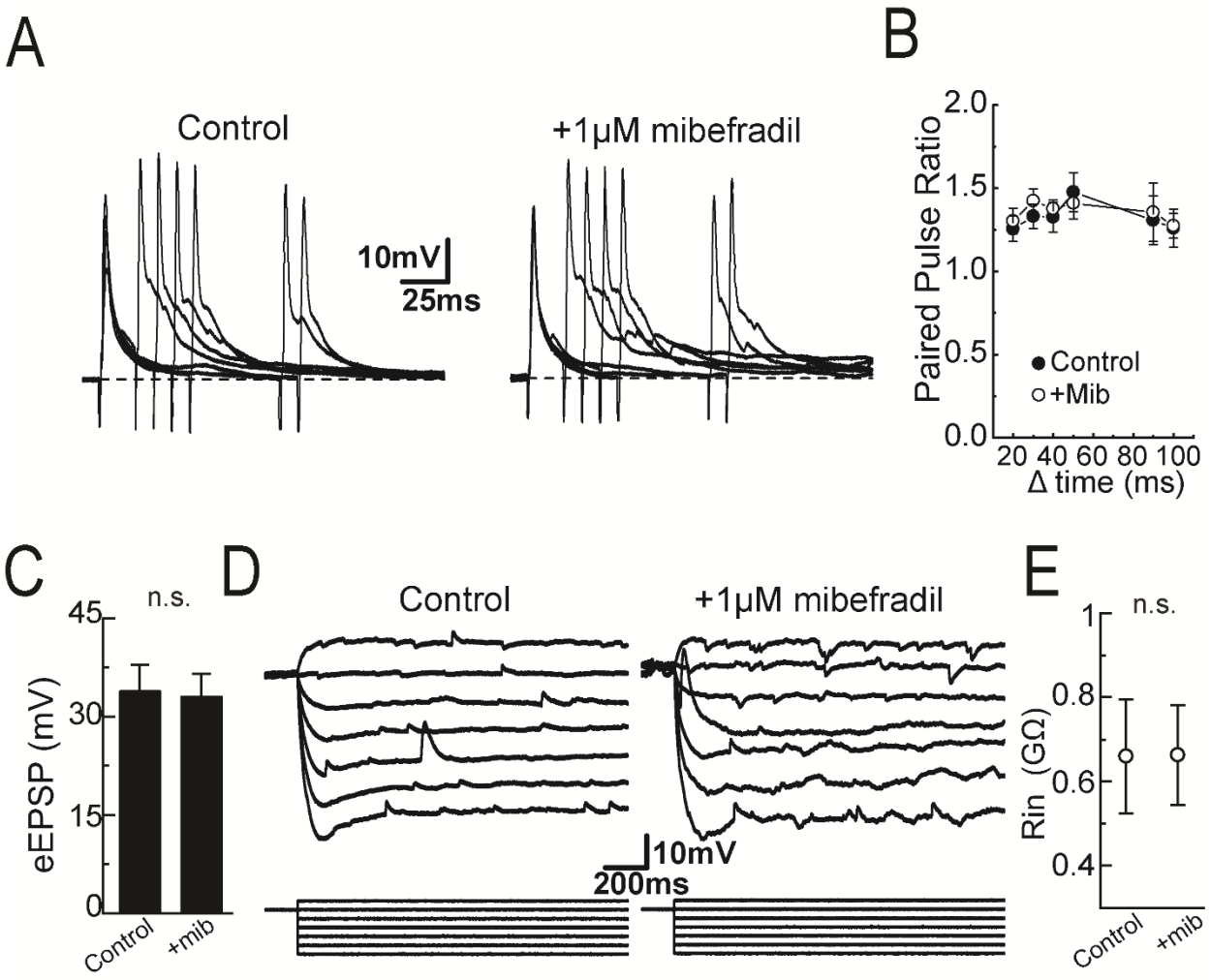

Figure 3.4: T-type calcium channels do not contribute to the eEPSP waveform

(A) Representative current-clamp paired pulse eEPSP recordings from the MLI of an Fmr1-KO mouse before (left), and after the addition of the T-type calcium blocker mibefradil. Multiple sweeps are overlaid with different inter-stimulation intervals. (B) Summary plot of the paired pulse ratio before and after the addition of mibefradil. (C) Summary plot of the average first eEPSP amplitude elicited before and after the addition of mibefradil. (D) Example traces of membrane potentials from currents injected (bottom) to probe the MLI input resistance before (left) and after (right) the addition of mibefradil. (E) Summary plot of the average input resistance of Fmr1-KO mice before and after mibefradil. Data was obtained by measuring the membrane potential response across the current steps shown in panel D. (Error bars s.e.m.)

First we tested for a possible role of I_T in a regulating the eEPSP waveform. Increased T-type Ca^{2+} current in *Fmr1*-KO mice could amplify the eEPSP response resulting in our observed hyperexcitability. We therefore performed stimulation experiments on MLIs from *Fmr1*-KO mice

in current-clamp mode with QX-314 to evaluate the impact of T-type Ca^{2+} on the eEPSP waveform. To do this we first recorded the typical large amplitude eEPSP as described in Figure 3.3 and, after a short baseline duration (10 min), washed in the specific T-type Ca^{2+} blocker, mibefradil. We used a paired pulse protocol to examine if mibefradil affects presynaptic release and a step protocol to measure input resistance. We found that mibefradil did not affect the presynaptic parallel fiber release as measured by our PPR protocol (Fig. 3.4*A,B*). Finally, mibefradil had no significant effect on the amplitude of the eEPSP waveform in *Fmr1*-KO mice nor did we see any changes to the input resistance of the neuron (control eEPSP amplitude 33.8 ±3.9 mV; +mib ePSP amplitude, 32.9 ±3.6mV, n=7, paired t-test t(6)= 0.774, p=0.46, Fig.3.4*C,D,E*). Together, these data suggest that T-type Ca^{2+} channels have very little modulatory effect on the eEPSP waveform and they do not contribute to the differences in eEPSP amplitude found between WT and *Fmr1* -KO mice.

MLI dendrites also express $K_V4.3$ channels which mediate the fast-inactivating I_A. These channels are which are found in complex with T-type Ca^{2+} channels and are known to strongly regulate MLI signaling properties (Molineux et al., 2005; Anderson et al., 2010; Anderson et al., 2013). We tested the differences in biophysical properties of isolated A-type current between WT and *Fmr1*-KO MLIs. To isolate I_A, we took advantage of the fact that they are relatively insensitive to TEA which blocks most other K^+ channels. We then performed activation and inactivation voltage-clamp protocols and plotted the responses onto a conductance/voltage plot and fit them with a Boltzmann function. We did not find any significant differences in either the $V_{1/2}$ of voltage-dependence of activation (WT: -31.7mV, n=12; *Fmr1*-KO: -34.9mV, n=9, unpaired t-test t(19) = -1.134, p=0.27) or steady-state inactivation (WT: -84.6mV, n=11; *Fmr1*-KO: -86.9mV,

n=9, unpaired t-test t(18) = 1.043, p=0.31) between WT and *Fmr1*-KO MLIs (Fig. 3.5*A,C,D,E*). Interestingly, we found that there was a significant decrease in the A-type K^+ current density from *Fmr1*-KO MLIs (WT: 1238.5 ± 48.8 pA/pF, *Fmr1*-KO: 536.7 ± 75.3 pA/pF, unpaired t-test t(19) = 8.431, p<0.00001) (Fig. 3.5*B*). While the nature of this deficit could play into the larger eEPSP amplitude in *Fmr1*-KO mice, it remains to be seen how exactly this interaction occurs. Due to the hyperpolarized $V_{1/2}$ of inactivation that A-type K^+ currents have in MLIs, it is difficult to imagine how this current could modulate the eEPSP amplitude. For instance, nearly all of the of the A-type K^+ current is inactivated at -60 mV holding potential which is where we performed our eEPSP stimulation experiments (Fig. 3.5*D*).

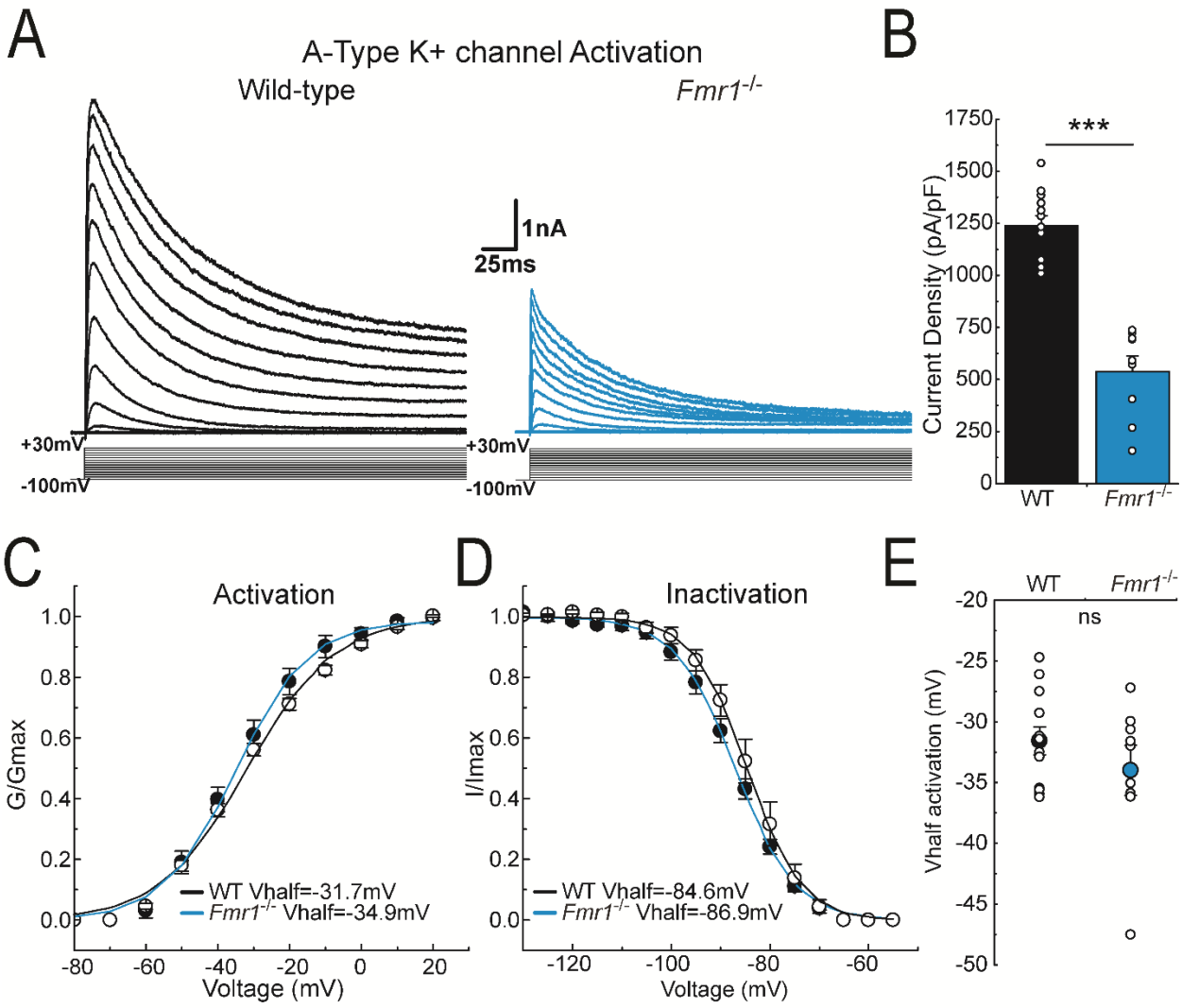

Figure 3.5: Fmr1-KO mice have reduced density of somatic A-type potassium currents
(A) Representative voltage-clamp recordings from the activation protocol of isolated A-type potassium currents from WT (left) and Fmr1-KO mice (right). (B) Summary plot of the A-type potassium channel current density as measured by the peak current amplitude to pF ratio. (C) Summary plot of voltage dependence of activation of A-type currents in WT and Fmr1-KO MLIs. (D) Summary plot of voltage dependence of inactivation of A-type currents in WT and Fmr1-KO MLIs. (E) Summary plot of $V_{1/2}$ for A-type activation in WT and Fmr1-KO MLIs. (Error bars s.e.m.)

FMRP regulates MLI eEPSP through a protein-protein interaction

In the last decade there has been a rapid accumulation of studies on a new functional role of FMRP as a direct regulator of ion channel function independent of translation. A particular focus has been on the N-terminal (1-297 amino acids) fragment of FMRP (N-FMRP) which regulates the biophysical properties of Slack, BK, SK, HCN and other K_Vs (Brown et al., 2010; Deng et al., 2013; Yang et al., 2018; Deng et al., 2019; Brandalise et al., 2020; Kshatri et al., 2020; Zhan et al., 2020). Furthermore, the reintroduction of N-FMRP can rescue multiple hyperexcitability defects in *Fmr1*-KO mice in different neuron types and brain regions (Deng et al., 2013; Deng et al., 2019; Zhan et al., 2020). The N-FMRP fragment lacks the mRNA binding RGG motif as well as most of the KH domains which are critical for control of mRNA translation (Vasilyev et al., 2015). Therefore these studies have implicated a new role for FMRP to regulate excitability through direct FMRP ion channel interactions independent of mRNA translation.

We tested if re-introducing the N-FMRP fragment (15nM) through our patch pipette could rescue dendritic hyperexcitability through an mRNA independent mechanism. We performed the same current clamp experiments as presented in Figure 3.3 and stimulated eEPSPs while N-FMRP dialyzed into the neuron through our intracellular patch-pipette solution. Over the 25 mins following breakthrough with internal N-FMRP, we observed a dramatic reduction in eEPSP amplitude in *Fmr1*-KO (*Fmr1*-KO Baseline: 38.02 ± 1.5mV, 25mins +N-FMRP: 17.4 ± 2.8mV, n=8, paired t-test t(7)=7.176, p= 0.00018) (Fig. 3.6*A,C*). After 25mins, the *Fmr1*-KO eEPSP amplitude with N-FMRP was not significantly different from the baseline WT eEPSP amplitude described in Figure 3.3 (*Fmr1*-KO 25mins +N-FMRP: 17.4 ± 2.8mV, n=8, WT baseline: 22.5 ± 3.9mV, n=13, unpaired t-test t(19)=0.877, p=0.39). N-FMRP did not have a significant effect on the eEPSP

amplitude in WT animals suggesting that endogenous FMRP levels maximally regulate MLI eEPSPs (WT Baseline: 25.6 ± 2.8mV, 25mins +N-FMRP: 28.8 ± 2.1mV, n=8, paired t-test t(7)=0.836, p= 0.43) (Fig. 3.6*B*).

Finally, we tested whether N-FMRP is acting to inhibit excitatory synaptic signaling or if it is affecting a dendritic filtering mechanism. To do this we performed additional voltage-clamp experiments measuring isolated AMPA receptor evoked excitatory post synaptic currents (eEPSCs) while internally perfusing N-FMRP. Unlike our current-clamp experiments, dialysis of N-FMRP did not have any on the eEPSC amplitude which remained at 97.4% of the baseline at 25mins of recording time (*Fmr1*-KO Baseline: 392.5 ± 83.7pA, 25mins +N-FMRP: 382.37 ± 71pA, paired t-test, t(6)=0.231, p=0.82) (Fig. 3.6*D*). In view of this, it seems most likely that N-FMRP modulates the dendritic filtering of AMPAR synapses by a FMRP protein-protein interaction involving an undetermined ion channel.

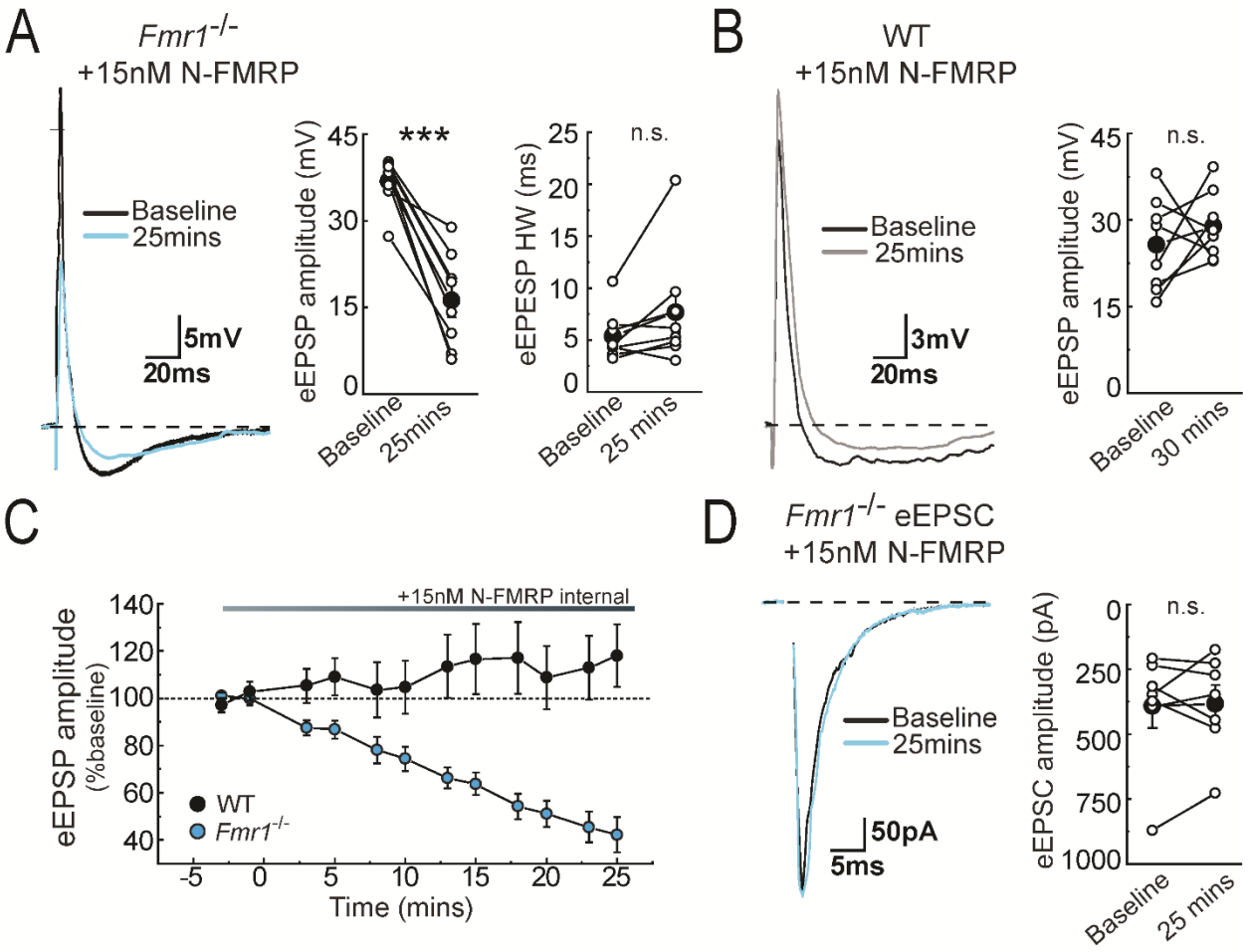

Figure 3.6: The reintroduction of N-FMRP reduces the eEPSP amplitude in Fmr1-KO mice

(A) Representative eEPSP recordings from an Fmr1-KO MLI at baseline and 25 mins after wash in of the N-FMRP peptide. Summary plots to the right of the traces show changes to eEPSP amplitude and half-width over the same time period. (B) Representative eEPSP recordings from a WT MLI at baseline and 25 mins after wash in of the N-FMRP peptide. Summary plots to the right of the traces show changes to eEPSP amplitude over the same time period. (C) Summary plot of the time course of the eEPSP amplitude during internal wash in of N-FMRP in WT and Fmr1-KO mice.) Representative eEPSC recordings from an Fmr1-KO MLI at baseline and 25 mins after wash in of the N-FMRP peptide. Summary plots to the right of the traces show changes to eEPSC amplitude over the same time period

3.6 Discussion

This study provides new insight into the pathophysiology of FXS and advances our knowledge of the translation independent role of FMRP. For the first time we have shown a new defect in dendritic signaling in cerebellar MLIs of *Fmr1*-KO mice. Consequently, MLIs from *Fmr1*-KO mice fire more APs from a similar synaptic input while having normal intrinsic firing properties. We found that MLI hyperexcitability was due to an amplified EPSP waveform resulting in nearly twice the depolarization amplitude in *Fmr1*-KO mice compared to WT. Surprisingly, there was no appreciable role for T-type calcium channels to affect the EPSP waveform but we did observe a notable decrease in somatically recorded A-type potassium current from *Fmr1*-KO mice. Finally, we were able to rescue the EPSP waveform by reintroduction of N-FMRP through our patch pipette suggesting that *Fmr1*-KO MLI hyperexcitability is primarily a translation independent defect.

Molecular layer interneuron hyperexcitablility and the cerebellar cortex circuit

Our observed hyperexcitability of MLIs from *Fmr1*-KO mice will likely modify the output of the cerebellar cortex as MLIs form an important inhibitory role within the cerebellar cortex circuit. The cerebellar molecular layer circuit consists of the parallel fibers which form excitatory synapses onto MLIs and PCs – the sole output from the cerebellar cortex (Apps and Garwicz, 2005). Within this circuit, MLIs provide feedforward inhibition onto nearby PCs following parallel fiber stimulation (Mittmann et al., 2005). Importantly, the robust MLI response to parallel fiber stimulation dictates their ability to inhibit cerebellar PCs and ultimately control the output of the cerebellar cortex (Häusser and Clark, 1997). The activation of MLI-PC inhibitory synapses dynamically alters the time window for synaptic integration in PCs (Häusser and Clark, 1997). However, MLIs also form a

complex interconnected micro-network with other MLIs which consists of inhibitory chemical GABAergic synapses and depolarizing electrical synapses which complicates understanding how they function in a complete *in vivo* circuit (Rieubland et al., 2014). What is known is that their relative location to the postsynaptic PC determines if the activation of a single MLI can strongly inhibit or disinhibit a PC (Dizon and Khodakhah, 2011; Arlt and Häusser, 2020).

A notable feature of cerebellar MLIs is that they have high input resistances and are more electrically compact compared to principal neurons and typical interneurons in the hippocampus and cortex, for example. These properties impacts their responses to synaptic inputs as individual quanta are sufficient to briefly control their firing properties (Carter and Regehr, 2002) while subthreshold dendritic depolarizations can increase neurotransmitter release (Christie et al., 2011). Effectively a few coincident EPSPs or a single IPSP has the ability to increase or decrease AP firing respectively. As MLIs are incredibly sensitive to synaptic inputs, the increase in EPSP amplitude that we have found in *Fmr1*-KO mice unsurprisingly matches the increase in AP generation from afferent stimulation (Figure 3.1 and 3.3). Consequently, we predict that there would be increased activity in MLI microcircuits and could have consequences for PC firing. This could also be balanced by an increased inhibitory synaptic frequency reducing MLI activity as their primary inhibitory synaptic connections is from other MLIs (Rieubland et al., 2014; Arlt and Häusser, 2020).

Global activity in MLIs is directly linked with a number of behaviours such as vestibulo-oculomotor reflex (VOR) gain control (Wulff et al., 2009) and oromotor movement rate (Astorga et al., 2017; Gaffield and Christie, 2017). At the cellular-circuit level it was recently shown that the plasticity rules for PF-PC synapses are altered by tuning the activity level of MLIs (Rowan et

al., 2018). Increasing the activity of MLIs changes a LTD response into an LTP response which underlies the motor learning occurring during VOR gain control (Rowan et al., 2018). Therefore we hypothesize that some motor learning problems found in both *Fmr1*-KO mice and human patients (Reiss et al., 1995; Bear et al., 2004; Koekkoek et al., 2005) could be attributable to the hyperexcitability of MLIs. In particular, it will be interesting to see how MLI hyperexcitability interacts with previous *Fmr1*-KO cerebellar defects such as enhanced parallel fiber-PC mGluR LTD (Koekkoek et al., 2005). These findings should also be considered in future experiments studying Fragile X-associated tremor/ataxia syndrome which predominantly has cerebellar motor learning deficits and occurs in patients with the FMR1 premutation (55-200 CGG repeats) (Hagerman et al., 2003; Foote et al., 2016). As the important role of MLI activity on cerebellar learning is advancing, the results from this study should be considered in future studies on FXS cerebellar dysfunctions. To properly understand the functional consequence of MLI hyperexcitability, *Fmr1* conditional KOs should be generated in MLIs under promotors for *c-kit* (Amat et al., 2017) or nNOS (Rowan et al., 2018).

A-type potassium currents are significantly smaller in *Fmr1*-KO mice

Interestingly, we found that there are significantly decreased A-type potassium currents in *Fmr1*-KO mice compared to WT mice. This is similar to observations which show a loss of A-type potassium currents from hippocampal dentate gyrus granule cells and CA1 pyramidal neurons (Gross et al., 2011; Routh et al., 2013). Surprisingly the decrease in A-type potassium currents did not have a significant effect on the intrinsic firing properties of *Fmr1*-KO mice since they are similar to those in WT mice (see Figure 3.2, see also Chapter 2 Figure 2.2). Furthermore, our observed decrease in A-type current density from *Fmr1*-KO MLIs is unlikely to account for the

differences in EPSP amplitude due to the following reasoning. First, our recorded steady state inactivation of A-type K^+ currents in MLIs is significantly hyperpolarized ($V_{1/2}$ =-86.9mV) in *Fmr1*-KO mice. Our eEPSP experiments were performed with a holding potential of -60mV where there are very few, if any, channels available for activation and thus they would not be expected to play a significant role. Previous studies have identified an important signaling role for A-type potassium currents but this research was done on rats which have a more right shifted A-type inactivation curve allowing for more A-type current to contribute at depolarized potentials (Molineux et al., 2005; Anderson et al., 2010).

Second, A-type potassium currents in MLIs undergo a significant hyperpolarizing shift in their voltage-dependence of activation following whole-cell patch breakthrough (Alexander et al., 2019). If A-type potassium currents were playing a significant role in modifying the eEPSP waveform, we would expect to see a similar shift following whole cell breakthrough. As noted in Chapter 2 Figure 2.3, MLI eEPSP amplitudes from *Fmr1*-KO mice are very stable over 30 minutes of recording and thus are insensitive to these shifts in A-type K^+ biophysical properties. Accordingly, it is unlikely that A-type K^+ currents can play a significant role in modulating the eEPSP waveform. Nevertheless, we cannot entirely rule out a role for A-type K^+ currents in modulating the eEPSP waveform as it is possible that dendritic A-type K^+ channels are functionally different compared to somatic channels. This has been see in other cell types (Hoffman et al., 1997; Routh et al., 2013) and we are unable to determine the properties of dendritic A-type K^+ currents from somatic whole cell recordings. Further experiments with simultaneous dendritic and somatic patches would shed light on this.

The reintroduction of the N-FMRP is a potent modulator of the MLI EPSP waveform

Recent advances over the last decade have firmly demonstrated a new role for FMRP forming direct protein-protein interactions with a number of different ion channels (Brown et al., 2010; Deng et al., 2013; Deng et al., 2019; Brandalise et al., 2020; Zhan et al., 2020). These defects were each shown to be rescued by reintroduction of the N-FMRP which notably does not contain the RNA binding motifs (Vasilyev et al., 2015). While this study does not identify a new target for FMRP, it further establishes a role for the N-FMRP to regulate dendritic signaling. Future experiments should identify the ion channel involved in regulating the amplitude of the EPSP waveform.

One likely candidate that could be modulated by N-FMRP in our experiments is the BK channel. MLIs have robust BK currents which are a large percentage of their depolarization-evoked potassium currents (Liu et al., 2011). In addition, FXS mouse models have consistently found dysregulations of BK channels across different brain regions and cell types including sensory cortex (Zhang et al., 2014b) and CA3 pyramidal neurons (Deng et al., 2013; Myrick et al., 2015). Finally, the N-terminal fragment of FMRP plays a key structural role in increasing BK channel current when it is in complex with the BK β4 auxiliary subunit (Myrick et al., 2015; Kshatri et al., 2020). This interaction can be abolished by the R138Q mutation which is a sporadic cause of FXS (Myrick et al., 2015; Kshatri et al., 2020). Our observations from the reintroduction of N-FMRP is consistent with these studies which show N-FMRP potentiating outward currents. Further confirmation with the R138Q mutation and directly measuring BK currents in MLIs from WT and *Fmr1*-KO mice should be done to elucidate if N-FMRP is regulating dendritic excitability through similar BK channel interactions.

In this study we reveal a novel hyperexcitablilty defect in the cerebellum of *Fmr1*-KO mice which increases MLI responsiveness to parallel fiber stimulation. In light of new discoveries highlighting the important role that MLI activity plays in cerebellar motor learning (Rowan et al., 2018), it will be important to test what impact MLI hyperexcitability has on the cerebellar circuit. In addition, this study further establishes the translation independent role of FMRP in regulating excitability. With this in mind, research into therapeutics treating people with FXS should consider a multifaceted approach that takes into account both the translation dependent and independent functions of FMRP. A potential treatment involving the reintroduction of FMRP through a tat-conjugate peptide has been recently considered as a novel therapeutic angle. This method was effective at rescuing ion channel deficits when the tat-conjugate was attached to N-FMRP (Zhan et al., 2020) but is toxic when the full FMRP protein was attached to the tat-sequence (Reis et al., 2004). Ultimately, future therapeutic development will depend on the ability to reintroduce functional FMRP in a safe and effective manner to restore proper translational control and translation independent ion channel modulation.

Acknowledgements

This work was supported by Canadian Institutes of Health Research Operating Grants CIHR MOP-342247 to D.B. We thank Ryan P.D. Alexander for help with analysis and comments on the manuscript and other members of the Bowie laboratory, for discussions and comments on the manuscript.

Author Contributions:

E.A.L. and D.B. designed research; E.A.L., performed research and analyzed data; E.A.L. and D.B. wrote the paper.

PART III: GENERAL DISCUSSION

D.1 General Thoughts

In this thesis, I have reviewed the literature on the functions of synapses in both health and disease and presented my new findings on inhibitory synaptic plasticity and how it pertains to our understanding of fragile-X syndrome. At the start, this work was motivated by a desire to understand the physiological signaling mechanisms behind recent discoveries on a role of ROS in the induction of iLTP (Accardi et al., 2014; Accardi et al., 2015). Moreover, I set out to explore the synaptic function of MLIs from *Fmr1*-KO mice, which I undertook due to a general lack of understanding of MLIs in FXS. As MLIs fulfill a key role by directly controlling PC firing properties and regulating the output of the cerebellar cortex (Mittmann et al., 2005; Jörntell et al., 2010), understanding their functional properties in *Fmr1*-KO mice is necessary to properly appreciate the pathophysiology of the disease as it relates to cerebellum function.

The discoveries of multiple defects in inhibitory signaling from Chapter 2 rely on the groundwork laid in Chapter 1. Specifically, we were able to directly test the consequences of disrupted NMDA receptor signaling in *Fmr1*-KO mice by using the knowledge developed in Chapter 1 and other Bowie lab observations (see Chapter 2 intrinsic plasticity and (Alexander and Bowie, 2020)). Based on our results from Chapter 1, we found a targeted molecule could rescue the inhibitory plasticity deficits found in *Fmr1*-KO mice. Chapters 1 and 2 thus highlight the benefit of carefully dissecting molecular signaling pathways. This could be even more significant if the results from Chapter 2 lead to the development of therapeutics for use in a clinical setting. Chapter 3 followed up on an observation which had been made during Chapter 2. Interestingly the large evoked EPSP amplitude in Chapter 3 could not be explained by differences in AMPA receptor currents, but rather involved changes to dendritic filtering. Altogether, this thesis has

revealed multiple defects in *Fmr1*-KO mice which had previously been unexplored. Additionally I have also proposed different avenues for rescuing said defects. Through the next few sections I will address some of the outstanding questions that arise from this work.

D.2 Cerebellum MLI plasticity and the impacts on the cerebellar circuit

So far, these results have focused on identifying the molecular mechanisms triggering iLTP in MLIs, but it is still unknown how this impacts PC firing. Ultimately, this will depend on the cerebellar circuit and, in particular, how MLIs function within this circuit. This will also rely on understanding how MLIs are regulated themselves. In an effort for simplicity, most studies on plasticity mechanisms focus on an individual synapse, which in this case maybe insufficient for making predictions on circuit output. In WT MLIs, activation of NMDA receptors from PF stimulation triggers two distinct plasticity mechanisms, an increase in intrinsic firing rate and a potentiation of inhibitory GABAergic signaling (see Chapter 1 and 2). At face value, these appear to be antagonistic mechanisms which could cancel each other out. Why would NMDA receptor activation increase MLI firing frequency through Na_V phosphorylation (Alexander et al., 2019; Alexander and Bowie, 2020), while also increasing the strength of inhibition onto MLIs by the same stimulation protocol (Larson et al., 2020)? To provide a hypothesis to answer this question, consideration will be given to the underlying effects of each phenomena, as well as how they may interact.

Increased firing of MLIs, or Intrinsic plasticity (IP), involves a left shift in the voltage-dependence of activation of Na_V channels which lowers the spike threshold to more hyperpolarized membrane potentials (Alexander et al., 2019). Recent observations from the Bowie lab have revealed that NMDA receptor activation induces IP leading to an increase in spike

frequency (Alexander and Bowie, 2020). The time course to reach peak changes in firing rate (see Chapter 2, Figure 2.2), is similar to that seen in iLTP (see Chapter 1, Figure 1.1) suggesting that these two mechanisms occur simultaneously following NMDA receptor activation. It remains to be determined what happens when these two plasticity mechanisms are induced and recorded simultaneously, but there are two outcomes which would likely occur. First, iLTP is likely to reduce the frequency and regularity of AP generation in MLIs. Inhibition is known to significantly decrease the firing rate, and increase the coefficient of variation in MLIs resulting in irregular spontaneous firing patterns (Häusser and Clark, 1997). Second, IP involves a hyperpolarization of spike threshold which would render MLIs more likely to fire APs to PF evoked EPSPs, effectively increasing their gain. Due to their high input resistance and electrical compactness, MLIs are already prone to firing APs following excitatory synaptic input (Carter and Regehr, 2002). It is likely that the effects of IP would make MLIs even more sensitive to excitatory synaptic input. When combined together, iLTP and IP could balance each other and prevent a significant change to the spontaneous MLI firing rate, while simultaneously increasing the probability for generating a spike after PF glutamate release. This would allow MLIs to maintain a consistent level of inhibition on PCs during spontaneous pacemaker activity, but dynamically tune their excitability during activity.

The consequence of this will likely result in changes to inhibition onto PCs during circuit activity. MLIs regulate PC activity through their spontaneous activity (Häusser and Clark, 1997) and feedforward inhibition (Mittmann et al., 2005; Coddington et al., 2013). Recordings from PCs during stimulation of PF afferents reveal that they generate a biphasic response consisting of an initial EPSP, followed by a delayed IPSP which rapidly repolarizes the membrane and silences

activity (Mittmann et al., 2005). The IPSPs are disynaptic and occur from a PF-MLI-PC feedforward inhibitory circuit. Similar to MLIs, inhibition onto PCs has a strong effect on spike regularity during basal activity. Experiments using $GABA_A$ receptor blockers (Häusser and Clark, 1997), or targeted knockouts of $GABA_A$ receptors expressed at MLI-PC synapses (Wulff et al., 2009), show an increase in the spike regularity of PCs. If the effects of IP and iLTP are to maintain a consistent spontaneous firing rate, then it is unlikely there would be any major effects on the spontaneous firing of PCs, including spike regularity or frequency. However it is likely that feedforward inhibition onto PCs would increase due to an increased responsiveness to PF-MLI glutamate release.

In addition to feedforward inhibition of PCs, MLIs also synapse onto other MLIs for the same inhibitory feedforward circuit with each other (Mittmann et al., 2005; Coddington et al., 2013). Moreover they also form electrical synapses with each other which makes functional microcircuits of MLIs that act together to regulate the inhibition of nearby PCs (Rieubland et al., 2014). Activation of a single MLI can also result in disinhibition of PCs through synapses within these microcircuits (Arlt and Häusser, 2020). The relative location of a granule cells plays an important role in determining if they will inhibit or disinhibit a PC due to MLI lateral inhibition motifs. PF activation is most likely to excite the closest PCs and inhibit PCs laterally (Dizon and Khodakhah, 2011). This has also been noted by CF activation which causes strong excitation on the PC that it is synapsing onto, or feedforward inhibition on other nearby PCs (Coddington et al., 2013). An important future direction for understanding the nature of iLTP, will be to identify if there are specific presynaptic GABAergic neurons which preferentially partner with potentiating

synapses. This could yield additional insights into the functional connectivity of the cerebellar MLI networks.

At the behavioural level, MLI inhibition onto PCs has an important role in motor learning. This was revealed by PC specific $GABA_A$ receptor knockout mice which had disruptions during the vestibulo-ocular reflex (VOR) gain control task (Wulff et al., 2009). Motor learning appears to be a MLI specific task as the absence of $GABA_A$ receptors at MLI-PC synapses only resulted in a mild impairment of baseline motor activity (Wulff et al., 2009). VOR gain control relies on LTD and LTP at PF-PC synapses (Boyden and Raymond, 2003). Recently experiments have revealed the mechanism by which MLIs contribute to this behaviour. MLI activity changes the induction of PF-PC LTD to LTP during associative learning which directly impacts the VOR gain control motor learning behaviour (Rowan et al., 2018). This is achieved by suppression of CF-mediated Ca^{2+} signals in PC dendrites during MLI inhibition (Rowan et al., 2018). This paper from Rowan *et al* has provided the clearest indication of what the functional consequences of IP and iLTP could be to MLIs and the cerebellar circuit. The effect of increasing MLI responsiveness is likely to be an important mechanism fine-tuning cerebellar learning. Behavioural *in vivo* experiments exploring the effect of eliminating iLTP (i.e. *Gabra3*-KO mice), IP, or both plasticity mechanisms in MLIs would shed light onto their roles on cerebellar motor learning tasks such as VOR gain control.

D.3 MLI defects in fragile-X syndrome

As discussed above, MLIs fulfill an important role in regulating activity throughout the cerebellar molecular layer. As research sheds more light on the important role of MLI activity in behaviour, new *in vivo* experiments should also be done in *Fmr1*-KO mice to test for defects in motor learning. The spatial and temporal spread of inhibition following CF activation depends largely on

NMDA receptor activation in MLIs (Coddington et al., 2013). Since NMDA receptor currents are lacking in *Fmr1*-KO mice, it is likely that there could be disruptions to feedforward inhibitory circuits even under basal conditions. However, a caveat to this hypothesis is that MLIs from *Fmr1*-KO mice have a greater eEPSP amplitude (Chapter 3) which could inadvertently be a compensatory mechanism for maintaining a consistent overall inhibitory tone onto PCs during feedforward inhibition.

A recent study has shown that PCs in *Fmr1*-KO mice have a greater mini IPSCs frequency which is attributed to an increase in basket cell presynaptic release (Yang et al., 2018). How this defect is related to the observations made in this thesis remains to be seen, but similar to the results seen in Chapter 3, GABA release from cerebellar basket cells is linked to a direct protein-protein interaction between N-FMRP and K^+ channels (Yang et al., 2018). Early work into cerebellar FXS pathophysiology revealed that there are significant defects in motor learning in both humans and animal models (Koekkoek et al., 2005), but there has yet to be an investigation into the specific role of MLI defects in relation to these observations. Since MLIs fulfill such a fundamental role in motor learning, future experiments on the impact of the defects described in this thesis could explain some of the FXS phenotypes that have previously been described.

D.4 The role of FMRP, from control of translation to modulation of ion channels across the CNS

The results from Chapters 2 and 3 have revealed two interesting, and importantly, different observations about the pathophysiology of FXS. Both studies have found defects in cellular signaling, but they are the result of two different roles for FMRP. In Chapter 2, I describe a novel excitatory signaling defect which is the result of reduced surface NMDA receptor

expression. The most likely cause of this disruption is due to translation dependent changes to neuroligin expression in MLIs (Dahlhaus and El-Husseini, 2010), which is critical for NMDA receptor signaling in MLIs (Zhang and Sudhof, 2016). This defect cannot be rescued by acute reintroduction of N-FMRP which fails to potentiate NMDA receptor signaling (see Fig. D.1). On the other hand, defects in dendritic filtering from Chapter 3 are directly related to a translation independent role of FMRP since reintroduction of N-FMRP rescues the eEPSP amplitude. While both chapters describe a new defect in FXS synaptic signaling and a treatment to reverse the defect, they rely on different roles of FMRP. Together these chapters illustrate the complexity for understanding the pathophysiology of FXS as it is necessary to consider the two main functions of FMRP, a regulator of translation (Udagawa et al., 2013), and a modulator of ion channel biophysical properties (Brown et al., 2010).

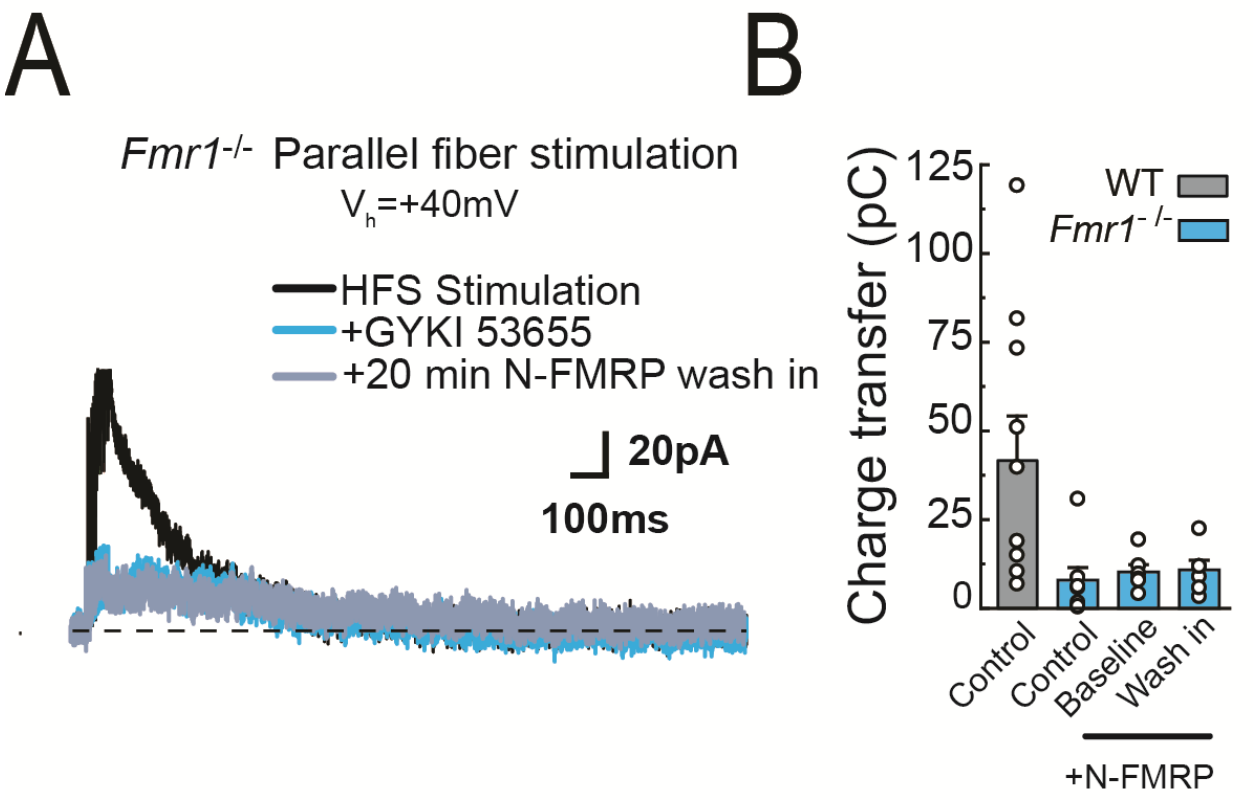

Figure D.1: Reintroduction of N-FMRP does not potentiate Fmr1-KO NMDAR currents
(A) Representative voltage clamp traces of EPSCs evoked from HFS parallel fiber stimulations from an Fmr1-KO mouse before treatment, after GYKI-53655 to block AMPA receptor currents, and after complete dialysis of N-FMRP. (B) Summary plot of the average charge transfer of isolated NMDA receptor currents from WT and Fmr1-KO mice. (Error bars, s.e.m).

When only considering the translation dependent roles of FMRP there is heterogeneity across the CNS in the defects due to a lack of FMRP (Bagni and Zukin, 2019). Much of this is due to how specialized the different neuron structure or functions can be from each other. Some defects that are consistently seen across the CNS involve the FMRP translational control of ion channels controlling cell excitability, including HCN, and K^+ channels (Contractor et al., 2015; Ferron, 2016). However, FMRP can only impact the mRNA that is already transcribed and accordingly, the effects depend on the cell transcriptome. Some observations can be attributable across the CNS, such as the effects of FMRP on the ubiquitous mTOR signaling pathway (Bagni

and Zukin, 2019; Gantois et al., 2019). It remains to be seen if the defects in NMDAR/nNOS signaling from Chapter 2 are restricted to the cerebellum, or are common to nNOS containing neurons across the CNS. NO is produced across the CNS but in discrete cell populations (Bredt et al., 1990) and has a number of impacts on behaviour such as drinking (Calapai et al., 1992), regulation of sleep (Kapás et al., 1994a; Kapás et al., 1994b), circadian rhythm (Watanabe et al., 1995), blood flow (Rancillac et al., 2006), and thermoregulation (De Luca et al., 1995). Notably there are dysfunctions to both circadian rhythms (Zhang et al., 2008) and sleep (Saré et al., 2017) in FXS animal models. Whether or not these FXS defects are attributable to a general nNOS deficit in the CNS remains to be seen, but should be examined in future studies.

The nature of the hyperexcitability and dendritic filtering defect outlined in Chapter 3 is a widespread observation in the FXS brain. Specifically there are many ion channels that have already been shown to be modulated by protein-protein interactions with N-FMRP. To date studies have been published demonstrating that FMRP directly interacts with Slack (Brown et al., 2010), $K_V1.2$ (Yang et al., 2018), A-type K^+ ($K_V4.3$) (Zhan et al., 2020), HCN (Brandalise et al., 2020), N-type Ca^{2+} (Ca_V 2.2) (Ferron et al., 2014), T-type Ca^{2+} ($Ca_V3.1$) (Zhan et al., 2020), SK2 (Deng et al., 2019), and BK (Deng et al., 2013) channels. These studies have found these interactions across the CNS including in the cerebellum (Yang et al., 2018; Zhan et al., 2020), hippocampus (Deng et al., 2013; Deng et al., 2019; Brandalise et al., 2020), prefrontal cortex (Brandalise et al., 2020), olfactory bulb (Brown et al., 2010), and dorsal root ganglia (Ferron et al., 2014). Therefore, the nature of FXS excitability defects due to the loss of FMRP has been well established across the CNS. The novelty from Chapter 3 is that this is the first study which has linked these defects to dendritic filtering. Most of the functional consequences have described defects in AP generation

(Deng et al., 2013; Deng et al., 2019), or presynaptic release (Yang et al., 2018). Meanwhile, other studies have found a role for FMRP to modulate proteins expressed in dendrites (Brandalise et al., 2020; Zhan et al., 2020), but have yet to show how they contribute to dendritic filtering.

An important take home from this work is that defects at the cellular level can arise due to different underlying reasons which are related to the two main functional roles of FMRP. As the pathophysiology of FXS is further studied, it is undoubtable that some defects will be generalizable to the rest of the CNS (i.e. mTOR signaling) (Gantois et al., 2019), while others are likely due to disruptions in cell specific machinery (i.e. ion channel dysregulation) (Brager and Johnston, 2014). Considerations to the specific, or generalizable nature of known defects should therefore be considered when developing therapeutics to target these defects. The lack of a viable therapeutic treatment could be due to strategies which have focused primarily on one aspect of the disease, while ignoring others. These ideas will be explored in more depth in the following section.

D.5 Fragile-X Syndrome, treating a neurodevelopmental disease

One of the major advances from describing the cell signaling defects in this thesis has been the findings that they can be rescued with the right treatment approach. In particular, the results from Chapter 2 suggest that targeting the NMDA receptor-nNOS signaling pathway could be useful in the treatment of FXS. Ultimately, it remains to be seen if Drug-X can rescue behavioural phenotypes in animal models, which would be an important first step before use in a clinical setting. It should also be noted that Drug-X would unlikely be a FXS cure, but rather, it could be used to ameliorate some FXS symptoms. In part this is because nNOS signaling is restricted to a subpopulation of neurons (Bredt et al., 1990), and these neurons are unlikely to account for the

entirety of the symptoms associated with FXS (Rajaratnam et al., 2017). Moreover, data within this thesis demonstrate that FMRP itself plays a critical role in cell signaling through its regulation of different ion channels. It is therefore likely that small molecule treatments will be unable to both rescue effects on their target, and overcome the lack of FMRP in regulating neuron excitability.

In light of the multiple roles of FMRP and the lack of one specific targetable pathway, drug development should become a more focused on ameliorating specific FXS symptoms. In the past most drug development has focused on generally improving all symptoms of FXS across the board (Berry-Kravis et al., 2018). One of the proposed reasons for an inability to find viable treatments for FXS has been that once early developmental milestones have passed, there is little that can be done in restoring normal behaviour. For instance reintroduction of functional ubiquitin protein ligase E3A (*Ube3a*) (Silva-Santos et al., 2015) or *Syngap1* (Barnes et al., 2015a) can rescue synaptic defects at any age, but behavioural rescue can only be made in younger animals. In *Fmr1*-KO animal models, chronic treatments with mGluR antagonists (Michalon et al., 2012; Gantois et al., 2013), or $GABA_B$ inhibitors (Henderson et al., 2012) can rescue behavioural phenotypes in older animals. The inability to reproduce promising results in FXS clinical trials could be due to differences in the development between humans and mice, which means younger patients could have more positive results in drug treatments. Considerations should be made to ensuring that drug treatments are designed to be given at the right developmental time points. Alternatively, more specific behavioural outcomes should be tested for in FXS clinical trials (Berry-Kravis et al., 2018). Metformin is a drug with has recently been considered for FXS treatment. It regulates mTOR signaling and has thus been found to restore normal protein

translation during mGluR-LTD (Gantois et al., 2017) and also has positive effects in a small clinical study (Dy et al., 2018). It remains to be seen if targeting the NMDA/nNOS pathway would provide therapeutic benefit to people with FXS, but it represents a new type of approach and could be a roadmap for future development. As research continues into NMDA/nNOS defects, the lessons discussed above should be considered for moving from research in animal defects to use in the clinical setting.

As discussed in Chapter 3, FMRP itself is an important molecule which regulates neuron function. It therefore stands to reason that any treatment which provides a complete rescue of behavioural defects should consider the reintroduction of normal levels of FMRP. This has been attempted by the use of tat-conjugate peptide which enables delivery of proteins into the brain across membranes (Schwarze et al., 1999). Tail injections of tat-FMRP are an effective way of reintroducing the N-terminal fragment of FMRP into neurons and to rescue animal behaviours (Zhan et al., 2020). Other studies have had less success with at the tat-conjugate approach. Attempts to reintroduce the whole FMRP protein with a tat-peptide was toxic in a cell culture preparation (Reis et al., 2004). Therefore more work needs to be done before this could be considered a viable treatment. Other studies have used viruses to induced expression of FMRP in neurons with some success, but the efficacy of this approach is limited due to variable expression patterns across the CNS (Zeier et al., 2009; Gholizadeh et al., 2014; Arsenault et al., 2016). Other approaches have tried to reverse FXS phenotypes by gene editing mGluR to reduce exaggerated mGluR5 signalling (Lee et al., 2018), or gene editing the removal of CGG repeats to allow for reintroduction of endogenous FMRP expression (Xie et al., 2016; Liu et al., 2018b). In the end, the success of these approaches will depend on the ability to restore normal levels of

FMRP across the entirety of the effected brain. What is evident is that a holistic approach to understanding the different functions of FMRP is needed to accurately understand the pathophysiology of FXS which is the first step to designing new therapeutic approaches.

CONCLUDING REMARKS

In **PART I** of this thesis I have provided a brief summary of the current field of synaptic physiology, with considerations given to synaptic anatomy and plasticity mechanisms. I have also summarized the current literature describing synaptic defects in the pathophysiology of FXS. In the experimental chapters of **PART II**, I have presented my original findings on inhibitory synaptic plasticity and defects in signaling in FXS. The first results chapter addressed outstanding questions from previous work regarding the role of ROS and GABAergic plasticity. Through whole-cell patch clamp electrophysiology and electrical afferent stimulations, I was able to demonstrate that cerebellar MLIs strengthen their GABAergic synapses through a ROS dependent pathway. Using an approach involving pharmacological and genetic tools, I was able to demonstrate that iLTP involves an NMDA-nNOS-PKC signaling pathway (see Chapter 1, Figure 1.8 for a complete summary). In Chapters 2 and 3, I examined the synaptic signaling of cerebellar MLIs in FXS. Prior to this work, the synaptic properties of MLIs had not been investigated in the context of FXS. The work in Chapter 2 relied on the knowledge that was gained from identifying the biochemical signaling pathway in Chapter 1. In Chapter 2, I have described defects in inhibitory plasticity from lack of NMDA receptor signaling. Moreover, the intracellular signaling pathways downstream of NMDA receptor activation remain functional in *Fmr1*-KO mice, and that small molecules (Drug-X) potentiating the signaling pathway identified in Chapter 1 could rescue inhibitory plasticity. Importantly, the work in this thesis also identified defects in blood flow in the brain of *Fmr1*-KO mice which has been relatively unexplored in the pathophysiology of FXS. Finally, Chapter 3 of this thesis came from an interesting observation that was made during my

recordings from *Fmr1*-KO mice. Early experiments performed for Chapter 2 had revealed that the eEPSP amplitude was consistently larger in *Fmr1*-KO mice. This was then demonstrated to increase the excitability of MLIs in response to afferent stimulation, and was linked to the absence of N-FMRP regulation. In both Chapter 2 and 3, I demonstrate molecular mechanisms which reverse the defects described in each chapter.

In **PART III** of this thesis, I have discussed the overall impact of this work and discussed how this work has advanced the fields of cerebellum physiology and FXS research. Moreover, I have discussed some of the outstanding questions resulting from this work as well as provide hypotheses which could explain these questions. I hope that at this point, the reader can take away two important concepts demonstrated in this thesis. First, there is great value in understanding the molecular mechanisms underlying the physiological regulation of synaptic transmission. This is a theme that I stressed in **PART I**, which was important for all of the main conclusions to follow in the results chapters from **PART II**. Second, when considering treatments for FXS, all of the roles of FMRP can impact the ultimate success of a therapeutic. The results from this thesis have focused on one cell type, but revealed defects in both the translation dependent, and independent roles of FMRP. As improvements are made in the development of targeted FXS therapeutics, it will be crucial to address how to replace the function of the multifaceted and enigmatic FMRP.

SUMMARY OF CONTRIBUTIONS TO ORIGINAL KNOWLEDGE

I. I have identified that iLTP is driven by NMDA receptors in cerebellar MLIs

II. I have found that NMDA receptor activation stimulates a nNOS-cGMP-NOX2 pathway to induce iLTP in MLIs

III. I have found that PKC activation occurs downstream of NOX2 activation and ROS production in the induction pathway of iLTP

IV. I have found that GABARAP is required to traffic $GABA_A$ receptors to the synapse during the expression of iLTP

V. I have found that NMDA receptor currents are reduced in MLIs lacking from *Fmr1*-KO mice

VI. I have found that the lack of NMDA receptor current impairs the induction of iLTP in *Fmr1*-KO mice

VII. I have found that by direct PKC activation, the iLTP induction signaling pathway downstream of NMDA receptor activation is functional in *Fmr1*-KO mice

VIII. I have found that iLTP can be rescued in *Fmr1*-KO mice by using Drug-X to boost the intracellular signaling pathway described in Chapter 1

IX. I have found that *Fmr1*-KO mice have defects in the regulation of blood flow through the cerebellum

X. I have found that MLIs from *Fmr1*-KO mice have increased excitability during glutamatergic transmission

XI. I have found that MLIs from WT and *Fmr1*-KO mice have similar AP properties

XII. I have found that *Fmr1*-KO mice have larger evoked PSP depolarizations compared to WT mice

XIII. I have found that *Fmr1*-KO mice have smaller A-type K^+ currents compared to WT mice

XIV. I have found that N-FMRP can reduce the evoked PSP amplitude in *Fmr1*-KO mice

LIST OF REFERENCES

Accardi MV, Brown PMGE, Miraucourt LS, Orser BA, Bowie D (2015) α6-Containing GABAA Receptors Are the Principal Mediators of Inhibitory Synapse Strengthening by Insulin in Cerebellar Granule Cells. The Journal of Neuroscience 35:9676-9688.

Accardi MV, Daniels BA, Brown PMGE, Fritschy J-M, Tyagarajan SK, Bowie D (2014) Mitochondrial reactive oxygen species regulate the strength of inhibitory GABA-mediated synaptic transmission. Nat Commun 5.

Alba A, Kano M, Chen C, Stanton ME, Fox GD, Herrup K, Zwingman TA, Tonegawa S (1994) Deficient cerebellar long-term depression and impaired motor learning in mGluR1 mutant mice. Cell 79:377-388.

Alexander RP, Bowie D (2020) Intrinsic plasticity of cerebellar stellate cells is mediated by NMDA receptor regulation of voltage-gated Na+ channels. The Journal of Physiology.

Alexander RPD, Mitry J, Sareen V, Khadra A, Bowie D (2019) Cerebellar Stellate Cell Excitability Is Coordinated by Shifts in the Gating Behavior of Voltage-Gated Na(+) and A-Type K(+) Channels. eNeuro 6.

Amat SB, Rowan MJ, Gaffield MA, Bonnan A, Kikuchi C, Taniguchi H, Christie JM (2017) Using c-kit to genetically target cerebellar molecular layer interneurons in adult mice. PloS one 12:e0179347.

Amin J, Weiss DS (1993) GABAA receptor needs two homologous domains of the & beta;-subunit for activation by GABA but not by pentobarbital. Nature 366:565-569.

Amir RE, Van den Veyver IB, Wan M, Tran CQ, Francke U, Zoghbi HY (1999) Rett syndrome is caused by mutations in X-linked MECP2, encoding methyl-CpG-binding protein 2. Nature Genetics 23:185-188.

Anderson D, Engbers JD, Heath NC, Bartoletti TM, Mehaffey WH, Zamponi GW, Turner RW (2013) The Cav3-Kv4 complex acts as a calcium sensor to maintain inhibitory charge transfer during extracellular calcium fluctuations. J Neurosci 33:7811-7824.

Anderson D, Mehaffey WH, Iftinca M, Rehak R, Engbers JDT, Hameed S, Zamponi GW, Turner RW (2010) Regulation of neuronal activity by Cav3-Kv4 channel signaling complexes. Nature Neuroscience 13:333-337.

Angelotti T, Macdonald R (1993) Assembly of GABAA receptor subunits: alpha 1 beta 1 and alpha 1 beta 1 gamma 2S subunits produce unique ion channels with dissimilar single- channel properties. The Journal of Neuroscience 13:1429-1440.

Apps R, Garwicz M (2005) Anatomical and physiological foundations of cerebellar information processing. Nature Reviews Neuroscience 6:297-311.

Arenz A, Silver RA, Schaefer AT, Margrie TW (2008) The contribution of single synapses to sensory representation in vivo. Science 321:977-980.

Arlt C, Häusser M (2020) Microcircuit Rules Governing Impact of Single Interneurons on Purkinje Cell Output In Vivo. Cell Reports 30:3020-3035.e3023.

Arsenault J, Gholizadeh S, Niibori Y, Pacey LK, Halder SK, Koxhioni E, Konno A, Hirai H, Hampson DR (2016) FMRP expression levels in mouse central nervous system neurons determine behavioral phenotype. Human gene therapy 27:982-996.

Ascher P, Nowak L (1988) The role of divalent cations in the N-methyl-D-aspartate responses of mouse central neurones in culture. The Journal of physiology 399:247-266.

Ashley CT, Wilkinson KD, Reines D, Warren ST (1993) FMR1 protein: conserved RNP family domains and selective RNA binding. Science 262:563-566.

Astorga G, Li D, Therreau L, Kassa M, Marty A, Llano I (2017) Concerted Interneuron Activity in the Cerebellar Molecular Layer During Rhythmic Oromotor Behaviors. The Journal of Neuroscience 37:11455-11468.

Atwood BK, Lovinger DM, Mathur BN (2014) Presynaptic long-term depression mediated by Gi/o-coupled receptors. Trends in Neurosciences 37:663-673.

Auerbach BD, Osterweil EK, Bear MF (2011) Mutations causing syndromic autism define an axis of synaptic pathophysiology. Nature 480:63-68.

Awapara J, Landua AJ, Fuerst R, Seale B (1950) Free γ-aminobutyric acid in brain. Journal of Biological Chemistry 187:35-39.

Ayata C, Ma J, Meng W, Huang P, Moskowitz MA (1996) L-NA-sensitive rCBF augmentation during vibrissal stimulation in type III nitric oxide synthase mutant mice. Journal of Cerebral Blood Flow & Metabolism 16:539-541.

Babiec WE, Guglietta R, Jami SA, Morishita W, Malenka RC, O'Dell TJ (2014) Ionotropic NMDA receptor signaling is required for the induction of long-term depression in the mouse hippocampal CA1 region. Journal of Neuroscience 34:5285-5290.

Bacaj T, Wu D, Yang X, Morishita W, Zhou P, Xu W, Malenka Robert C, Südhof Thomas C (2013) Synaptotagmin-1 and Synaptotagmin-7 Trigger Synchronous and Asynchronous Phases of Neurotransmitter Release. Neuron 80:947-959.

Badura A, Verpeut JL, Metzger JW, Pereira TD, Pisano TJ, Deverett B, Bakshinskaya DE, Wang SS (2018) Normal cognitive and social development require posterior cerebellar activity. Elife 7:e36401.

Bagni C, Zukin RS (2019) A Synaptic Perspective of Fragile X Syndrome and Autism Spectrum Disorders. Neuron 101:1070-1088.

Bagni C, Tassone F, Neri G, Hagerman R (2012) Fragile X syndrome: causes, diagnosis, mechanisms, and therapeutics. The Journal of clinical investigation 122:4314-4322.

Balcar VJ, Johnston GA (1972) Glutamate uptake by brain slices and its relation to the depolarization of neurones by acidic amino acids. J Neurobiol 3:295-301.

Bali M, Akabas MH (2007) The Location of a Closed Channel Gate in the GABAA Receptor Channel. Journal of General Physiology 129:145-159.

Banerjee A, Ifrim MF, Valdez AN, Raj N, Bassell GJ (2018) Aberrant RNA translation in fragile X syndrome: From FMRP mechanisms to emerging therapeutic strategies. Brain Research 1693:24-36.

Banko JL, Hou L, Poulin F, Sonenberg N, Klann E (2006) Regulation of Eukaryotic Initiation Factor 4E by Converging Signaling Pathways during Metabotropic Glutamate Receptor-Dependent Long-Term Depression. The Journal of Neuroscience 26:2167-2173.

Bannai H, Lévi S, Schweizer C, Inoue T, Launey T, Racine V, Sibarita J-B, Mikoshiba K, Triller A (2009) Activity-Dependent Tuning of Inhibitory Neurotransmission Based on GABAAR Diffusion Dynamics. Neuron 62:670-682.

Barberis A, Mozrzymas JW, Ortinski PI, Vicini S (2007) Desensitization and binding properties determine distinct α1β2γ2 and α3β2γ2 GABAA receptor-channel kinetic behavior. European Journal of Neuroscience 25:2726-2740.

Barnard EA, Darlison MG, Seeburg P (1987) Molecular biology of the GABAA receptor: the receptor/channel superfamily. Trends in Neurosciences 10:502-509.

Barnes SA, Wijetunge LS, Jackson AD, Katsanevaki D, Osterweil EK, Komiyama NH, Grant SG, Bear MF, Nägerl UV, Kind PC (2015a) Convergence of hippocampal pathophysiology in Syngap+/− and Fmr1−/y mice. Journal of Neuroscience 35:15073-15081.

Barnes SJ, Sammons RP, Jacobsen RI, Mackie J, Keller GB, Keck T (2015b) Subnetwork-specific homeostatic plasticity in mouse visual cortex in vivo. Neuron 86:1290-1303.

Bayer KU, LeBel E, McDonald GL, O'Leary H, Schulman H, De Koninck P (2006) Transition from reversible to persistent binding of CaMKII to postsynaptic sites and NR2B. J Neurosci 26:1164-1174.

Bean BP (2007) The action potential in mammalian central neurons. Nature Reviews Neuroscience 8:451-465.

Bear MF, Huber KM, Warren ST (2004) The mGluR theory of fragile X mental retardation. Trends Neurosci 27:370-377.

Beattie EC, Stellwagen D, Morishita W, Bresnahan JC, Ha BK, Von Zastrow M, Beattie MS, Malenka RC (2002) Control of Synaptic Strength by Glial TNFα. Science 295:2282-2285.

Behr J, Wozny C, Fidzinski P, Schmitz D (2009) Synaptic plasticity in the subiculum. Progress in neurobiology 89:334-342.

Bello O, Blair K, Chapleau C, Larimore JL (2013) Is memantine a potential therapeutic for Rett syndrome? Front Neurosci 7:245.

Beltrán González AN, López Pazos MI, Calvo DJ (2020) Reactive Oxygen Species in the Regulation of the GABA Mediated Inhibitory Neurotransmission. Neuroscience 439:137-145.

Ben-Ari Y (2002) Excitatory actions of gaba during development: the nature of the nurture. Nature Reviews Neuroscience 3:728-739.

Ben-Ari Y (2010) Kainate and temporal lobe epilepsies: Three decades of progress. Epilepsia 51:40-40.

Ben-Ari Y, Gaiarsa J-L, Tyzio R, Khazipov R (2007) GABA: A Pioneer Transmitter That Excites Immature Neurons and Generates Primitive Oscillations. Physiological Reviews 87:1215-1284.

Benhassine N, Berger T (2008) Large-conductance calcium-dependent potassium channels prevent dendritic excitability in neocortical pyramidal neurons. Pflügers Archiv - European Journal of Physiology 457:1133.

Benkwitz C, Banks MI, Pearce RA (2004) Influence of GABAAReceptor γ2Splice Variants on Receptor Kinetics and Isoflurane Modulation. Anesthesiology: The Journal of the American Society of Anesthesiologists 101:924-936.

Berkefeld H, Sailer CA, Bildl W, Rohde V, Thumfart J-O, Eble S, Klugbauer N, Reisinger E, Bischofberger J, Oliver D, Knaus H-G, Schulte U, Fakler B (2006) BK-Cav Channel Complexes Mediate Rapid and Localized Ca2+-Activated K+ Signaling. Science 314:615-620.

Berl S, Waelsch H (1958) DETERMINATION OF GLUTAMIC ACID, GLUTAMINE, GLUTATHIONE AND γ-AMINOBUTYRIC ACID AND THEIR DISTRIBUTION IN BRAIN TISSUE. Journal of Neurochemistry 3:161-169.

Berry-Kravis E (2002) Epilepsy in fragile X syndrome. Developmental medicine and child neurology 44:724-728.

Berry-Kravis EM, Lindemann L, Jønch AE, Apostol G, Bear MF, Carpenter RL, Crawley JN, Curie A, Des Portes V, Hossain F, Gasparini F, Gomez-Mancilla B, Hessl D, Loth E, Scharf SH, Wang PP, Von Raison F, Hagerman R, Spooren W, Jacquemont S (2018) Drug development for neurodevelopmental disorders: lessons learned from fragile X syndrome. Nature Reviews Drug Discovery 17:280-299.

Betancur C (2011) Etiological heterogeneity in autism spectrum disorders: More than 100 genetic and genomic disorders and still counting. Brain Research 1380:42-77.

Betz WJ (1970) Depression of transmitter release at the neuromuscular junction of the frog. The Journal of Physiology 206:629-644.

Biesold D, Inanami O, Sato A, Sato Y (1989) Stimulation of the nucleus basalis of Meynert increases cerebral cortical blood flow in rats. Neuroscience letters 98:39-44.

Bliss TV, Lømo T (1973) Long-lasting potentiation of synaptic transmission in the dentate area of the anaesthetized rabbit following stimulation of the perforant path. The Journal of physiology 232:331-356.

Bock T, Stuart GJ (2016) The Impact of BK Channels on Cellular Excitability Depends on their Subcellular Location. Frontiers in Cellular Neuroscience 10.

Bocquet N, Nury H, Baaden M, Le Poupon C, Changeux J-P, Delarue M, Corringer P-J (2009) X-ray structure of a pentameric ligand-gated ion channel in an apparently open conformation. Nature 457:111-114.

Böhme I, Rabe H, Lüddens H (2004) Four Amino Acids in the α Subunits Determine the γ-Aminobutyric Acid Sensitivities of GABAA Receptor Subtypes. Journal of Biological Chemistry 279:35193-35200.

Boileau AJ, Evers AR, Davis AF, Czajkowski C (1999) Mapping the agonist binding site of the GABAAReceptor: Evidence for a β-strand. Journal of Neuroscience 19:4847-4854.

Bolduc M-e, Limperopoulos C (2009) Neurodevelopmental outcomes in children with cerebellar malformations: a systematic review. Developmental Medicine & Child Neurology 51:256-267.

Bon CLM, Garthwaite J (2003) On the Role of Nitric Oxide in Hippocampal Long-Term Potentiation. The Journal of Neuroscience 23:1941-1948.

Bormann J, Hamill OP, Sakmann B (1987) Mechanism of anion permeation through channels gated by glycine and gamma-aminobutyric acid in mouse cultured spinal neurones. The Journal of physiology 385:243-286.

Bostrom CA, Majaess N-M, Morch K, White E, Eadie BD, Christie BR (2013) Rescue of NMDAR-Dependent Synaptic Plasticity in Fmr1 Knock-Out Mice. Cerebral Cortex 25:271-279.

Bourgeron T (2015) From the genetic architecture to synaptic plasticity in autism spectrum disorder. Nat Rev Neurosci 16:551-563.

Bourne JN, Harris KM (2008) Balancing Structure and Function at Hippocampal Dendritic Spines. Annual Review of Neuroscience 31:47-67.

Bowery N, Hill D, Hudson A, Doble A, Middlemiss D, Shaw J, Turnbull M (1980) (–) Baclofen decreases neurotransmitter release in the mammalian CNS by an action at a novel GABA receptor. Nature 283:92-94.

Bowie D, Mayer ML (1995) Inward rectification of both AMPA and kainate subtype glutamate receptors generated by polyamine-mediated ion channel block. Neuron 15:453-462.

Boyden ES, Raymond JL (2003) Active reversal of motor memories reveals rules governing memory encoding. Neuron 39:1031-1042.

Brager DH, Johnston D (2014) Channelopathies and dendritic dysfunction in fragile X syndrome. Brain Research Bulletin 103:11-17.

Branco T, Häusser M (2011) Synaptic Integration Gradients in Single Cortical Pyramidal Cell Dendrites. Neuron 69:885-892.

Brandalise F, Kalmbach BE, Mehta P, Thornton O, Johnston D, Zemelman BV, Brager DH (2020) Fragile X Mental Retardation Protein Bidirectionally Controls Dendritic I_h in a Cell Type-Specific Manner between Mouse Hippocampus and Prefrontal Cortex. The Journal of Neuroscience 40:5327-5340.

Bredt DS (1999) Endogenous nitric oxide synthesis: biological functions and pathophysiology. Free Radic Res 31:577-596.

Bredt DS, Snyder SH (1994) NITRIC OXIDE: A Physiologic Messenger Molecule. Annual Review of Biochemistry 63:175-195.

Bredt DS, Hwang PM, Snyder SH (1990) Localization of nitric oxide synthase indicating a neural role for nitric oxide. Nature 347:768-770.

Brejc K, van Dijk WJ, Klaassen RV, Schuurmans M, van der Oost J, Smit AB, Sixma TK (2001) Crystal structure of an ACh-binding protein reveals the ligand-binding domain of nicotinic receptors. Nature 411:269-276.

Brenman JE, Christopherson KS, Craven SE, McGee AW, Bredt DS (1996a) Cloning and characterization of postsynaptic density 93, a nitric oxide synthase interacting protein. J Neurosci 16:7407-7415.

Brenman JE, Chao DS, Gee SH, McGee AW, Craven SE, Santillano DR, Wu Z, Huang F, Xia H, Peters MF, Froehner SC, Bredt DS (1996b) Interaction of nitric oxide synthase with the postsynaptic density protein PSD-95 and alpha1-syntrophin mediated by PDZ domains. Cell 84:757-767.

Brickley SG, Revilla V, Cull-Candy SG, Wisden W, Farrant M (2001) Adaptive regulation of neuronal excitability by a voltage- independent potassium conductance. Nature 409:88-92.

Brock L, Coombs J, Eccles J (1952) The recording of potentials from motoneurones with an intracellular electrode. The Journal of physiology 117:431.

Brown AM, Arancillo M, Lin T, Catt DR, Zhou J, Lackey EP, Stay TL, Zuo Z, White JJ, Sillitoe RV (2019) Molecular layer interneurons shape the spike activity of cerebellar Purkinje cells. Scientific Reports 9:1742.

Brown GC (2010) Nitric oxide and neuronal death. Nitric Oxide 23:153-165.

Brown GL, Dale HH, Feldberg W (1936) Reactions of the normal mammalian muscle to acetylcholine and to eserine. The Journal of Physiology 87:394.

Brown MR, Kronengold J, Gazula V-R, Chen Y, Strumbos JG, Sigworth FJ, Navaratnam D, Kaczmarek LK (2010) Fragile X mental retardation protein controls gating of the sodium-activated potassium channel Slack. Nature Neuroscience 13:819-821.

Brown PMGE, McGuire H, Bowie D (2017) Stargazin and cornichon-3 relieve polyamine block of AMPA receptors by enhancing blocker permeation. Journal of General Physiology 150:67-82.

Brown V, Jin P, Ceman S, Darnell JC, O'Donnell WT, Tenenbaum SA, Jin X, Feng Y, Wilkinson KD, Keene JD, Darnell RB, Warren ST (2001) Microarray Identification of FMRP-Associated Brain mRNAs and Altered mRNA Translational Profiles in Fragile X Syndrome. Cell 107:477-487.

Bu DF, Erlander MG, Hitz BC, Tillakaratne NJ, Kaufman DL, Wagner-McPherson CB, Evans GA, Tobin AJ (1992) Two human glutamate decarboxylases, 65-kDa GAD and 67-kDa GAD, are each encoded by a single gene. Proceedings of the National Academy of Sciences 89:2115-2119.

Burnashev N, Rozov A (2005) Presynaptic Ca2+ dynamics, Ca2+ buffers and synaptic efficacy. Cell Calcium 37:489-495.

Burnashev N, Monyer H, Seeburg PH, Sakmann B (1992) Divalent ion permeability of AMPA receptor channels is dominated by the edited form of a single subunit. Neuron 8:189-198.

Burrone J, O'Byrne M, Murthy VN (2002) Multiple forms of synaptic plasticity triggered by selective suppression of activity in individual neurons. Nature 420:414-418.

Cahill E, Pascoli V, Trifilieff P, Savoldi D, Kappès V, Lüscher C, Caboche J, Vanhoutte P (2014) D1R/GluN1 complexes in the striatum integrate dopamine and glutamate signalling to control synaptic plasticity and cocaine-induced responses. Molecular Psychiatry 19:1295-1304.

Calapai G, Squadrito F, Altavilla D, Zingarelli B, Campo GM, Cilia M, Caputi AP (1992) Evidence that nitric oxide modulates drinking behaviour. Neuropharmacology 31:761-764.

Carland JE, Moorhouse AJ, Barry PH, Johnston GA, Chebib M (2004) Charged residues at the 2′ position of human GABAC ρ1 receptors invert ion selectivity and influence open state probability. Journal of Biological Chemistry 279:54153-54160.

Carta I, Chen CH, Schott AL, Dorizan S, Khodakhah K (2019) Cerebellar modulation of the reward circuitry and social behavior. Science 363:eaav0581.

Carter AG, Regehr WG (2000) Prolonged synaptic currents and glutamate spillover at the parallel fiber to stellate cell synapse. Journal of Neuroscience 20:4423-4434.

Carter AG, Regehr WG (2002) Quantal events shape cerebellar interneuron firing. Nature Neuroscience 5:1309-1318.

Carter BC, Jahr CE (2016) Postsynaptic, not presynaptic NMDA receptors are required for spike-timing-dependent LTD induction. Nature Neuroscience 19:1218-1224.

Cash S, Yuste R (1999) Linear Summation of Excitatory Inputs by CA1 Pyramidal Neurons. Neuron 22:383-394.

Castillo PE (2012) Presynaptic LTP and LTD of Excitatory and Inhibitory Synapses. Cold Spring Harbor Perspectives in Biology 4.

Castro-Alamancos MA, Calcagnotto ME (1999) Presynaptic Long-Term Potentiation in Corticothalamic Synapses. The Journal of Neuroscience 19:9090-9097.

Catsman-Berrevoets CE, Aarsen FK (2010) The spectrum of neurobehavioural deficits in the Posterior Fossa Syndrome in children after cerebellar tumour surgery. Cortex 46:933-946.

Catterall WA, Few AP (2008) Calcium Channel Regulation and Presynaptic Plasticity. Neuron 59:882-901.

Cauli B, Tong X-K, Rancillac A, Serluca N, Lambolez B, Rossier J, Hamel E (2004) Cortical GABA Interneurons in Neurovascular Coupling: Relays for Subcortical Vasoactive Pathways. The Journal of Neuroscience 24:8940-8949.

Celie PHN, van Rossum-Fikkert SE, van Dijk WJ, Brejc K, Smit AB, Sixma TK (2004) Nicotine and Carbamylcholine Binding to Nicotinic Acetylcholine Receptors as Studied in AChBP Crystal Structures. Neuron 41:907-914.

Chachlaki K, Garthwaite J, Prevot V (2017) The gentle art of saying NO: how nitric oxide gets things done in the hypothalamus. Nat Rev Endocrinol 13:521-535.

Chadderton P, Margrie TW, Hausser M (2004) Integration of quanta in cerebellar granule cells during sensory processing. Nature 428:856-860.

Chen C, Jonas P (2017) Synaptotagmins: That's Why So Many. Neuron 94:694-696.

Chen C, Satterfield R, Young SM, Jonas P (2017) Triple Function of Synaptotagmin 7 Ensures Efficiency of High-Frequency Transmission at Central GABAergic Synapses. Cell Reports 21:2082-2089.

Chen L, Toth M (2001) Fragile X mice develop sensory hyperreactivity to auditory stimuli. Neuroscience 103:1043-1050.

Chen L, Bao S, Qiao X, Thompson RF (1999) Impaired cerebellar synapse maturation in waggler, a mutant mouse with a disrupted neuronal calcium channel γ subunit. Proceedings of the National Academy of Sciences 96:12132-12137.

Chen L, Wang H, Vicini S, Olsen RW (2000a) The γ-aminobutyric acid type A (GABA_A) receptor-associated protein (GABARAP) promotes GABA_A receptor clustering and

modulates the channel kinetics. Proceedings of the National Academy of Sciences 97:11557-11562.

Chen L, Chetkovich DM, Petralia RS, Sweeney NT, Kawasaki Y, Wenthold RJ, Bredt DS, Nicoll RA (2000b) Stargazin regulates synaptic targeting of AMPA receptors by two distinct mechanisms. Nature 408:936-943.

Chen WR, Midtgaard J, Shepherd GM (1997) Forward and backward propagation of dendritic impulses and their synaptic control in mitral cells. Science 278:463-467.

Chen X, Winters CA, Reese TS (2008) Life Inside a Thin Section: Tomography. The Journal of Neuroscience 28:9321-9327.

Chen X, Aslam M, Gollisch T, Allen K, von Engelhardt J (2018) CKAMP44 modulates integration of visual inputs in the lateral geniculate nucleus. Nature communications 9:1-13.

Chiu CQ, Barberis A, Higley MJ (2019) Preserving the balance: diverse forms of long-term GABAergic synaptic plasticity. Nature Reviews Neuroscience 20:272-281.

Chiu CQ, Lur G, Morse TM, Carnevale NT, Ellis-Davies GCR, Higley MJ (2013) Compartmentalization of GABAergic Inhibition by Dendritic Spines. Science 340:759-762.

Chiu CQ, Martenson JS, Yamazaki M, Natsume R, Sakimura K, Tomita S, Tavalin SJ, Higley MJ (2018) Input-Specific NMDAR-Dependent Potentiation of Dendritic GABAergic Inhibition. Neuron 97:368-377.e363.

Cho K-O, Hunt CA, Kennedy MB (1992) The rat brain postsynaptic density fraction contains a homolog of the Drosophila discs-large tumor suppressor protein. Neuron 9:929-942.

Choi D, Farb D, Fischbach G (1977) Chlordiazepoxide selectively augments GABA action in spinal cord cell cultures. Nature 269:342-344.

Chou T-H, Tajima N, Romero-Hernandez A, Furukawa H (2020) Structural Basis of Functional Transitions in Mammalian NMDA Receptors. Cell 182:357-371.e313.

Chowdhury S, Shepherd JD, Okuno H, Lyford G, Petralia RS, Plath N, Kuhl D, Huganir RL, Worley PF (2006) Arc/Arg3. 1 interacts with the endocytic machinery to regulate AMPA receptor trafficking. Neuron 52:445-459.

Christie JM, Chiu DN, Jahr CE (2011) Ca(2+)-dependent enhancement of release by subthreshold somatic depolarization. Nat Neurosci 14:62-68.

Chung HJ, Steinberg JP, Huganir RL, Linden DJ (2003) Requirement of AMPA receptor GluR2 phosphorylation for cerebellar long-term depression. Science 300:1751-1755.

Chung HJ, Xia J, Scannevin RH, Zhang X, Huganir RL (2000) Phosphorylation of the AMPA Receptor Subunit GluR2 Differentially Regulates Its Interaction with PDZ Domain-Containing Proteins. The Journal of Neuroscience 20:7258-7267.

Clark BA, Cull-Candy SG (2002) Activity-Dependent Recruitment of Extrasynaptic NMDA Receptor Activation at an AMPA Receptor-Only Synapse. The Journal of Neuroscience 22:4428-4436.

Clayton GH, Owens GC, Wolff JS, Roderic LS (1998) Ontogeny of cation–Cl− cotransporter expression in rat neocortex1Published on the World Wide Web on 27 May 1998.1. Developmental Brain Research 109:281-292.

Clements JD, Westbrook GL (1991) Activation kinetics reveal the number of glutamate and glycine binding sites on the N-methyl-d-aspartate receptor. Neuron 7:605-613.

Cochilla AJ, Alford S (1998) Metabotropic Glutamate Receptor–Mediated Control of Neurotransmitter Release. Neuron 20:1007-1016.

Coddington LT, Rudolph S, Vande Lune P, Overstreet-Wadiche L, Wadiche JI (2013) Spillover-mediated feedforward inhibition functionally segregates interneuron activity. Neuron 78:1050-1062.

Collingridge GL, Peineau S, Howland JG, Wang YT (2010) Long-term depression in the CNS. Nature Reviews Neuroscience 11:459-473.

Collins SC, Bray SM, Suhl JA, Cutler DJ, Coffee B, Zwick ME, Warren ST (2010) Identification of novel FMR1 variants by massively parallel sequencing in developmentally delayed males. American Journal of Medical Genetics Part A 152A:2512-2520.

Comery TA, Harris JB, Willems PJ, Oostra BA, Irwin SA, Weiler IJ, Greenough WT (1997) Abnormal dendritic spines in fragile X knockout mice: maturation and pruning deficits. Proc Natl Acad Sci U S A 94:5401-5404.

Conquet F, Bashir ZI, Davies CH, Daniel H, Ferraguti F, Bordi F, Franz-Bacon K, Reggiani A, Matarese V, Condé F (1994) Motor deficit and impairment of synaptic plasticity in mice lacking mGluR1. Nature 372:237-243.

Constanti A (1979) The GABA dose/conductance relationship on lobster muscle. Journal de physiologie 75:645-649.

Contractor A, Mulle C, Swanson GT (2011) Kainate receptors coming of age: milestones of two decades of research. Trends in neurosciences 34:154-163.

Contractor A, Klyachko VA, Portera-Cailliau C (2015) Altered Neuronal and Circuit Excitability in Fragile X Syndrome. Neuron 87:699-715.

Coombs ID, Soto D, Zonouzi M, Renzi M, Shelley C, Farrant M, Cull-Candy SG (2012) Cornichons Modify Channel Properties of Recombinant and Glial AMPA Receptors. The Journal of Neuroscience 32:9796-9804.

Coombs J, Eccles JC, Fatt P (1955) The specific ionic conductances and the ionic movements across the motoneuronal membrane that produce the inhibitory post-synaptic potential. The Journal of physiology 130:326-373.

Corringer P-J, Bertrand S, Galzi J-L, Devillers-Thiéry A, Changeux J-P, Bertrand D (1999) Mutational Analysis of the Charge Selectivity Filter of the α7 Nicotinic Acetylcholine Receptor. Neuron 22:831-843.

Craig AM, Blackstone CD, Huganir RL, Banker G (1993) The distribution of glutamate receptors in cultured rat hippocampal neurons: postsynaptic clustering of AMPA selective subunits. Neuron 10:1055-1068.

Cupolillo D, Hoxha E, Faralli A, De Luca A, Rossi F, Tempia F, Carulli D (2016) Autistic-Like Traits and Cerebellar Dysfunction in Purkinje Cell PTEN Knock-Out Mice. Neuropsychopharmacology 41:1457-1466.

Curtis D, Watkins J (1960a) The excitation and depression of spinal neurones by structurally related amino acids. Journal of neurochemistry 6:117-141.

Curtis D, Phillis J, Watkins J (1959) Chemical excitation of spinal neurones. Nature 183:611-612.

Curtis D, Phillis J, Watkins J (1960) The chemical excitation of spinal neurones by certain acidic amino acids. The Journal of physiology 150:656.

Curtis DR, Watkins JC (1960b) THE EXCITATION AND DEPRESSION OF SPINAL NEURONES BY STRUCTURALLY RELATED AMINO ACIDS. Journal of Neurochemistry 6:117-141.

Curtis DR, Duggan AW, Felix D, Johnston GAR, McLennan H (1971) Antagonism between bicuculline and GABA in the cat brain. Brain Research 33:57-73.

Dahlhaus R, El-Husseini A (2010) Altered neuroligin expression is involved in social deficits in a mouse model of the fragile X syndrome. Behavioural brain research 208:96-105.

Dale HH, Gaddum JH (1930) Reactions of denervated voluntary muscle, and their bearing on the mode of action of parasympathetic and related nerves. The Journal of Physiology 70:109.

Dale HH, Feldberg W, Vogt M (1936) Release of acetylcholine at voluntary motor nerve endings. The Journal of physiology 86:353.

Darnell Jennifer C, Van Driesche Sarah J, Zhang C, Hung Ka Ying S, Mele A, Fraser Claire E, Stone Elizabeth F, Chen C, Fak John J, Chi Sung W, Licatalosi Donny D, Richter Joel D, Darnell Robert B (2011) FMRP Stalls Ribosomal Translocation on mRNAs Linked to Synaptic Function and Autism. Cell 146:247-261.

Dawe GB, Musgaard M, Aurousseau MR, Nayeem N, Green T, Biggin PC, Bowie D (2016) Distinct structural pathways coordinate the activation of AMPA receptor-auxiliary subunit complexes. Neuron 89:1264-1276.

Dawe GB, Kadir MF, Venskutonytė R, Perozzo AM, Yan Y, Alexander RPD, Navarrete C, Santander EA, Arsenault M, Fuentes C, Aurousseau MRP, Frydenvang K, Barrera NP, Kastrup JS, Edwardson JM, Bowie D (2019) Nanoscale Mobility of the Apo State and TARP Stoichiometry Dictate the Gating Behavior of Alternatively Spliced AMPA Receptors. Neuron 102:976-992.e975.

De Boulle K, Verkerk AJMH, Reyniers E, Vits L, Hendrickx J, Van Roy B, Van Den Bos F, de Graaff E, Oostra BA, Willems PJ (1993) A point mutation in the FMR-1 gene associated with fragile X mental retardation. Nature Genetics 3:31-35.

De Luca B, Monda M, Sullo A (1995) Changes in eating behavior and thermogenic activity following inhibition of nitric oxide formation. American Journal of Physiology-Regulatory, Integrative and Comparative Physiology 268:R1533-R1538.

De Robertis ED, Bennett HS (1955) Some features of the submicroscopic morphology of synapses in frog and earthworm. The Journal of Cell Biology 1:47-58.

De Zeeuw CI, Hansel C, Bian F, Koekkoek SKE, van Alphen AM, Linden DJ, Oberdick J (1998) Expression of a Protein Kinase C Inhibitor in Purkinje Cells Blocks Cerebellar LTD and Adaptation of the Vestibulo-Ocular Reflex. Neuron 20:495-508.

De Rubeis S, Pasciuto E, Li Ka W, Fernández E, Di Marino D, Buzzi A, Ostroff Linnaea E, Klann E, Zwartkruis FJT, Komiyama Noboru H, Grant SGN, Poujol C, Choquet D, Achsel T, Posthuma D, Smit August B, Bagni C (2013) CYFIP1 Coordinates mRNA Translation and Cytoskeleton Remodeling to Ensure Proper Dendritic Spine Formation. Neuron 79:1169-1182.

Debanne D, Inglebert Y, Russier M (2019) Plasticity of intrinsic neuronal excitability. Current Opinion in Neurobiology 54:73-82.

Deisz RA, Fortin G, Zieglgansberger W (1991) Voltage dependence of excitatory postsynaptic potentials of rat neocortical neurons. Journal of Neurophysiology 65:371-382.

Dejanovic B, Schwarz G (2014) Neuronal nitric oxide synthase-dependent S-nitrosylation of gephyrin regulates gephyrin clustering at GABAergic synapses. Journal of Neuroscience 34:7763-7768.

Dejanovic B, Semtner M, Ebert S, Lamkemeyer T, Neuser F, Lüscher B, Meier JC, Schwarz G (2014) Palmitoylation of gephyrin controls receptor clustering and plasticity of GABAergic synapses. PLoS Biol 12:e1001908.

del Castillo J, Katz B (1954) Quantal components of the end-plate potential. The Journal of Physiology 124:560-573.

Deng P-Y, Sojka D, Klyachko VA (2011) Abnormal Presynaptic Short-Term Plasticity and Information Processing in a Mouse Model of Fragile X Syndrome. The Journal of Neuroscience 31:10971-10982.

Deng P-Y, Carlin D, Oh YM, Myrick LK, Warren ST, Cavalli V, Klyachko VA (2019) Voltage-Independent SK-Channel Dysfunction Causes Neuronal Hyperexcitability in the Hippocampus of Fmr1 Knock-Out Mice. The Journal of Neuroscience 39:28-43.

Deng P-Y, Rotman Z, Blundon Jay A, Cho Y, Cui J, Cavalli V, Zakharenko Stanislav S, Klyachko Vitaly A (2013) FMRP Regulates Neurotransmitter Release and Synaptic Information Transmission by Modulating Action Potential Duration via BK Channels. Neuron 77:696-711.

Deverett B, Koay SA, Oostland M, Wang SS (2018) Cerebellar involvement in an evidence-accumulation decision-making task. Elife 7:e36781.

Devys D, Lutz Y, Rouyer N, Bellocq J-P, Mandel J-L (1993) The FMR–1 protein is cytoplasmic, most abundant in neurons and appears normal in carriers of a fragile X premutation. Nature genetics 4:335-340.

Dickinson BC, Chang CJ (2011) Chemistry and biology of reactive oxygen species in signaling or stress responses. Nature chemical biology 7:504.

Diering GH, Huganir RL (2018) The AMPA Receptor Code of Synaptic Plasticity. Neuron 100:314-329.

Dixon C, Sah P, Lynch JW, Keramidas A (2014) GABAA Receptor α and γ Subunits Shape Synaptic Currents via Different Mechanisms. Journal of Biological Chemistry 289:5399-5411.

Dizon MJ, Khodakhah K (2011) The Role of Interneurons in Shaping Purkinje Cell Responses in the Cerebellar Cortex. The Journal of Neuroscience 31:10463-10473.

Dölen G, Osterweil E, Rao BSS, Smith GB, Auerbach BD, Chattarji S, Bear MF (2007) Correction of Fragile X Syndrome in Mice. Neuron 56:955-962.

Donevan SD, Rogawski MA (1995) Intracellular polyamines mediate inward rectification of Ca(2+)-permeable alpha-amino-3-hydroxy-5-methyl-4-isoxazolepropionic acid receptors. Proceedings of the National Academy of Sciences 92:9298-9302.

Dong H, O'Brien RJ, Fung ET, Lanahan AA, Worley PF, Huganir RL (1997) GRIP: a synaptic PDZ domain-containing protein that interacts with AMPA receptors. Nature 386:279-284.

Dong H, Zhang P, Song I, Petralia RS, Liao D, Huganir RL (1999) Characterization of the glutamate receptor-interacting proteins GRIP1 and GRIP2. Journal of Neuroscience 19:6930-6941.

Dore K, Malinow R (2020) Elevated PSD-95 Blocks Ion-flux Independent LTD: A Potential New Role for PSD-95 in Synaptic Plasticity. Neuroscience.

Dore K, Aow J, Malinow R (2015) Agonist binding to the NMDA receptor drives movement of its cytoplasmic domain without ion flow. Proceedings of the National Academy of Sciences 112:14705-14710.

Dudek SM, Bear MF (1992) Homosynaptic long-term depression in area CA1 of hippocampus and effects of N-methyl-D-aspartate receptor blockade. Proceedings of the National Academy of Sciences 89:4363-4367.

Dugan LL, Sensi SL, Canzoniero LM, Handran SD, Rothman SM, Lin TS, Goldberg MP, Choi DW (1995) Mitochondrial production of reactive oxygen species in cortical neurons following exposure to N-methyl-D-aspartate. J Neurosci 15:6377-6388.

Durand CM, Betancur C, Boeckers TM, Bockmann J, Chaste P, Fauchereau F, Nygren G, Rastam M, Gillberg IC, Anckarsäter H (2007) Mutations in the gene encoding the synaptic scaffolding protein SHANK3 are associated with autism spectrum disorders. Nature genetics 39:25-27.

Dy ABC, Tassone F, Eldeeb M, Salcedo-Arellano MJ, Tartaglia N, Hagerman R (2018) Metformin as targeted treatment in fragile X syndrome. Clinical Genetics 93:216-222.

Eccles J (1937) Synaptic and neuro-muscular transmission. Physiological Reviews 17:538-555.

Eccles JC, Katz B, Kuffler SW (1941) Nature of the" endplate potential" in curarized muscle. Journal of Neurophysiology 4:362-387.

Edbauer D, Neilson JR, Foster KA, Wang C-F, Seeburg DP, Batterton MN, Tada T, Dolan BM, Sharp PA, Sheng M (2010) Regulation of Synaptic Structure and Function by FMRP-Associated MicroRNAs miR-125b and miR-132. Neuron 65:373-384.

Erlander MG, Tillakaratne NJK, Feldblum S, Patel N, Tobin AJ (1991) Two genes encode distinct glutamate decarboxylases. Neuron 7:91-100.

Faraci FM, Breese KR (1993) Nitric oxide mediates vasodilatation in response to activation of N-methyl-D-aspartate receptors in brain. Circulation Research 72:476-480.

Farrant M, Nusser Z (2005) Variations on an inhibitory theme: phasic and tonic activation of GABAA receptors. Nature Reviews Neuroscience 6:215-229.

Farrant M, Kaila K (2007) The cellular, molecular and ionic basis of GABAA receptor signalling. Progress in brain research 160:59-87.

Farrow P, Khodosevich K, Sapir Y, Schulmann A, Aslam M, Stern-Bach Y, Monyer H, von Engelhardt J (2015) Auxiliary subunits of the CKAMP family differentially modulate AMPA receptor properties. Elife 4:e09693.

Fatt P, Katz B (1951) An analysis of the end-plate potential recorded with an intra-cellular electrode. The Journal of physiology 115:320.

Fatt P, Katz B (1952) Spontaneous subthreshold activity at motor nerve endings. The Journal of Physiology 117:109-128.

Ferron L (2016) Fragile X mental retardation protein controls ion channel expression and activity. The Journal of Physiology 594:5861-5867.

Ferron L, Nieto-Rostro M, Cassidy JS, Dolphin AC (2014) Fragile X mental retardation protein controls synaptic vesicle exocytosis by modulating N-type calcium channel density. Nature Communications 5:3628.

Fisher JL, Macdonald RL (1997) Single channel properties of recombinant GABAA receptors containing γ2 or δ subtypes expressed with α1 and β3 subtypes in mouse L929 Cells. The Journal of Physiology 505:283-297.

Flores CE, Nikonenko I, Mendez P, Fritschy J-M, Tyagarajan SK, Muller D (2015) Activity-dependent inhibitory synapse remodeling through gephyrin phosphorylation. Proceedings of the National Academy of Sciences 112:E65-E72.

Foote M, Arque G, Berman RF, Santos M (2016) Fragile X-Associated Tremor/Ataxia Syndrome (FXTAS) Motor Dysfunction Modeled in Mice. The Cerebellum 15:611-622.

Forstermann U, Gorsky LD, Pollock JS, Schmidt HH, Heller M, Murad F (1990) Regional distribution of EDRF/NO-synthesizing enzyme(s) in rat brain. Biochem Biophys Res Commun 168:727-732.

Forsythe ID, Westbrook GL (1988) Slow excitatory postsynaptic currents mediated by N-methyl-D-aspartate receptors on cultured mouse central neurones. The Journal of Physiology 396:515-533.

Francis SH, Busch JL, Corbin JD (2010) cGMP-Dependent Protein Kinases and cGMP Phosphodiesterases in Nitric Oxide and cGMP Action. Pharmacological Reviews 62:525-563.

Fritschy J-M, Panzanelli P (2014) GABAA receptors and plasticity of inhibitory neurotransmission in the central nervous system. European Journal of Neuroscience 39:1845-1865.

Fritschy J-M, Panzanelli P, Tyagarajan SK (2012) Molecular and functional heterogeneity of GABAergic synapses. Cellular and Molecular Life Sciences 69:2485-2499.

Fritschy JM, Panzanelli P (2006) Molecular and synaptic organization of GABAA receptors in the cerebellum: Effects of targeted subunit gene deletions. Cerebellum 5:275-285.

Fujii S, Saito K, Miyakawa H, Ito K-i, Kato H (1991) Reversal of long-term potentiation (depotentiation) induced by tetanus stimulation of the input to CA1 neurons of guinea pig hippocampal slices. Brain research 555:112-122.

Fulton JF (1951) Physiology of the nervous system, 3d ed., rev. Edition. New York: Oxford University Press.

Gaffield MA, Christie JM (2017) Movement Rate Is Encoded and Influenced by Widespread, Coherent Activity of Cerebellar Molecular Layer Interneurons. The Journal of Neuroscience 37:4751-4765.

Gaffield MA, Bonnan A, Christie JM (2019) Conversion of Graded Presynaptic Climbing Fiber Activity into Graded Postsynaptic Ca2+ Signals by Purkinje Cell Dendrites. Neuron 102:762-769.e764.

Gallagher SM, Daly CA, Bear MF, Huber KM (2004) Extracellular signal-regulated protein kinase activation is required for metabotropic glutamate receptor-dependent long-term depression in hippocampal area CA1. Journal of Neuroscience 24:4859-4864.

Galzi J-L, Devillers-Thiery A, Hussy N, Bertrand S, Changeux J-P, Bertrand D (1992) Mutations in the channel domain of a neuronal nicotinic receptor convert ion selectivity from cationic to anionic. Nature 359:500-505.

Gantois I, Popic J, Khoutorsky A, Sonenberg N (2019) Metformin for Treatment of Fragile X Syndrome and Other Neurological Disorders. Annual Review of Medicine 70:167-181.

Gantois I, Pop AS, de Esch CE, Buijsen RA, Pooters T, Gomez-Mancilla B, Gasparini F, Oostra BA, D'Hooge R, Willemsen R (2013) Chronic administration of AFQ056/Mavoglurant restores social behaviour in Fmr1 knockout mice. Behavioural brain research 239:72-79.

Gantois I, Khoutorsky A, Popic J, Aguilar-Valles A, Freemantle E, Cao R, Sharma V, Pooters T, Nagpal A, Skalecka A (2017) Metformin ameliorates core deficits in a mouse model of fragile X syndrome. Nature medicine 23:674.

Garthwaite J (2008) Concepts of neural nitric oxide-mediated transmission. Eur J Neurosci 27:2783-2802.

Garthwaite J (2016) From synaptically localized to volume transmission by nitric oxide. The Journal of Physiology 594:9-18.

Garthwaite J (2019) NO as a multimodal transmitter in the brain: discovery and current status. Br J Pharmacol 176:197-211.

Geiger JR, Lübke J, Roth A, Frotscher M, Jonas P (1997) Submillisecond AMPA receptor-mediated signaling at a principal neuron–interneuron synapse. Neuron 18:1009-1023.

Geiger JR, Melcher T, Koh D-S, Sakmann B, Seeburg PH, Jonas P, Monyer H (1995) Relative abundance of subunit mRNAs determines gating and Ca2+ permeability of AMPA receptors in principal neurons and interneurons in rat CNS. Neuron 15:193-204.

Geppert M, Goda Y, Hammer RE, Li C, Rosahl TW, Stevens CF, Südhof TC (1994) Synaptotagmin I: a major Ca2+ sensor for transmitter release at a central synapse. Cell 79:717-727.

Gerdeman GL, Ronesi J, Lovinger DM (2002) Postsynaptic endocannabinoid release is critical to long-term depression in the striatum. Nature Neuroscience 5:446-451.

Gholizadeh S, Arsenault J, Xuan ICY, Pacey LK, Hampson DR (2014) Reduced phenotypic severity following adeno-associated virus-mediated Fmr1 gene delivery in fragile X mice. Neuropsychopharmacology 39:3100-3111.

Ghosh H, Auguadri L, Battaglia S, Simone Thirouin Z, Zemoura K, Messner S, Acuña MA, Wildner H, Yévenes GE, Dieter A, Kawasaki H, O. Hottiger M, Zeilhofer HU, Fritschy J-M, Tyagarajan SK (2016) Several posttranslational modifications act in concert to regulate gephyrin scaffolding and GABAergic transmission. Nature Communications 7:13365.

Gidon A, Segev I (2012) Principles Governing the Operation of Synaptic Inhibition in Dendrites. Neuron 75:330-341.

Gielen M, Thomas P, Smart TG (2015) The desensitization gate of inhibitory Cys-loop receptors. Nature Communications 6:6829.

Gingrich K, Roberts W, Kass R (1995) Dependence of the GABAA receptor gating kinetics on the alpha-subunit isoform: implications for structure-function relations and synaptic transmission. The Journal of Physiology 489:529-543.

Girouard H, Wang G, Gallo EF, Anrather J, Zhou P, Pickel VM, Iadecola C (2009) NMDA Receptor Activation Increases Free Radical Production through Nitric Oxide and NOX2. The Journal of Neuroscience 29:2545-2552.

Giuffrida R, Musumeci S, D'Antoni S, Bonaccorso CM, Giuffrida-Stella AM, Oostra BA, Catania MV (2005) A reduced number of metabotropic glutamate subtype 5 receptors are associated with constitutive homer proteins in a mouse model of fragile X syndrome. Journal of Neuroscience 25:8908-8916.

Gkogkas Christos G, Khoutorsky A, Cao R, Jafarnejad Seyed M, Prager-Khoutorsky M, Giannakas N, Kaminari A, Fragkouli A, Nader K, Price Theodore J, Konicek Bruce W, Graff Jeremy R, Tzinia Athina K, Lacaille J-C, Sonenberg N (2014) Pharmacogenetic Inhibition of eIF4E-Dependent Mmp9 mRNA Translation Reverses Fragile X Syndrome-like Phenotypes. Cell Reports 9:1742-1755.

Gladding CM, Collett VJ, Jia Z, Bashir ZI, Collingridge GL, Molnár E (2009) Tyrosine dephosphorylation regulates AMPAR internalisation in mGluR-LTD. Molecular and Cellular Neuroscience 40:267-279.

Glasgow NG, Siegler Retchless B, Johnson JW (2015) Molecular bases of NMDA receptor subtype-dependent properties. The Journal of Physiology 593:83-95.

Gnegy ME (2000) Ca2+/calmodulin signaling in NMDA-induced synaptic plasticity. Crit Rev Neurobiol 14:91-129.

Gocel J, Larson J (2012) Synaptic NMDA receptor-mediated currents in anterior piriform cortex are reduced in the adult fragile X mouse. Neuroscience 221:170-181.

Golding NL, Ferragamo MJ, Oertel D (1999) Role of intrinsic conductances underlying responses to transients in octopus cells of the cochlear nucleus. Journal of Neuroscience 19:2897-2905.

Goy MF (1991) cGMP: the wayward child of the cyclic nucleotide family. Trends in neurosciences 14:293-299.

Granger AJ, Shi Y, Lu W, Cerpas M, Nicoll RA (2013) LTP requires a reserve pool of glutamate receptors independent of subunit type. Nature 493:495-500.

Grant SG (2012) Synaptopathies: diseases of the synaptome. Current opinion in neurobiology 22:522-529.

Greenough WT, Klintsova AY, Irwin SA, Galvez R, Bates KE, Weiler IJ (2001) Synaptic regulation of protein synthesis and the fragile X protein. Proc Natl Acad Sci U S A 98:7101-7106.

Gross C, Yao X, Pong DL, Jeromin A, Bassell GJ (2011) Fragile X Mental Retardation Protein Regulates Protein Expression and mRNA Translation of the Potassium Channel Kv4.2. The Journal of Neuroscience 31:5693-5698.

Gu N, Hu H, Vervaeke K, Storm JF (2008) SK (KCa2) Channels Do Not Control Somatic Excitability in CA1 Pyramidal Neurons But Can Be Activated by Dendritic Excitatory Synapses and Regulate Their Impact. Journal of Neurophysiology 100:2589-2604.

Gulledge AT, Stuart GJ (2003) Excitatory Actions of GABA in the Cortex. Neuron 37:299-309.

Gunthorpe MJ, Lummis SC (2001) Conversion of the ion selectivity of the 5-HT3Areceptor from cationic to anionic reveals a conserved feature of the ligand-gated ion channel superfamily. Journal of Biological Chemistry 276:10977-10983.

Guo W, Ceolin L, Collins Katie A, Perroy J, Huber Kimberly M (2015) Elevated CaMKIIα and Hyperphosphorylation of Homer Mediate Circuit Dysfunction in a Fragile X Syndrome Mouse Model. Cell Reports 13:2297-2311.

Gustafsson B, Wigstrom H, Abraham W, Huang Y (1987) Long-term potentiation in the hippocampus using depolarizing current pulses as the conditioning stimulus to single volley synaptic potentials. Journal of Neuroscience 7:774-780.

Gutierrez-Castellanos N, Da Silva-Matos CM, Zhou K, Canto CB, Renner MC, Koene LMC, Ozyildirim O, Sprengel R, Kessels HW, De Zeeuw CI (2017) Motor Learning Requires Purkinje Cell Synaptic Potentiation through Activation of AMPA-Receptor Subunit GluA3. Neuron 93:409-424.

Haas KF, Macdonald RL (1999) GABAA receptor subunit γ2 and δ subtypes confer unique kinetic properties on recombinant GABAA receptor currents in mouse fibroblasts. The Journal of Physiology 514:27-45.

Hagerman PJ, Greco CM, Hagerman RJ (2003) A cerebellar tremor/ataxia syndrome among fragile X premutation carriers. Cytogenetic and Genome Research 100:206-212.

Haj-Dahmane S, Shen R-Y (2010) Regulation of plasticity of glutamate synapses by endocannabinoids and the cyclic-AMP/protein kinase A pathway in midbrain dopamine neurons. The Journal of Physiology 588:2589-2604.

Hall SS, Dougherty RF, Reiss AL (2016) Profiles of aberrant white matter microstructure in fragile X syndrome. NeuroImage: Clinical 11:133-138.

Hampson DR, Blatt GJ (2015) Autism spectrum disorders and neuropathology of the cerebellum. Front Neurosci 9:420.

Hansen KB, Yi F, Perszyk RE, Furukawa H, Wollmuth LP, Gibb AJ, Traynelis SF (2018) Structure, function, and allosteric modulation of NMDA receptors. Journal of General Physiology 150:1081-1105.

Hansen SB, Wang H-L, Taylor P, Sine SM (2008) An Ion Selectivity Filter in the Extracellular Domain of Cys-loop Receptors Reveals Determinants for Ion Conductance. Journal of Biological Chemistry 283:36066-36070.

Hardingham GE, Bading H (2003) The Yin and Yang of NMDA receptor signalling. Trends Neurosci 26:81-89.

Hartmann J, Karl Rosa M, Alexander Ryan PD, Adelsberger H, Brill Monika S, Rühlmann C, Ansel A, Sakimura K, Baba Y, Kurosaki T, Misgeld T, Konnerth A (2014) STIM1 Controls Neuronal Ca2+ Signaling, mGluR1-Dependent Synaptic Transmission, and Cerebellar Motor Behavior. Neuron 82:635-644.

Hashimoto K, Fukaya M, Qiao X, Sakimura K, Watanabe M, Kano M (1999) Impairment of AMPA receptor function in cerebellar granule cells of ataxic mutant mouse stargazer. Journal of Neuroscience 19:6027-6036.

Häusser M, Clark BA (1997) Tonic Synaptic Inhibition Modulates Neuronal Output Pattern and Spatiotemporal Synaptic Integration. Neuron 19:665-678.

Hay N, Sonenberg N (2004) Upstream and downstream of mTOR. Genes & development 18:1926-1945.

Hayashi T, Nagai K (1956) Action of B-amino acids on the motor cortex of higher animals, especially.-amino-O-oxybutyric acid on the real inhibitory principle in brain. Abstr XX int physiol Congr:410.

Hays SA, Huber KM, Gibson JR (2011) Altered neocortical rhythmic activity states in Fmr1 KO mice are due to enhanced mGluR5 signaling and involve changes in excitatory circuitry. J Neurosci 31:14223-14234.

He Q, Nomura T, Xu J, Contractor A (2014) The developmental switch in GABA polarity is delayed in fragile X mice. J Neurosci 34:446-450.

He Q, Duguid I, Clark B, Panzanelli P, Patel B, Thomas P, Fritschy J-M, Smart TG (2015) Interneuron- and GABAA receptor-specific inhibitory synaptic plasticity in cerebellar Purkinje cells. Nature Communications 6:7364.

Heavner WE, Smith SEP (2020) Resolving the Synaptic versus Developmental Dichotomy of Autism Risk Genes. Trends in Neurosciences 43:227-241.

Hebb DO (1949) The organization of behavior: A neuropsychological theory: Psychology Press.

Henderson C, Wijetunge L, Kinoshita MN, Shumway M, Hammond RS, Postma FR, Brynczka C, Rush R, Thomas A, Paylor R (2012) Reversal of disease-related pathologies in the fragile X mouse model by selective activation of GABAB receptors with arbaclofen. Science translational medicine 4:152ra128-152ra128.

Hengen KB, Lambo ME, Van Hooser SD, Katz DB, Turrigiano GG (2013) Firing rate homeostasis in visual cortex of freely behaving rodents. Neuron 80:335-342.

Hensch TK, Fagiolini M, Mataga N, Stryker MP, Baekkeskov S, Kash SF (1998) Local GABA circuit control of experience-dependent plasticity in developing visual cortex. Science 282:1504-1508.

Herguedas B, Watson JF, Ho H, Cais O, García-Nafría J, Greger IH (2019) Architecture of the heteromeric GluA1/2 AMPA receptor in complex with the auxiliary subunit TARP γ8. Science 364:eaav9011.

Hestrin S, Nicoll R, Perkel D, Sah P (1990) Analysis of excitatory synaptic action in pyramidal cells using whole-cell recording from rat hippocampal slices. The Journal of Physiology 422:203-225.

Hilf RJC, Dutzler R (2008) X-ray structure of a prokaryotic pentameric ligand-gated ion channel. Nature 452:375-379.

Hill DR, Bowery NG (1981) 3H-baclofen and 3H-GABA bind to bicuculline-insensitive GABAB sites in rat brain. Nature 290:149-152.

Hinds HL, Ashley CT, Sutcliffe JS, Nelson DL, Warren ST, Housman DE, Schalling M (1993) Tissue specific expression of FMR–1 provides evidence for a functional role in fragile X syndrome. Nature Genetics 3:36-43.

Hoffman DA, Magee JC, Colbert CM, Johnston D (1997) K+ channel regulation of signal propagation in dendrites of hippocampal pyramidal neurons. Nature 387:869-875.

Hou L, Klann E (2004) Activation of the Phosphoinositide 3-Kinase-Akt-Mammalian Target of Rapamycin Signaling Pathway Is Required for Metabotropic Glutamate Receptor-Dependent Long-Term Depression. The Journal of Neuroscience 24:6352-6361.

Hu C, Chen W, Myers SJ, Yuan H, Traynelis SF (2016) Human GRIN2B variants in neurodevelopmental disorders. J Pharmacol Sci 132:115-121.

Huang PL, Dawson TM, Bredt DS, Snyder SH, Fishman MC (1993) Targeted disruption of the neuronal nitric oxide synthase gene. Cell 75:1273-1286.

Huber KM, Kayser MS, Bear MF (2000) Role for Rapid Dendritic Protein Synthesis in Hippocampal mGluR-Dependent Long-Term Depression. Science 288:1254-1256.

Huber KM, Roder JC, Bear MF (2001) Chemical Induction of mGluR5- and Protein Synthesis–Dependent Long-Term Depression in Hippocampal Area CA1. Journal of Neurophysiology 86:321-325.

Huber KM, Gallagher SM, Warren ST, Bear MF (2002) Altered synaptic plasticity in a mouse model of fragile X mental retardation. Proc Natl Acad Sci U S A 99:7746-7750.

Huganir Richard L, Nicoll Roger A (2013) AMPARs and Synaptic Plasticity: The Last 25 Years. Neuron 80:704-717.

Hume R, Dingledine R, Heinemann S (1991) Identification of a site in glutamate receptor subunits that controls calcium permeability. Science 253:1028-1031.

Ignarro LJ, Harbison RG, Wood KS, Kadowitz PJ (1986) Activation of purified soluble guanylate cyclase by endothelium-derived relaxing factor from intrapulmonary artery and vein: stimulation by acetylcholine, bradykinin and arachidonic acid. Journal of Pharmacology and Experimental Therapeutics 237:893-900.

Ip JPK, Mellios N, Sur M (2018) Rett syndrome: insights into genetic, molecular and circuit mechanisms. Nature Reviews Neuroscience 19:368-382.

Iremonger KJ, Bains JS (2009) Retrograde Opioid Signaling Regulates Glutamatergic Transmission in the Hypothalamus. The Journal of Neuroscience 29:7349-7358.

Isaacson Jeffry S, Scanziani M (2011) How Inhibition Shapes Cortical Activity. Neuron 72:231-243.

Ito-Ishida A, Kakegawa W, Yuzaki M (2006) ERK1/2 but not p38 MAP kinase is essential for the long-term depression in mouse cerebellar slices. European Journal of Neuroscience 24:1617-1622.

Ito M (2006) Cerebellar circuitry as a neuronal machine. Progress in neurobiology 78:272-303.

Ito M, Sakurai M, Tongroach P (1982) Climbing fibre induced depression of both mossy fibre responsiveness and glutamate sensitivity of cerebellar Purkinje cells. The Journal of Physiology 324:113-134.

Jackman SL, Regehr WG (2017) The Mechanisms and Functions of Synaptic Facilitation. Neuron 94:447-464.

Jackman SL, Turecek J, Belinsky JE, Regehr WG (2016) The calcium sensor synaptotagmin 7 is required for synaptic facilitation. Nature 529:88-91.

Jackson Alexander C, Nicoll Roger A (2011) The Expanding Social Network of Ionotropic Glutamate Receptors: TARPs and Other Transmembrane Auxiliary Subunits. Neuron 70:178-199.

Jacob TC, Moss SJ, Jurd R (2008) GABA(A) receptor trafficking and its role in the dynamic modulation of neuronal inhibition. Nat Rev Neurosci 9:331-343.

Jacob TC, Bogdanov YD, Magnus C, Saliba RS, Kittler JT, Haydon PG, Moss SJ (2005) Gephyrin Regulates the Cell Surface Dynamics of Synaptic GABA_A Receptors. The Journal of Neuroscience 25:10469-10478.

Jamain S et al. (2003) Mutations of the X-linked genes encoding neuroligins NLGN3 and NLGN4 are associated with autism. Nature Genetics 34:27-29.

Jensen ML, Timmermann DB, Johansen TH, Schousboe A, Varming T, Ahring PK (2002) The β subunit determines the ion selectivity of the GABAA receptor. Journal of Biological Chemistry 277:41438-41447.

Jeong J-W, Tiwari V, Behen M, Chugani H, Chugani D (2014) In vivo detection of reduced Purkinje cell fibers with diffusion MRI tractography in children with autistic spectrum disorders. Frontiers in Human Neuroscience 8.

Jeste SS, Varcin KJ, Hellemann GS, Gulsrud AC, Bhatt R, Kasari C, Wu JY, Sahin M, Nelson CA (2016) Symptom profiles of autism spectrum disorder in tuberous sclerosis complex. Neurology 87:766-772.

Johnson JW, Ascher P (1987) Glycine potentiates the NMDA response in cultured mouse brain neurons. Nature 325:529-531.

Jones A, Korpi ER, McKernan RM, Pelz R, Nusser Z, Mäkelä R, Mellor JR, Pollard S, Bahn S, Stephenson FA, Randall AD, Sieghart W, Somogyi P, Smith AJH, Wisden W (1997) Ligand-Gated Ion Channel Subunit Partnerships: GABA_AReceptor α₆ Subunit Gene Inactivation Inhibits δ Subunit Expression. The Journal of Neuroscience 17:1350-1362.

Jones MV, Westbrook GL (1995) Desensitized states prolong GABAA channel responses to brief agonist pulses. Neuron 15:181-191.

Jones SL, To M-S, Stuart GJ (2017) Dendritic small conductance calcium-activated potassium channels activated by action potentials suppress EPSPs and gate spike-timing dependent synaptic plasticity. Elife 6:e30333.

Jorntell H, Ekerot CF (2006) Properties of somatosensory synaptic integration in cerebellar granule cells in vivo. J Neurosci 26:11786-11797.

Jörntell H, Bengtsson F, Schonewille M, De Zeeuw CI (2010) Cerebellar molecular layer interneurons – computational properties and roles in learning. Trends in Neurosciences 33:524-532.

Jung H, Gkogkas CG, Sonenberg N, Holt CE (2014) Remote control of gene function by local translation. Cell 157:26-40.

Kaeser PS, Regehr WG (2017) The readily releasable pool of synaptic vesicles. Current Opinion in Neurobiology 43:63-70.

Kaila K, Price TJ, Payne JA, Puskarjov M, Voipio J (2014) Cation-chloride cotransporters in neuronal development, plasticity and disease. Nature Reviews Neuroscience 15:637-654.

Kalmbach BE, Johnston D, Brager DH (2015) Cell-type specific channelopathies in the prefrontal cortex of the fmr1-/y mouse model of fragile X syndrome. Eneuro 2.

Kamboj SK, Swanson GT, Cull-Candy SG (1995) Intracellular spermine confers rectification on rat calcium-permeable AMPA and kainate receptors. The Journal of Physiology 486:297-303.

Kano M, Rexhausen U, Dreessen J, Konnerth A (1992) Synaptic excitation produces a long-lasting rebound potentiation of inhibitory synaptic signals in cerebellar Purkinje cells. Nature 356:601-604.

Kano M, Kano M, Fukunaga K, Konnerth A (1996) Ca2+-induced rebound potentiation of γ-aminobutyric acid-mediated currents requires activation of Ca2+/calmodulin-dependent kinase II. Proceedings of the National Academy of Sciences 93:13351-13356.

Kapás L, Fang J, Krueger JM (1994a) Inhibition of nitric oxide synthesis inhibits rat sleep. Brain Research 664:189-196.

Kapás L, Shibata M, Kimura M, Krueger JM (1994b) Inhibition of nitric oxide synthesis suppresses sleep in rabbits. American Journal of Physiology-Regulatory, Integrative and Comparative Physiology 266:R151-R157.

Kaplan JS, Mohr C, Rossi DJ (2013) Opposite actions of alcohol on tonic GABA(A) receptor currents mediated by nNOS and PKC activity. Nat Neurosci 16:1783-1793.

Karlin A, Akabas MH (1995) Toward a structural basis for the function of nicotinic acetylcholine receptors and their cousins. Neuron 15:1231-1244.

Kato AS, Siuda ER, Nisenbaum ES, Bredt DS (2008) AMPA Receptor Subunit-Specific Regulation by a Distinct Family of Type II TARPs. Neuron 59:986-996.

Kato AS, Zhou W, Milstein AD, Knierman MD, Siuda ER, Dotzlaf JE, Yu H, Hale JE, Nisenbaum ES, Nicoll RA, Bredt DS (2007) New Transmembrane AMPA Receptor Regulatory Protein Isoform, γ-7, Differentially Regulates AMPA Receptors. The Journal of Neuroscience 27:4969-4977.

Kato AS, Gill MB, Ho MT, Yu H, Tu Y, Siuda ER, Wang H, Qian Y-W, Nisenbaum ES, Tomita S, Bredt DS (2010) Hippocampal AMPA Receptor Gating Controlled by Both TARP and Cornichon Proteins. Neuron 68:1082-1096.

Katz B, Kuffler SW (1941) Multiple motor innervation of the frog's sartorius muscle. Journal of Neurophysiology 4:209-223.

Katz B, Miledi R (1968) The role of calcium in neuromuscular facilitation. The Journal of physiology 195:481-492.

Kaufman DL, McGinnis JF, Krieger NR, Tobin AJ (1986) Brain glutamate decarboxylase cloned in lambda gt-11: fusion protein produces gamma-aminobutyric acid. Science 232:1138-1140.

Kawaguchi S-y, Hirano T (2000) Suppression of Inhibitory Synaptic Potentiation by Presynaptic Activity through Postsynaptic GABAB Receptors in a Purkinje Neuron. Neuron 27:339-347.

Keck T, Keller GB, Jacobsen RI, Eysel UT, Bonhoeffer T, Hübener M (2013) Synaptic scaling and homeostatic plasticity in the mouse visual cortex in vivo. Neuron 80:327-334.

Keck T, Toyoizumi T, Chen L, Doiron B, Feldman DE, Fox K, Gerstner W, Haydon PG, Hübener M, Lee H-K, Lisman JE, Rose T, Sengpiel F, Stellwagen D, Stryker MP, Turrigiano GG, Rossum MCv (2017)

Integrating Hebbian and homeostatic plasticity: the current state of the field and future research directions. Philosophical Transactions of the Royal Society B: Biological Sciences 372:20160158.

Keramidas A, Harrison NL (2009) The activation mechanism of α1β2γ2S and α3β3γ2S GABAA receptors. Journal of General Physiology 135:59-75.

Keramidas A, Moorhouse AJ, French CR, Schofield PR, Barry PH (2000) M2 pore mutations convert the glycine receptor channel from being anion-to cation-selective. Biophysical Journal 79:247-259.

Keramidas A, Moorhouse AJ, Pierce KD, Schofield PR, Barry PH (2002) Cation-selective mutations in the M2 domain of the inhibitory glycine receptor channel reveal determinants of ion-charge selectivity. The Journal of general physiology 119:393-410.

Kessels HW, Malinow R (2009) Synaptic AMPA Receptor Plasticity and Behavior. Neuron 61:340-350.

Khodosevich K, Jacobi E, Farrow P, Schulmann A, Rusu A, Zhang L, Sprengel R, Monyer H, von Engelhardt J (2014) Coexpressed Auxiliary Subunits Exhibit Distinct Modulatory Profiles on AMPA Receptor Function. Neuron 83:601-615.

Kim E, Sheng M (2004) PDZ domain proteins of synapses. Nature Reviews Neuroscience 5:771-781.

Kim H-G, Kishikawa S, Higgins AW, Seong I-S, Donovan DJ, Shen Y, Lally E, Weiss LA, Najm J, Kutsche K (2008) Disruption of neurexin 1 associated with autism spectrum disorder. The American Journal of Human Genetics 82:199-207.

Kiss JP, Vizi ES (2001) Nitric oxide: a novel link between synaptic and nonsynaptic transmission. Trends Neurosci 24:211-215.

Kittler JT, Rostaing P, Schiavo G, Fritschy JM, Olsen R, Triller A, Moss SJ (2001) The subcellular distribution of GABARAP and its ability to interact with NSF suggest a role for this protein in the intracellular transport of GABA(A) receptors. Mol Cell Neurosci 18:13-25.

Klausberger T, Somogyi P (2008) Neuronal Diversity and Temporal Dynamics: The Unity of Hippocampal Circuit Operations. Science 321:53-57.

Kneussel M, Brandstatter JH, Gasnier B, Feng G, Sanes JR, Betz H (2001) Gephyrin-independent clustering of postsynaptic GABA(A) receptor subtypes. Mol Cell Neurosci 17:973-982.

Knock GA, Ward JP (2011) Redox regulation of protein kinases as a modulator of vascular function. Antioxidants & redox signaling 15:1531-1547.

Kobayashi K, Manabe T, Takahashi T (1996) Presynaptic Long-Term Depression at the Hippocampal Mossy Fiber--CA3 Synapse. Science 273:648-650.

Kobayashi Y, Kaufman DL, Tobin AJ (1987) Glutamic acid decarboxylase cDNA: nucleotide sequence encoding an enzymatically active fusion protein. Journal of Neuroscience 7:2768-2772.

Koekkoek SK et al. (2005) Deletion of FMR1 in Purkinje cells enhances parallel fiber LTD, enlarges spines, and attenuates cerebellar eyelid conditioning in Fragile X syndrome. Neuron 47:339-352.

Koh DS, Geiger JR, Jonas P, Sakmann B (1995) Ca(2+)-permeable AMPA and NMDA receptor channels in basket cells of rat hippocampal dentate gyrus. The Journal of Physiology 485:383-402.

Köhr G, Eckardt S, Lüddens H, Monyer H, Seeburg PH (1994) NMDA receptor channels: Subunit-specific potentiation by reducing agents. Neuron 12:1031-1040.

Kole MH, Ilschner SU, Kampa BM, Williams SR, Ruben PC, Stuart GJ (2008) Action potential generation requires a high sodium channel density in the axon initial segment. Nature neuroscience 11:178-186.

Konnerth A, Dreessen J, Augustine GJ (1992) Brief dendritic calcium signals initiate long-lasting synaptic depression in cerebellar Purkinje cells. Proceedings of the National Academy of Sciences 89:7051-7055.

Kornau H, Schenker L, Kennedy M, Seeburg P (1995) Domain interaction between NMDA receptor subunits and the postsynaptic density protein PSD-95. Science 269:1737-1740.

Kowalczyk S, Winkelmann A, Smolinsky B, Forstera B, Neundorf I, Schwarz G, Meier JC (2013) Direct binding of GABAA receptor beta2 and beta3 subunits to gephyrin. Eur J Neurosci 37:544-554.

Krawczun M, Jenkins E, Brown W (1985) Analysis of the fragile-X chromosome: localization and detection of the fragile site in high resolution preparations. Human genetics 69:209-211.

Krnjević K (2010) When and why amino acids? J Physiol 588:33-44.

Krnjević K, Schwartz S (1967) The action of γ-aminobutyric acid on cortical neurones. Experimental brain research 3:320-336.

Kshatri A, Cerrada A, Gimeno R, Bartolomé-Martín D, Rojas P, Giraldez T (2020) Differential regulation of BK channels by fragile X mental retardation protein. Journal of General Physiology 152.

Kuffler SW, Edwards C (1958) MECHANISM OF GAMMA AMINOBUTYRIC ACID (GABA) ACTION AND ITS RELATION TO SYNAPTIC INHIBITION. Journal of Neurophysiology 21:589-610.

Kullmann DM, Moreau AW, Bakiri Y, Nicholson E (2012) Plasticity of inhibition. Neuron 75:951-962.

Lachance-Touchette P, Brown P, Meloche C, Kinirons P, Lapointe L, Lacasse H, Lortie A, Carmant L, Bedford F, Bowie D, Cossette P (2011) Novel α1 and γ2 GABAA receptor subunit mutations in families with idiopathic generalized epilepsy. European Journal of Neuroscience 34:237-249.

Langley JN (1905) On the reaction of cells and of nerve-endings to certain poisons, chiefly as regards the reaction of striated muscle to nicotine and to curari. The Journal of Physiology 33:374-413.

Larson EA, Accardi MV, Wang Y, D'Antoni M, Karimi B, Siddiqui TJ, Bowie D (2020) Nitric oxide signaling strengthens inhibitory synapses of cerebellar molecular layer interneurons through a GABARAP-dependent mechanism. Journal of Neuroscience 40:3348-3359.

Laurie D, Wisden W, Seeburg P (1992a) The distribution of thirteen GABAA receptor subunit mRNAs in the rat brain. III. Embryonic and postnatal development. The Journal of Neuroscience 12:4151-4172.

Laurie D, Seeburg P, Wisden W (1992b) The distribution of 13 GABAA receptor subunit mRNAs in the rat brain. II. Olfactory bulb and cerebellum. The Journal of Neuroscience 12:1063-1076.

Laurie DJ, Seeburg PH, Wisden W (1992c) The distribution of 13 GABAA receptor subunit mRNAs in the rat brain. II. Olfactory bulb and cerebellum. J Neurosci 12:1063-1076.

Lavoie AM, Tingey JJ, Harrison NL, Pritchett DB, Twyman RE (1997) Activation and deactivation rates of recombinant GABA(A) receptor channels are dependent on alpha-subunit isoform. Biophysical Journal 73:2518-2526.

Lee B, Lee K, Panda S, Gonzales-Rojas R, Chong A, Bugay V, Park HM, Brenner R, Murthy N, Lee HY (2018) Nanoparticle delivery of CRISPR into the brain rescues a mouse model of fragile X syndrome from exaggerated repetitive behaviours. Nature Biomedical Engineering 2:497-507.

Lee DZ, Chung JM, Chung K, Kang M-G (2012) Reactive oxygen species (ROS) modulate AMPA receptor phosphorylation and cell-surface localization in concert with pain-related behavior. PAIN® 153:1905-1915.

Lee H-K, Kameyama K, Huganir RL, Bear MF (1998) NMDA Induces Long-Term Synaptic Depression and Dephosphorylation of the GluR1 Subunit of AMPA Receptors in Hippocampus. Neuron 21:1151-1162.

Lee H-K, Takamiya K, He K, Song L, Huganir RL (2010) Specific Roles of AMPA Receptor Subunit GluR1 (GluA1) Phosphorylation Sites in Regulating Synaptic Plasticity in the CA1 Region of Hippocampus. Journal of Neurophysiology 103:479-489.

Lee H-K, Takamiya K, Han J-S, Man H, Kim C-H, Rumbaugh G, Yu S, Ding L, He C, Petralia RS (2003) Phosphorylation of the AMPA receptor GluR1 subunit is required for synaptic plasticity and retention of spatial memory. Cell 112:631-643.

Lee WY, Sine SM (2005) Principal pathway coupling agonist binding to channel gating in nicotinic receptors. Nature 438:243-247.

Leonard AS, Davare MA, Horne MC, Garner CC, Hell JW (1998) SAP97 Is Associated with the α-Amino-3-hydroxy-5-methylisoxazole-4-propionic Acid Receptor GluR1 Subunit. Journal of Biological Chemistry 273:19518-19524.

Leonard AS, Lim IA, Hemsworth DE, Horne MC, Hell JW (1999) Calcium/calmodulin-dependent protein kinase II is associated with the N-methyl-D-aspartate receptor. Proceedings of the National Academy of Sciences 96:3239-3244.

Lester RA, Clements JD, Westbrook GL, Jahr CE (1990) Channel kinetics determine the time course of NMDA receptor-mediated synaptic currents. Nature 346:565-567.

Letts VA, Felix R, Biddlecome GH, Arikkath J, Mahaffey CL, Valenzuela A, Bartlett FS, Mori Y, Campbell KP, Frankel WN (1998) The mouse stargazer gene encodes a neuronal Ca2+-channel γ subunit. Nature Genetics 19:340-347.

Lev-Ram V, Wong ST, Storm DR, Tsien RY (2002) A new form of cerebellar long-term potentiation is postsynaptic and depends on nitric oxide but not cAMP. Proceedings of the National Academy of Sciences 99:8389-8393.

Lévi S, Logan SM, Tovar KR, Craig AM (2004) Gephyrin is critical for glycine receptor clustering but not for the formation of functional GABAergic synapses in hippocampal neurons. Journal of Neuroscience 24:207-217.

Li Z, Ji G, Neugebauer V (2011) Mitochondrial Reactive Oxygen Species Are Activated by mGluR5 through IP3 and Activate ERK and PKA to Increase Excitability of Amygdala Neurons and Pain Behavior. The Journal of Neuroscience 31:1114-1127.

Limperopoulos C, Bassan H, Gauvreau K, Robertson RL, Sullivan NR, Benson CB, Avery L, Stewart J, Soul JS, Ringer SA (2007) Does cerebellar injury in premature infants contribute to the high prevalence of long-term cognitive, learning, and behavioral disability in survivors? Pediatrics 120:584-593.

Lindauer U, Megow D, Matsuda H, Dirnagl U (1999) Nitric oxide: a modulator, but not a mediator, of neurovascular coupling in rat somatosensory cortex. American Journal of Physiology-Heart and Circulatory Physiology 277:H799-H811.

Linden D, Connor J (1991) Participation of postsynaptic PKC in cerebellar long-term depression in culture. Science 254:1656-1659.

Linden DJ, Dickinson MH, Smeyne M, Connor JA (1991) A long-term depression of AMPA currents in cultured cerebellar purkinje neurons. Neuron 7:81-89.

Lipton Jonathan O, Sahin M (2014) The Neurology of mTOR. Neuron 84:275-291.

Lisman J (1989) A mechanism for the Hebb and the anti-Hebb processes underlying learning and memory. Proceedings of the National Academy of Sciences 86:9574-9578.

Lisman JE, Goldring MA (1988) Feasibility of long-term storage of graded information by the Ca2+/calmodulin-dependent protein kinase molecules of the postsynaptic density. Proceedings of the National Academy of Sciences 85:5320-5324.

Liu J, Chang L, Song Y, Li H, Wu Y (2019) The Role of NMDA Receptors in Alzheimer's Disease. Front Neurosci 13:43.

Liu S-QJ, Cull-Candy SG (2000) Synaptic activity at calcium-permeable AMPA receptors induces a switch in receptor subtype. Nature 405:454-458.

Liu S, Xu L, Guan F, Liu Y-T, Cui Y, Zhang Q, Zheng X, Bi G-Q, Zhou ZH, Zhang X, Ye S (2018a) Cryo-EM structure of the human α5β3 GABAA receptor. Cell Research 28:958-961.

Liu SJ, Cull-Candy SG (2002) Activity-Dependent Change in AMPA Receptor Properties in Cerebellar Stellate Cells. The Journal of Neuroscience 22:3881-3889.

Liu XS, Wu H, Krzisch M, Wu X, Graef J, Muffat J, Hnisz D, Li CH, Yuan B, Xu C, Li Y, Vershkov D, Cacace A, Young RA, Jaenisch R (2018b) Rescue of Fragile X Syndrome Neurons by DNA Methylation Editing of the FMR1 Gene. Cell 172:979-992.e976.

Liu Y, Savtchouk I, Acharjee S, Liu SJ (2011) Inhibition of Ca2+-activated large-conductance K+ channel activity alters synaptic AMPA receptor phenotype in mouse cerebellar stellate cells. Journal of Neurophysiology 106:144-152.

Lodge D (2009) The history of the pharmacology and cloning of ionotropic glutamate receptors and the development of idiosyncratic nomenclature. Neuropharmacology 56:6-21.

Loewi O (1921) Über humorale übertragbarkeit der Herznervenwirkung. Pflüger's Archiv für die gesamte Physiologie des Menschen und der Tiere 189:239-242.

Lomeli H, Mosbacher J, Melcher T, Hoger T, Geiger, Kuner T, Monyer H, Higuchi M, Bach A, Seeburg P (1994) Control of kinetic properties of AMPA receptor channels by nuclear RNA editing. Science 266:1709-1713.

Losonczy A, Magee JC (2006) Integrative Properties of Radial Oblique Dendrites in Hippocampal CA1 Pyramidal Neurons. Neuron 50:291-307.

Lozano R, Rosero CA, Hagerman RJ (2014a) Fragile X spectrum disorders. Intractable & rare diseases research 3:134-146.

Lozano R, Hare EB, Hagerman RJ (2014b) Modulation of the GABAergic pathway for the treatment of fragile X syndrome. Neuropsychiatr Dis Treat 10:1769-1779.

Lu W, Roche KW (2012) Posttranslational regulation of AMPA receptor trafficking and function. Current opinion in neurobiology 22:470-479.

Lu YF, Kandel ER, Hawkins RD (1999) Nitric oxide signaling contributes to late-phase LTP and CREB phosphorylation in the hippocampus. J Neurosci 19:10250-10261.

Lüddens H, Wisden W (1991) Function and pharmacology of multiple GABAA receptor subunits. Trends in pharmacological sciences 12:49-51.

Lummis SCR, L. Beene D, Harrison NJ, Lester HA, Dougherty DA (2005) A Cation-π Binding Interaction with a Tyrosine in the Binding Site of the GABAC Receptor. Chemistry & Biology 12:993-997.

Luo F, Südhof TC (2017) Synaptotagmin-7-Mediated Asynchronous Release Boosts High-Fidelity Synchronous Transmission at a Central Synapse. Neuron 94:826-839.e823.

Luscher B, Fuchs T, Kilpatrick CL (2011) GABAA receptor trafficking-mediated plasticity of inhibitory synapses. Neuron 70:385-409.

Lynch G, Larson J, Kelso S, Barrionuevo G, Schottler F (1983) Intracellular injections of EGTA block induction of hippocampal long-term potentiation. Nature 305:719-721.

MacDermott AB, Mayer ML, Westbrook GL, Smith SJ, Barker JL (1986) NMDA-receptor activation increases cytoplasmic calcium concentration in cultured spinal cord neurones. Nature 321:519-522.

Macdonald RL, Barker JL (1978) Different actions of anticonvulsant and anesthetic barbiturates revealed by use of cultured mammalian neurons. Science 200:775-777.

Macdonald RL, Rogers CJ, Twyman RE (1989) Kinetic properties of the GABAA receptor main conductance state of mouse spinal cord neurones in culture. The Journal of Physiology 410:479-499.

MacLean DM, Bowie D (2011) Transmembrane AMPA receptor regulatory protein regulation of competitive antagonism: a problem of interpretation. The Journal of Physiology 589:5383-5390.

Maconochie DJ, Zempel JM, Steinbach JH (1994) How quickly can GABAA receptors open? Neuron 12:61-71.

Magee JC (1998) Dendritic hyperpolarization-activated currents modify the integrative properties of hippocampal CA1 pyramidal neurons. Journal of Neuroscience 18:7613-7624.

Malenka R, Kauer J, Zucker R, Nicoll R (1988) Postsynaptic calcium is sufficient for potentiation of hippocampal synaptic transmission. Science 242:81-84.

Malenka RC, Bear MF (2004) LTP and LTD: an embarrassment of riches. Neuron 44:5-21.

Malenka RC, Kauer JA, Perkel DJ, Mauk MD, Kelly PT, Nicoll RA, Waxham MN (1989) An essential role for postsynaptic calmodulin and protein kinase activity in long-term potentiation. Nature 340:554-557.

Malinow R, Miller JP (1986) Postsynaptic hyperpolarization during conditioning reversibly blocks induction of long-term potentiation. Nature 320:529-530.

Mannaioni G, Marino MJ, Valenti O, Traynelis SF, Conn PJ (2001) Metabotropic Glutamate Receptors 1 and 5 Differentially Regulate CA1 Pyramidal Cell Function. The Journal of Neuroscience 21:5925-5934.

Mapelli J, Gandolfi D, Vilella A, Zoli M, Bigiani A (2016) Heterosynaptic GABAergic plasticity bidirectionally driven by the activity of pre- and postsynaptic NMDA receptors. Proc Natl Acad Sci U S A 113:9898-9903.

Mapelli L, Gagliano G, Soda T, Laforenza U, Moccia F, D'Angelo EU (2017) Granular Layer Neurons Control Cerebellar Neurovascular Coupling Through an NMDA Receptor/NO-Dependent System. J Neurosci 37:1340-1351.

Maric HM, Kasaragod VB, Hausrat TJ, Kneussel M, Tretter V, Stromgaard K, Schindelin H (2014) Molecular basis of the alternative recruitment of GABA(A) versus glycine receptors through gephyrin. Nat Commun 5:5767.

Marsden KC, Beattie JB, Friedenthal J, Carroll RC (2007) NMDA receptor activation potentiates inhibitory transmission through GABA receptor-associated protein-dependent exocytosis of GABA(A) receptors. J Neurosci 27:14326-14337.

Marsden KC, Shemesh A, Bayer KU, Carroll RC (2010) Selective translocation of Ca²⁺/calmodulin protein kinase IIα (CaMKIIα) to inhibitory synapses. Proceedings of the National Academy of Sciences 107:20559-20564.

Martin JP, Bell J (1943) A pedigree of mental defect showing sex-linkage. Journal of neurology and psychiatry 6:154.

Martina M, Royer S, Paré D (2001) Cell-Type-Specific GABA Responses and Chloride Homeostasis in the Cortex and Amygdala. Journal of Neurophysiology 86:2887-2895.

Masiulis S, Desai R, Uchański T, Serna Martin I, Laverty D, Karia D, Malinauskas T, Zivanov J, Pardon E, Kotecha A, Steyaert J, Miller KW, Aricescu AR (2019) GABAA receptor signalling mechanisms revealed by structural pharmacology. Nature 565:454-459.

Mathur BN, Capik NA, Alvarez VA, Lovinger DM (2011) Serotonin Induces Long-Term Depression at Corticostriatal Synapses. The Journal of Neuroscience 31:7402-7411.

Matsuda S, Mikawa S, Hirai H (1999) Phosphorylation of Serine-880 in GluR2 by Protein Kinase C Prevents Its C Terminus from Binding with Glutamate Receptor-Interacting Protein. Journal of Neurochemistry 73:1765-1768.

Mayer ML, Westbrook GL, Guthrie PB (1984) Voltage-dependent block by Mg 2+ of NMDA responses in spinal cord neurones. Nature 309:261-263.

McGee TP, Bats C, Farrant M, Cull-Candy SG (2015) Auxiliary Subunit GSG1L Acts to Suppress Calcium-Permeable AMPA Receptor Function. The Journal of Neuroscience 35:16171-16179.

McLaughlin BJ, Wood JG, Saito K, Barber R, Vaughn JE, Roberts E, Wu J-Y (1974) The fine structural localization of glutamate decarboxylase in synaptic terminals of rodent cerebellum. Brain research 76:377-391.

Meng Y, Zhang Y, Jia Z (2003) Synaptic Transmission and Plasticity in the Absence of AMPA Glutamate Receptor GluR2 and GluR3. Neuron 39:163-176.

Menuz K, Stroud RM, Nicoll RA, Hays FA (2007) TARP auxiliary subunits switch AMPA receptor antagonists into partial agonists. Science 318:815-817.

Michalon A, Sidorov M, Ballard TM, Ozmen L, Spooren W, Wettstein JG, Jaeschke G, Bear MF, Lindemann L (2012) Chronic pharmacological mGlu5 inhibition corrects fragile X in adult mice. Neuron 74:49-56.

Miller PS, Smart TG (2010) Binding, activation and modulation of Cys-loop receptors. Trends in Pharmacological Sciences 31:161-174.

Miller PS, Aricescu AR (2014) Crystal structure of a human GABAA receptor. Nature 512:270-275.

Miller SG, Kennedy MB (1986) Regulation of brain Type II Ca2+ calmodulin-dependent protein kinase by autophosphorylation: A Ca2+-triggered molecular switch. Cell 44:861-870.

Milnerwood AJ, Raymond LA (2010) Early synaptic pathophysiology in neurodegeneration: insights from Huntington's disease. Trends Neurosci 33:513-523.

Milstein AD, Zhou W, Karimzadegan S, Bredt DS, Nicoll RA (2007) TARP Subtypes Differentially and Dose-Dependently Control Synaptic AMPA Receptor Gating. Neuron 55:905-918.

Mittmann W, Koch U, Hausser M (2005) Feed-forward inhibition shapes the spike output of cerebellar Purkinje cells. J Physiol 563:369-378.

Molineux ML, Fernandez FR, Mehaffey WH, Turner RW (2005) A-Type and T-Type Currents Interact to Produce a Novel Spike Latency-Voltage Relationship in Cerebellar Stellate Cells. The Journal of Neuroscience 25:10863-10873.

Monday HR, Castillo PE (2017) Closing the gap: long-term presynaptic plasticity in brain function and disease. Current Opinion in Neurobiology 45:106-112.

Monteiro P, Feng G (2017) SHANK proteins: roles at the synapse and in autism spectrum disorder. Nature Reviews Neuroscience 18:147.

Moss SJ, Smart TG (1996) Modulation Of Amind Acid-Gated Ion Channels By Protein Phoshorlation. In: International review of neurobiology, pp 1-52: Elsevier.

Mothet J-P, Parent AT, Wolosker H, Brady RO, Linden DJ, Ferris CD, Rogawski MA, Snyder SH (2000) d-Serine is an endogenous ligand for the glycine site of the N-methyl-d-aspartate receptor. Proceedings of the National Academy of Sciences 97:4926-4931.

Moult PR, Gladding CM, Sanderson TM, Fitzjohn SM, Bashir ZI, Molnar E, Collingridge GL (2006) Tyrosine phosphatases regulate AMPA receptor trafficking during metabotropic glutamate receptor-mediated long-term depression. Journal of Neuroscience 26:2544-2554.

Muddashetty Ravi S, Nalavadi Vijayalaxmi C, Gross C, Yao X, Xing L, Laur O, Warren Stephen T, Bassell Gary J (2011) Reversible Inhibition of PSD-95 mRNA Translation by miR-125a, FMRP Phosphorylation, and mGluR Signaling. Molecular Cell 42:673-688.

Mukherjee J, Kretschmannova K, Gouzer G, Maric HM, Ramsden S, Tretter V, Harvey K, Davies PA, Triller A, Schindelin H, Moss SJ (2011) The residence time of GABA(A)Rs at inhibitory synapses is determined by direct binding of the receptor alpha1 subunit to gephyrin. J Neurosci 31:14677-14687.

Mulkey RM, Endo S, Shenolikar S, Malenka RC (1994) Involvement of a calcineurin/ inhibitor-1 phosphatase cascade in hippocampal long-term depression. Nature 369:486-488.

Musumeci SA, Bosco P, Calabrese G, Bakker C, De Sarro GB, Elia M, Ferri R, Oostra BA (2000) Audiogenic seizures susceptibility in transgenic mice with fragile X syndrome. Epilepsia 41:19-23.

Myoga MH, Beierlein M, Regehr WG (2009) Somatic spikes regulate dendritic signaling in small neurons in the absence of backpropagating action potentials. Journal of Neuroscience 29:7803-7814.

Myrick LK, Nakamoto-Kinoshita M, Lindor NM, Kirmani S, Cheng X, Warren ST (2014) Fragile X syndrome due to a missense mutation. European Journal of Human Genetics 22:1185-1189.

Myrick LK, Deng P-Y, Hashimoto H, Oh YM, Cho Y, Poidevin MJ, Suhl JA, Visootsak J, Cavalli V, Jin P, Cheng X, Warren ST, Klyachko VA (2015) Independent role for presynaptic FMRP revealed by an FMR1 missense mutation associated with intellectual disability and seizures. Proceedings of the National Academy of Sciences 112:949-956.

Nabavi S, Kessels HW, Alfonso S, Aow J, Fox R, Malinow R (2013) Metabotropic NMDA receptor function is required for NMDA receptor-dependent long-term depression. Proceedings of the National Academy of Sciences 110:4027-4032.

Nakahiro M, Arakawa O, Narahashi T, Ukai S, Kato Y, Nishinuma K, Nishimura T (1992) Dimethyl sulfoxide (DMSO) blocks GABA-induced current in rat dorsal root ganglion neurons. Neuroscience letters 138:5-8.

Nakamura Y, Darnieder LM, Deeb TZ, Moss SJ (2015) Regulation of GABAARs by phosphorylation. In: Advances in pharmacology, pp 97-146: Elsevier.

Napoli I, Mercaldo V, Boyl PP, Eleuteri B, Zalfa F, De Rubeis S, Di Marino D, Mohr E, Massimi M, Falconi M, Witke W, Costa-Mattioli M, Sonenberg N, Achsel T, Bagni C (2008) The Fragile X Syndrome Protein Represses Activity-Dependent Translation through CYFIP1, a New 4E-BP. Cell 134:1042-1054.

Nelson Sacha B, Valakh V (2015) Excitatory/Inhibitory Balance and Circuit Homeostasis in Autism Spectrum Disorders. Neuron 87:684-698.

Ngo-Anh TJ, Bloodgood BL, Lin M, Sabatini BL, Maylie J, Adelman JP (2005) SK channels and NMDA receptors form a Ca2+-mediated feedback loop in dendritic spines. Nature Neuroscience 8:642-649.

Nicoll RA (1988) The coupling of neurotransmitter receptors to ion channels in the brain. Science 241:545-551.

Nicoll RA (2017) A Brief History of Long-Term Potentiation. Neuron 93:281-290.

Nicoll RA, Schmitz D (2005) Synaptic plasticity at hippocampal mossy fibre synapses. Nature Reviews Neuroscience 6:863-876.

Nisticò R, Pignatelli M, Piccinin S, Mercuri NB, Collingridge G (2012) Targeting Synaptic Dysfunction in Alzheimer's Disease Therapy. Molecular Neurobiology 46:572-587.

Niswender CM, Conn PJ (2010) Metabotropic Glutamate Receptors: Physiology, Pharmacology, and Disease. Annual Review of Pharmacology and Toxicology 50:295-322.

Noebels J, Qiao X, Bronson R, Spencer C, Davisson M (1990) Stargazer: a new neurological mutant on chromosome 15 in the mouse with prolonged cortical seizures. Epilepsy research 7:129-135.

Nosyreva ED, Huber KM (2006) Metabotropic receptor-dependent long-term depression persists in the absence of protein synthesis in the mouse model of fragile X syndrome. Journal of neurophysiology 95:3291-3295.

Nowak L, Bregestovski P, Ascher P, Herbet A, Prochiantz A (1984) Magnesium gates glutamate-activated channels in mouse central neurones. Nature 307:462-465.

Nugent FS, Penick EC, Kauer JA (2007) Opioids block long-term potentiation of inhibitory synapses. Nature 446:1086-1090.

Nugent FS, Niehaus JL, Kauer JA (2009) PKG and PKA signaling in LTP at GABAergic synapses. Neuropsychopharmacology 34:1829-1842.

Nusser Z, Sieghart W, Somogyi P (1998) Segregation of Different GABA_A Receptors to Synaptic and Extrasynaptic Membranes of Cerebellar Granule Cells. The Journal of Neuroscience 18:1693-1703.

Nusser Z, Sieghart W, Stephenson F, Somogyi P (1996) The alpha 6 subunit of the GABAA receptor is concentrated in both inhibitory and excitatory synapses on cerebellar granule cells. The Journal of Neuroscience 16:103-114.

Nusser Z, Ahmad Z, Tretter V, Fuchs K, Wisden W, Sieghart W, Somogyi P (1999) Alterations in the expression of GABAA receptor subunits in cerebellar granule cells after the disruption of the α6 subunit gene. European Journal of Neuroscience 11:1685-1697.

O'Donnell WT, Warren ST (2002) A decade of molecular studies of fragile X syndrome. Annu Rev Neurosci 25:315-338.

Oliet SHR, Malenka RC, Nicoll RA (1997) Two Distinct Forms of Long-Term Depression Coexist in CA1 Hippocampal Pyramidal Cells. Neuron 18:969-982.

Olsen RW, DeLorey T (1999) GABA and glycine. Basic neurochemistry: molecular, cellular and medical aspects 6.

Olsen RW, Sieghart W (2008) International Union of Pharmacology. LXX. Subtypes of γ-Aminobutyric Acid_A Receptors: Classification on the Basis of Subunit Composition, Pharmacology, and Function. Update. Pharmacological Reviews 60:243-260.

Padgett CL, Hanek AP, Lester HA, Dougherty DA, Lummis SCR (2007) Unnatural Amino Acid Mutagenesis of the GABA_A Receptor Binding Site Residues Reveals a Novel Cation–π Interaction between GABA and β₂Tyr97. The Journal of Neuroscience 27:886-892.

Palay SL (1956) Synapses in the central nervous system. The Journal of biophysical and biochemical cytology 2:193.

Palay SL, Palade GE (1955) THE FINE STRUCTURE OF NEURONS. The Journal of Biophysical and Biochemical Cytology 1:69-88.

Palmer RMJ, Ferrige AG, Moncada S (1987) Nitric oxide release accounts for the biological activity of endothelium-derived relaxing factor. Nature 327:524-526.

Paluszkiewicz SM, Martin BS, Huntsman MM (2011) Fragile X syndrome: the GABAergic system and circuit dysfunction. Dev Neurosci 33:349-364.

Pan B, Hillard CJ, Liu Q-s (2008) Endocannabinoid Signaling Mediates Cocaine-Induced Inhibitory Synaptic Plasticity in Midbrain Dopamine Neurons. The Journal of Neuroscience 28:1385-1397.

Panzanelli P, Gunn BG, Schlatter MC, Benke D, Tyagarajan SK, Scheiffele P, Belelli D, Lambert JJ, Rudolph U, Fritschy JM (2011) Distinct mechanisms regulate GABAA receptor and gephyrin clustering at perisomatic and axo-axonic synapses on CA1 pyramidal cells. J Physiol 589:4959-4980.

Paoletti P, Bellone C, Zhou Q (2013a) NMDA receptor subunit diversity: impact on receptor properties, synaptic plasticity and disease. Nat Rev Neurosci 14:383-400.

Paoletti P, Bellone C, Zhou Q (2013b) NMDA receptor subunit diversity: impact on receptor properties, synaptic plasticity and disease. Nature Reviews Neuroscience 14:383-400.

Paraskevopoulou F, Herman MA, Rosenmund C (2019) Glutamatergic Innervation onto Striatal Neurons Potentiates GABAergic Synaptic Output. J Neurosci 39:4448-4460.

Parenti I, Rabaneda LG, Schoen H, Novarino G (2020) Neurodevelopmental Disorders: From Genetics to Functional Pathways. Trends in Neurosciences 43:608-621.

Partin KM, Fleck MW, Mayer ML (1996) AMPA Receptor Flip/Flop Mutants Affecting Deactivation, Desensitization, and Modulation by Cyclothiazide, Aniracetam, and Thiocyanate. The Journal of Neuroscience 16:6634-6647.

Pelkey KA, Chittajallu R, Craig MT, Tricoire L, Wester JC, McBain CJ (2017) Hippocampal GABAergic Inhibitory Interneurons. Physiological Reviews 97:1619-1747.

Penagarikano O, Mulle JG, Warren ST (2007) The Pathophysiology of Fragile X Syndrome. Annual Review of Genomics and Human Genetics 8:109-129.

Penna A, Wang D-S, Yu J, Lecker I, Brown PMGE, Bowie D, Orser BA (2014) Hydrogen Peroxide Increases GABA_A Receptor-Mediated Tonic Current in Hippocampal Neurons. The Journal of Neuroscience 34:10624-10634.

Peter S, ten Brinke MM, Stedehouder J, Reinelt CM, Wu B, Zhou H, Zhou K, Boele H-J, Kushner SA, Lee MG, Schmeisser MJ, Boeckers TM, Schonewille M, Hoebeek FE, De Zeeuw CI (2016) Dysfunctional cerebellar Purkinje cells contribute to autism-like behaviour in Shank2-deficient mice. Nature Communications 7:12627.

Petrini EM, Barberis A (2014) Diffusion dynamics of synaptic molecules during inhibitory postsynaptic plasticity. Front Cell Neurosci 8:300.

Petrini EM, Nieus T, Ravasenga T, Succol F, Guazzi S, Benfenati F, Barberis A (2011) Influence of GABAAR monoliganded states on GABAergic responses. Journal of Neuroscience 31:1752-1761.

Petrini EM, Ravasenga T, Hausrat TJ, Iurilli G, Olcese U, Racine V, Sibarita J-B, Jacob TC, Moss SJ, Benfenati F, Medini P, Kneussel M, Barberis A (2014) Synaptic recruitment of gephyrin regulates surface GABAA receptor dynamics for the expression of inhibitory LTP. Nature Communications 5:3921.

Phillips C (1959) Actions of antidromic pyramidal volleys on single Betz cells in the cat. Quarterly Journal of Experimental Physiology and Cognate Medical Sciences: Translation and Integration 44:1-25.

Phulera S, Zhu H, Yu J, Claxton DP, Yoder N, Yoshioka C, Gouaux E (2018) Cryo-EM structure of the benzodiazepine-sensitive α1β1γ2S tri-heteromeric GABAA receptor in complex with GABA. Elife 7:e39383.

Pieretti M, Zhang F, Fu Y-H, Warren ST, Oostra BA, Caskey CT, Nelson DL (1991) Absence of expression of the FMR-1 gene in fragile X syndrome. Cell 66:817-822.

Pinheiro PS, Mulle C (2008) Presynaptic glutamate receptors: physiological functions and mechanisms of action. Nature Reviews Neuroscience 9:423-436.

Poulter M, Barker J, O'carroll A, Lolait S, Mahan L (1992) Differential and transient expression of GABAA receptor alpha-subunit mRNAs in the developing rat CNS. Journal of Neuroscience 12:2888-2900.

Pribiag H, Peng H, Shah WA, Stellwagen D, Carbonetto S (2014) Dystroglycan mediates homeostatic synaptic plasticity at GABAergic synapses. Proc Natl Acad Sci U S A 111:6810-6815.

Priel A, Kolleker A, Ayalon G, Gillor M, Osten P, Stern-Bach Y (2005) Stargazin Reduces Desensitization and Slows Deactivation of the AMPA-Type Glutamate Receptors. The Journal of Neuroscience 25:2682-2686.

Puia G, Santi M, Vicini S, Pritchett DB, Purdy RH, Paul SM, Seeburg PH, Costa E (1990) Neurosteroids act on recombinant human GABAA receptors. Neuron 4:759-765.

Qiu D-l, Knöpfel T (2007) An NMDA Receptor/Nitric Oxide Cascade in Presynaptic Parallel Fiber–Purkinje Neuron Long-Term Potentiation. The Journal of Neuroscience 27:3408-3415.

Rajaratnam A, Shergill J, Salcedo-Arellano M, Saldarriaga W, Duan X, Hagerman R (2017) Fragile X syndrome and fragile X-associated disorders. F1000Res 6:2112-2112.

Ramaswami G, Geschwind DH (2018) Chapter 21 - Genetics of autism spectrum disorder. In: Handbook of Clinical Neurology (Geschwind DH, Paulson HL, Klein C, eds), pp 321-329: Elsevier.

Ramon y Cajal S (1911) Histologie du système nerveux de l'homme et des vertébrés. Maloine, Paris 2:153-173.

Ramos A, Hollingworth D, Adinolfi S, Castets M, Kelly G, Frenkiel TA, Bardoni B, Pastore A (2006) The Structure of the N-Terminal Domain of the Fragile X Mental Retardation Protein: A Platform for Protein-Protein Interaction. Structure 14:21-31.

Rancillac A, Crépel F (2004) Synapses between parallel fibres and stellate cells express long-term changes in synaptic efficacy in rat cerebellum. The Journal of Physiology 554:707-720.

Rancillac A, Rossier J, Guille M, Tong XK, Geoffroy H, Amatore C, Arbault S, Hamel E, Cauli B (2006) Glutamatergic Control of Microvascular Tone by Distinct GABA Neurons in the Cerebellum. J Neurosci 26:6997-7006.

Rancz EA, Ishikawa T, Duguid I, Chadderton P, Mahon S, Hausser M (2007) High-fidelity transmission of sensory information by single cerebellar mossy fibre boutons. Nature 450:1245-1248.

Rasband MN (2010) The axon initial segment and the maintenance of neuronal polarity. Nature Reviews Neuroscience 11:552-562.

Regehr WG (2012) Short-Term Presynaptic Plasticity. Cold Spring Harbor Perspectives in Biology 4.

Reis SA, Willemsen R, van Unen L, Hoogeveen AT, Oostra BA (2004) Prospects of TAT-Mediated Protein Therapy for Fragile X Syndrome. Journal of Molecular Histology 35:389-395.

Reiss AL, Abrams MT, Greenlaw R, Freund L, Denckla MB (1995) Neurodevelopmental effects of the FMR-1 full mutation in humans. Nature Medicine 1:159-167.

Reith RM, McKenna J, Wu H, Hashmi SS, Cho S-H, Dash PK, Gambello MJ (2013) Loss of Tsc2 in Purkinje cells is associated with autistic-like behavior in a mouse model of tuberous sclerosis complex. Neurobiology of Disease 51:93-103.

Renner MC, Albers EH, Gutierrez-Castellanos N, Reinders NR, van Huijstee AN, Xiong H, Lodder TR, Kessels HW (2017) Synaptic plasticity through activation of GluA3-containing AMPA-receptors. Elife 6:e25462.

Reynolds IJ, Hastings TG (1995) Glutamate induces the production of reactive oxygen species in cultured forebrain neurons following NMDA receptor activation. J Neurosci 15:3318-3327.

Richter JD, Bassell GJ, Klann E (2015) Dysregulation and restoration of translational homeostasis in fragile X syndrome. Nature Reviews Neuroscience 16:595-605.

Rieubland S, Roth A, Häusser M (2014) Structured Connectivity in Cerebellar Inhibitory Networks. Neuron 81:913-929.

Rivera C, Voipio J, Payne JA, Ruusuvuori E, Lahtinen H, Lamsa K, Pirvola U, Saarma M, Kaila K (1999) The K+/Cl− co-transporter KCC2 renders GABA hyperpolarizing during neuronal maturation. Nature 397:251-255.

Roberts E, Frankel S (1950) gamma-Aminobutyric acid in brain: its formation from glutamic acid. J Biol Chem 187:55-63.

Roberts PJ (1974) Amino acid release from isolated rat dorsal root ganglia. Brain Res 74:327-332.

Rodrigo J, Springall DR, Uttenthal O, Bentura ML, Abadia-Molina F, Riveros-Moreno V, Martinez-Murillo R, Polak JM, Moncada S (1994) Localization of nitric oxide synthase in the adult rat brain. Philos Trans R Soc Lond B Biol Sci 345:175-221.

Rotschafer S, Razak K (2013) Altered auditory processing in a mouse model of fragile X syndrome. Brain Research 1506:12-24.

Routh BN, Johnston D, Brager DH (2013) Loss of Functional A-Type Potassium Channels in the Dendrites of CA1 Pyramidal Neurons from a Mouse Model of Fragile X Syndrome. The Journal of Neuroscience 33:19442-19450.

Roux L, Buzsáki G (2015) Tasks for inhibitory interneurons in intact brain circuits. Neuropharmacology 88:10-23.

Rowan MJM, Bonnan A, Zhang K, Amat SB, Kikuchi C, Taniguchi H, Augustine GJ, Christie JM (2018) Graded Control of Climbing-Fiber-Mediated Plasticity and Learning by Inhibition in the Cerebellum. Neuron 99:999-1015.e1016.

Rubenstein J, Merzenich MM (2003) Model of autism: increased ratio of excitation/inhibition in key neural systems. Genes, Brain and Behavior 2:255-267.

Rudelli R, Brown W, Wisniewski K, Jenkins E, Laure-Kamionowska M, Connell F, Wisniewski H (1985) Adult fragile X syndrome. Acta neuropathologica 67:289-295.

Rudolph U, Mohler H (2014) GABAA receptor subtypes: Therapeutic potential in Down syndrome, affective disorders, schizophrenia, and autism. Annu Rev Pharmacol Toxicol 54:483-507.

Rudy B, Fishell G, Lee S, Hjerling-Leffler J (2011) Three groups of interneurons account for nearly 100% of neocortical GABAergic neurons. Developmental neurobiology 71:45-61.

Rutherford LC, Nelson SB, Turrigiano GG (1998) BDNF Has Opposite Effects on the Quantal Amplitude of Pyramidal Neuron and Interneuron Excitatory Synapses. Neuron 21:521-530.

Saal D, Dong Y, Bonci A, Malenka RC (2003) Drugs of Abuse and Stress Trigger a Common Synaptic Adaptation in Dopamine Neurons. Neuron 37:577-582.

Sabatini BL, Regehr WG (1996) Timing of neurotransmission at fast synapses in the mammalian brain. Nature 384:170-172.

Sagher O, Zhang X-Q, Szeto W, Thai QA, Jin Y, Kassell NF, Lee KS (1993) Live Computerized Videomicroscopy of Cerebral Microvessels in Brain Slices. Journal of Cerebral Blood Flow & Metabolism 13:676-682.

Sah P, Hestrin S, Nicoll R (1990) Properties of excitatory postsynaptic currents recorded in vitro from rat hippocampal interneurones. The Journal of Physiology 430:605-616.

Sakmann B, Hamill OP, Bormann J (1983) Patch-clamp measurements of elementary chloride currents activated by the putative inhibitory transmitter GABA and glycine in mammalian spinal neurons. Journal of neural transmission Supplementum 18:83-95.

Sakurai M (1990) Calcium is an intracellular mediator of the climbing fiber in induction of cerebellar long-term depression. Proceedings of the National Academy of Sciences 87:3383-3385.

Salin PA, Malenka RC, Nicoll RA (1996) Cyclic AMP mediates a presynaptic form of LTP at cerebellar parallel fiber synapses. Neuron 16:797-803.

Sanderson JL, Gorski JA, Dell'Acqua ML (2016) NMDA receptor-dependent LTD requires transient synaptic incorporation of Ca2+-permeable AMPARs mediated by AKAP150-anchored PKA and calcineurin. Neuron 89:1000-1015.

Sanhueza M, Lisman J (2013) The CaMKII/NMDAR complex as a molecular memory. Mol Brain 6:10.

Santoro MR, Bray SM, Warren ST (2012) Molecular Mechanisms of Fragile X Syndrome: A Twenty-Year Perspective. Annual Review of Pathology: Mechanisms of Disease 7:219-245.

Saré RM, Harkless L, Levine M, Torossian A, Sheeler CA, Smith CB (2017) Deficient Sleep in Mouse Models of Fragile X Syndrome. Frontiers in Molecular Neuroscience 10.

Sathyanesan A, Zhou J, Scafidi J, Heck DH, Sillitoe RV, Gallo V (2019) Emerging connections between cerebellar development, behaviour and complex brain disorders. Nature Reviews Neuroscience 20:298-313.

Saviane C, Silver RA (2006) Fast vesicle reloading and a large pool sustain high bandwidth transmission at a central synapse. Nature 439:983-987.

Scharf SH, Jaeschke G, Wettstein JG, Lindemann L (2015) Metabotropic glutamate receptor 5 as drug target for Fragile X syndrome. Curr Opin Pharmacol 20:124-134.

Schmahmann JD, Sherman JC (1998) The cerebellar cognitive affective syndrome. Brain 121:561-579.

Schmahmann JD, Guell X, Stoodley CJ, Halko MA (2019) The Theory and Neuroscience of Cerebellar Cognition. Annual Review of Neuroscience 42:337-364.

Schneggenburger R (1996) Simultaneous measurement of Ca2+ influx and reversal potentials in recombinant N-methyl-D-aspartate receptor channels. Biophysical journal 70:2165-2174.

Schnell E, Sizemore M, Karimzadegan S, Chen L, Bredt DS, Nicoll RA (2002) Direct interactions between PSD-95 and stargazin control synaptic AMPA receptor number. Proceedings of the National Academy of Sciences 99:13902-13907.

Schwarze SR, Ho A, Vocero-Akbani A, Dowdy SF (1999) In Vivo Protein Transduction: Delivery of a Biologically Active Protein into the Mouse. Science 285:1569-1572.

Schwenk J, Harmel N, Zolles G, Bildl W, Kulik A, Heimrich B, Chisaka O, Jonas P, Schulte U, Fakler B (2009) Functional proteomics identify cornichon proteins as auxiliary subunits of AMPA receptors. Science 323:1313-1319.

Semyanov A, Walker MC, Kullmann DM, Silver RA (2004) Tonically active GABAA receptors: modulating gain and maintaining the tone. Trends in Neurosciences 27:262-269.

Serulle Y, Zhang S, Ninan I, Puzzo D, McCarthy M, Khatri L, Arancio O, Ziff EB (2007) A GluR1-cGKII interaction regulates AMPA receptor trafficking. Neuron 56:670-688.

Shanks Natalie F, Savas Jeffrey N, Maruo T, Cais O, Hirao A, Oe S, Ghosh A, Noda Y, Greger Ingo H, Yates John R, Nakagawa T (2012) Differences in AMPA and Kainate Receptor Interactomes Facilitate Identification of AMPA Receptor Auxiliary Subunit GSG1L. Cell Reports 1:590-598.

Sharma A, Hoeffer CA, Takayasu Y, Miyawaki T, McBride SM, Klann E, Zukin RS (2010) Dysregulation of mTOR Signaling in Fragile X Syndrome. The Journal of Neuroscience 30:694-702.

Sheng M, Sala C (2001) PDZ Domains and the Organization of Supramolecular Complexes. Annual Review of Neuroscience 24:1-29.

Sheng M, Kim E (2011) The postsynaptic organization of synapses. Cold Spring Harbor perspectives in biology 3:a005678.

Sheng M, Sabatini BL, Südhof TC (2012) Synapses and Alzheimer's Disease. Cold Spring Harbor Perspectives in Biology 4.

Shepherd JD, Rumbaugh G, Wu J, Chowdhury S, Plath N, Kuhl D, Huganir RL, Worley PF (2006) Arc/Arg3.1 Mediates Homeostatic Synaptic Scaling of AMPA Receptors. Neuron 52:475-484.

Sherrington CS (1906) The integrative action of the nervous system. CT US: Yale University Press.

Shigemoto R, Abe T, Nomura S, Nakanishi S, Hirano T (1994) Antibodies inactivating mGluR1 metabotropic glutamate receptor block long-term depression in cultured Purkinje cells. Neuron 12:1245-1255.

Sigel E, Steinmann ME (2012) Structure, Function, and Modulation of GABAA Receptors. Journal of Biological Chemistry 287:40224-40231.

Silva-Santos S, Van Woerden GM, Bruinsma CF, Mientjes E, Jolfaei MA, Distel B, Kushner SA, Elgersma Y (2015) Ube3a reinstatement identifies distinct developmental windows in a murine Angelman syndrome model. The Journal of clinical investigation 125:2069-2076.

Silverman W, Lubin R, Jenkins EC, Brown WT (1983) The strength of association between fragile(X) chromosome presence and mental retardation. Clinical Genetics 23:436-440.

Simon J, Wakimoto H, Fujita N, Lalande M, Barnard EA (2004) Analysis of the Set of GABAA Receptor Genes in the Human Genome. Journal of Biological Chemistry 279:41422-41435.

Siomi H, Siomi MC, Nussbaum RL, Dreyfuss G (1993) The protein product of the fragile X gene, FMR1, has characteristics of an RNA-binding protein. Cell 74:291-298.

Sitzmann AF, Hagelstrom RT, Tassone F, Hagerman RJ, Butler MG (2018) Rare FMR1 gene mutations causing fragile X syndrome: A review. American Journal of Medical Genetics Part A 176:11-18.

Sivakumaran S, Mohajerani MH, Cherubini E (2009) At Immature Mossy-Fiber–CA3 Synapses, Correlated Presynaptic and Postsynaptic Activity Persistently Enhances GABA Release and Network Excitability via BDNF and cAMP-Dependent PKA. The Journal of Neuroscience 29:2637-2647.

Sjöström PJ, Turrigiano GG, Nelson SB (2003) Neocortical LTD via Coincident Activation of Presynaptic NMDA and Cannabinoid Receptors. Neuron 39:641-654.

Skefos J, Cummings C, Enzer K, Holiday J, Weed K, Levy E, Yuce T, Kemper T, Bauman M (2014) Regional alterations in purkinje cell density in patients with autism. PloS one 9:e81255.

Smith GB, Olsen RW (1995) Functional domains of GABAA receptors. Trends in Pharmacological Sciences 16:162-168.

Sobolevsky AI, Rosconi MP, Gouaux E (2009) X-ray structure, symmetry and mechanism of an AMPA-subtype glutamate receptor. Nature 462:745-756.

Soghomonian J-J, Martin DL (1998) Two isoforms of glutamate decarboxylase: why? Trends in pharmacological sciences 19:500-505.

Sommer B, Köhler M, Sprengel R, Seeburg PH (1991) RNA editing in brain controls a determinant of ion flow in glutamate-gated channels. Cell 67:11-19.

Sommer B, Keinanen K, Verdoorn TA, Wisden W, Burnashev N, Herb A, Kohler M, Takagi T, Sakmann B, Seeburg PH (1990) Flip and flop: a cell-specific functional switch in glutamate-operated channels of the CNS. Science 249:1580-1585.

Sotelo C (2003) Viewing the brain through the master hand of Ramon y Cajal. Nature Reviews Neuroscience 4:71-77.

Sotelo C (2020) The History of the Synapse. The Anatomical Record 303:1252-1279.

Soto D, Coombs ID, Kelly L, Farrant M, Cull-Candy SG (2007) Stargazin attenuates intracellular polyamine block of calcium-permeable AMPA receptors. Nature neuroscience 10:1260-1267.

Soto D, Coombs ID, Gratacos-Batlle E, Farrant M, Cull-Candy SG (2014) Molecular mechanisms contributing to TARP regulation of channel conductance and polyamine block of calcium-permeable AMPA receptors. Journal of Neuroscience 34:11673-11683.

Soto D, Coombs ID, Renzi M, Zonouzi M, Farrant M, Cull-Candy SG (2009) Selective regulation of long-form calcium-permeable AMPA receptors by an atypical TARP, γ-5. Nature neuroscience 12:277.

Southam E, Garthwaite J (1993) The nitric oxide-cyclic GMP signalling pathway in rat brain. Neuropharmacology 32:1267-1277.

Southam E, East SJ, Garthwaite J (1991) Excitatory amino acid receptors coupled to the nitric oxide/cyclic GMP pathway in rat cerebellum during development. J Neurochem 56:2072-2081.

Spruston N, Johnston D (1992) Perforated patch-clamp analysis of the passive membrane properties of three classes of hippocampal neurons. Journal of Neurophysiology 67:508-529.

Spruston N, Jaffe DB, Johnston D (1994) Dendritic attenuation of synaptic potentials and currents: the role of passive membrane properties. Trends in Neurosciences 17:161-166.

Staubli U, Lynch G (1990) Stable depression of potentiated synaptic responses in the hippocampus with 1–5 Hz stimulation. Brain research 513:113-118.

Stefanis C, Jasper H (1964) Recurrent collateral inhibition in pyramidal tract neurons. Journal of Neurophysiology 27:855-877.

Stein IS, Gray JA, Zito K (2015) Non-Ionotropic NMDA Receptor Signaling Drives Activity-Induced Dendritic Spine Shrinkage. The Journal of Neuroscience 35:12303-12308.

Steinberg JP, Takamiya K, Shen Y, Xia J, Rubio ME, Yu S, Jin W, Thomas GM, Linden DJ, Huganir RL (2006) Targeted in vivo mutations of the AMPA receptor subunit GluR2 and its interacting protein PICK1 eliminate cerebellar long-term depression. Neuron 49:845-860.

Steinert JR, Chernova T, Forsythe ID (2010) Nitric oxide signaling in brain function, dysfunction, and dementia. Neuroscientist 16:435-452.

Stellwagen D, Malenka RC (2006) Synaptic scaling mediated by glial TNF-α. Nature 440:1054-1059.

Stoodley CJ, Schmahmann JD (2009) Functional topography in the human cerebellum: a meta-analysis of neuroimaging studies. Neuroimage 44:489-501.

Strauss KA, Puffenberger EG, Huentelman MJ, Gottlieb S, Dobrin SE, Parod JM, Stephan DA, Morton DH (2006) Recessive symptomatic focal epilepsy and mutant contactin-associated protein-like 2. New England Journal of Medicine 354:1370-1377.

Streng ML, Krook-Magnuson E (2020) The cerebellum and epilepsy. Epilepsy & Behavior:106909.

Strumbos JG, Brown MR, Kronengold J, Polley DB, Kaczmarek LK (2010) Fragile X Mental Retardation Protein Is Required for Rapid Experience-Dependent Regulation of the Potassium Channel Kv3.1b. The Journal of Neuroscience 30:10263-10271.

Stuart G, Sakmann B (1995) Amplification of EPSPs by axosomatic sodium channels in neocortical pyramidal neurons. Neuron 15:1065-1076.

Stuart G, Spruston N (1998) Determinants of voltage attenuation in neocortical pyramidal neuron dendrites. Journal of Neuroscience 18:3501-3510.

Stuart G, Spruston N, Häusser M (2016) Dendrites. In, Third edition. Edition. Oxford, UK: Oxford University Press.

Südhof Thomas C (2012) The Presynaptic Active Zone. Neuron 75:11-25.

Südhof TC (2018) Towards an Understanding of Synapse Formation. Neuron 100:276-293.

Sun Q, Srinivas KV, Sotayo A, Siegelbaum SA (2014) Dendritic Na+ spikes enable cortical input to drive action potential output from hippocampal CA2 pyramidal neurons. Elife 3:e04551.

Sur C, Wafford KA, Reynolds DS, Hadingham KL, Bromidge F, Macaulay A, Collinson N, O'Meara G, Howell O, Newman R (2001) Loss of the major GABAA receptor subtype in the brain is not lethal in mice. Journal of Neuroscience 21:3409-3418.

Sutton RB, Fasshauer D, Jahn R, Brunger AT (1998) Crystal structure of a SNARE complex involved in synaptic exocytosis at 2.4 Å resolution. Nature 395:347-353.

Suvrathan A, Payne HL, Raymond JL (2016) Timing Rules for Synaptic Plasticity Matched to Behavioral Function. Neuron 92:959-967.

Suvrathan A, Hoeffer CA, Wong H, Klann E, Chattarji S (2010) Characterization and reversal of synaptic defects in the amygdala in a mouse model of fragile X syndrome. Proc Natl Acad Sci U S A 107:11591-11596.

Swanson MR, Wolff JJ, Shen MD, Styner M, Estes A, Gerig G, McKinstry RC, Botteron KN, Piven J, Hazlett HC (2018) Development of white matter circuitry in infants with fragile X syndrome. JAMA psychiatry 75:505-513.

Szapiro G, Barbour B (2007) Multiple climbing fibers signal to molecular layer interneurons exclusively via glutamate spillover. Nat Neurosci 10:735-742.

Takamiya K, Mao L, Huganir RL, Linden DJ (2008) The glutamate receptor-interacting protein family of GluR2-binding proteins is required for long-term synaptic depression expression in cerebellar Purkinje cells. Journal of Neuroscience 28:5752-5755.

Takeuchi A, Takeuchi N (1969) A study of the action of picrotoxin on the inhibitory neuromuscular junction of the crayfish. The Journal of physiology 205:377-391.

Terrier J, Lüscher C, Pascoli V (2016) Cell-Type Specific Insertion of GluA2-Lacking AMPARs with Cocaine Exposure Leading to Sensitization, Cue-Induced Seeking, and Incubation of Craving. Neuropsychopharmacology 41:1779-1789.

Thomas MJ, Malenka RC (2003) Synaptic plasticity in the mesolimbic dopamine system. Philosophical Transactions of the Royal Society of London Series B: Biological Sciences 358:815-819.

Tian N, Petersen C, Kash S, Baekkeskov S, Copenhagen D, Nicoll R (1999) The role of the synthetic enzyme GAD65 in the control of neuronal γ-aminobutyric acid release. Proceedings of the National Academy of Sciences 96:12911-12916.

Todd PK, Mack KJ, Malter JS (2003) The fragile X mental retardation protein is required for type-I metabotropic glutamate receptor-dependent translation of PSD-95. Proceedings of the National Academy of Sciences 100:14374-14378.

Toft AKH, Lundbye CJ, Banke TG (2016) Dysregulated NMDA-receptor signaling inhibits long-term depression in a mouse model of fragile X syndrome. Journal of Neuroscience 36:9817-9827.

Tomita S, Chen L, Kawasaki Y, Petralia RS, Wenthold RJ, Nicoll RA, Bredt DS (2003) Functional studies and distribution define a family of transmembrane AMPA receptor regulatory proteins. Journal of Cell Biology 161:805-816.

Tomita S, Adesnik H, Sekiguchi M, Zhang W, Wada K, Howe JR, Nicoll RA, Bredt DS (2005) Stargazin modulates AMPA receptor gating and trafficking by distinct domains. Nature 435:1052-1058.

Toussay X, Basu K, Lacoste B, Hamel E (2013) Locus Coeruleus Stimulation Recruits a Broad Cortical Neuronal Network and Increases Cortical Perfusion. The Journal of Neuroscience 33:3390-3401.

Traynelis SF, Wollmuth LP, McBain CJ, Menniti FS, Vance KM, Ogden KK, Hansen KB, Yuan H, Myers SJ, Dingledine R (2010) Glutamate Receptor Ion Channels: Structure, Regulation, and Function. Pharmacological Reviews 62:405-496.

Tretter V, Jacob TC, Mukherjee J, Fritschy JM, Pangalos MN, Moss SJ (2008) The clustering of GABA(A) receptor subtypes at inhibitory synapses is facilitated via the direct binding of receptor alpha 2 subunits to gephyrin. J Neurosci 28:1356-1365.

Tretter V, Mukherjee J, Maric H, Schindelin H, Sieghart W, Moss S (2012) Gephyrin, the enigmatic organizer at GABAergic synapses. Frontiers in Cellular Neuroscience 6.

Tretter V, Kerschner B, Milenkovic I, Ramsden SL, Ramerstorfer J, Saiepour L, Maric H-M, Moss SJ, Schindelin H, Harvey RJ, Sieghart W, Harvey K (2011) Molecular Basis of the γ-Aminobutyric Acid A Receptor α3 Subunit Interaction with the Clustering Protein Gephyrin. Journal of Biological Chemistry 286:37702-37711.

Trigiani LJ, Royea J, Tong X-K, Hamel E (2019) Comparative benefits of simvastatin and exercise in a mouse model of vascular cognitive impairment and dementia. The FASEB Journal 33:13280-13293.

Triller A, Choquet D (2008) New concepts in synaptic biology derived from single-molecule imaging. Neuron 59:359-374.

Tsai NP, Wilkerson JR, Guo W, Maksimova MA, DeMartino GN, Cowan CW, Huber KM (2012) Multiple autism-linked genes mediate synapse elimination via proteasomal degradation of a synaptic scaffold PSD-95. Cell 151:1581-1594.

Turecek J, Regehr WG (2018) Synaptotagmin 7 Mediates Both Facilitation and Asynchronous Release at Granule Cell Synapses. The Journal of Neuroscience 38:3240-3251.

Turecek J, Jackman SL, Regehr WG (2017) Synaptotagmin 7 confers frequency invariance onto specialized depressing synapses. Nature 551:503-506.

Turrigiano GG (2008) The Self-Tuning Neuron: Synaptic Scaling of Excitatory Synapses. Cell 135:422-435.

Turrigiano GG, Leslie KR, Desai NS, Rutherford LC, Nelson SB (1998) Activity-dependent scaling of quantal amplitude in neocortical neurons. Nature 391:892-896.

Twomey EC, Yelshanskaya MV, Grassucci RA, Frank J, Sobolevsky AI (2016) Elucidation of AMPA receptor–stargazin complexes by cryo–electron microscopy. Science 353:83-86.

Tyagarajan SK, Fritschy J-M (2014) Gephyrin: a master regulator of neuronal function? Nature Reviews Neuroscience 15:141-156.

Tyagarajan SK, Ghosh H, Yévenes GE, Imanishi SY, Zeilhofer HU, Gerrits B, Fritschy J-M (2013) Extracellular Signal-regulated Kinase and Glycogen Synthase Kinase 3β Regulate Gephyrin Postsynaptic Aggregation and GABAergic Synaptic Function in a Calpain-dependent Mechanism. Journal of Biological Chemistry 288:9634-9647.

Tyagarajan SK, Ghosh H, Yévenes GE, Nikonenko I, Ebeling C, Schwerdel C, Sidler C, Zeilhofer HU, Gerrits B, Muller D, Fritschy J-M (2011) Regulation of GABAergic synapse formation and plasticity by GSK3β-dependent phosphorylation of gephyrin. Proceedings of the National Academy of Sciences 108:379-384.

Udagawa T, Farny NG, Jakovcevski M, Kaphzan H, Alarcon JM, Anilkumar S, Ivshina M, Hurt JA, Nagaoka K, Nalavadi VC, Lorenz LJ, Bassell GJ, Akbarian S, Chattarji S, Klann E, Richter JD (2013) Genetic and acute CPEB1 depletion ameliorate fragile X pathophysiology. Nature Medicine 19:1473-1477.

Udenfriend S (1950) Identification of γ-aminobutyric acid in brain by the isotope derivative method. Journal of Biological Chemistry 187:65-69.

Ueno S, Bracamontes J, Zorumski C, Weiss DS, Steinbach JH (1997) Bicuculline and Gabazine Are Allosteric Inhibitors of Channel Opening of the GABA_A Receptor. The Journal of Neuroscience 17:625-634.

Ungless MA, Whistler JL, Malenka RC, Bonci A (2001) Single cocaine exposure in vivo induces long-term potentiation in dopamine neurons. Nature 411:583-587.

Urban NN, Castro JB (2005) Tuft calcium spikes in accessory olfactory bulb mitral cells. Journal of Neuroscience 25:5024-5028.

Urban NN, Henze DA, Barrionuevo G (1998) Amplification of Perforant-Path EPSPs in CA3 Pyramidal Cells by LVA Calcium and Sodium Channels. Journal of Neurophysiology 80:1558-1561.

Vaags AK, Lionel AC, Sato D, Goodenberger M, Stein QP, Curran S, Ogilvie C, Ahn JW, Drmic I, Senman L (2012) Rare deletions at the neurexin 3 locus in autism spectrum disorder. The American Journal of Human Genetics 90:133-141.

van der Molen MJ, Stam CJ, van der Molen MW (2014) Resting-state EEG oscillatory dynamics in fragile X syndrome: abnormal functional connectivity and brain network organization. PloS one 9:e88451.

Vasilyev N, Polonskaia A, Darnell JC, Darnell RB, Patel DJ, Serganov A (2015) Crystal structure reveals specific recognition of a G-quadruplex RNA by a β-turn in the RGG motif of FMRP. Proceedings of the National Academy of Sciences 112:E5391-E5400.

Verdoorn T, Burnashev N, Monyer H, Seeburg P, Sakmann B (1991) Structural determinants of ion flow through recombinant glutamate receptor channels. Science 252:1715-1718.

Verdoorn TA, Draguhn A, Ymer S, Seeburg PH, Sakmann B (1990) Functional properties of recombinant rat GABAA receptors depend upon subunit composition. Neuron 4:919-928.

Verkerk AJ, Pieretti M, Sutcliffe JS, Fu Y-H, Kuhl DP, Pizzuti A, Reiner O, Richards S, Victoria MF, Zhang F (1991) Identification of a gene (FMR-1) containing a CGG repeat coincident with a breakpoint cluster region exhibiting length variation in fragile X syndrome. Cell 65:905-914.

Villalon-Reina J, Jahanshad N, Beaton E, Toga AW, Thompson PM, Simon TJ (2013) White matter microstructural abnormalities in girls with chromosome 22q11.2 deletion syndrome, Fragile X or Turner syndrome as evidenced by diffusion tensor imaging. NeuroImage 81:441-454.

Vincent SR, Kimura H (1992) Histochemical mapping of nitric oxide synthase in the rat brain. Neuroscience 46:755-784.

Volianskis A, France G, Jensen MS, Bortolotto ZA, Jane DE, Collingridge GL (2015) Long-term potentiation and the role of N-methyl-D-aspartate receptors. Brain research 1621:5-16.

von Engelhardt J, Mack V, Sprengel R, Kavenstock N, Li KW, Stern-Bach Y, Smit AB, Seeburg PH, Monyer H (2010) CKAMP44: A Brain-Specific Protein Attenuating Short-Term Synaptic Plasticity in the Dentate Gyrus. Science 327:1518-1522.

Wall MJ, Collins DR, Chery SL, Allen ZD, Pastuzyn ED, George AJ, Nikolova VD, Moy SS, Philpot BD, Shepherd JD, Müller J, Ehlers MD, Mabb AM, Corrêa SAL (2018) The Temporal Dynamics of Arc Expression Regulate Cognitive Flexibility. Neuron 98:1124-1132.e1127.

Wang H, Bedford FK, Brandon NJ, Moss SJ, Olsen RW (1999) GABA(A)-receptor-associated protein links GABA(A) receptors and the cytoskeleton. Nature 397:69-72.

Wang J, Ethridge LE, Mosconi MW, White SP, Binder DK, Pedapati EV, Erickson CA, Byerly MJ, Sweeney JA (2017) A resting EEG study of neocortical hyperexcitability and altered functional connectivity in fragile X syndrome. Journal of Neurodevelopmental Disorders 9:11.

Wang SS, Kloth AD, Badura A (2014) The cerebellum, sensitive periods, and autism. Neuron 83:518-532.

Watanabe A, Ono M, Shibata S, Watanabe S (1995) Effect of a nitric oxide synthase inhibitor, N-nitro-L-arginine methylester, on light-induced phase delay of circadian rhythm of wheel-running activity in golden hamsters. Neuroscience letters 192:25-28.

Watkins JC, Jane DE (2006) The glutamate story. Br J Pharmacol 147 Suppl 1:S100-108.

Waung MW, Pfeiffer BE, Nosyreva ED, Ronesi JA, Huber KM (2008) Rapid Translation of Arc/Arg3.1 Selectively Mediates mGluR-Dependent LTD through Persistent Increases in AMPAR Endocytosis Rate. Neuron 59:84-97.

Weaving LS, Christodoulou J, Williamson SL, Friend KL, McKenzie OLD, Archer H, Evans J, Clarke A, Pelka GJ, Tam PPL, Watson C, Lahooti H, Ellaway CJ, Bennetts B, Leonard H, Gécz J (2004) Mutations of CDKL5 Cause a Severe Neurodevelopmental Disorder with Infantile Spasms and Mental Retardation. The American Journal of Human Genetics 75:1079-1093.

Weiergräber OH, Stangler T, Thielmann Y, Mohrlüder J, Wiesehan K, Willbold D (2008) Ligand Binding Mode of GABAA Receptor-Associated Protein. Journal of Molecular Biology 381:1320-1331.

Werman R, Davidoff R, Aprison M (1967) Is Glycine a Neurotransmitter?: Inhibition of Motoneurones by Iontophoresis of Glycine. Nature 214:681-683.

Whitney ER, Kemper TL, Bauman ML, Rosene DL, Blatt GJ (2008) Cerebellar Purkinje cells are reduced in a subpopulation of autistic brains: a stereological experiment using calbindin-D28k. The Cerebellum 7:406-416.

Williams SR, Stuart GJ (2000) Site independence of EPSP time course is mediated by dendritic I h in neocortical pyramidal neurons. Journal of neurophysiology 83:3177-3182.

Wotring V, Miller T, Weiss DS (2003) Mutations at the GABA receptor selectivity filter: a possible role for effective charges. The Journal of physiology 548:527-540.

Wu J-Y, Matsuda T, Roberts E (1973) Purification and Characterization of Glutamate Decarboxylase from Mouse Brain. Journal of Biological Chemistry 248:3029-3034.

Wulff P, Schonewille M, Renzi M, Viltono L, Sassoè-Pognetto M, Badura A, Gao Z, Hoebeek FE, van Dorp S, Wisden W, Farrant M, De Zeeuw CI (2009) Synaptic inhibition of Purkinje cells mediates consolidation of vestibulo-cerebellar motor learning. Nature Neuroscience 12:1042-1049.

Xia J, Zhang X, Staudinger J, Huganir RL (1999) Clustering of AMPA receptors by the synaptic PDZ domain–containing protein PICK1. Neuron 22:179-187.

Xie N, Gong H, Suhl JA, Chopra P, Wang T, Warren ST (2016) Reactivation of FMR1 by CRISPR/Cas9-Mediated Deletion of the Expanded CGG-Repeat of the Fragile X Chromosome. PLOS ONE 11:e0165499.

Xu J, Wu L-G (2005) The Decrease in the Presynaptic Calcium Current Is a Major Cause of Short-Term Depression at a Calyx-Type Synapse. Neuron 46:633-645.

Yamada J, Okabe A, Toyoda H, Kilb W, Luhmann HJ, Fukuda A (2004) Cl− uptake promoting depolarizing GABA actions in immature rat neocortical neurones is mediated by NKCC1. The Journal of physiology 557:829-841.

Yang G, Chen G, Ebner TJ, Iadecola C (1999) Nitric oxide is the predominant mediator of cerebellar hyperemia during somatosensory activation in rats. American Journal of Physiology-Regulatory, Integrative and Comparative Physiology 277:R1760-R1770.

Yang G, Huard JMT, Beitz AJ, Ross ME, Iadecola C (2000) Stellate Neurons Mediate Functional Hyperemia in the Cerebellar Molecular Layer. The Journal of Neuroscience 20:6968-6973.

Yang Y-M, Arsenault J, Bah A, Krzeminski M, Fekete A, Chao OY, Pacey LK, Wang A, Forman-Kay J, Hampson DR, Wang L-Y (2018) Identification of a molecular locus for normalizing dysregulated GABA release from interneurons in the Fragile X brain. Molecular Psychiatry.

Yee BK, Keist R, von Boehmer L, Studer R, Benke D, Hagenbuch N, Dong Y, Malenka RC, Fritschy J-M, Bluethmann H, Feldon J, Möhler H, Rudolph U (2005) A schizophrenia-related sensorimotor deficit links α3-containing GABAA receptors to a dopamine hyperfunction. Proceedings of the National Academy of Sciences of the United States of America 102:17154-17159.

Zalfa F, Eleuteri B, Dickson KS, Mercaldo V, De Rubeis S, di Penta A, Tabolacci E, Chiurazzi P, Neri G, Grant SGN, Bagni C (2007) A new function for the fragile X mental retardation protein in regulation of PSD-95 mRNA stability. Nature Neuroscience 10:578-587.

Zamanillo D, Sprengel R, Hvalby Ø, Jensen V, Burnashev N, Rozov A, Kaiser KMM, Köster HJ, Borchardt T, Worley P, Lübke J, Frotscher M, Kelly PH, Sommer B, Andersen P, Seeburg PH, Sakmann B (1999) Importance of AMPA Receptors for Hippocampal Synaptic Plasticity But Not for Spatial Learning. Science 284:1805-1811.

Zeier Z, Kumar A, Bodhinathan K, Feller JA, Foster TC, Bloom DC (2009) Fragile X mental retardation protein replacement restores hippocampal synaptic function in a mouse model of fragile X syndrome. Gene therapy 16:1122-1129.

Zeisel A, Hochgerner H, Lonnerberg P, Johnsson A, Memic F, van der Zwan J, Haring M, Braun E, Borm LE, La Manno G, Codeluppi S, Furlan A, Lee K, Skene N, Harris KD, Hjerling-Leffler J, Arenas E, Ernfors P, Marklund U, Linnarsson S (2018) Molecular Architecture of the Mouse Nervous System. Cell 174:999-1014 e1022.

Zhan X, Asmara H, Cheng N, Sahu G, Sanchez E, Zhang F-X, Zamponi GW, Rho JM, Turner RW (2020) FMRP(1–297)-tat restores ion channel and synaptic function in a model of Fragile X syndrome. Nature Communications 11:2755.

Zhang B, Sudhof TC (2016) Neuroligins Are Selectively Essential for NMDAR Signaling in Cerebellar Stellate Interneurons. J Neurosci 36:9070-9083.

Zhang D, Pan Z-H, Awobuluyi M, Lipton SA (2001) Structure and function of GABAC receptors: a comparison of native versus recombinant receptors. Trends in Pharmacological Sciences 22:121-132.

Zhang J, Fang Z, Jud C, Vansteensel MJ, Kaasik K, Lee CC, Albrecht U, Tamanini F, Meijer JH, Oostra BA (2008) Fragile X-related proteins regulate mammalian circadian behavioral rhythms. The American Journal of Human Genetics 83:43-52.

Zhang W, Devi SPS, Tomita S, Howe JR (2014a) Auxiliary proteins promote modal gating of AMPA-and kainate-type glutamate receptors. European Journal of Neuroscience 39:1138-1147.

Zhang Y, Brown MR, Hyland C, Chen Y, Kronengold J, Fleming MR, Kohn AB, Moroz LL, Kaczmarek LK (2012) Regulation of Neuronal Excitability by Interaction of Fragile X Mental Retardation Protein with Slack Potassium Channels. The Journal of Neuroscience 32:15318-15327.

Zhang Y, Bonnan A, Bony G, Ferezou I, Pietropaolo S, Ginger M, Sans N, Rossier J, Oostra B, LeMasson G, Frick A (2014b) Dendritic channelopathies contribute to neocortical and sensory hyperexcitability in Fmr1−/y mice. Nature Neuroscience 17:1701-1709.

Zhou J, Parada LF (2012) PTEN signaling in autism spectrum disorders. Current Opinion in Neurobiology 22:873-879.

Zhou Q, Zhou P, Wang AL, Wu D, Zhao M, Südhof TC, Brunger AT (2017) The primed SNARE–complexin–synaptotagmin complex for neuronal exocytosis. Nature 548:420-425.

Zhou Z, Liu A, Xia S, Leung C, Qi J, Meng Y, Xie W, Park P, Collingridge GL, Jia Z (2018) The C-terminal tails of endogenous GluA1 and GluA2 differentially contribute to hippocampal synaptic plasticity and learning. Nature Neuroscience 21:50-62.

Zhu PJ, Chen C-J, Mays J, Stoica L, Costa-Mattioli M (2018a) mTORC2, but not mTORC1, is required for hippocampal mGluR-LTD and associated behaviors. Nature Neuroscience 21:799-802.

Zhu S, Noviello CM, Teng J, Walsh RM, Kim JJ, Hibbs RE (2018b) Structure of a human synaptic GABAA receptor. Nature 559:67-72.

Zoghbi HY, Bear MF (2012) Synaptic dysfunction in neurodevelopmental disorders associated with autism and intellectual disabilities. Cold Spring Harbor perspectives in biology 4:a009886.

Zucker RS, Regehr WG (2002) Short-Term Synaptic Plasticity. Annual Review of Physiology 64:355-405.

APPENDIX I: REPRINTS OF PUBLISHED CHAPTERS

Cellular/Molecular

Nitric Oxide Signaling Strengthens Inhibitory Synapses of Cerebellar Molecular Layer Interneurons through a GABARAP-Dependent Mechanism

Erik A. Larson,[1,3] Michael V. Accardi,[2,3] Ying Wang,[4,5,6] Martina D'Antoni,[1,3] Benyamin Karimi,[4,5,6] Tabrez J. Siddiqui,[4,5,6] and Derek Bowie[3]

[1]Integrated Program in Neuroscience, McGill University, Montréal, Québec, Canada H3A 2B4, [2]Graduate Program in Pharmacology, McGill University, Montréal, Québec, Canada H3G 1Y6, [3]Department of Pharmacology and Therapeutics, McGill University, Montréal H3G 0B1, Québec, Canada, [4]Department of Physiology and Pathophysiology, Max Rady College of Medicine, Rady Faculty of Health Sciences, University of Manitoba, Winnipeg, Manitoba, Canada R3E 0J9, [5]Neuroscience Research Program, Kleysen Institute for Advanced Medicine, Health Sciences Centre, Winnipeg, Manitoba, Canada R3E 3J7, and [6]The Children's Hospital Research Institute of Manitoba, Winnipeg, Manitoba Canada R3E 3P4

Nitric oxide (NO) is an important signaling molecule that fulfills diverse functional roles as a neurotransmitter or diffusible second messenger in the developing and adult CNS. Although the impact of NO on different behaviors such as movement, sleep, learning, and memory has been well documented, the identity of its molecular and cellular targets is still an area of ongoing investigation. Here, we identify a novel role for NO in strengthening inhibitory $GABA_A$ receptor-mediated transmission in molecular layer interneurons of the mouse cerebellum. NO levels are elevated by the activity of neuronal NO synthase (nNOS) following Ca^{2+} entry through extrasynaptic NMDA-type ionotropic glutamate receptors (NMDARs). NO activates protein kinase G with the subsequent production of cGMP, which prompts the stimulation of NADPH oxidase and protein kinase C (PKC). The activation of PKC promotes the selective strengthening of α3-containing $GABA_A$Rs synapses through a GABA receptor-associated protein-dependent mechanism. Given the widespread but cell type-specific expression of the NMDAR/nNOS complex in the mammalian brain, our data suggest that NMDARs may uniquely strengthen inhibitory GABAergic transmission in these cells through a novel NO-mediated pathway.

Key words: **cerebellum; electrophysiology; GABA receptor; GABARAP; inhibitory synapse; plasticity**

Significance Statement

Long-term changes in the efficacy of GABAergic transmission is mediated by multiple presynaptic and postsynaptic mechanisms. A prominent pathway involves crosstalk between excitatory and inhibitory synapses whereby Ca^{2+}-entering through postsynaptic NMDARs promotes the recruitment and strengthening of $GABA_A$ receptor synapses via Ca^{2+}/calmodulin-dependent protein kinase II. Although Ca^{2+} transport by NMDARs is also tightly coupled to nNOS activity and NO production, it has yet to be determined whether this pathway affects inhibitory synapses. Here, we show that activation of NMDARs trigger a NO-dependent pathway that strengthens inhibitory GABAergic synapses of cerebellar molecular layer interneurons. Given the widespread expression of NMDARs and nNOS in the mammalian brain, we speculate that NO control of GABAergic synapse efficacy may be more widespread than has been appreciated.

Introduction

The NMDA receptor (NMDAR) is an abundant neurotransmitter-gated ion-channel that orchestrates the formation, maintenance, and plasticity of almost all glutamatergic synapses in the developing and adult brain (Hardingham and Bading, 2003; Paoletti et al., 2013). It is implicated in numerous neurologic diseases from neurodevelopmental disorders (Bello et al., 2013; Hu et al., 2016) to neurodegenerative disease including Huntington's (Milnerwood and Raymond, 2010) and Alzheimer's disease (Liu et al., 2019). Two synergistic features of the NMDAR critical for its role in synaptic signaling are its slow channel gating (Glasgow

Received Sep. 12, 2019; revised Jan. 13, 2020; accepted Mar. 3, 2020.

Author contributions: E.A.L., M.V.A., T.J.S., and D.B. designed research; E.A.L., M.V.A., Y.W., M.D., and B.K. performed research; E.A.L., M.V.A., Y.W., M.D., B.K., T.J.S., and D.B. analyzed data; E.A.L., T.J.S., and D.B. wrote the paper.

This work was supported by Canadian Institutes of Health Research Operating Grants CIHR MOP-342247 to D.B. and by CIHR MOP-142209 to T.J.S. We thank members of the Bowie laboratory for discussions and comments on the paper.

The authors declare no competing financial interests.

Correspondence should be addressed to Derek Bowie at derek.bowie@mcgill.ca.

https://doi.org/10.1523/JNEUROSCI.2211-19.2020

Copyright © 2020 the authors

et al., 2015) and high Ca^{2+} permeability (Gnegy, 2000). These properties of the NMDAR act together to ensure that the presynaptic release of L-glutamate elevates postsynaptic Ca^{2+} and triggers a cascade of Ca^{2+}-dependent biochemical events inside the cell. Much of the activity initiated by NMDARs is relayed through the actions of Ca^{2+}/calmodulin-dependent protein kinase II (CaMKII; Sanhueza and Lisman, 2013), which is anchored to the NMDAR (Bayer et al., 2006) and thus ideally suited to act as a signaling hub. For example, it has been shown that this pathway originating at glutamatergic synapses strengthens GABAergic synapses (Marsden et al., 2007; Petrini et al., 2014; Chiu et al., 2018).

NMDA receptor signaling is also tightly coupled to neuronal nitric oxide synthase (nNOS) activity through the postsynaptic scaffold of PSD-95 and -93 (Brenman et al., 1996a,b). By elevating cytosolic Ca^{2+}, synaptic NMDARs activate nNOS generating nitric oxide (NO), which has a variety of roles in neuronal communication and blood vessel modulation (Bredt, 1999; Kiss and Vizi, 2001). Accordingly, NO participates in numerous CNS functions including learning and memory, sleep and feeding behavior, movement, pain, anxiety, and reproductive activity (Garthwaite, 2019). An area of ongoing investigation is to identify the molecular and cellular targets of NO. What is known is that physiological levels of NO elevated by NMDAR stimulation act as a retrograde signal (Garthwaite, 2016), stimulate gene expression (Lu et al., 1999) and/or promote AMPA receptor (AMPAR) trafficking (Serulle et al., 2007). Conversely, excessive levels of NO promote neurotoxicity (Brown, 2010).

Here, we identify a new role for NO in strengthening GABAergic synapses of cerebellar molecular layer inhibitory neurons. We show that an elevation in cytosolic Ca^{2+} mediated by NMDARs triggers a cascade of signaling events that begin with nNOS activation and release of NO, which through the generation of cGMP activates protein kinase G (PKG). This pathway stimulates NADPH oxidase and protein kinase C (PKC) to strengthen α3-containing $GABA_A$ receptor ($GABA_AR$) synapses through a GABA receptor-associated protein (GABARAP)-dependent mechanism. Given the widespread but cell-type-specific expression of the NMDAR/nNOS complex in the mammalian CNS, our data suggest that NMDARs may uniquely strengthen inhibitory GABAergic transmission through a novel NO-mediated pathway in cerebellar molecular layer interneurons (MLIs) and other nNOS-positive ($nNOS^+$) neurons.

Materials and Methods

Animals

Wild-type mice with a C57BL/6 background were obtained from Charles River Laboratories and maintained as a breeding colony at McGill University. Mice (male and female) used for the experiments ranged from 18 to 30 d old. All experiments have been approved and were performed in accordance with the guidelines of the Canadian Council on Animal Care and were approved by the Animal Care Committee of McGill University. Breeder pairs of *Gabra3* KO (1-Gabra3tm2Uru/Uru), C57BL/6 background, were kindly provided by Dr. Rudolph (Harvard Medical School, McLean Hospital; Yee et al., 2005).

Cerebellum slice preparation

Mice were anaesthetized with isoflurane and immediately decapitated. The cerebellum was rapidly removed from the whole brain while submerged in oxygenated (95% O_2, 5% CO_2) ice-cold cutting solution, which contained the following (in mM): 235 sucrose, 2.5 KCl, 1.25 NaH_2PO_4, 28 $NaHCO_3$, 0.5 $CaCl_2$, 7 $MgSO_4$, 28 D-glucose, pH 7.4, 305–315 mOsm/L. The tissue was maintained in ice-cold solution while sagittal slices of cerebellar vermis (300 μm) were cut using a vibrating tissue slicer (Leica VT1200, Leica Instruments). The slices were transferred to oxygenated artificial CSF (aCSF) and held at room temperature (20–23° C) for at least 1 h before recordings were performed. aCSF contained the following (in mM): 125 NaCl, 2.5 KCl, 1.25 NaH_2PO_4, 26 $NaHCO_3$, 2 $CaCl_2$, 1 $MgCl_2$, 25 D-glucose, pH 7.4, 305–315 mOsm/L.

Electrophysiology

Slice experiments were performed on an Olympus BX51 upright microscope equipped with differential interference contrast/infrared optics. Whole-cell patch-clamp recordings were made from visually-identified MLIs, primarily in lobules IV and V, which were distinguished from misplaced or migrating granule cells by their soma diameter (8–9 μm) and location in the molecular layer. For current-clamp experiments, patch pipettes were prepared from thick-walled borosilicate glass [GC150F-10, outer diameter (o.d.): 1.5 mm, inner diameter (i.d.): 0.86 mm; Harvard Apparatus] and had open tip resistances of 4–10 MΩ when filled with an intracellular solution that contained the following (in mM): 126 K-gluconate, 0.05 $CaCl_2$, 0.15 K_4BAPTA, 4 NaCl, 1 $MgSO_4$, 5 HEPES, 3 Mg-ATP, 0.1 NaGTP, 15 D-glucose, 2 QX314 to block voltage-activated Na^+ channels, and 0.5 mg/ml Lucifer yellow as a *post hoc* dye indicator, pH 7.4 with KOH, 300–310 mOsm/L. High BAPTA intracellular current-clamp solution contained the following (in mM): 110 K-gluconate, 0.05 $CaCl_2$, 10 K_4BAPTA, 4 NaCl, 5 HEPES, 4 Mg-ATP, 0.1NaGTP, 15 D-glucose, and 2 QX314, pH 7.4 with KOH, 300–310 mOsm/L. Voltage-clamp recordings were made with patch pipettes prepared as described but filled with an intracellular solution that contained the following (in mM): 140 CsCl, 4 NaCl, 0.5 $CaCl_2$, 10 HEPES, 5 EGTA, 2 Mg-ATP, 2 QX314, pH 7.4 with CsOH, 300–310 mOsm/L. High BAPTA voltage-clamp solution contained 110 CsCl, 4 NaCl, 10 HEPES, 10 Cs_4BAPTA, 2 Mg-ATP, 2 QX314, pH 7.4 with CsOH, 300–310 mOsm/L. Specific *n* numbers reported refer to technical replications (i.e., patch-clamp recordings), while each experiment was replicated using at least three different mice.

In each case, recordings were made with a MultiClamp 700A amplifier (Molecular Devices) in voltage- or current-clamp mode. Series resistance and whole-cell capacitance were corrected and estimated by cancelling the fast current transients evoked at the onset and offset of brief (10–20 ms) 5 mV voltage-command steps. Series resistance during postsynaptic whole-cell recording (10–25 MΩ) was checked for stability throughout the experiments (<20% drift tolerance). The capacitance of the MLIs was in the range of 5–14 pF. The bath was continuously perfused at room temperature (22–23°C) with aCSF at a rate of 1–2 ml/min. We chose to perform recordings at room temperature rather than physiological temperature because it tended to increase the viability of the slice tissue and slowed the time course of synaptic events making them easier to resolve. Membrane currents were filtered at 5 kHz with an 8-pole low-pass Bessel filter (Frequency Devices) and digitized at 25 kHz with a Digidata 1322A data acquisition board and Clampex9 (Molecular Devices) software. Curve fitting and figure preparation of all electrophysiology data were performed using Origin 7.0 (OriginLab), Microsoft Excel, and Clampfit 10 (Molecular Devices) software.

For extracellular stimulation, thin walled borosilicate glass electrodes (o.d. 1.65 mm, i.d. 1.15 mm; King Precision Glass) were used with a tip resistance of < 3 MΩ when filled with aCSF. The ground electrode for the stimulation circuit was made with a platinum wire wrapped around the stimulation electrode. The stimulating electrode was positioned in the molecular layer at or just beneath the slice surface. Voltage pulses (10–25 V in amplitude, 200–400 μs in duration) were applied at low-frequency stimulation (0.1 Hz) through the stimulating electrode. To minimize variability between responses, the stimulating electrode was positioned 50–100 μm away from the recorded cell. The stimulus voltage used during each experiment was at the lowest intensity to elicit the maximal evoked excitatory post synaptic potential/inhibitory post synaptic current (eEPSP/IPSC) response within the range described above. Stimulation strength and duration were kept constant throughout the experiment. For high-frequency stimulation (HFS), trains of six stimuli were delivered at 100 Hz (intertrain interval of 20 s) as described previously (Li et al., 2011). This HFS protocol has been previously shown to generate reactive oxygen species

(ROS; Li et al., 2011) and mimics somatosensory stimulation patterns (Jörntell and Ekerot, 2006; Saviane and Silver, 2006; Rancz et al., 2007; Arenz et al., 2008; Coddington et al., 2013). The HFS was performed every 5 min to ensure a continual accumulation of ROS. During the voltage-clamp experiments of evoked GABA currents (compare Fig. 2), we performed the HFS protocol at a holding potential of +40 mV to relieve Mg^{2+} block of NMDARs. We performed the single stimulation recordings at −60 mV to isolate the response from NMDA currents and used GYKI 53 655 to pharmacologically block AMPA currents. For all experiments that included perfusion of either pharmacological or peptide blocker compounds in the internal solution we waited 15 min before beginning the HFS induction protocol. In experiments where the antioxidant *N*-acetyl-cysteine (NAC) was included in the patch electrode solution, we unexpectedly observed that NAC alone increased the amplitude of baseline responses to 191.5% ± 36 ($n = 4$) of the starting response, which stabilized 20 min after whole-cell breakthrough. Because this was not observed in the absence of NAC ($Peak_{15}$: 100.2 ± 5.5%, $n = 21$), we concluded that the resting redox state of the cell affects the synaptic properties of MLIs. Antioxidants have been shown to potentiate both AMPARs (Lee et al., 2012) and NMDARs (Köhr et al., 1994). As our plasticity mechanism relies on NMDAR activation we would expect that any potentiating effect of NAC on the NMDAR current would be more likely to strengthen long term potentiation of inhibitory synapses (iLTP). Given this, HFS was commenced only after the effect of NAC on basal synaptic properties stabilized.

Pharmacological compounds

NMDAR antagonist, D-(-)−2-amino-5-phosphonopentanoic acid(D-APV; 10 μM), AMPA antagonist 1-(4-aminophenyl)-3-methylcarbamyl-4-methyl-3,4-dihydro-7,8-methylenedioxy-5H-2,3-benzodiazepine hydrochloride (GYKI 53 655; 10 μM), and the $GABA_A$Rs antagonist bicuculline (10 μM) were purchased from Tocris Bioscience. Stock solutions of these antagonists were prepared in water and were stored at −20°C and working solutions were diluted with aCSF shortly before application to the bath. NAC (1 mM; Sigma-Aldrich), protein kinase A (PKA) inhibitor fragment (6–22) amide (PKA 6-22; 5 μM; Tocris Bioscience), Ruthenium red (1 μM; Tocris Bioscience), and cGMP analog pCPT-cGMP (10 μM; Tocris Bioscience) were prepared as a stock solution in water and dissolved in patch electrode solution on the day of the experiment. Apocynin (Apo; 100 μM; Tocris Bioscience), 3-bromo-7-nitroindazole (3-Br-7-NI; 10 μM; Tocris Bioscience), KN-93 (5 μM; Tocris Bioscience), Gö 6983 (5 μM; Tocris Bioscience), phorbol 12-myristate 13-acetate (PMA; 100 nM; Tocris Bioscience), 1H-[1,2,4]oxadiazolo[4,3-a]quinoxalin-1-one (ODQ; 10 μM; Tocris Bioscience), KT 5823 (5 μM; Tocris Bioscience), and antimycin-A (2 μM; Sigma-Aldrich) were dissolved in DMSO and stored at −20°C. The K1 GABARAP, K1 GABARAP scrambled, and α3-derived peptides (all 100 μM; Genscript) were dissolved in DMSO and stored at −20°C. The final maximum DMSO concentration for all experiments (0.1% v/v) had no effect on GABAergic responses, which was consistent with other studies (Nakahiro et al., 1992).

cDNA constructs

HA-GABAR-α3 contains the signal sequence of rat neuroligin1, the HA tag and mature sequence of rat GABAR-α3 (NM_017069) included in the Clontech EGFP-C1 vector. Human GABAR-β2 (NM_000813) and human GABAR-γ2 (NM_000816) were cloned into the pcDNA3 vector. Mouse GABARAP (BC030350) was C-terminally tagged with CFP in the Clontech ECFP-N1 vector. Rat gephyrin (NM_022865), N-terminally tagged with YFP, was cloned in the Clontech EYFP-C1 vector. All expression constructs were driven by the CMV promoter.

Coimmunoprecipitation protocol

Semi-confluent HEK 293 cells were plated on 60 mm dishes and transfected with YFP-Gephyrin, GABARAP-CFP or negative control YFP. Cotransfections were done with equivalent amounts of HA-GABAR-α3, GABAR-β2, and GABAR-γ2 (short). Cells were then allowed to grow for 24 h post-transfection. Protein-G Sepharose bead slurry (50 μl) was incubated with 5 μg of rat anti-HA antibody (3F10, Sigma-Aldrich) for 4 h at 4°C. Cells were subsequently washed twice and collected in cold PBS. Harvested cells were lysed using 250 μl of complexiolyte-48 (Logopharm) and further disrupted by passaging 10–15 times through a 25G needle. Lysed cells were incubated at 4°C for 1 h on an end-over rotator. Subsequently, lysates were centrifuged at 14,000 × *g* at 4°C for 10 min. The resulting supernatants were incubated overnight at 4°C with Protein-G beads conjugated with anti-HA antibody. The beads were washed 3–4 times with complexiolyte-48 dilution buffer and eluted in 2× SDS-PAGE sample buffer. The resulting eluates along with 10 μl of the supernatants used as expression control (input) were subjected to SDS-PAGE electrophoresis, immunoblotted on PVDF membranes, and probed with rabbit anti-GFP antibody (A11122, Life Technologies; 1:1000) followed by anti-rabbit HRP antibody (4030-05, Southern Biotech; 1:7000). The blots were developed using chemiluminescence in the ChemiDoc imaging system (Bio-Rad). For peptide interference experiments, the same protocol was followed with a third of the antibody, beads and lysates used. The scrambled GABARAP and GABARAP peptides were added to the lysates just before they were added to the beads with a final concentration 2.5 mM.

Statistical analysis

Data were analyzed using SPSS (IBM) and custom statistical software kindly provided by Joe Rochford (McGill University). All data were tested for normality and appropriate parametric or nonparametric tests were conducted accordingly. For all repeated-measures ANOVA presented, Tukey's *post hoc* tests were conducted as indicated in the figure legends. For all Friedman tests, a Wilcoxon signed rank test with a Bonferroni–Holmes correction was conducted on the combinations. All statistical analysis of amplitudes (repeated-measures ANOVA or Friedman tests) were conducted comparing the baseline 5 min average of the datasets and each subsequent 5 min intervals following treatment up to 25 min posttreatment.

Results

HFS of glutamatergic synapses strengthens inhibitory transmission

To study activity-dependent plasticity of GABAergic synapses, we performed whole-cell current- and voltage-clamp electrophysiological recordings on cerebellar MLIs which receive synaptic input from both excitatory and inhibitory neurons (Fig. 1*A*). Current-clamp recordings were performed to examine the effect of GABAergic signaling on neuronal excitability whereas we used voltage-clamp recordings to study the $GABA_A$R response in isolation. Previous work from our laboratory has shown that GABAergic synapses of MLIs can be strengthened by elevating cytosolic ROS with the mitochondrial uncoupler, antimycin A (Accardi et al., 2014). It remains to be established, however, whether cytosolic ROS levels can be elevated by physiologically relevant stimuli, for example, through synaptic transmission. Because MLIs express extrasynaptic NMDARs (Clark and Cull-Candy, 2002), we reasoned that activation of these receptors by neurotransmitter spillover from glutamatergic fibers might elevate cytosolic ROS through a non-canonical signaling pathway that was previously described in cultured neurons (Dugan et al., 1995; Reynolds and Hastings, 1995).

To test this, we performed stimulation experiments of MLI glutamatergic synapses using a field-stimulating electrode placed in the molecular layer of the cerebellum to activate the parallel fiber axons from granule cells (Fig. 1*A*). Using this approach, two types of responses were observed in current-clamp recordings (Fig. 1*B*,*C*). In most of the recordings ($n = 10$), a single stimulation elicited a compound response composed of an initial EPSP that overlapped with an IPSP (Fig. 1*B*) suggesting that both excitatory parallel fiber-MLI (PF-MLI) synapses and inhibitory synapses had been stimulated. MLIs receive input from many inhibitory cells in the cerebellar cortex; therefore, the

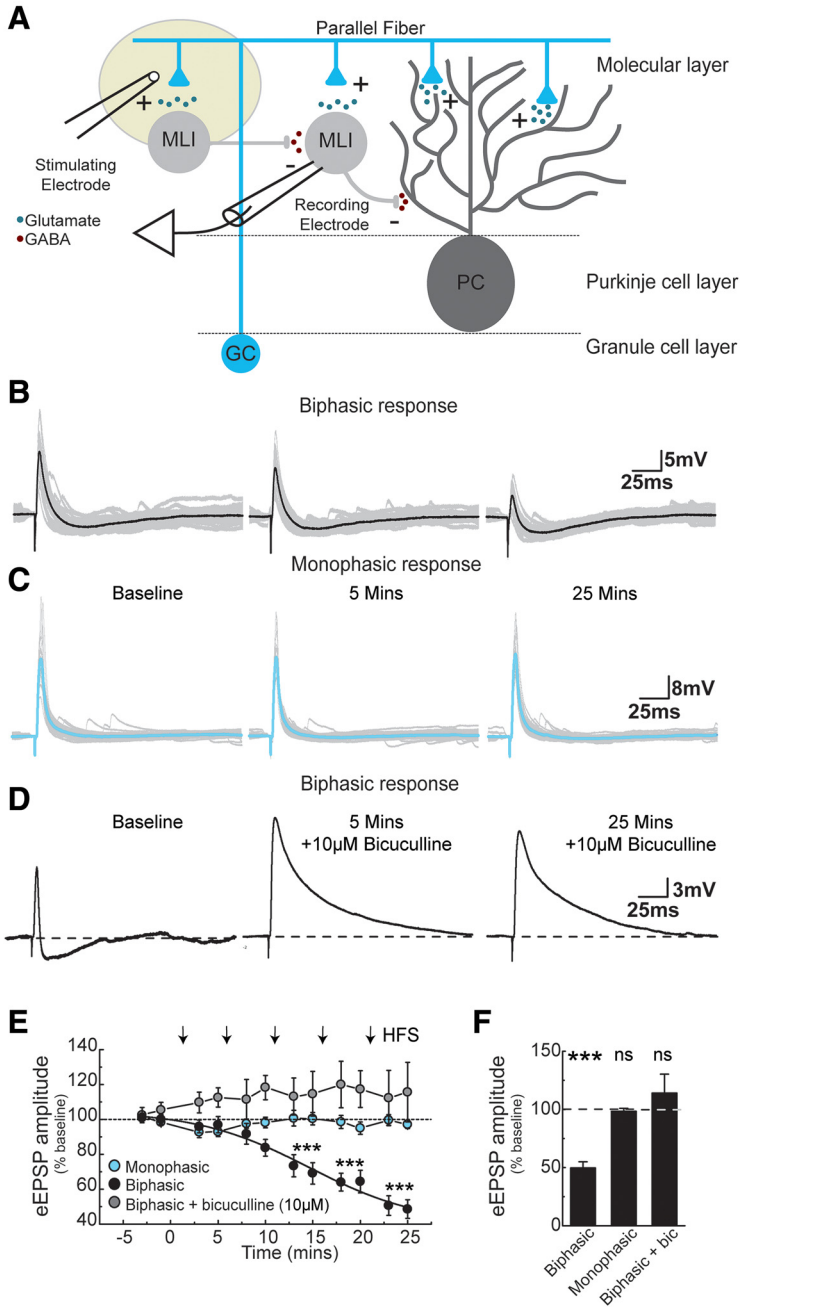

Figure 1. Repetitive stimulation of MLI excitatory synapses strengthens inhibitory neurotransmission. ***A***, Schematic illustrating the arrangement of stimulating and recording electrodes. Stimulating electrode was positioned to focally depolarize (yellow circle) excitatory and inhibitory axons of cells innervating MLIs. PC, Purkinje cell; GC, granule cell. ***B***, ***C***, Representative current-clamp recordings from two MLIs with either a biphasic (***B***; cell 141105r2) or monophasic (***C***; cell 141125r3) response at three time points; before (baseline) and after (5 min or 25 min) HFS. ***D***, Representative current-clamp recordings from a MLI with a biphasic response at three time points; before (baseline) and 5 min after application of the $GABA_A$Rs antagonist bicuculline and 25 min after HFS + bicuculline treatment (cell 150225r1). ***E***, Time course plot of the eEPSP amplitude before and after HFS from monophasic ($n = 7$) or biphasic ($n = 10$) cells or biphasic cells in the presence of the bicuculline ($n = 4$). ***F***, Summary plot of the eEPSP amplitude at 25 min following HFS shown as a percentage of the initial baseline. Tukey's *post hoc* contrasts: $^{***}p < 0.001$. ns, not significant.

observed inhibitory signal could arise from the axons of adjacent MLIs and/or Lugaro and globular cells (Fritschy and Panzanelli, 2006). In other recordings ($n = 8$), field stimulation evoked a monophasic EPSP without any detectable hyperpolarization, suggesting that only PF-MLI excitatory synapses were activated (Fig. 1*C*).

To study GABAergic synapse plasticity, we adapted a HFS protocol used in other studies to elevate ROS (Li et al., 2011). This HFS protocol is also in line with *in vivo* firing rates of cerebellar granule cells and the frequency of synaptic transmission for cerebellar MLIs (Chadderton et al., 2004). Using this protocol, a decline in the eEPSP amplitude was observed in recordings with a biphasic response over the 25 min following HFS ($Peak_{25}$: 48.6 ± 5% of initial response, $n = 10$, $F_{(5,45)} = 34.55$, $p < 0.00{,}001$, repeated-measures ANOVA; Fig. 1*B*,*E*,*F*). In contrast, the EPSP amplitude was unchanged in cells exhibiting a monophasic response ($Peak_{25}$: 98.3 ± 2%, $n = 8$, $F_{(5,40)} = 1.70$, $p = 0.15$, repeated-measures ANOVA) suggesting that HFS did not directly affect the efficacy of glutamatergic transmission (Fig. 1*C*,*E*,*F*). We therefore reasoned that the decline elicited by HFS in cells with a biphasic response was due to a strengthening of inhibitory transmission. In agreement with this, application of 10 μM bicuculline, to block $GABA_A$Rs and the observed hyperpolarization, prevented the decline in the eEPSP amplitude ($Peak_{25}$: 115.6 ± 17%, $n = 4$, $\chi^2_{(5)} = 2.74$, $p = 0.74$, Friedman test; Fig. 1*D*–*F*).

To better quantify the increase in GABAergic transmission, we performed the same HFS protocol in voltage-clamp mode and measured the evoked IPSCs (eIPSCs; Fig. 2). We observed a twofold increase in the eIPSC amplitude following the HFS protocol (HFS $Peak_{25}$: 200.3 ± 35%, $n = 7$, $F_{(5,30)} = 5.97$, $p = 0.0006$, repeated-measures ANOVA), which was accompanied by a slowing in decay kinetics (Fig. 2*A*–*D*). This latter observation is consistent with our previous finding showing that elevation in ROS levels promotes the recruitment of α3-containing $GABA_A$R into inhibitory MLI synapses (Accardi et al., 2014). Potentiation was absent in experiments where the recorded cell did not receive HFS reaffirming that GABAergic transmission is stable under basal conditions (Control $Peak_{25}$: 105.5 ± 8%, $n = 8$, $\chi^2_{(5)} = 2.67$, $p = 0.75$, Friedman test). Furthermore, the potentiation of eIPSC amplitude was present only when the HFS protocol was paired with a depolarization to +40 mV and not when HFS was performed at −60 mV ($Peak_{25}$: 95.6 ± 9%, $n = 6$, $\chi^2_{(5)} = 0.57$, $p = 0.98$, Friedman test; Fig. 2*A*–*C*). This latter finding suggests that the induction of long-term potentiation in GABAergic transmission (i.e., iLTP) may be postsynaptic and also involve an elevation in cytosolic Ca^{2+}. In agreement with this, inclusion of 10 mM BAPTA, to chelate cytosolic Ca^{2+}, eliminated the increase in eIPSC amplitude ($Peak_{25}$: 89 ± 5%,

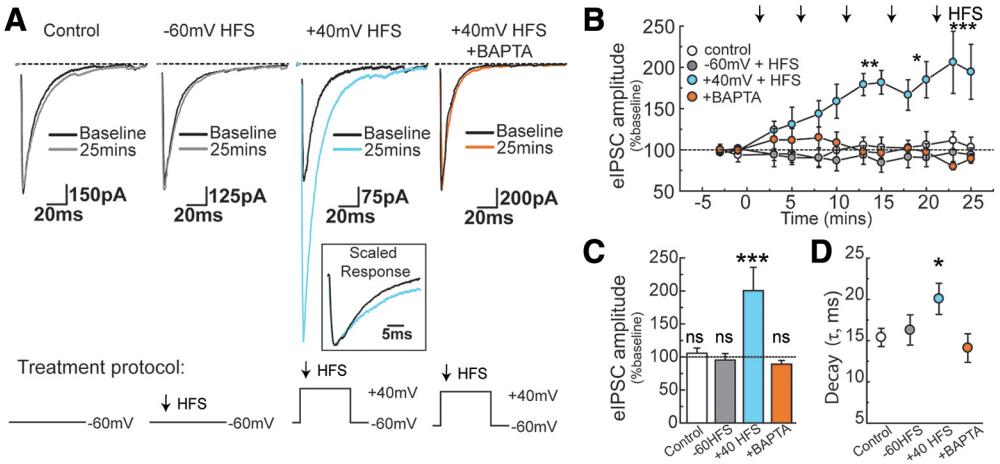

Figure 2. High-frequency stimulation evokes an increase in eIPSC amplitude and a slowing of decay kinetics. ***A***, $GABA_AR$ currents from different MLIs just before the start (i.e., baseline) of the HFS protocol at $t = 0$ min and after 25 min (cell numbers, Control: 160718r1, −60HFS: 171101r1, +40HFS: 160714r1, +BAPTA: 171019r1). Inset, Scaled response from the same trace as the +40HFS demonstrating the slowing of decay kinetics following the HFS treatment. Stimulation artifacts have been removed for clarity. ***B***, Summary plot of the time course of eIPSC amplitude during and following HFS expressed as a percentage of the baseline. ***C***, Summary bar graph of the eIPSC amplitude observed in different experimental conditions at 25 min after HFS and expressed as a percentage of the baseline. ***D***, Summary plot comparing the decay kinetics of eIPSCs at 25 min in different experimental conditions after HFS. Error bars indicate SEM. Tukey's *post hoc* contrasts: $^*p < 0.05$, $^{**}p < 0.01$, $^{***}p < 0.001$. ns, not significant.

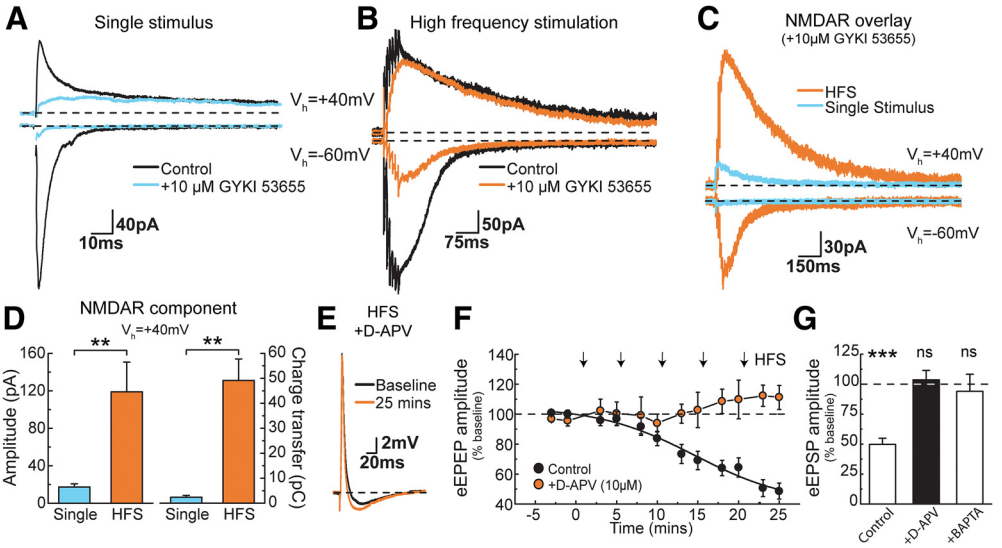

Figure 3. GABAergic synapses are strengthened by the activation of extrasynaptic NMDARs. ***A***, Representative traces of evoked currents from a single stimulus at +40 mV (top) or −60 mV (bottom) membrane potential (cell 150317r1). Traces in blue or black denote responses observed in the presence or absence of the AMPAR antagonist, GYKI 53 655 (10 μM), respectively. ***B***, Representative traces of evoked currents (from the same cell as *A*) during a 100 Hz 6 train stimulus (or HFS) at a membrane potential of +40 mV (top) and −60 mV (bottom) in the presence (orange trace) and absence (black trace) of GYKI 53 655. ***C***, Overlay of pharmacologically-isolated NMDAR currents (same traces as in ***A*** and ***B***) following a single stimulus (blue trace) or during a 100 Hz 6 stimulus train (orange trace, HFS) at +40 mV and −60 mV membrane potential. Stimulation artifacts have been removed for clarity. ***D***, Bar graph of the peak amplitude (left; $t_{(9)} = 3.43$, $p = 0.007$, paired *t* test) or charge transfer (right; $t_{(9)} = 3.32$, $p = 0.009$, paired *t* test) of NMDAR responses following a single stimulus or during a HFS train. ***E***, Representative current-clamp recordings from a MLI with a biphasic response in the presence of the NMDAR antagonist D-APV before and after HFS treatment (cell 150203r2). ***F***, Time course plot of the eEPSP amplitude before and after HFS in the presence ($n = 4$; open circle) and absence ($n = 10$; filled circles) of D-APV. Arrows indicate when the HFS protocol was performed. *G*, Summary plot of the eEPSP amplitude at 25 min following HFS expressed as a percentage of the baseline. Error bars indicate SEM. Control data represents the biphasic response from Figure 1 and is shown for comparison purposes. $^{**}p < 0.01$, $^{***}p < 0.001$. ns, not significant.

$n = 5$, $\chi^2_{(5)} = 9.45$, $p = 0.06$, Friedman test) and prevented the slowing in decay kinetics (control τ, 15.3 ± 1.1 ms, +40 mV HFS τ: 20.1 ± 1.9 ms, +BAPTA τ: 14.1 ± 1.7 ms) observed when HFS was paired with a depolarization step to +40 mV (Fig. 2*A–D*).

Activation of NMDARs strengthens postsynaptic inhibitory synapses

Previous work has shown that fast glutamatergic signaling in MLIs is primarily mediated by synaptic AMPARs, with a smaller contribution from extrasynaptic NMDARs (Clark and Cull-Candy, 2002). To determine the impact of each receptor subtype following a single stimulus or HFS, we compared the effect of AMPAR and NMDAR selective antagonists on the glutamatergic response (Fig. 3*A–D*). Given the strong voltage-dependent block of NMDARs by external Mg^{2+} at negative membrane potentials, we recorded membrane currents at both −60 and +40 mV. As previously reported (Clark and Cull-Candy, 2002), most of the glutamatergic response from a single stimulation at a holding potential of −60 mV was blocked by the selective AMPAR antagonist, GYKI 53 655 (10 μM) demonstrating the predominant

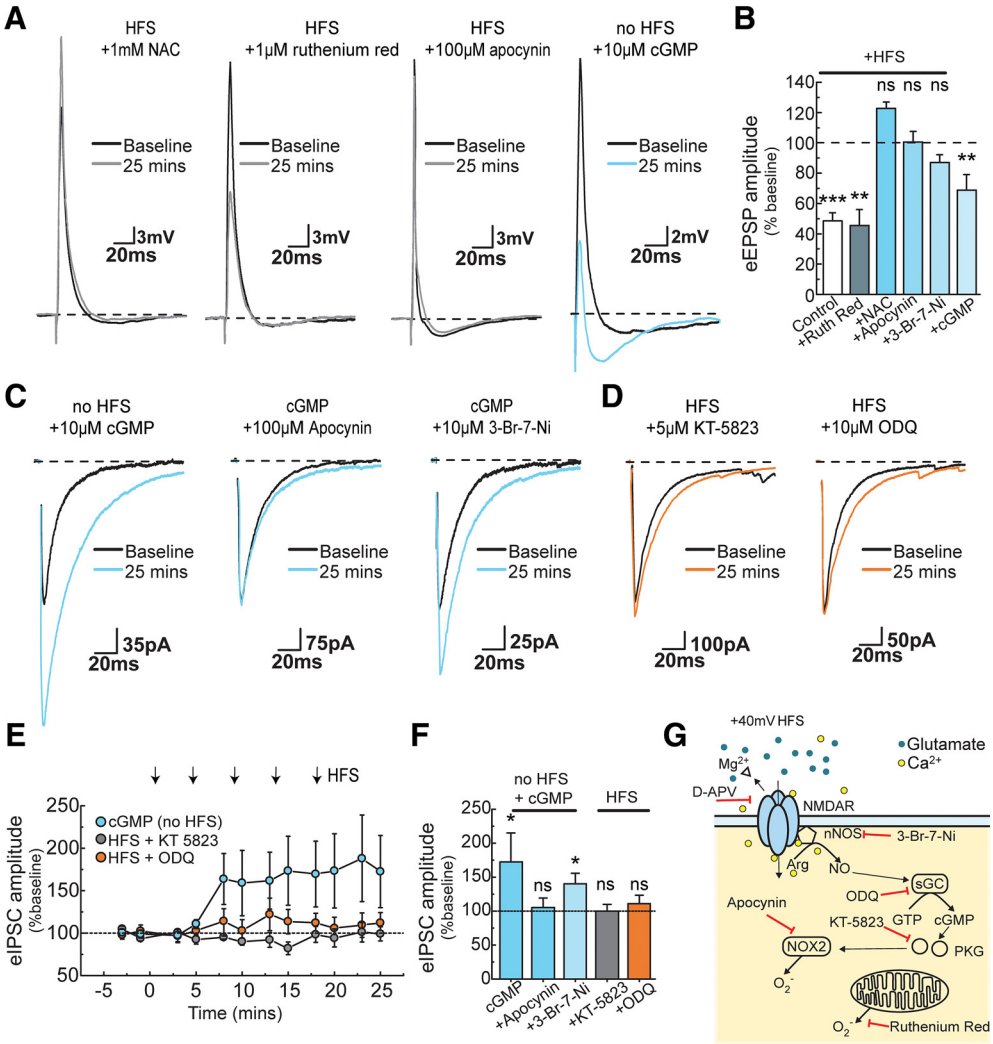

Figure 4. Inhibition of NO synthase and NADPH oxidase blocks iLTP. ***A***, Representative recordings from four different MLIs in current-clamp showing the response to patch electrode perfusion with different pharmacological agents. The first three traces (left to right, cell numbers: 151105r2, 150423r1, 150302r1) show the overlay of responses before (black) and after (gray) HFS. In each case, the recording electrode solution contained either NAC (cell 151105r2), RR (cell 150423r1), or Apo (cell 150302r1). The rightmost trace shows the overlay of two averaged EPSPs at the beginning (black) of patch perfusion with cGMP and after 25 min (blue; cell 190530r2). ***B***, Summary bar graph of the eEPSP amplitude at 25 min under different conditions expressed as a percentage of the baseline. Error bars indicate SEM. ***C***, Representative $GABA_AR$ membrane currents from three different voltage-clamped MLIs at the start (black) and after 25 min (blue) of internal patch perfusion with cGMP (cell numbers left to right: 190122r1, 190311r2, 190530r2). ***D***, Representative $GABA_AR$ currents from two different voltage-clamped MLIs at baseline (black) and 25 min after HFS (orange) with internal patch perfusion of KT-5823 (PKG inhibitor, cell 191214r2) or ODQ (guanylate cyclase inhibitor, cell 191217r2). ***E***, Summary plot of the time course of eIPSC amplitude during internal perfusion of cGMP or HFS treatment. ***F***, Summary bar graph of the change in eIPSC amplitude after 25 min perfusion with internal perfusion of cGMP or HFS treatment with pharmacological blockers. Data are expressed as a percentage of the baseline. ***G***, Schematic diagram outlining the key signaling steps triggered by Ca^{2+} influx through NMDARs. An elevation in cytosolic Ca^{2+}, activates nNOS which generates NO from arginine (Arg). NO's action on guanylate cyclase (sGC) generates cGMP from GTP which, in turn, signals to PKG and NOX2 to generate the ROS, superoxide (O_2^-). Line markers in red denote the pharmacological target of 3-Br-7-Ni (nNOS), Apo (NOX2), RR (mitochondria), D-APV (NMDAR), KT-5823 (PKG), and ODQ (sGC). Error bars indicate SEM. *$p < 0.05$, **$p < 0.01$, ***$p < 0.001$. ns, not significant.

contribution of postsynaptic AMPARs (Fig. 3*A*,*D*). In contrast, the glutamatergic response after HFS stimulation at +40 mV, exhibited a greater APV-sensitive component due to a greater contribution of NMDARs (Fig. 3*B*–*D*). In keeping with this, the charge transfer (Q) observed in control conditions at +40 mV ($Q = 49.1 \pm 8.6$ pC, $n = 10$) was similar to the charge transfer measured following bath application of 10 μM GYKI 53 655 to isolate the NMDAR response ($Q = 41.7 \pm 12.3$ pC, $n = 10$, $W_{(9)} = 12$, $p = 0.25$, Wilcoxon signed rank test; Fig. 3*B*–*D*). To directly test the hypothesis that NMDAR activation is required for strengthening GABAergic signaling, we repeated the HFS protocol in slices pre-incubated with 10 μM D-APV to block NMDARs (Fig. 3*E*–*G*). Under these conditions, the reduction in peak eEPSP of the biphasic response failed to occur ($Peak_{25}$: 111.2 ± 8%, $n = 4$, $F_{(5,15)} = 0.33$, $p = 0.88$, repeated-measures ANOVA; Fig. 3*E*–*G*) establishing that extrasynaptic NMDARs couple signaling between glutamatergic and GABAergic synapses in cerebellar MLIs. In agreement with our previous result in voltage-clamp (Fig. 2), inclusion of high concentrations of BAPTA in the patch electrode also eliminated the reduction in the eEPSP amplitude (Fig. 3*G*) demonstrating that NMDARs strengthen GABAergic transmission through an elevation in cytosolic Ca^{2+}.

NMDA receptors strengthen GABAergic synapses via a NO-dependent pathway

Since NMDARs can elevate ROS levels in other neurons (Dugan et al., 1995; Reynolds and Hastings, 1995) and strengthen GABAergic signaling in cerebellar MLIs (Accardi et al., 2014),

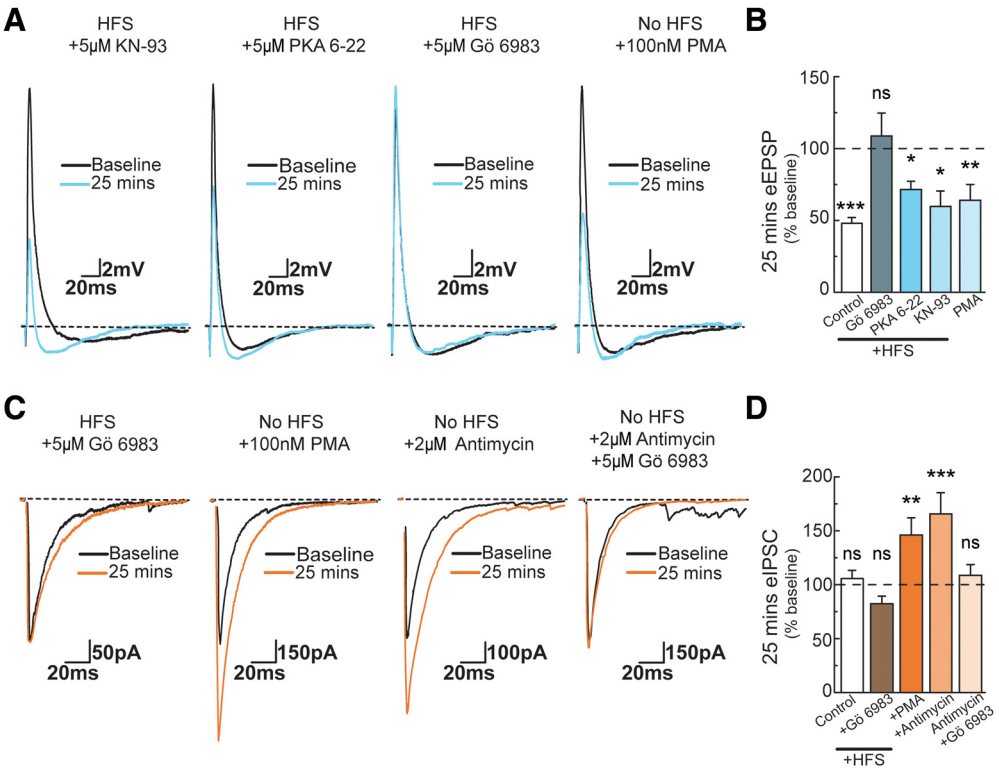

Figure 5. Activation of protein kinase C strengthens GABAergic synapses. ***A***, Representative recordings from four different MLIs in current-clamp showing the response to patch electrode perfusion with different kinase inhibitors or activators. The first three traces (left to right) show the overlay of responses before (black) and after (blue) HFS. In each case, the recording electrode solution contained either KN-93 (cell 150904r1), PKA 6-22 (cell 150717r2) or Gö 6983 (cell 150629r2). The rightmost trace shows the overlay of two averaged EPSPs at the beginning (black) of patch perfusion with the phorbol ester, PMA, and after 25 min (blue; cell 160204r2). ***B***, Summary bar graph of the eEPSP amplitude at 25 min under different conditions expressed as a percentage of the baseline. Error bars show SEM. ***C***, Representative $GABA_AR$ membrane currents from four different MLIs in the voltage-clamp configuration. Synaptically-evoked membrane currents observed before the onset of HFS (black) and after 25 min (orange) in the presence of the PKC inhibitor, Gö 6983 (left; cell 171027r1). The remaining traces correspond to eIPSCs observed at the start (black) and after 25 min (orange) of patch perfusion with PMA (cell 160825r1), antimycin A (cell 190630r1), and antimycin A + Gö 6983 (cell 190704r1). ***D***, Summary bar graph of the data shown in ***C*** expressed as a percentage of the baseline. Error bars indicate SEM. $^*p < 0.05$, $^{**}p < 0.01$, $^{***}p < 0.001$. ns, not significant.

we tested whether a ROS-dependent mechanism could be responsible for the induction of iLTP in this study. To do this, we first included the antioxidant, N-acetylcysteine (NAC, 1 mM), in the patch electrode solution (Fig. 4*A*) which, as anticipated, eliminated the decline in the net depolarization following HFS ($Peak_{25}$: 117 ± 21%, $n = 4$, $F_{(5,15)} = 0.35$, $p = 0.87$, repeated-measures ANOVA; Fig. 4*B*). Because intracellular NAC does not antagonize $GABA_AR$ responses (Accardi et al., 2014, 2015), we concluded that the failure of the HFS protocol to reduce the net depolarization was due to the antioxidant properties of NAC. To determine the origin of ROS production, the pharmacological agents 3-Br-7-Nitroindazole (3-Br-7-Ni; 10 μM), Apo (100 μM), and ruthenium red (RR; 1 μM) were included in the patch electrode solution to selectively inhibit the activity of neuronal NOS (nNOS or NOS-1), NADPH oxidase (NOX2), and the mitochondrial Ca^{2+} uniporter, respectively. Although 3-Br-7-Ni also inhibits the other NOS isoforms, iNOS (or NOS-2), and eNOS (NOS-3), RNAseq and data from nNOS-specific KO animals reveal that only nNOS is expressed in cerebellar MLIs (Huang et al., 1993; Zeisel et al., 2018). The decline in the net depolarization was greatly attenuated by pharmacological block of nNOS and NOX2 with peak responses at 25 min of 87.1 ± 5% (3-Br-7-Ni: $n = 5$, $F_{(5,20)} = 2.40$, $p = 0.073$, repeated-measures ANOVA) and 100.6 ± 7% (Apo: $n = 5$, $\chi^2_{(5)} = 6.371$, $p = 0.272$, Friedman test), respectively (Fig. 4*A*,*B*). In contrast, inhibition of the mitochondrial Ca^{2+} uniporter with 1 μM RR did not affect the ability of the HFS protocol to attenuate the eEPSP amplitude ($Peak_{25}$: 45.5 ± 10%, $n = 4$, $\chi^2_{(5)} = 17.857$, $p = 0.003$, Friedman test; Fig. 4*A*,*B*). These results demonstrate that nNOS and NOX2 are responsible for the iLTP observed following NMDAR activation.

The fact that iLTP can be eliminated by pharmacological block of nNOS or NOX2 suggests both enzymes share a common signaling pathway. Because prior work has shown that nNOS activity is upstream of NOX2 in neurons (Girouard et al., 2009), we reasoned that a similar sequence of events may occur in MLIs. For example, a rise in NO levels through nNOS activity is known to first elevate cGMP levels via guanylate cyclase which in turn activates PKG with downstream activation of NOX2 (Girouard et al., 2009). To determine whether a similar sequence of events occurs in MLIs, we directly stimulated PKG by perfusing a non-hydrolyzable cGMP analog through our patch pipette (Fig. 4*A*–*C*,*E*,*F*). In separate current- and voltage-clamp experiments, direct activation of PKG resulted in a decrease in eEPSP amplitude ($Peak_{25}$: 68.7 ± 10%, $n = 7$, $F_{(6,30)} = 4.56$, $p = 0.003$, repeated-measures ANOVA) and a potentiation of the eIPSC amplitude ($Peak_{25}$: 180.3 ± 10%, $n = 6$, $F_{(5,25)} = 3.09$, $p = 0.02$, repeated-measures ANOVA), respectively (Fig. 4*A*,*C*) demonstrating that iLTP is regulated by cGMP. Consistent with our HFS treatment, intracellular perfusion of cGMP also resulted in a slowing of decay kinetics (cGMP τ: 21.8 ± 3.7 ms). Furthermore, pharmacological block of nNOS with 3-Br-7-Ni failed to eliminate the eIPSC potentiation ($Peak_{25}$: 139.9 ± 15%, $n = 6$, $F_{(5,25)} = 2.87$, $p = 0.03$, repeated-measures ANOVA) whereas block of

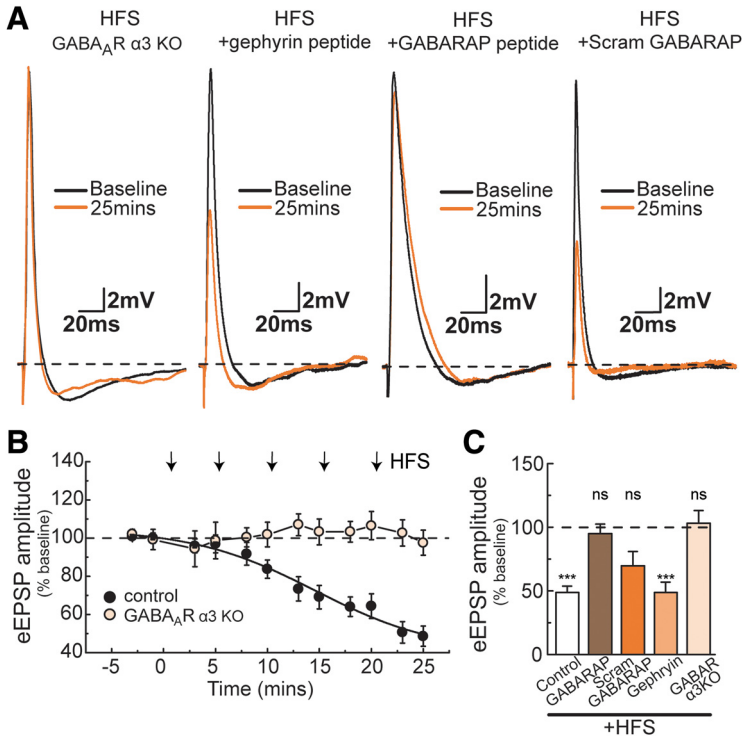

Figure 6. iLTP is dependent on α3-containing GABA$_A$ receptors and GABARAP. ***A***, Overlay of eEPSP recordings from four different MLIs in current-clamp configuration before the start of HFS (black) and after 25 min (orange). Left to right, Representative examples of recordings from MLIs from a GABA$_A$R α3 KO mouse (cell 151110r1) and wild-type cells perfused with the gephyrin interfering peptide (cell 150612r1), GABARAP interfering peptide (cell 150518r1) and scrambled GABARAP peptide (cell 150908r1). ***B***, Time course of the averaged eEPSP amplitude before and after HFS for the biphasic response from Figure 1 and in recordings from GABA$_A$R α3 KO mice. ***C***, Summary bar graph of eEPSP amplitude at 25 min following HFS expressed as a percentage of the baseline. Error bars indicate SEM. ***$p < 0.001$. ns, not significant.

NOX2 activity with Apo eliminated the effect of the cGMP analog (Peak$_{25}$: 105 ± 14%, $n = 6$, $\chi^2_{(5)} = 5.33$, $p = 0.37$, Friedman test; Fig. 4*C*,*F*). Conversely, including the PKG antagonist, KT-5823 (5 μM), in our internal patch solution eliminated any potentiation of the eIPSC amplitude following HFS (Peak$_{25}$: 99.3 ± 8%, $n = 7$, $F_{(6,30)} = 0.92$, $p = 0.48$, repeated-measures ANOVA; Fig. 4*D*–*F*). Finally, pharmacological block of guanylate cyclase by internal perfusion of ODQ (10 μM) also prevented any potentiation of the eIPSC following HFS (Peak$_{25}$: 112 ± 12%, $n = 7$, $F_{(6,30)} = 0.78$, $p = 0.57$, repeated-measures ANOVA; Fig. 4*D*–*F*). Together, these data demonstrate that nNOS activation is upstream of NOX2 in a PKG-dependent pathway as summarized in Figure 4*G*.

PKC strengthens GABAergic synapses following NMDA receptor activation

Several kinases have been shown to regulate the strength of GABAergic synapses by triggering the recruitment of synaptic GABA$_A$Rs (Luscher et al., 2011). Many of these kinases also possess ROS-sensitive amino-acid residues in their regulatory or catalytic domains which can affect kinase activity. Specifically PKA, PKC, and CaMKII can be activated by ROS in addition to their canonical activation pathways (Knock and Ward, 2011). Given this, we reasoned that the iLTP observed in the present study could be because of ROS action on kinase activity.

To test this, we performed the HFS experiment while perfusing individual MLIs with either KN-93 (5 μM), protein kinase inhibitor-(6-22)-amide peptide (5 μM) or Gö 6983 (5 μM) to selectively inhibit CaMKII, PKA, and PKC, respectively (Fig. 5). Pharmacological inhibition of PKA and CaMKII still resulted in a decline in the eEPSP amplitude following HFS with peak responses after 25 min of 71.5 ± 5% ($n = 6$, $\chi^2_{(5)} = 23.23$, $p = 0.0003$, Friedman test) and 57.2 ± 9%, respectively ($n = 4$, $\chi^2_{(5)} = 11.43$, $p = 0.04$, Friedman test; Fig. 5*A*,*B*). In contrast, inhibition of PKC by 5 μM Gö 6983 eliminated the induction of iLTP by the HFS protocol (Fig. 5*A*) with peak responses at 25 min of 108.7 ± 16% ($n = 5$, $\chi^2_{(5)} = 5.43$, $p = 0.36$, Friedman test; Fig. 5*B*). Similarly, inclusion of 5 μM Gö 6983 in voltage-clamp experiments also prevented iLTP (Fig. 5*C*,*D*). In support of this, direct activation of PKC with PMA (100 nM), elicited a similar time-dependent onset of iLTP in both current- and voltage-clamp experiments (Fig. 5*A*–*D*). We observed a decrease in the eEPSP to 63.9 ± 12% of the baseline eEPSP ($n = 4$, $\chi^2_{(4)} = 13.8$, $p = 0.008$, Friedman test) in current-clamp recordings and an increase to 146 ± 16% of the baseline eIPSC ($n = 6$, repeated-measures ANOVA, $F_{(4,20)} = 4.77$, $p = 0.007$) in voltage-clamp (Fig. 5*A*–*D*). Interestingly, we also observed iLTP following the inclusion of the metabolic uncoupler, antimycin A, to generate mitochondrial ROS in MLIs which was eliminated by the PKC inhibitor (Fig. 5*C*,*D*). This latter finding demonstrates that our previous study linking mitochondrial ROS (mROS) to the strengthening of GABAergic signaling in cerebellar MLIs is mediated through PKC (Accardi et al., 2014). A similar PKC-dependent pathway may also explain the effect of mROS on α6-containing GABA$_A$Rs of cerebellar granule cells (Accardi et al., 2015). Together, these data show that ROS-induced iLTP in MLIs relies on a PKC-dependent signaling pathway.

Synapse strengthening requires GABARAP and recruitment of α3-containing GABA$_A$ receptors

Although MLIs express both α1- and α3-containing GABA$_A$ receptors (Laurie et al., 1992), previous work from our laboratory has shown that ROS-mediated synapse strengthening relies exclusively on the recruitment of postsynaptic α3-containing receptors (Accardi et al., 2014). Though more numerous, α1-containing GABA$_A$R synapses are unaffected by ROS in both stellate and granule cells of the cerebellum (Accardi et al., 2014, 2015). To determine whether NMDAR-dependent strengthening of GABAergic transmission also relies on α3-containing receptors, we repeated the HFS protocol in cerebellar slices from α3 KO mice (Fig. 6). As anticipated, GABAergic strengthening elicited by HFS was absent in MLIs lacking the α3-subunit (Peak$_{25}$: 115.3 ± 15%, $n = 7$, $\chi^2_{(5)} = 6.59$, $p = 0.25$, Friedman test; Fig. 6*A*–*C*) confirming that the strengthening of MLI inhibitory synapses is subunit-dependent.

GABA$_A$Rs interact with a number of scaffolding proteins which regulate receptor trafficking and clustering at inhibitory

synapses. To investigate which protein interactions are responsible for synaptic targeting of α3-containing $GABA_A$Rs, we focused on two prominent $GABA_A$R scaffolding proteins linked to inhibitory synapse plasticity (Petrini and Barberis, 2014): gephyrin (Tyagarajan and Fritschy, 2014) and GABARAP (Wang et al., 1999). Previous work has identified that gephyrin binds directly to the GABA α3-subunit (Tretter et al., 2011) while GABARAP is known to bind to the γ2-subunit (Wang et al., 1999). In keeping with this, coexpression of recombinant $\alpha3\beta2\gamma2$ $GABA_A$ receptors in HEK293 cells with either gephyrin or GABARAP revealed that both scaffolding proteins coimmunoprecipitate with the ion-channel complex (Fig. 7). Consequently, we used two short-chain peptides, namely α3-derived peptide (Tretter et al., 2011; Maric et al., 2014) and K1 GABARAP peptide (Weiergräber et al., 2008), to interfere with the binding of gephyrin or GABARAP, respectively, to recombinantly expressed α3-containing $GABA_A$Rs (see Materials and Methods; Fig. 7*B*). These peptides were then used in separate electrophysiology experiments to test for the role of gephyrin and/or GABARAP in MLI inhibitory synapse strengthening.

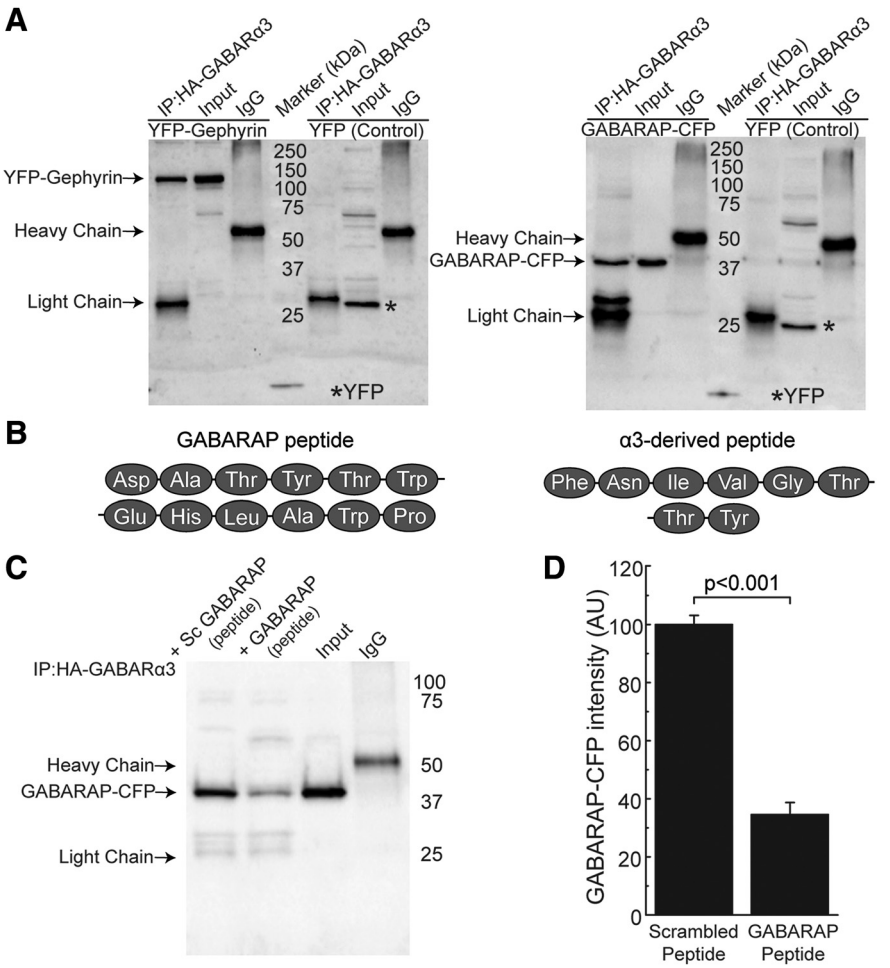

Figure 7. Co-assembly of α3-containing $GABA_A$ receptors with GABARAP can be disrupted by short-chain interfering peptides. ***A***, Western blots of lysates from HEK 293 cells transfected with HA-GABAR-α3, GABAR-β2, and GABAR-γ2 (short) to form $\alpha3\beta2\gamma2$ GABAR channels that have been coexpressed with either Gephyrin-YFP (left) or GABARAP-CFP (right). ***A***, Left, Blot with eluates and inputs ($n = 3$) of cell lysates immunoprecipitated with an anti-HA antibody and analyzed by immunoblotting with an anti-GFP antibody. YFP is presented as a negative control (note that the anti-GFP antibody recognizes both YFP and CFP). Right, Blot with eluates and inputs ($n = 3$) of cell lysates immunoprecipitated with an anti-HA antibody and analyzed by immunoblotting with an anti-GFP antibody. ***B***, Primary amino-acid sequence of the K1-GABARAP blocking peptide and the α3-derived-gephyrin blocking peptide. *C*, Scrambled GABARAP peptide or GABARAP peptide were added to lysates from the same transfections and pulled down with anti-HA antibody. Immunoblotting was performed with an anti-GFP antibody, as in ***A***. ***D***, Bar graph comparing GABARAP immunoblot levels after pre-incubation with GABARAP or scrambled peptide. $p < 0.001$, $n = 4$, Student's *t* test. Error bars indicate SEM.

Each peptide was included in the patch electrode solution during HFS protocols to interfere with the binding of the target protein (Fig. 6*A*,*C*). In all cases, we waited 15 min from breakthrough before beginning the HFS protocol to allow the peptide to dialyze throughout the neuron and prevent protein–protein interactions. We observed that the rate and degree of onset of synapse strengthening induced by HFS was unaffected by the α3-derived, gephyrin-inhibiting peptide ($Peak_{25}$: 48.7 ± 8%, $n = 5$, $F_{(4,20)} = 6.86$, $p = 0.0007$, repeated-measures ANOVA; Fig. 6*A*,*C* suggesting that α3-containing $GABA_A$Rs are not recruited to inhibitory synapses via a gephyrin-dependent mechanism. In contrast, inclusion of the K1 GABARAP peptide in the patch electrode solution eliminated the induction of synapse strengthening (Fig. 6*A*, *C*; $F_{(5,40)} = 1.22$, $p = 0.35$, repeated-measures ANOVA) indicating that GABARAP is required for the synaptic recruitment of α3-containing $GABA_A$Rs. In agreement with this, pre-incubation of the K1 GABARAP peptide with lysates of cells coexpressing α3-containing $GABA_A$Rs disrupted GABARAP binding establishing the specificity of the interaction (Fig. 7*C*,*D*). Moreover, a scrambled version of the K1 GABARAP peptide failed to disrupt the binding of GABARAP to the GABAR complex (Fig. 7*C*,*D*). Additionally, the scrambled peptide failed to prevent the induction of iLTP by the HFS protocol ($n = 4$, 69.6 ± 11%; Fig. 6*A*,*C*) further confirming the specificity of the K1 GABARAP peptide interaction with α3-containing $GABA_A$Rs.

Discussion

The present study advances our understanding of how NO signaling regulates the excitatory/inhibitory balance in the mammalian brain in several new and important ways. First, we show that NO generated by NMDAR activation strengthens inhibitory GABAergic synapses through a series of sequential steps involving nNOS, NADPH oxidase, and PKC as outlined in Figure 8 These observations are distinct from previous work, which has shown that NMDARs strengthen $GABA_A$ receptor synapses through a different pathway involving CaMKII. Second, we show that the strengthening of α3-containing $GABA_A$R synapses in MLIs is reliant on the scaffolding protein, GABARAP, rather than gephyrin. Our data does not exclude a role for gephyrin

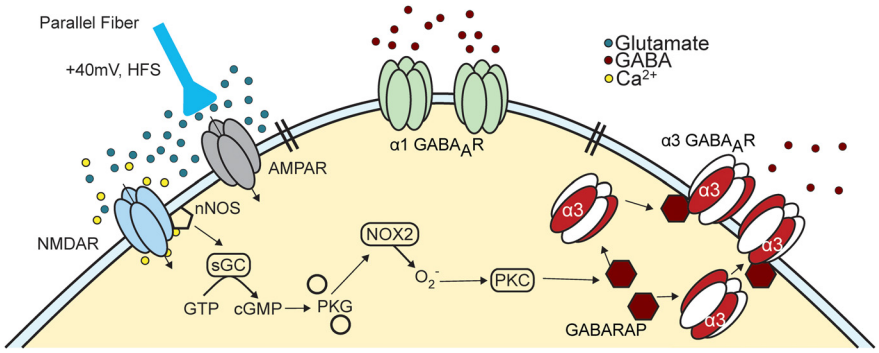

Figure 8. Summary of iLTP signaling pathway. Schematic summarizing the main signaling events and molecules that lead to the selective recruitment of α3-containing $GABA_AR$s into inhibitory synapses of cerebellar MLIs. HFS of parallel fibers from granule cells stimulates extrasynaptic NMDARs of MLIs and activates nNOS through the influx of external Ca^{2+}. nNOS generates NO, which acts on guanylate cyclase (sGC) elevating cGMP which, in turn, stimulates PKG and NOX2. We speculate the production of superoxide by NOX2 leads to the activation of PKC and the recruitment of $GABA_AR$s via a GABARAP-dependent pathway. This signaling pathway selectively acts on α3-containing $GABA_AR$s and does not affect synapses containing α1-$GABA_AR$s.

at α3-receptor synapses but nevertheless highlights that GABARAP has a prominent role in the recruitment process. Finally, given the widespread but cell-selective expression of the NMDAR/nNOS complex, our findings suggest that NO control of GABAergic synapses through NMDARs may be more widespread in the vertebrate brain than has been appreciated.

NO strengthens inhibitory GABAergic synapses following NMDAR activation

Multiple presynaptic and postsynaptic mechanisms elicit long-term changes in the efficacy of GABAergic synapses (Kullmann et al., 2012) with one of the most prominent pathways involving an increase in the number of $GABA_A$ receptors per synapse (Luscher et al., 2011). NMDAR-mediated strengthening of GABAergic synapses has been linked to an increase in cytoplasmic Ca^{2+} and subsequent activation of CaMKII (Marsden et al., 2007; Luscher et al., 2011; Chiu et al., 2019). Although Ca^{2+} entry through NMDARs is still a requirement in inhibitory synapse strengthening of MLIs, we excluded a role for CaMKII because its specific kinase inhibitor, KN-93, did not affect synaptic plasticity (compare Fig. 5).

A recent study has shown that postsynaptic NMDARs of granule cells can enhance inhibitory transmission by the retrograde action of NO on presynaptic GABA terminals of Golgi cells in the rat cerebellum (Mapelli et al., 2016). Although we cannot completely exclude a presynaptic role of NO in the present study on the mouse cerebellum, our data suggest that almost all the molecular events triggered by NMDARs in MLIs are predominantly postsynaptic. For example, it is unlikely that a presynaptic mechanism could explain the effect of internal patch perfusion of the GABARAP blocking peptide on inhibitory synapse strengthening (Figs. 6, 7) given that the peptide is membrane impermeant and thus confined to the cytoplasm of the recorded cell. Likewise, the effect of internal patch perfusion with cGMP and its inhibition by Apo (Fig. 4) suggests that the signaling pathway involving both cGMP and NOX2 is postsynaptic. Furthermore, if NO was acting through a purely presynaptic mechanism, enhanced release of presynaptic GABA by NO would be expected to be observed at all inhibitory synapses. However, our data demonstrate that the enhancement of GABAergic transmission by NMDARs and NO occurs only at α3-containing inhibitory synapses and not α1-receptor synapses (Fig. 6). It is possible that NO has both presynaptic and postsynaptic targets at inhibitory synapses of MLIs. In this case, NO would selectively enhance presynaptic GABA release from α3- and not α1-receptor synapses while triggering the postsynaptic cell to generate NO, cGMP, activate NOX2 and PKC, and finally promote the recruitment of postsynaptic α3-receptors.

Interestingly, a similar dual effect of NO might be at play at the inhibitory Golgi cell-granule cell synapse. In agreement with this, we have previously shown that reactive oxygen species enhance recruitment of postsynaptic α6- but not α1-containing $GABA_AR$s in mouse granule cells (Accardi et al., 2015), whereas others have shown a presynaptic action of NO on GABA release from rat Golgi cells (Mapelli et al., 2016). Differential regulation of input-specific GABAergic synapses onto the same neuron has recently been described in the cerebral cortex (Chiu et al., 2018) and striatum (Paraskevopoulou et al., 2019), consequently, it is possible that a similar arrangement is found in both inhibitory synapses of MLIs and granule cells of the cerebellum. An important caveat to both presynaptic and postsynaptic roles of NO in granule cells, however, is that nNOS expression in the presynaptic terminals of Golgi cells is high in the rat but almost completely absent from the mouse, particularly mice with the C57BL/6 background used in this study (Kaplan et al., 2013). Accordingly, NO may act primarily on presynaptic Golgi cell terminals in the rat and through a postsynaptic pathway in granule cells of the mouse. Whether nNOS expression at MLI inhibitory synapses is similarly species-dependent has yet to be examined.

GABAergic synapse strengthening is dependent on the scaffolding protein, GABARAP

Our experiments establish a key role for GABARAP in the strengthening of GABAergic synapses. Although different mechanisms may anchor $GABA_AR$s at central synapses, the prevalent view is that gephyrin plays a prominent role in binding the α1–3 (Tretter et al., 2008; Mukherjee et al., 2011; Tretter et al., 2011) and/or β2–3 (Kowalczyk et al., 2013) $GABA_AR$ subunits to the cytoskeleton (Tyagarajan and Fritschy, 2014). Although gephyrin-independent clustering of postsynaptic $GABA_AR$s has been reported (Kneussel et al., 2001; Levi et al., 2004; Panzanelli et al., 2011) the role of other accessory proteins, such as GABARAP (Wang et al., 1999) and/or the dystrophin–glycoprotein complex (Pribiag et al., 2014), has received less attention. Our data argue in favor of GABARAP playing an important role in the recruitment of α3-containing $GABA_AR$s during synapse strengthening (compare Fig. 6). Although, we cannot exclude a role for gephyrin at α3-receptor synapses, costaining for the α3 subunit and gephyrin show very little overlap (Accardi et al., 2014) suggesting that α3 $GABA_AR$ subunits may associate with another trafficking/scaffolding protein in MLIs. Our findings are consistent with studies on cultured hippocampal neurons showing that there are low GABARAP levels at inhibitory synapses under basal conditions (Kittler et al., 2001) and that the levels increase following

chemically-induced strengthening of inhibitory synapses (Marsden et al., 2007).

Widespread and cell-selective expression of nNOS$^+$ neurons in the mammalian brain

nNOS$^+$ neurons are expressed throughout the CNS (Vincent and Kimura, 1992; Southam and Garthwaite, 1993; Rodrigo et al., 1994) and are involved in many different CNS functions that include learning and memory, sleep, feeding behaviors, movement, pain, anxiety, and reproductive activity (Garthwaite, 2008; Steinert et al., 2010; Chachlaki et al., 2017; Garthwaite, 2019). It has long been recognized that nNOS activation and the downstream production of cGMP is linked to glutamatergic signaling, primarily through NMDARs in the cerebellum (Southam et al., 1991). Of note, nNOS activity is highest in the cerebellum compared with other brain regions (Förstermann et al., 1990) because of several nNOS$^+$ neuronal types, including granule cells and MLIs, but is curiously absent from Purkinje cells, the sole output neuron of the cerebellar cortex (Vincent and Kimura, 1992; Rodrigo et al., 1994). Our data establish a new function for nNOS in MLIs, which is part of a sequential signaling pathway that strengthens inhibitory GABAergic synapses following NMDAR activation. NMDARs of MLIs are also involved in the tight coupling between neuronal communication and local blood flow during functional hyperemia where activation of NMDARs generates NO, which promotes vasodilation of local capillaries (Rancillac et al., 2006).

Together, these observations suggest that NMDARs expressed by MLIs fulfill multiple functions that control the excitability of MLIs while impacting the physiological state of the surrounding cells and tissue. In keeping with this, unpublished data from our laboratory reveals that NMDARs also directly modulate MLI excitability (RPD Alexander and D. Bowie, unpublished observation) through a signaling pathway that leads to a hyperpolarizing shift in sodium channel (Nav) activation and inactivation recently described (Alexander et al., 2019). Interestingly, this pathway does not involve PKC but instead signals through the actions of CaMKII (Alexander and Bowie, unpublished observation) suggesting that Ca^{2+} influx through NMDARs in MLIs triggers a bifurcating pathway involving both CaMKII and nNOS. Given the multiple actions of NMDARs and nNOS in MLIs, it is tempting to speculate that similar roles are found in other nNOS$^+$ cells of the CNS. On that note, NMDAR activation and the generation of ROS or NO also lead to the strengthening of GABAergic transmission in cerebellar granule cells (Accardi et al., 2015; Mapelli et al., 2016) and vasodilation of local blood vessels (Mapelli et al., 2017) in a manner reminiscent of MLIs. Given this, it would be interesting in future studies to examine whether NMDAR activation of other nNOS$^+$ neurons outside the cerebellum similarly regulate GABAR plasticity and local blood flow.

References

Accardi MV, Brown P, Miraucourt LS, Orser BA, Bowie D (2015) α6-Containing GABAA receptors are the principal mediators of inhibitory synapse strengthening by insulin in cerebellar granule cells. J Neurosci 35:9676–9688.

Accardi MV, Daniels BA, Brown P, Fritschy JM, Tyagarajan SK, Bowie D (2014) Mitochondrial reactive oxygen species regulate the strength of inhibitory GABA-mediated synaptic transmission. Nat Commun 5: 3168.

Alexander RPD, Mitry J, Sareen V, Khadra A, Bowie D (2019) Cerebellar stellate cell excitability is coordinated by shifts in the gating behavior of voltage-gated Na(+) and A-type K(+) channels. eNeuro 6:ENEURO. 0126-19.2019.

Arenz A, Silver RA, Schaefer AT, Margrie TW (2008) The contribution of single synapses to sensory representation *in vivo*. Science 321:977–980.

Bayer KU, LeBel E, McDonald GL, O'Leary H, Schulman H, De Koninck P (2006) Transition from reversible to persistent binding of CaMKII to postsynaptic sites and NR2B. J Neurosci 26:1164–1174.

Bello O, Blair K, Chapleau C, Larimore JL (2013) Is memantine a potential therapeutic for Rett syndrome? Front Neurosci 7:245.

Bredt DS (1999) Endogenous nitric oxide synthesis: biological functions and pathophysiology. Free Radic Res 31:577–596.

Brenman JE, Christopherson KS, Craven SE, McGee AW, Bredt DS (1996a) Cloning and characterization of postsynaptic density 93, a nitric oxide synthase interacting protein. J Neurosci 16:7407–7415.

Brenman JE, Chao DS, Gee SH, McGee AW, Craven SE, Santillano DR, Wu Z, Huang F, Xia H, Peters MF, Froehner SC, Bredt DS (1996b) Interaction of nitric oxide synthase with the postsynaptic density protein PSD-95 and α1-syntrophin mediated by PDZ domains. Cell 84:757–767.

Brown GC (2010) Nitric oxide and neuronal death. Nitric Oxide 23:153–165.

Chachlaki K, Garthwaite J, Prevot V (2017) The gentle art of saying NO: how nitric oxide gets things done in the hypothalamus. Nat Rev Endocrinol 13:521–535.

Chadderton P, Margrie TW, Hausser M (2004) Integration of quanta in cerebellar granule cells during sensory processing. Nature 428:856–860.

Chiu CQ, Barberis A, Higley MJ (2019) Preserving the balance: diverse forms of long-term GABAergic synaptic plasticity. Nat Rev Neurosci 20:272–281.

Chiu CQ, Martenson JS, Yamazaki M, Natsume R, Sakimura K, Tomita S, Tavalin SJ, Higley MJ (2018) Input-specific NMDAR-dependent potentiation of dendritic GABAergic inhibition. Neuron 97:368–377.e3.

Clark BA, Cull-Candy SG (2002) Activity-dependent recruitment of extrasynaptic NMDA receptor activation at an AMPA receptor-only synapse. J Neurosci 22:4428–4436.

Coddington LT, Rudolph S, Vande Lune P, Overstreet-Wadiche L, Wadiche JI (2013) Spillover-mediated feedforward inhibition functionally segregates interneuron activity. Neuron 78:1050–1062.

Dugan LL, Sensi SL, Canzoniero LM, Handran SD, Rothman SM, Lin TS, Goldberg MP, Choi DW (1995) Mitochondrial production of reactive oxygen species in cortical neurons following exposure to N-methyl-D-aspartate. J Neurosci 15:6377–6388.

Förstermann U, Gorsky LD, Pollock JS, Schmidt HH, Heller M, Murad F (1990) Regional distribution of EDRF/NO-synthesizing enzyme(s) in rat brain. Biochem Biophys Res Commun 168:727–732.

Fritschy JM, Panzanelli P (2006) Molecular and synaptic organization of GABAA receptors in the cerebellum: effects of targeted subunit gene deletions. Cerebellum 5:275–285.

Garthwaite J (2008) Concepts of neural nitric oxide-mediated transmission. Eur J Neurosci 27:2783–2802.

Garthwaite J (2016) From synaptically localized to volume transmission by nitric oxide. J Physiol 594:9–18.

Garthwaite J (2019) NO as a multimodal transmitter in the brain: discovery and current status. Br J Pharmacol 176:197–211.

Girouard H, Wang G, Gallo EF, Anrather J, Zhou P, Pickel VM, Iadecola C (2009) NMDA receptor activation increases free radical production through nitric oxide and NOX2. J Neurosci 29:2545–2552.

Glasgow NG, Siegler Retchless B, Johnson JW (2015) Molecular bases of NMDA receptor subtype-dependent properties. J Physiol 593:83–95.

Gnegy ME (2000) Ca^{2+}/calmodulin signaling in NMDA-induced synaptic plasticity. Crit Rev Neurobiol 14:91–129.

Hardingham GE, Bading H (2003) The Yin and Yang of NMDA receptor signalling. Trends Neurosci 26:81–89.

Hu C, Chen W, Myers SJ, Yuan H, Traynelis SF (2016) Human GRIN2B variants in neurodevelopmental disorders. J Pharmacol Sci 132:115–121.

Huang PL, Dawson TM, Bredt DS, Snyder SH, Fishman MC (1993) Targeted disruption of the neuronal nitric oxide synthase gene. Cell 75:1273–1286.

Jörntell H, Ekerot CF (2006) Properties of somatosensory synaptic integration in cerebellar granule cells *in vivo*. J Neurosci 26:11786–11797.

Kaplan JS, Mohr C, Rossi DJ (2013) Opposite actions of alcohol on tonic GABA(A) receptor currents mediated by nNOS and PKC activity. Nat Neurosci 16:1783–1793.

Kiss JP, Vizi ES (2001) Nitric oxide: a novel link between synaptic and nonsynaptic transmission. Trends Neurosci 24:211–215.

Kittler JT, Rostaing P, Schiavo G, Fritschy JM, Olsen R, Triller A, Moss SJ (2001) The subcellular distribution of GABARAP and its ability to interact with NSF suggest a role for this protein in the intracellular transport of GABA(A) receptors. Mol Cell Neurosci 18:13–25.

Kneussel M, Brandstatter JH, Gasnier B, Feng G, Sanes JR, Betz H (2001) Gephyrin-independent clustering of postsynaptic GABA(A) receptor subtypes. Mol Cell Neurosci 17:973–982.

Knock GA, Ward JP (2011) Redox regulation of protein kinases as a modulator of vascular function. Antioxid Redox Signal 15:1531–1547.

Köhr G, Eckardt S, Lüddens H, Monyer H, Seeburg PH (1994) NMDA receptor channels: subunit-specific potentiation by reducing agents. Neuron 12:1031–1040.

Kowalczyk S, Winkelmann A, Smolinsky B, Forstera B, Neundorf I, Schwarz G, Meier JC (2013) Direct binding of GABAA receptor $\beta 2$ and $\beta 3$ subunits to gephyrin. Eur J Neurosci 37:544–554.

Kullmann DM, Moreau AW, Bakiri Y, Nicholson E (2012) Plasticity of inhibition. Neuron 75:951–962.

Laurie DJ, Seeburg PH, Wisden W (1992) The distribution of 13 GABAA receptor subunit mRNAs in the rat brain: II. Olfactory bulb and cerebellum. J Neurosci 12:1063–1076.

Lee DZ, Chung JM, Chung K, Kang M-G (2012) Reactive oxygen species (ROS) modulate AMPA receptor phosphorylation and cell-surface localization in concert with pain-related behavior. PAIN 153:1905–1915.

Levi S, Logan SM, Tovar KR, Craig AM (2004) Gephyrin is critical for glycine receptor clustering but not for the formation of functional GABAergic synapses in hippocampal neurons. J Neurosci 24:207–217.

Li Z, Ji G, Neugebauer V (2011) Mitochondrial reactive oxygen species are activated by mGluR5 through IP3 and activate ERK and PKA to increase excitability of amygdala neurons and pain behavior. J Neurosci 31:1114–1127.

Liu J, Chang L, Song Y, Li H, Wu Y (2019) The role of NMDA receptors in Alzheimer's disease. Front Neurosci 13:43.

Lu YF, Kandel ER, Hawkins RD (1999) Nitric oxide signaling contributes to late-phase LTP and CREB phosphorylation in the hippocampus. J Neurosci 19:10250–10261.

Luscher B, Fuchs T, Kilpatrick CL (2011) GABAA receptor trafficking-mediated plasticity of inhibitory synapses. Neuron 70:385–409.

Mapelli J, Gandolfi D, Vilella A, Zoli M, Bigiani A (2016) Heterosynaptic GABAergic plasticity bidirectionally driven by the activity of pre- and postsynaptic NMDA receptors. Proc Natl Acad Sci U S A 113:9898–9903.

Mapelli L, Gagliano G, Soda T, Laforenza U, Moccia F, D'Angelo EU (2017) Granular layer neurons control cerebellar neurovascular coupling through an NMDA receptor/NO-dependent system. J Neurosci 37:1340–1351.

Maric HM, Kasaragod VB, Hausrat TJ, Kneussel M, Tretter V, Stromgaard K, Schindelin H (2014) Molecular basis of the alternative recruitment of GABA(A) versus glycine receptors through gephyrin. Nat Commun 5:5767.

Marsden KC, Beattie JB, Friedenthal J, Carroll RC (2007) NMDA receptor activation potentiates inhibitory transmission through GABA receptor-associated protein-dependent exocytosis of GABA(A) receptors. J Neurosci 27:14326–14337.

Milnerwood AJ, Raymond LA (2010) Early synaptic pathophysiology in neurodegeneration: insights from Huntington's disease. Trends Neurosci 33:513–523.

Mukherjee J, Kretschmannova K, Gouzer G, Maric HM, Ramsden S, Tretter V, Harvey K, Davies PA, Triller A, Schindelin H, Moss SJ (2011) The residence time of GABA(A)Rs at inhibitory synapses is determined by direct binding of the receptor $\alpha 1$ subunit to gephyrin. J Neurosci 31:14677–14687.

Nakahiro M, Arakawa O, Narahashi T, Ukai S, Kato Y, Nishinuma K, Nishimura T (1992) Dimethyl sulfoxide (DMSO) blocks GABA-induced current in rat dorsal root ganglion neurons. Neurosci Lett 138:5–8.

Panzanelli P, Gunn BG, Schlatter MC, Benke D, Tyagarajan SK, Scheiffele P, Belelli D, Lambert JJ, Rudolph U, Fritschy JM (2011) Distinct mechanisms regulate GABAA receptor and gephyrin clustering at perisomatic and axo-axonic synapses on CA1 pyramidal cells. J Physiol 589:4959–4980.

Paoletti P, Bellone C, Zhou Q (2013) NMDA receptor subunit diversity: impact on receptor properties, synaptic plasticity and disease. Nat Rev Neurosci 14:383–400.

Paraskevopoulou F, Herman MA, Rosenmund C (2019) Glutamatergic Innervation onto Striatal Neurons Potentiates GABAergic Synaptic Output. J Neurosci 39:4448–4460.

Petrini EM, Barberis A (2014) Diffusion dynamics of synaptic molecules during inhibitory postsynaptic plasticity. Front Cell Neurosci 8:300.

Petrini EM, Ravasenga T, Hausrat TJ, Iurilli G, Olcese U, Racine V, Sibarita JB, Jacob TC, Moss SJ, Benfenati F, Medini P, Kneussel M, Barberis A (2014) Synaptic recruitment of gephyrin regulates surface GABAA receptor dynamics for the expression of inhibitory LTP. Nat Commun 5:3921.

Pribiag H, Peng H, Shah WA, Stellwagen D, Carbonetto S (2014) Dystroglycan mediates homeostatic synaptic plasticity at GABAergic synapses. Proc Natl Acad Sci U S A 111:6810–6815.

Rancillac A, Rossier J, Guille M, Tong XK, Geoffroy H, Amatore C, Arbault S, Hamel E, Cauli B (2006) Glutamatergic control of microvascular tone by distinct GABA neurons in the cerebellum. J Neurosci 26:6997–7006.

Rancz EA, Ishikawa T, Duguid I, Chadderton P, Mahon S, Hausser M (2007) High-fidelity transmission of sensory information by single cerebellar mossy fibre boutons. Nature 450:1245–1248.

Reynolds IJ, Hastings TG (1995) Glutamate induces the production of reactive oxygen species in cultured forebrain neurons following NMDA receptor activation. J Neurosci 15:3318–3327.

Rodrigo J, Springall DR, Uttenthal O, Bentura ML, Abadia-Molina F, Riveros-Moreno V, Martínez-Murillo R, Polak JM, Moncada S (1994) Localization of nitric oxide synthase in the adult rat brain. Philos Trans R Soc Lond B Biol Sci 345:175–221.

Sanhueza M, Lisman J (2013) The CaMKII/NMDAR complex as a molecular memory. Mol Brain 6:10.

Saviane C, Silver RA (2006) Fast vesicle reloading and a large pool sustain high bandwidth transmission at a central synapse. Nature 439:983–987.

Serulle Y, Zhang S, Ninan I, Puzzo D, McCarthy M, Khatri L, Arancio O, Ziff EB (2007) A GluR1-cGKII interaction regulates AMPA receptor trafficking. Neuron 56:670–688.

Southam E, Garthwaite J (1993) The nitric oxide-cyclic GMP signalling pathway in rat brain. Neuropharmacology 32:1267–1277.

Southam E, East SJ, Garthwaite J (1991) Excitatory amino acid receptors coupled to the nitric oxide/cyclic GMP pathway in rat cerebellum during development. J Neurochem 56:2072–2081.

Steinert JR, Chernova T, Forsythe ID (2010) Nitric oxide signaling in brain function, dysfunction, and dementia. Neuroscientist 16:435–452.

Tretter V, Jacob TC, Mukherjee J, Fritschy JM, Pangalos MN, Moss SJ (2008) The clustering of $GABA_A$ receptor subtypes at inhibitory synapses is facilitated via the direct binding of receptor alpha 2 subunits to gephyrin. J Neurosci 28:1356–1365.

Tretter V, Kerschner B, Milenkovic I, Ramsden SL, Ramerstorfer J, Saiepour L, Maric HM, Moss SJ, Schindelin H, Harvey RJ, Sieghart W, Harvey K (2011) Molecular basis of the γ-aminobutyric acid A receptor $\alpha 3$ subunit interaction with the clustering protein gephyrin. J Biol Chem 286:37702–37711.

Tyagarajan SK, Fritschy JM (2014) Gephyrin: a master regulator of neuronal function? Nat Rev Neurosci 15:141–156.

Vincent SR, Kimura H (1992) Histochemical mapping of nitric oxide synthase in the rat brain. Neuroscience 46:755–784.

Wang H, Bedford FK, Brandon NJ, Moss SJ, Olsen RW (1999) GABA(A)-receptor-associated protein links GABA(A) receptors and the cytoskeleton. Nature 397:69–72.

Weiergräber OH, Stangler T, Thielmann Y, Mohrlüder J, Wiesehan K, Willbold D (2008) Ligand binding mode of GABAA receptor-associated protein. J Mol Biol 381:1320–1331.

Yee BK, Keist R, von Boehmer L, Studer R, Benke D, Hagenbuch N, Dong Y, Malenka RC, Fritschy J-M, Bluethmann H, Feldon J, Möhler H, Rudolph U (2005) A schizophrenia-related sensorimotor deficit links $\alpha 3$-containing GABAA receptors to a dopamine hyperfunction. Proc Natl Acad Sci U S A 102:17154–17159.

Zeisel A, Hochgerner H, Lönnerberg P, Johnsson A, Memic F, van der Zwan J, Haring M, Braun E, Borm LE, La Manno G, Codeluppi S, Furlan A, Lee K, Skene N, Harris KD, Hjerling-Leffler J, Arenas E, Ernfors P, Marklund U, Linnarsson S (2018) Molecular Architecture of the Mouse Nervous System. Cell 174:999–1014.e22.